THE MECHANISMS AND KINETICS OF BIOLOGICAL TREATMENT OF METAL-CONTAINING EFFLUENT

Report to the
WATER RESEARCH COMMISSION

by

GS Hansford
University of Cape Town

WRC Report No 1080/1/04
ISBN No 1-77005-141-4

MARCH 2004

Disclaimer

This report emanates from a project financed by the Water Research Commission (WRC) and is approved for publication. Approval does not signify that the contents necessarily reflect the views and policies of the WRC or the members of the project steering committee, nor does mention of trade names or commercial products constitute endorsement or recommendation for use.

SUMMARY

This project was initiated in order to provide a fundamental understanding of the mechanism and kinetics of the biological treatment of metal-sulfate-containing effluents such as acid mine drainage. It also has the objective of supporting process development investigations being carried out at other institutions, under Water Research Commission support. The results presented in this report cover the work outlined in the PhD thesis of S. Moosa and the MSc (Eng.) theses of N. E. Ristow and A. Knobel as well as the postdoctoral work of M. Nemati and M. R. Kosseva.

The conclusions of each investigation are summarised in detail at the end of each chapter, and Chapters 7 gives the overall conclusions and Chapter 8 the recommendations that have led to the further investigation being carried out in Project 1251.

The report covers four areas investigated in the project:

1. A review of the literature to define the state-of-the-art on the mechanism and kinetics of microbial sulfate reduction and provide rate equations for modelling bacterial sulfate reduction.
2. The development of two simulation models one using AQUASIM to predict the performance of the pilot plant for sludge hydrolysis and sulfate reduction developed by Rhodes University and the other a more general description of bacterial sulfate reduction.
3. Experimental investigations on the kinetics of bacterial sulfate reduction using, in one case, acetate and the other, ethanol.
4. Theoretical and experimental studies of metal precipitation.

The results of these areas of investigation can be summarised as follows:

1. The review of the literature provided a description of the pathway from complex organics through to sulfate reduction and methane formation. For most of the steps in these pathways, kinetic studies have been reported and rate equations and kinetic constants determined. However, in several of the steps the data was neither available nor applicable to the conditions applying in sulfate reduction. Rates of hydrolysis

were not well described and there was no published information on the effect of sulfate or sulfide and pH on the rates of hydrolysis. Through all the steps, the studies were aimed at anaerobic digestion and only included effects of sulfide inhibition at relatively low levels of sulfide. There is therefore the need to investigate the kinetics of acidogenesis, acetogenesis, and the kinetics of acetate utilising and hydrogen-utilising sulfate reducing bacteria at high concentrations of sulfate and sulfide. Investigation of the sulfate reducing bacteria at high sulfate loadings was initiated in this project. Further study of this as well as the other sub-processes will be investigated in WRC Project 1251.

2. In the development of the simulation models, it was decided to use published rate equations and kinetic parameters even though these were only available for low levels of sulfide inhibition. Two approaches were adopted in the modelling. Using the package AQUASIM developed for modelling wastewater treatment processes, a simulation model was developed for predicting the performance of the falling sludge bed bioreactor tested by Professor P. Rose of Rhodes University. This proved to be quite successful although the model could not be tested exhaustively due to the lack of steady state operating data from the pilot plant.

   The other simulation model, using a high level mathematical language, is more general and fundamental in nature, taking into account chemical and biological reactions as well as vapour-liquid equilibrium pertinent to the treatment systems. It was calibrated against steady state operating data published by Maree and co-workers. Neither simulation model was complete, and the work will be continued under 1251 both to refine and extend the model in terms of newly available information and to inform the experimental investigation.

3. Experimental investigations on the kinetics of bacterial sulfate reduction using acetate and using ethanol were carried out. The former was extensive based on chemostat culture in a well-mixed stirred tank. It investigated kinetics of sulfate reduction and bacterial growth as a function of sulfate loading (affected by both residence time and feed concentration) and temperature. The investigation using ethanol was only preliminary. Both showed that the kinetics are inhibited by sulfide and possibly by sulfate. For the case of the acetate-based sulfate reduction, the effect of sulfate concentration and temperature are reported and a rate equation describing the kinetics proposed.

4. Experimental precipitation studies showed that the pellet reactor is an appropriate technology for the precipitation of a metal hydroxy-carbonate salt from a synthetic nickel sulfate stream. The system produces no sludge, but rather, a dense precipitate, permitting easy solid-liquid separation and allowing reuse of the metal. The results suggest that fines are formed mostly by the spontaneous nucleation of solid phase in the liquid medium generated by a high supersaturation zone, often at the reactant inlet. The Patterson *et al.* (1977) solubility diagram can predict accurately the nickel conversion when two solid phases are taken into account: nickel hydroxide and nickel carbonate. The model is employed to determine the pH zone of the lowest soluble nickel concentration, i.e. the maximal conversion to solid nickel. The equilibrium model may not be used to predict removal efficiency, since it does not take into account fines formation. The kinetics of precipitation are fast, and the soluble species reach near equilibrium with the solid phase only after 20 centimetres of bed.

The recommendations of the investigations can be summarised as follows:

1. The possible inhibitory effect of high concentrations of sulfate *per se* on the sulfate reducing bacteria should be investigated
2. The literature review showed that while the kinetics of microorganisms involved in anaerobic digestion are available, there is very little kinetic information of the bacterial reduction of sulfate. In particular, little is reported on how the kinetics are affected by high concentrations of sulfide. It is recommended that this be thoroughly investigated.
3. The use of immobilisation to increase the concentration of sulfate reducing bacteria should be investigated.
4. The precipitation of iron carbonate and sulfide should be thoroughly investigated in the presence of sulfate reducing microorganisms.
5. The two simulation models are to be reconciled into a comprehensive modelling package including a kinetic description of all the microbial and physicochemical processes involved.

This will be undertaken in WRC Project 1251.

TABLE OF CONTENTS

Page Number

1 INTRODUCTION

Mining, mineral and chemical processing, electricity generation and many other industries produce wastewater that is acidic, has a high sulfate concentration and frequently high concentrations of dissolved metals. Bioprocesses for the treatment of acid mine drainage and other such acidic high sulfate wastewater offer advantages over physicochemical and passive treatment systems. The major advantages are the production of clean water, and the positive permanent removal of the metals.

Current and past mining activity and industrial activity leads to the discharge of large quantities of acidic wastewater high in sulfate and dissolved metals. This occurs in an area where there is a high demand for water for both domestic and industrial use. Traditionally, effluents, rich in sulfates and heavy metals, are treated by lime neutralisation, during which, the acidity of the waste stream is decreased, with the subsequent precipitation of heavy metals as hydroxides. Alternately, passive treatment, based on biological and physicochemical processes such as oxidation, reduction, adsorption and precipitation, may take place in large dams or reed beds (Kuyacek & St Germain, 1994). Disposal of sludge or reed mats at the end of the process requires further consideration.

Through this project, fundamental information to enable the development and optimisation of bioprocesses for treating these wastewaters to provide both clean water and to recover metals is sought. Disposal of concentrated brines and gypsum precipitates is eliminated through active biological treatment, as is the potential for long-term slow pollution from passive systems. Differential precipitation and separation of the dissolved metals in the active process has the potential to close the materials cycle for those metals. At best, the recovered metals could be returned to appropriate processes. At worst, a multi-component metal sulfide or carbonate precipitate is more stable, more compact and easier to de-water than the equivalent hydroxide precipitate.

Bioprocessing of acid mine drainage using bacterial sulfate reduction (Maree *et al.*, 1987; Barnes *et al.*, 1991; Stucki *et al.*, 1993; du Preez and Maree, 1994) with the recovery of metals has been demonstrated and has been in operation for some time in Europe and the United States of America. Those processes rely on the use of relatively expensive electron donors for the reduction of the sulfate and may not be generally economically applicable in South Africa. The use of other organic sources as electron donors shows promise (Colleran *et al.*, 1995; Hansen,

1988; Postgate, 1984; Widdel & Hansen, 1992). One of these is the use of sewage as proposed in the WRC projects 869 and 972 being investigated by the Department of Microbiology at Rhodes University. This project proposes to complement those projects by providing complementary engineering input into their development.

The development of simulation models to allow process optimisation forms the key emphasis of this project. A review of the literature on anaerobic digestion and bacterial sulfate reduction shows that, while a number of published models with kinetic parameters exist, there is no coherent approach for use in simulation and design. This project aims to review available kinetic data and models, verify the applicability of these for the systems of interest, and further develop kinetic models to handle environments not adequately described. Based on these kinetic models, simulations both specific to the WRC projects 869 and 972 and of general applicability to this class of processes will be developed. The development of the Rhodes University process for the treatment of acid mine drainage will be greatly facilitated by this complementary project which will permit optimisation and identification of the experimental windows to be investigated more extensively.

The specific objectives of WRC research contract 1080 are thus as follows:

1. A review of the literature to define the state-of-the-art on the mechanism and kinetics of microbial sulfate reduction and provide rate equations for modelling bacterial sulfate reduction.

2. Develop a mathematical model describing the biological treatment of Acid Mine Drainage and other high sulfate, metal-containing effluents. Incorporate this into two simulation models; one using AQUASIM to predict the performance of the pilot plant for sludge hydrolysis and sulfate reduction developed by Rhodes University and the other a more general description of bacterial sulfate reduction.

3. Experimental investigations on the kinetics of bacterial sulfate reduction using in one case, acetate, and the other, ethanol. Establish the kinetics of the critical sub-processes in order to inform and refine the predictive models

4. Theoretical and experimental studies of metal precipitation, in particular, the experimental investigation of metal removal as carbonate or sulfide salts in order to maximise clean water recovery.

2 REVIEW OF MECHANISMS AND KINETICS OF ANAEROBIC DIGESTION INCLUDING SULFATE REDUCTION

During the biological sulfate reduction process sulfate acts as the terminal electron acceptor for the degradation of organic compounds. The result of this reaction is a reduction in the sulfate concentration, an increase in the pH due to the consumption of protons, and the production of alkalinity, while the sulfide produced can be used to precipitate heavy metals, thereby treating the sulfate, pH and metals. The sulfate reducing bacteria (SRB) require an organic electron donor. These substrates can be in the form of a simple compound such as hydrogen gas, or a complex combination of compounds, such as solid waste. In order to minimise costs, primary settled sewage sludge was chosen as the organic electron donor for the process. The sulfate reducing bacteria are not able to use the particulate organic matter, and this needs to be degraded anaerobically to simple soluble organic compounds.

2.1 OVERVIEW OF THE BIOLOGICAL REACTIONS IN AN ANAEROBIC SYSTEM

Within a high sulfate anaerobic system, utilizing insoluble primary sludge as a carbon source, the following reactions can be expected to occur:

- Colonization of the sludge particles by acid fermenting bacteria. The particles are hydrolysed by enzymes secreted by the bacteria. The carbohydrate fraction is broken down to sugars, the protein fraction to amino acids and the lipid portion to long chain fatty acids (LCFAs) and polyols such as glycerol.
- Acid fermentation (acidogenesis) of sugars and amino acids to hydrogen, carbon dioxide and short chain fatty acids (SCFAs).
- Beta-oxidation of the long chain fatty acids to yield acetate, propionate and hydrogen.
- Acetogenesis of propionate and other SCFAs to acetate, hydrogen and carbon dioxide.
- Methanogenesis using hydrogen and acetate as substrate
- Sulfate reduction utilizing hydrogen, acetate, propionate and potentially other intermediate SCFAs as substrates.
- Homoacetogenesis, i.e. the production of acetate from hydrogen and carbon dioxide.

A diagram showing the interacting flows of substrates between each biological process is shown in Figure 2.1.

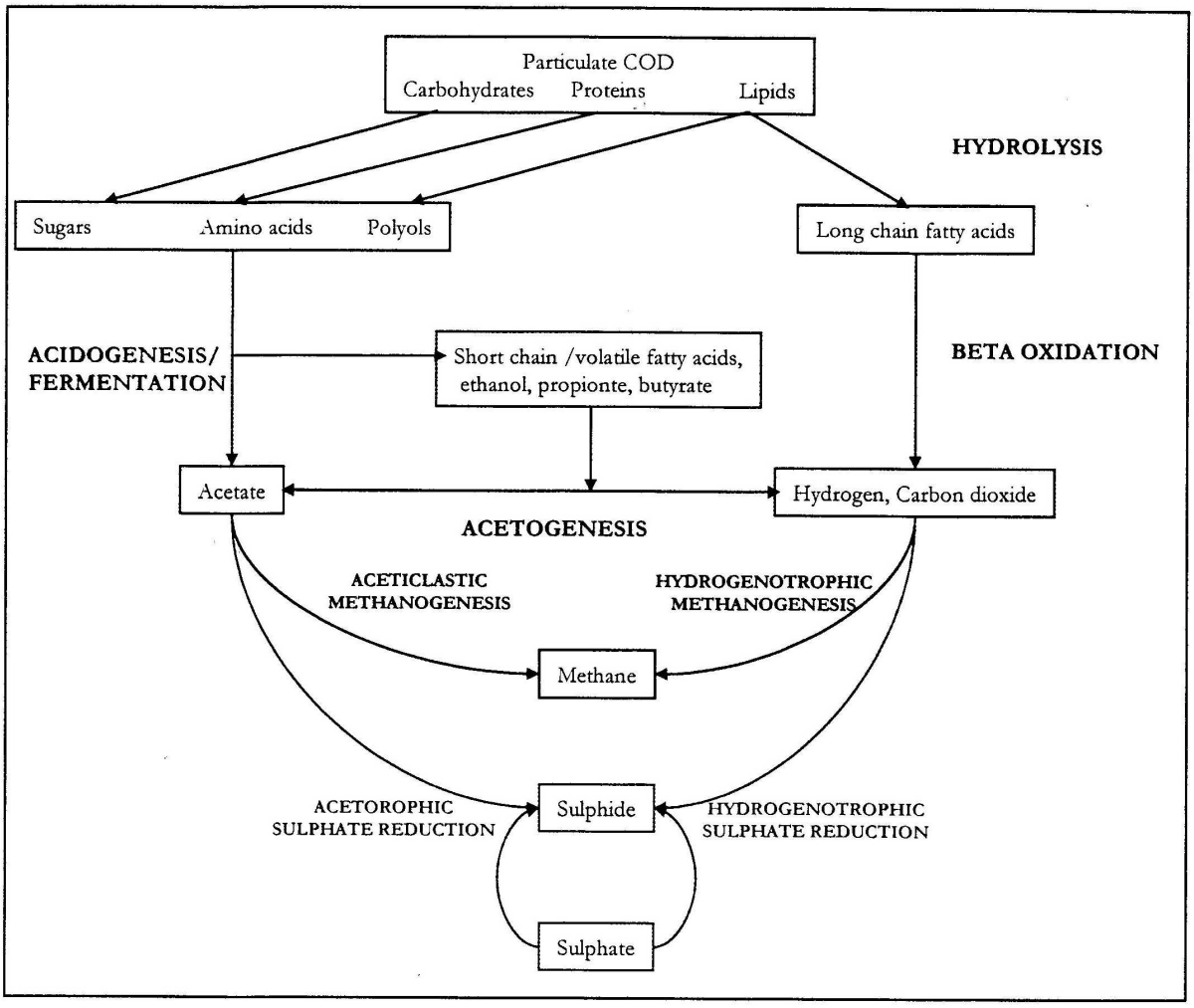

Figure 2.1: Microbial ecology and major substrate flows in an anaerobic system.

2.2 PRELIMINARY DISCUSSION OF KINETICS

Before reviewing the kinetic data and reaction stoichiometry of the various microbial processes involved in anaerobic digestion and sulfate reduction, it is convenient to provide an overview of the various mathematical expressions used to describe microbial biological kinetics. For reasons that will become apparent, the kinetic forms may be broken into two groups:

- the degradation of insoluble components described by first order kinetics
- Monod and related kinetics describing the uptake of soluble substrates.

2.2.1 FIRST ORDER KINETICS OF THE CATABOLISM OF INSOLUBLE SUBSTRATES

The breakdown of insoluble particles to soluble components represents the cumulative effects of a number of processes including: the colonization of the particles by bacteria, the mass transport of enzymes into the particles, and the degradation of a number of components at varying rates. This is usually most easily represented by an empirical first order expression of the form:

$$r_x = -kX \qquad [2.1]$$

where:

r_x = volumetric rate of reduction (mg l d^{-1})

k = first order rate constant (d^{-1})

X = mass concentration of insoluble compound (mg l^{-1})

In most cases a fraction of the substrate is resistant to breakdown. Equation 2.1 is modified to take this into account, giving:

$$r_x = -k(X - X_\infty) \qquad [2.2]$$

where X_∞ is the mass concentration of the nondegradable fraction (mg l^{-1}).

2.2.2 MONOD AND RELATED GROWTH KINETICS (SOLUBLE SUBSTRATES)

The volumetric net rate of biomass production r_{cells} (mg l d^{-1}) is usually determined from:

$$r_{cells} = (\mu - b)X_{cells} \qquad [2.3]$$

$$r_{cells} = \mu_{obs}X_{cells} \qquad [2.4]$$

where μ is the specific biomass growth rate (d^{-1}), b is the specific biomass loss rate due to cell death (d^{-1}), X_{cells} is the biomass concentration (mg l^{-1}) and μ_{obs} is the observed or net specific growth rate (d^{-1}). The volumetric rate of substrate utilization r_s (mg l d^{-1}) is given by:

$$r_s = -\frac{\mu X_{cells}}{Y} \qquad [2.5]$$

where Y is the biomass yield coefficient (mg cells / mg substrate).

The specific biomass growth rate (μ) is a function of the substrate concentration, and is potentially dependent on inhibitory or regulatory factors. Based on these considerations several expressions for determining μ have been proposed.

The most simple of these is to assume a constant value for μ, in which case equations 2.3 and 2.5 become first order expressions. In practice it is found that, while this is usually the case at high substrate concentrations, when the substrate concentration is low, deviation from first order is observed. This effect can be accounted for by the Monod model:

$$\mu = \frac{\mu_m [S]}{K_s + [S]} \qquad [2.6]$$

where μ_m is the maximum specific growth rate (d^{-1}), S is the soluble substrate concentration (mg l^{-1}) and K_s is the Monod half velocity constant (mg l^{-1}). K_s gives a measure of affinity for substrate and has the effect of providing a minimum substrate threshold below which substrate uptake is significantly reduced - a phenomenon which occurs in practice. Frequently, the specific rate of substrate utilization k (mg substrate mg $cells^{-1}$ d^{-1}) is reported instead of μ_m. The two are related by the expression:

$$k = \frac{\mu}{Y} \qquad [2.7]$$

In some instances two or more substrates may be limiting, in which case a multiple term Monod equation (Bailey and Ollis, 1986) is useful.

$$\mu = \mu_m \frac{S_1}{K_{s1} + S_1} \frac{S_2}{K_{s2} + S_2} \cdots \frac{S_n}{K_{sn} + S_n} \qquad [2.8]$$

A reduced growth rate may occur due to the presence of inhibitory compounds in the system. These could be substances present in the feed (e.g. heavy metals), substances produced by the

species under consideration (product inhibition), substances produced by a different, possibly competing, species or even high levels of substrate. Several models have been put forward to account for this. Non-competitive inhibition combines an inhibition factor with equation 2.6 giving:

$$\mu = \mu_m \frac{S_1}{K_s + S_1} \frac{K_I}{K_I + I} \qquad [2.9]$$

where K_I is the inhibition constant (mg l^{-1}) and I is the concentration of the inhibitory substance (mg l^{-1}). In the case of non-competitive inhibition K_I may be regarded as the concentration of the inhibitory compound which results in a 50% decrease in specific growth. A modified form of equation 2.9 has been proposed by Reis *et al.* (1990) and is given by:

$$\mu = \mu_m \frac{S_1}{K_s + S_1} \frac{1}{1 + (I / K_I)^n} \qquad [2.10]$$

Other inhibition models are uncompetitive inhibition:

$$\mu = \frac{\mu_m}{(1 + \frac{I}{K_I})(1 + \frac{K_m}{S})} \qquad [2.11]$$

and competitive inhibition:

$$\mu = \frac{\mu_m S}{K_s[1 + \frac{I}{K_I}] + S} \qquad [2.12]$$

where K_I and I have the same meaning. A better understanding of the effect the various inhibitory equations have on the specific growth rate, can be obtained from examining plots of μ/μ_m versus substrate concentration. Plots of this sort along with a plot of a standard Monod equation for comparison are given in Figure 2.2.

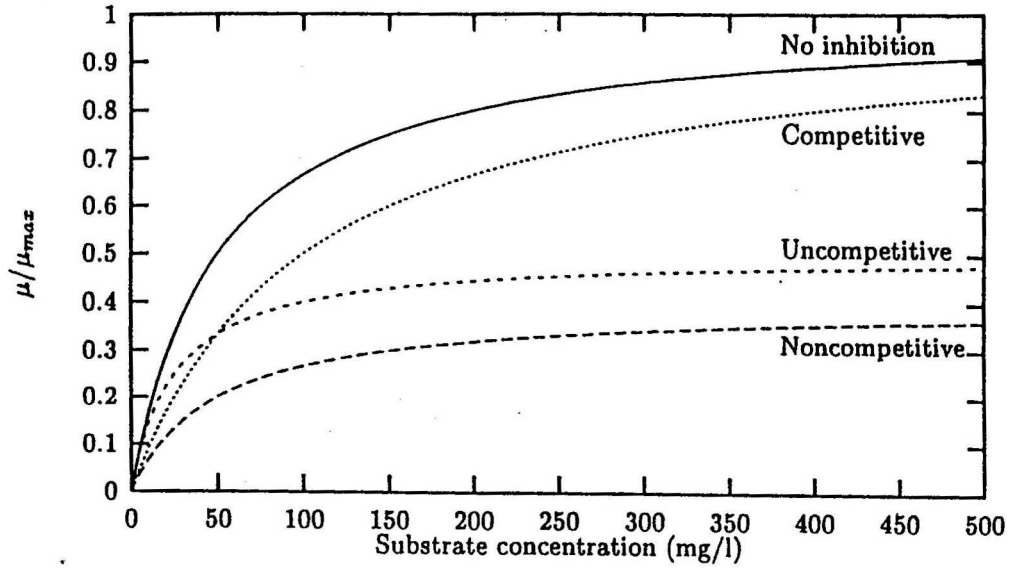

(a) $K_I = 100$

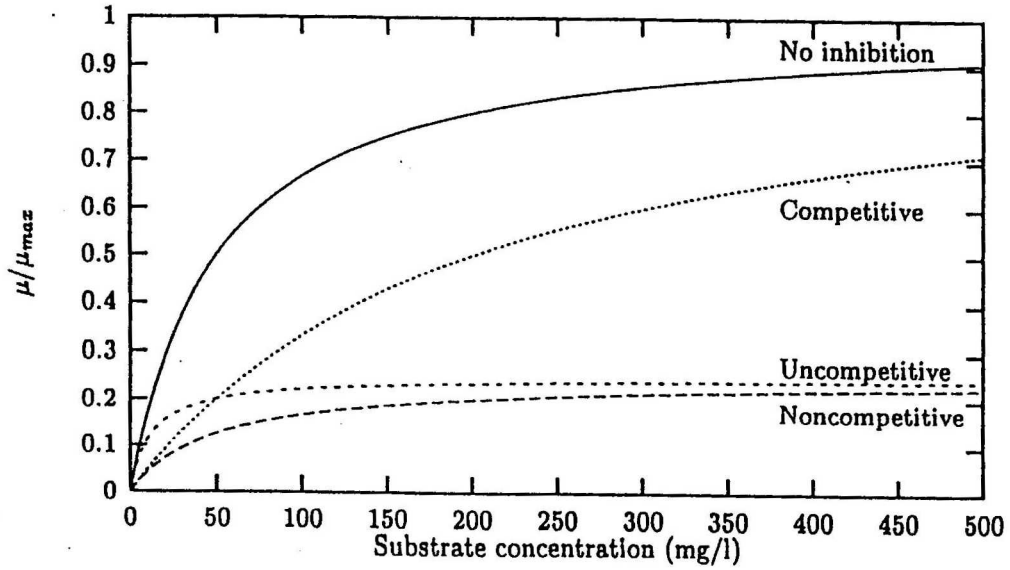

(b) $K_I = 50$

Figure 2.2: Illustrative plots of inhibition functions. $K_s = 50$, I = 150.

Three observations can be made. Firstly it is apparent that although all of the plots use the same values of K_I and K_S and the same concentration of I, the levels of inhibition are very different. A second point worth noting is that a lower K_I results in a greater degree of inhibition. The third point relates to the concentration ranges at which the inhibition functions have their greatest effect. Non-competitive inhibition exerts a constant inhibitory effect over the entire concentration span, uncompetitive inhibition results in greater inhibition at higher substrate concentrations, while the converse is true for competitive inhibition. This is illustrated in Figure 2.3 where a plot of $\mu_{inhibited}/\mu_{noninhibited}$ against substrate concentration for the three functions is given.

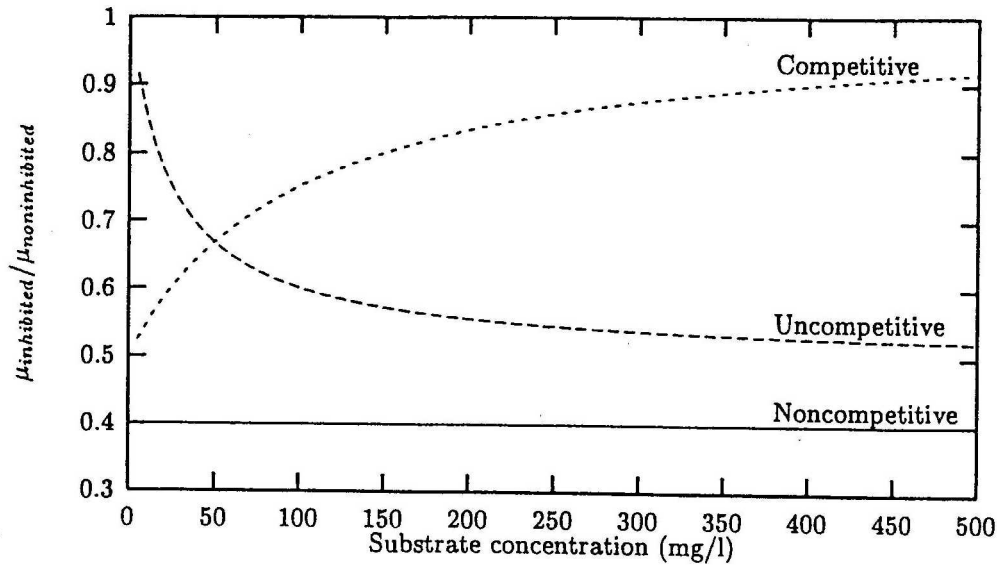

Figure 2.3 : Inhibition as a function of substrate concentration for various inhition functions. K_I = 100, K_s = 50, I = 150.

An alternative way of accounting for inhibition is to include an 'on/off' switching function as a factor of μ. A suitable expression is the sigmoidal function:

$$\xi_{SF} = = \frac{1}{1+e^{\alpha(C-\beta)}} \qquad [2.13]$$

where ξ_{SF} varies between 0 and 1; C is some reactor condition affecting the reaction rate; β is the value of this condition at $\mu = \frac{1}{2}\mu_m$; and α sets the steepness of the curve and whether the function is switched on or off. An example plot of Equation 2.13 is given in Figure 2.4.

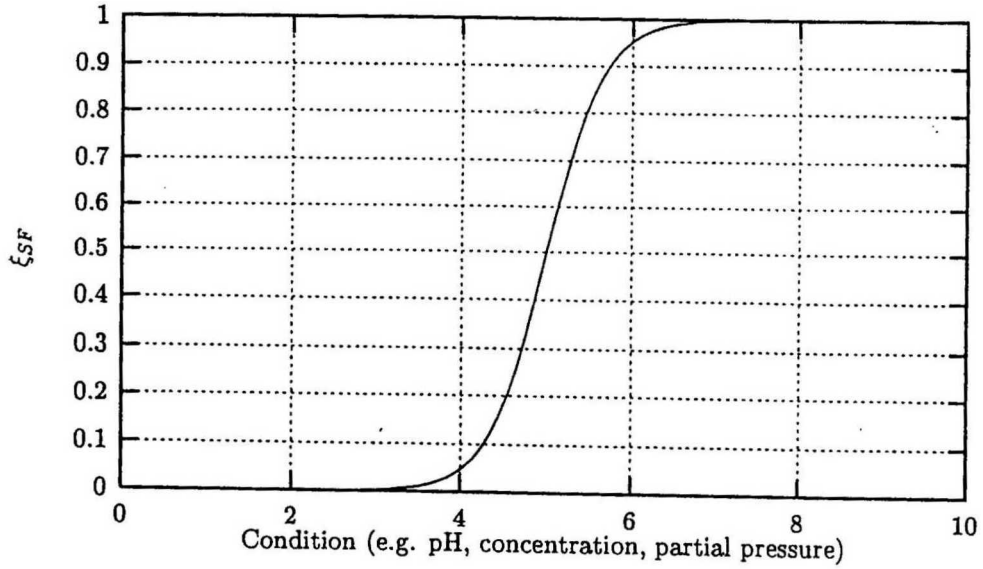

Figure 2.4 : Plot of $\xi_{SF} = = \frac{1}{1+e^{\alpha(C-\beta)}}$ with $\alpha = 3$, $\beta = 5$

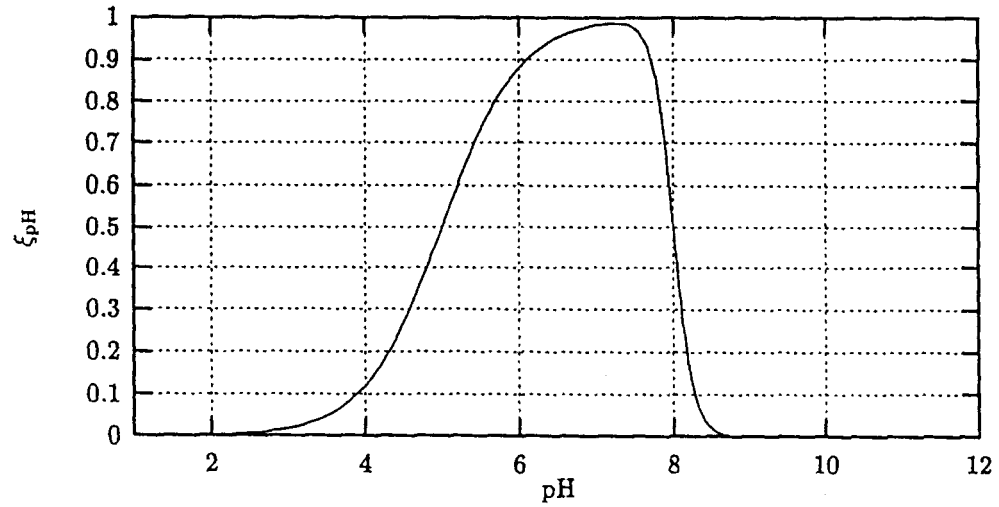

Figure 2.5: Illustrative plots of the pH switching function (Eqn 2.14) with $\alpha_{LL} = 2$, $\alpha_{UL} = 8$, $pH_{LL} = 5$, $pH_{UL} = 8$.

A particularly useful application of switching functions is to account for the inhibitory effects of pH. Most biological reactions occur only within a specific pH range- the reaction rate rapidly dropping to zero at too low or high pH values. The product of two switching functions provides an easy way to account for this, i.e.:

$$\xi_{pH} = (1+e^{-\alpha_{LL}(pH-pH_{LL})})^{-1} (1+e^{-\alpha_{UL}(pH-pHU_{L})})^{-1} \quad [2.14]$$

where ξ_{pH} takes on a value between 0 and 1; pH_{LL} and pH_{UL} are upper and lower pH limits, defined as the values at which $\mu = \frac{1}{2}\mu_m$ due to pH effects; and α_{LL} and α_{UL} are positive values

which effect the steepness of the curve. Higher α values result in a more rapid onset of inhibition.

An illustrative plot of Equation 2.14 is shown in Figure 2.5. Values of $\alpha_{LL} = 2$ and $\alpha_{UL} = 8$ are used resulting in a gradual onset of inhibition at the lower pH end but a more rapid onset at the upper values.

From the above it is apparent that the specific growth rate can be affected by a number of factors. It is convenient to express μ as a product of μ_m and several modifying factors, i.e.:

$$\mu = \mu_m \prod_i \xi_i \qquad [2.15]$$

where ξ_i are appropriate factors. A summary of ξ_i terms is given in Table 2.1.

Table 2.1: ξ factors modifying the specific biomass growth rate. Parameters are defined in the text.

Notation	Description	Form
ξ_{SU}	Substrate utilisation	$\frac{S}{K_S + S}$
ξ_{NI}	Non-competitive inhibition	$\frac{K_I}{K_I + 1}$
ξ_{NIn}	Non-competitive inhibition (variation)	$\frac{1}{1 + \left(\frac{I}{K_I}\right)^n}$
ξ_{UI}	Substrate utilisation with uncompetitive inhibition	$\frac{S}{K_S + S\left(1 + \frac{I}{K_I}\right)}$
ξ_{CI}	Substrate utilisation with competitive inhibition	$\frac{S}{S + K_S\left(1 + \frac{I}{K_I}\right)}$
ξ_{SF}	On/Off switching function	$\frac{1}{1 + e^{\alpha(C-\beta)}}$
ξ_{pH}	pH inhibition on/off switching function	$\left(1 + e^{\alpha_{LL}(pH-pH_{LL})}\right)^{-1} \times \left(1 + e^{\alpha_{UL}(pH-pH_{UL})}\right)^{-1}$

2.3 HYDROLYSIS OF INSOLUBLE SUBSTRATES

2.3.1 OVERVIEW

Primary sludge originates from the solid component of raw sewage settled prior to any biological treatment. The sludge consists mainly of insoluble lipids, proteins and carbohydrates. During hydrolysis, the exterior of the particles is colonized by acid forming bacteria. The bacteria secrete hydrolytic enzymes that are responsible for the extracellular hydrolysis of sludge. Specifically, the following reactions may be expected to occur:

- The hydrolysis of amide bonds of proteins to yield amino acids
- The hydrolysis of ester bonds of lipids to yield long chain fatty acids, glycerol (and other polyols) and alcohols.
- The hydrolysis of glycoside bonds of polysaccharides to yield dimeric and monomeric sugars.

With respect to the subsequent fermentation and anaerobic oxidation steps, the extracellular hydrolysis of sludge is rate limiting (Eastman and Ferguson, 1981). Consequently it is difficult to experimentally determine the rate of hydrolysis alone. For the reason the hydrolysis and acid fermentation steps are often modelled as a single step.

The composition of primary sludge as taken from several sources is shown in Table 2.2.

Table 2.2 : Composition of primary sludge as a percentage of dry matter. After Pavlostathis and Giraldo-Gomez (1991).

Component	O'Rouke (1968)	Eastman and Ferguson (1981)	Higgens *et al.* (1982)
Volatile solids	79.7	73.5	75
Lipids	18.6	21	10.3
Cellulose	18.2	19.9 [2]	32.2
Hemicellulose	-	-	2.5
Lignin	-	-	13.6
Crude protein	17.2	28.7	19
Volatile acids	3.5 [1]	5	6.4 [3]
Ash	20.3	26.5	25

[1]Expressed as acetic acid, [2]Measured as total carbohydrates, [3]Total free fatty acids

2.3.2 KINETICS OF HYDROLYSIS

The rate of hydrolysis has been shown to be dependent on a large number of factors. These include:

- Temperature. The rate of hydrolysis increases exponentially with an increase in temperature. (Gujer and Zehnder, 1983)

- pH. Near neutral conditions results in better hydrolysis than acid conditions. (Eastman and Ferguson, 1983)
- Microbial biomass and hence the level of hydrolytic enzymes.
- Particle geometry (surface area and size)
- The different rates of hydrolysis for the lipid, carbohydrate and protein fractions.
- The fact that the various components may be intimately bound.

The last two points are significant in that a slowly degrading component may shield an easily degraded component from enzymatic attack. In particular the lipid portion that degrades slowly may protect the protein and carbohydrate fractions.

Typically a first order function is used to model anaerobic sludge hydrolysis (Eastman and Ferguson, 1981; Lilley *et al*, 1990; Eliosov and Argaman, 1995; Shimizu *et al*., 1993), although other expressions such as the Contois equation have been used to describe hydrolysis in aerobic systems (Dold *et al*., 1980). The first order approach has been shown to fit experimental data extremely well. As Eastman and Ferguson (1981) have put it 'The first order hydrolysis function is an empirical expression that reflects the cumulative effects of all microscopic processes occurring in the digesters.'.

As discussed in section 2.2.1, the first order expression describing the rate of degradation of a component of the sludge r_x (mg l^{-1} d^{-1}) is given by a form of equation 2.2:

$$r_X = -k_h (X - X_\infty) \qquad [2.16]$$

$$= -k_h X_{deg} \qquad [2.17]$$

where k_h is the overall hydrolysis rate constant (d^{-1}), X is the total concentration of a sludge component, X_∞ is the concentration of the 'nondegradable' fraction and X_{deg} that of the degradable function. (All concentrations in mg l^{-1}). The rate of hydrolysis is hence a function of the degradable particulate matter remaining and not of the total particulate matter remaining. Failure to account for the nondegradable portion of the substrate will lead to erroneously reduced rates (Pavlostathis and Giraldo-Gomez, 1991).

The nondegradable portion reported by workers differs (Table 2.3). It is suggested that several factors influence the portion of the sludge that can be regarded as degradable. These are:

- pH
- Temperature

- Whether the sludge component is genuinely nondegradable or just very slowly degradable. For example some workers (e.g. Eastman and Ferguson, 1981) regard the lipid portion as nondegradable while others (e.g. O'Rourke, 1968) regard it as a slowly degradable component.
- Sludge composition. As mentioned this is a complicated by the fact that a nondegradable or slowly degradable component may protect a faster degrading component from hydrolysis.

Therefore, in any numerical comparison of the data of various workers, both the hydrolysis rate constant and the portion of the sludge reported as being nondegradable are required.

First order sludge hydrolysis kinetic data reported in the literature may broadly be divided into three categories:

- Rate data for the hydrolysis of sludge as a whole.
- Rate data for subportions (e.g. the lipid fraction) determined from the hydrolysis of sludge.
- Rate data for subportions but determined from artificial single component 'sludges'.

The last approach is not likely to be useful since the effect of sludge morphology is not taken into account. The second approach has advantage that more precise stoichiometric relationships linked to the rates of hydrolysis may formulate.

First order hydrolysis rate data for a number of different sludge types, as taken from a broad selection of the literature, are given in Table 2.3.

Table 2.3: First order rate constants of primary sludge hydrolysis. Taken in part from Gujer and Zehnder (1983) and Pavlostathis and Giraldo-Gomez (1991). Eperimental conditions are as follows: B Batch, C continuous and SC Semi-continuous.

Component	Conditions	pH	T °C	k d^{-1}	Degradable fraction	References
Overall sludge						
Primary sludge	B, C,SC		20	0.16 [1]	~0.34	Lilley *et al.* (1990)
Primary sludge	SC	5.13-6.67	35	3.00 [1]	~0.31	Eastmann and Ferguson (1981)
Primary sludge			33	0.32		Kaspar (1977)
Primary sludge			35	0.4 -1.2		Pavlostathis and Giraldo-Gomez (1991) using data from O'Rouke (1968)
Primary and waste activated sludge			25	0.077	0.8	Gujer and Zehnder (1983)using data from Pfeffer (1968)
Primary and waste activated sludge			35	0.15	0.8	Gujer and Zehnder (1983)using data from Pfeffer (1968)
Activated sludge				0.2– 0.6		Pavlostathis and Giraldo-Gomez (1991) using data from Ghosh(1981)
Activated sludge	C	7	37	0.16	0.65	Shimizu *et al.* (1993)
Solublized activated sludge	C	7	37	1.2	0.9	Shimizu *et al.* (1993)
Algae			20	0.11-0.32		Foree and McCarty (1969)
Sludge Protein						
	SC	5.13-6.67	35		0.5-0.57	Eastman and Ferguson (1981)
			15	0.01-0.03		Gujer and Zehnder (1983)using data from O'Rouke (1968)
			20	0.01-0.08		Gujer and Zehnder (1983)using data from O'Rouke (1968)
			25	0.01-0.09		Gujer and Zehnder (1983)using data from O'Rouke (1968)
			35	0.01-0.10		Gujer and Zehnder (1983)using data from O'Rouke (1968)
		5.14	35	0.28	0	Pavlostathis and Giraldo-Gomez (1991) using data from Eastman and Ferguson (1981)
		5.85	35	0.39	0	Pavlostathis and Giraldo-Gomez (1991) using data from Eastman and Ferguson (1981)
		6.67	35	0.69	0	Pavlostathis and Giraldo-Gomez (1991) using data from Eastman and Ferguson (1981)
			35	0.2-0.8		Pavlostathis and Giraldo-Gomez (1991) using data from O'Rouke (1968)
	C	7	37	1.3	0.95	Shimizu *et al.* (1993)
Sludge Carbohydrates						
	SC		35		0.64-0.7	Eastman and Ferguson (1981)
			15	0.03-0.10		Gujer and Zehnder (1983)using data from O'Rouke (1968)
			20	0.09-0.14		Gujer and Zehnder (1983)using data from O'Rouke (1968)
			25	0.16-0.29		Gujer and Zehnder (1983)using data from O'Rouke (1968)
			35	0.21-1.95		Gujer and Zehnder (1983)using data from O'Rouke (1968)
		5.14	35	0.3	0	Pavlostathis and Giraldo-Gomez (1991) using data from Eastman and Ferguson (1981)
		5.85	35	0.41	0	Pavlostathis and Giraldo-Gomez (1991) using data from Eastman and Ferguson (1981)
		6.67	35	0.58	0	Pavlostathis and Giraldo-Gomez (1991) using data from Eastman and Ferguson (1981)
			35	2.4-4.1		Pavlostathis and Giraldo-Gomez (1991) using data from O'Rouke (1968)
	C	7.0	37	0.52-1.2	0.9	Shimizu *et al.* (1993)
Sludge lipids						
	SC		35		0	Eastman and Ferguson (1981)
			15	0		Gujer and Zehnder (1983)using data from O'Rouke (1968)
			20	0-0.05		Gujer and Zehnder (1983)using data from O'Rouke (1968)
			25	0-0.09		Gujer and Zehnder (1983)using data from O'Rouke (1968)
			35	0.01-0.17		Gujer and Zehnder (1983)using data from O'Rouke (1968)
			35	0.3-0.7		Pavlostathis and Giraldo-Gomez (1991) using data from O'Rouke (1968)
	C	7.0	37	0.76	0.88	Shimizu *et al.* (1993)
Pure protein						
Casein				0.35		Nagase and Matsuo (1982)
Gelatin				0.60		Nagase and Matsuo (1982)
Zein				0.04		Greco *et al.* (1983)
Pure carbohydrates						
Cellulose	B		37	2.88		Stack and Cotta (1986)
Cellulose	C			1.18		Pavlostathis *et al.* (1988a,b)
Corn stover	SC		35	0.076 -0.18	0.8	Doyle *et al* (1983)

[1]Includes fermentation

2.3.3 STOICHIOMETRY OF HYDROLYSIS

The poorly defined nature of sludge makes it difficult to write definite stoichiometric relationships for its hydrolysis. Although broadly speaking, sludge consists of lipid, protein and carbohydrate fractions, within these fractions numerous different molecular species can be expected to occur. One solution to this problem is to use a pseudo (or real) molecule to represent the entire fraction. For example the protein fraction has been represented variously as $C_{16}H_{30}O_8N_4$ (Vasiliev *et al.*, 1993), $C_{39}H_{63}O_{13}N_{10}$ (Shimizu *et al.*, 1993) and $(C_4H_6O_2N)_n$ (Eastman and Ferguson, 1981). Since the ultimate products of protein hydrolysis are amino acids, a better generic formula for protein would be one built from an 'average' amino acid. An average of the twenty amino acids gives the formula as approximately $(C_5H_9O_3N)_n$. Protein hydrolysis is then represented by the reaction:

$$(C_5H_7O_2N)_n + nH_2O \rightarrow nC_5H_9O_3N \qquad [2.18]$$

In a similar manner $(C_6H_{10}O_5)_n$ (i.e. starch or cellulose) may be taken as the formula for the carbohydrate fraction, the hydrolysis of which would then be given by:

$$(C_6H_{10}O_5)_n + nH_2O \rightarrow nC_6H_{12}O_6 \qquad [2.19]$$

Since the lipid fraction consists mostly of triglycerides, a suitable generic triglyceride formula can be used. For example Eastman and Ferguson (1981) have used palmitic acid as the basis of the lipid fraction. McMurry (1992) gives palmitic acid, stearic acid, oleic acid and linoleic acid as being the most abundant naturally occurring fatty acids. Since molecular formulae of these compounds are reasonably similar, a triglyceride of one of these can be taken as being representative of the degradable lipid fraction. If palmitic acid is used, the stoichiometric reaction of lipid hydrolysis is:

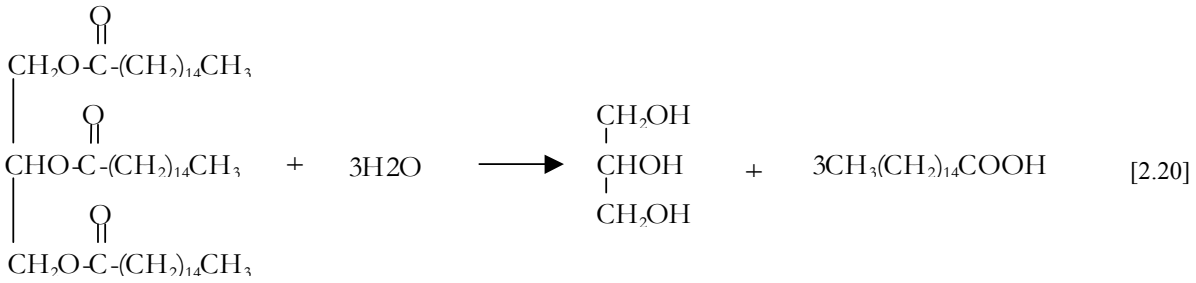

[2.20]

2.4 ACIDOGENESIS

The amino acids, sugars and polyols resulting from hydrolysis are broken down further by fermentation or acidogenesis. The main products of this are: hydrogen; carbon dioxide and the short chain fatty acids, lactate, butyrate, propionate and acetate. Other higher order acids such as valeric acid and caprionic acid are also produced to a lesser extent.

2.4.1 GLUCOSE FERMENTATION

Substrate Uptake and Hydrogen Inhibition and Product Regulation

Acid forming bacteria ferment glucose to produce a mixture of acetic, propionic, butyric and lactic acids. The respective stoichiometric reactions are:

$$C_6H_{12}O_6 + 2H_2O \rightarrow 2CH_3COOH + 2CO_2 + 4H_2 \quad [2.21]$$

$$C_6H_{12}O_6 + 2H_2 \rightarrow 2CH_3CH_2COOH + 2H_2O \quad [2.22]$$

$$C_6H_{12}O_6 \rightarrow 2CH_3CH_2CH_2COOH + 2CO_2 + 2H_2 \quad [2.23]$$

$$C_6H_{12}O_6 \rightarrow 2CH_3CHOHCOOH \quad [2.24]$$

The first reaction is favoured by the bacteria as it provides the largest energy yield (Mosey, 1983). The other reactions are said to occur as a response to elevated hydrogen concentrations. A convincing theory to account for this has been proposed by Mosey (1983) with modifications by Costello *et al* (1991). The essence of the theory is that the different cell pathways metabolizing the substrate are regulated by the relative concentrations of NADH and NAD^+. By assuming a constant internal cell pH of 7, and using the Nernst equation, Mosey was able to relate the ratio of the two concentrations to the hydrogen partial pressure. His equation is: $[NADH]/[NAD^+] = 1500P_{H2}$.

In Mosey's scheme an increase in hydrogen partial pressure shifts the fermentation reaction away from the production of acetic acid towards the production of butyric and propionic acids. In addition to this, elevated hydrogen levels result in a decreased rate of glucose uptake. The rate of glucose uptake for energy production only, R_{GL} ($mg1^{-1}d^{-1}$) is given by a non-competitive inhibition model:

$$R_{Gl} = -\frac{kXS}{K_S + S}\frac{1}{1+\frac{[NADH]}{[NAD^+]}} \quad [2.25]$$

$$= -\frac{kXS}{K_S + S}\frac{1}{1+1500P_{H_2}} \quad [2.26]$$

$$= -\frac{kXS}{K_S + S}\frac{K_{I,H_2}}{K_{I,H_2} + P_{H_2}} \quad [2.27]$$

where the symbols have the definitions as given in Section 2.2.2. The rate constant k is used rather than the standard μ due to the varying biomass yield. This is explained in more detail below. The reported values of the kinetic constants are k=268mg glucose . (mg biomass)$^{-1}$. d^{-1}, K_S = 23mg glucose^{-1} and b = 0.02d^{-1}.

The rates of acid production are given as functions of the glucose uptake rate, and of the NADH/NAD$^+$ ratio or hydrogen partial pressure (in atm):

$$r_{AcH} = \frac{2R_{Gl}}{\left(1+\frac{[NADH]}{[NAD^+]}\right)^2\left(1+\frac{[NAD^+]}{[NADH]}\right)} - \frac{2R_{Gl}}{\left(1+\frac{[NADH]}{[NAD^+]}\right)^2} \quad [2.28]$$

$$= \frac{2R_{Gl}}{\left(1+\frac{P_{H_2}}{K_{I,H_2}}\right)^2\left(1+\frac{K_{I,H_2}}{P_{H_2}}\right)} - \frac{2R_{Gl}}{\left(1+\frac{P_{H_2}}{K_{I,H_2}}\right)^2} \quad [2.29]$$

$$r_{PrH} = \frac{-2R_{Gl}}{\left(1+\frac{[NADH]}{[NAD^+]}\right)\left(1+\frac{[NAD^+]}{[NADH]}\right)} \quad [2.30]$$

$$= \frac{-2R_{Gl}}{\left(1+\frac{P_{H_2}}{K_{I,H_2}}\right)\left(1+\frac{K_{I,H_2}}{P_{H_2}}\right)} \quad [2.31]$$

$$r_{BuH} = \frac{-2R_{Gl}}{\left(1+\frac{[NADH]}{[NAD^+]}\right)^2\left(1+\frac{[NAD^+]}{[NADH]}\right)} \quad [2.32]$$

$$= \frac{-2R_{Gl}}{\left(1+\frac{P_{H_2}}{K_{I,H_2}}\right)^2\left(1+\frac{K_{I,H_2}}{P_{H_2}}\right)} \quad [2.33]$$

In all equations the inhibition constant $K_{I,H2}$ is equal to 1500^{-1} atm^{-1}. Alternatively the temperature dependency of this constant can be calculated from the following expression derived by Costello *et al*:

$$\log_{10}\left(K_{I,H_2}\right) = \frac{1139}{T} - 7 \qquad [2.34]$$

where T is the temperature in Kelvin.

The scheme of Costello *et al* differs in that they assume that acetic acid, butyric acid and lactic acid (and not propionic acid) are the three products of glucose fermentation. They also assume that a second group of bacteria is responsible for the further breakdown of lactic acid to either acetic acid (under low hydrogen conditions) or propionic acid (under high hydrogen conditions). Analyzing the metabolic pathways and relating the $NADH/NAD^+$ ratio to the hydrogen partial pressure in the same manner as Mosey, they obtain the same expression for glucose uptake (equation 2.27) and the following expressions for the production of volatile fatty acids:

$$r_{AcH} = \frac{-2R_{Gl}}{\left(1 + \frac{P_{H_2}}{K_{I,H_2}}\right)^2} \qquad [2.35]$$

$$r_{BuH} = \frac{-R_{Gl}\frac{P_{H_2}}{K_{I,H_2}}}{\left(1 + \frac{P_{H_2}}{K_{I,H_2}}\right)^2} \qquad [2.36]$$

$$r_{LsH} = \frac{-2R_{Gl}\frac{P_{H_2}}{K_{I,H_2}}}{\left(1 + \frac{P_{H_2}}{K_{I,H_2}}\right)} \qquad [2.37]$$

Substrate Uptake without Hydrogen Regulation

Alternatively, if the hydrogen partial pressure remains low, normal Monod kinetics can be used to describe glucose fermentation. Zoetemeyer *et al* (1982a) report $\mu_{max} = 7.9d^{-1}$ and Y = 0.134 giving k = 59mg glucose . (mg biomass)$^{-1}$. d^{-1}; and Moletta *et al* (1986) give $\mu_{max} = 1.5\ d^{-1}$ and Y = 0.82 giving k = 1.8 mg glucose . (mg biomass)$^{-1}$. d^{-1}.

Acid Production Inhibition

A further refinement to the kinetics of the acidogenesis of glucose is the inclusion of the inhibitory effects of the acids produced. The proposed mechanism assumes that only the undissociated acids are freely permeable to the cell membrane (Zoetemeyer *et al*, 1982b). Once inside the cell, the acids lower the pH and disrupt cell functioning. Since energy is required to expel the acids, a lower growth rate results.

Costello *et al* found that a non-competitive model described the effects of product inhibition in acidogenesis. Equation 2.27 should then be modified to:

$$R_{Gl} = -\frac{kXS}{K_S + S}\frac{K_{I,VFA}}{K_{I,VFA} + I_{VFA}}\frac{K_{I,H_2}}{K_{I,H_2} + P_{H_2}} \qquad [2.38]$$

where I_{VFA} is the total concentration of all undissociated short chain fatty acids and K_{IVFA} is the inhibition constant (in molar rather than the usual mass units). It is assumed here that a single expression may be used to account for the effect of all volatile acids, since the dissociation constants for the acids are similar. A value of $K_{I,Gf,vfa}$ = 10 mmol/l is reported by Costello *et al*.

Using the notation introduced earlier, equation 2.38 can be shortened to:

$$R_{Gl} = \xi_{SU,Gl} \cdot \xi_{NC,VFA} \cdot \xi_{NC,H_2} \qquad [2.39]$$

pH Inhibition

Zoetemeyer *et al* (1982a) measured the maximum specific growth rate of acidogenic bacteria fed glucose over a pH range of 4.5 to 7.9. They found that the optimal pH was around 6.0 with the maximum specific growth rate rapidly decreasing to 50% at pH 5 and gradually decreasing to 25% at pH 8.0. Hilton and Oleszkiewicz (1988) report a similar trend over a pH range of 6.0 to 8.0 for the utilization of lactose (a galactose-glucose disaccharide). Based on the data of Zoetemeyer *et al*, the parameters for the pH inhibition function, as defined in equation 2.14, are estimated as α_{LL} = 4, α_{UL} = 0.5, pH_{LL} = 5 and pH_{UL} = 10.5. A plot of this function is given in Figure 2.6 and shows a reasonable approximation to that given by Zoetemeyer *et al*. Equation 2.39 is then further modified to include pH inhibition to give:

$$R_{Gl} = \xi_{SU,Gl} \cdot \xi_{NC,VFA} \cdot \xi_{NC,H_2} \cdot \xi_{pH} \qquad [2.40]$$

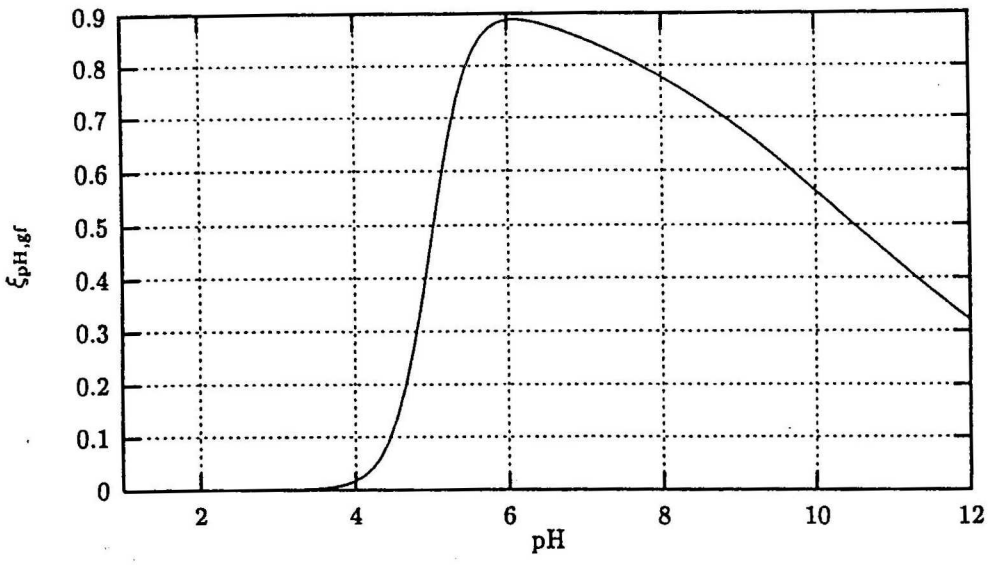

Figure 2.6: Plot of pH inhibition of glucose fermentation based on data from Zoetenmeyer *et al.* (1982a). $\alpha_{LL} = 4$, $\alpha_{UL} = 0.5$, $pH_{LL} = 5$, $pH_{UL} = 10.5$.

Hydrogen Sulfide Inhibition

Hilton and Oleszkiewicz (1988) examined the effect of sulfide concentration on lactose uptake over a pH range of 6.0 to 8.0. They concluded that unionized H_2S was inhibitory but did not report inhibition constants. They also found that the optimal pH shifted to around 7.0 in the presence of sulfide. This is due to the lower fraction of unionized H_2S at this pH. Hence in modelling a high sulfate reducing system, the effect of sulfide concentration on sugar uptake needs to be included. A term for sulfide inhibition should be incorporated into Equation 2.40.

Cell Synthesis

Due to the different amounts of energy produced in each pathway the biomass yield will vary. Using the scheme of Costello *et al*, the overall rate of biomass production of glucose fermenters can be calculated from:

$$r_{gF} = Y'_{AcH} \cdot r_{AcH} + Y'_{BuH} \cdot r_{BuH} + Y'_{LaH} \cdot r_{LaH} \qquad [2.41]$$

Mosey (1983) and Costello *et al* (1991) estimated the yield coefficients Y_i^1 from a rule of thumb that states that approximately 10g of biomass are produced for each mole of ATP generated (Bauchop and Elsden, 1960). The respective yields given by these workers for reactions 2.21 to 2.24 are four, three, two and two ATP molecules per molecule of glucose consumed. These

values correspond to product based yields of Y^1_{ACH}=0.33, Y^1_{PrH}=0.13, Y^1_{BuH}=0.34 and Y^1_{LaH}=0.11.

Assuming a cell formula of $C_5H_7O_2N$, the reaction describing the production of biomass from glucose is:

$$5C_6H_{12}O_6 + 6NH_3 \rightarrow 6C_5H_7O_2N + 18H_2O \quad [2.42]$$

2.4.2 LACTIC ACID FERMENTATION

Substrate Uptake and Hydrogen Inhibition and Regulation

Lactic acid has been shown to be a major intermediate in anaerobic digestion (Zeller *et al*, 1994). In the model of Costello *et al*, lactic acid produced by glucose fermentation is broken down to different ratios of acetic and propionic acids depending on the hydrogen partial pressure. The reactions given are:

$$CH_3CHOHCOOH + H_2 \rightarrow CH_3CH_2COOH + H_2O \quad [2.43]$$

$$CH_3CHOHCOOH + H_2O \rightarrow CH_3COOH + CO_2 + 2H_2 \quad [2.44]$$

Using a similar argument to that applied to glucose fermentation, the hydrogen regulated kinetics of lactate uptake (for energy production only) and acetic and propionic acid were derived:

$$R_{LaH} = -\frac{kXS}{K_S + S_{LaH}} \frac{1}{1 + \frac{P_{H_2}}{K_{I,H_2}}} \quad [2.45]$$

$$r_{PrH} = -\frac{\frac{R_{LaH} P_{H_2}}{K_{I,H_2}}}{1 + \frac{P_{H_2}}{K_{I,H_2}}} \quad [2.46]$$

$$r_{AcH} = -\frac{R_{LaH}}{1 + \frac{P_{H_2}}{K_{I,H_2}}} \quad [2.47]$$

The kinetic constants used in the model were k=46 mg glucose . (mg biomass)$^{-1}$. d^{-1}, K_S = 34 mg^{-1} and b = 0.02 d^{-1}. As before, the inhibition constant $K_{I,H2}$ is calculated using Equation 2.34.

Substrate Uptake without Hydrogen Regulation

If hydrogen levels can be assumed to be low, the Monod equation on its own can be used. Zeller *et al* (1994) give Monod kinetic parameters of μ_{max} = 16.8d^{-1} and K_S=225 mg/l for *Clostridium propionicum* growing on lactate.

Acid Production Inhibition

As with glucose fermentation, lactate acidogenesis is inhibited by undissociated fatty acids. As before, a non-competitive model has been used (Costello *et al*, 1991a,b). Equation 2.45 should therefore be multiplied by a suitable factor ($\xi_{NC,VFA}$). Costello *et al* used a value of $K_{I,VFA}$ = 10 mmole/l.

pH Inhibition

Costello *et al.* assume that since the lactate acidogenic bacteria are in close symbiosis with the glucose acidogens, the optimal pH ranges must be similar. Based on this assumption, the pH inhibition parameters estimated for glucose fermenters may be used to calculate ξ_{pH} for lactate fermenters.

Hydrogen Sulfide Inhibition

No specific mention of hydrogen sulfide inhibition of lactate fermenting bacteria has been found in the literature. However, based on the fact that sulfide has been shown to be inhibitory to almost all of the other microbial processes occurring in an anaerobic system, it is reasonable to assume that lactate fermenters will be similarly affected. A suitable inhibition term should hence be included when calculating the uptake rate of lactate.

Cell Synthesis

Based on ATP yields of 0.5 and 1.0 mole per mole lactate consumed for reactions 2.43 and 2.44 respectively (Costello *et al*, 1991a), the biomass product based yields are estimated as Y^1_{PrH} = 0.067 and Y^1_{AcH} = 0.17. The biomass synthesis reaction is:

$$5CH_3CHOHCOOH + NH_3 \rightarrow 3C_5H_7O_2N + 9H_2O \qquad [2.48]$$

Amino Acid Fermentation

Assuming that the formula $C_5H_9O_3N$ is a valid approximation for the average of all amino acids produced in hydrolysis, the reactions for the production of the four principle fatty acids are:

$$C_5H_9O_3N + 3H_2O \rightarrow 3CH_3COOH + CO_2 + 2H_2 + NH_3 \quad [2.49]$$

$$C_5H_9O_3N + 3H_2O \rightarrow CH_3CH_2COOH + 2CO_2 + 3H_2 + NH_3 \quad [2.50]$$

$$C_5H_9O_3N + H_2O \rightarrow CH_3CH_2CH_2COOH + CO_2 + NH_3 \quad [2.51]$$

$$C_5H_9O_3N + 4H_2O \rightarrow CH_3CHOHCOOH + 2CO_2 + 4H_2 + NH_3 \quad [2.52]$$

No data for the kinetics of amino acid acetogenesis are available in the literature. In the absence of any useful data, a rate similar to that of glucose fermentation can be tentatively assumed. Alternatively, since protein hydrolysis has been shown to be rate limiting in the conversion of protein to acids, a rate constant at least one order of magnitude greater than that for hydrolysis could be assumed.

Of the four reactions given above, only reaction 2.51 does not result in the production of hydrogen. Therefore, it could be assumed that a shift to butyrate production would result from an increase in hydrogen partial pressure. However, in the absence of any evidence, it is simpler to assume a fixed ratio of acid production. In the study of Eastman and Ferguson (1981) on the hydrolysis and acidogenesis of primary sludge, it was found that the production of acetic and propionic acids were roughly equal (on a COD basis). Although their work dealt with a mixture on carbohydrate and nitrogenous material, it is assumed here that this ratio will also be valid for the acidogenesis of amino acids alone.

The relevant biomass synthesis equation is:

$$C_5H_9O_3N \rightarrow C_5H_7O_2N + H_2O \quad [2.54]$$

A yield of 0.48g cell COD/g COD utilized is assumed (Eastman and Ferguson, 1981). Based on a cell COD of 1.41 and a generic amino acid COD of 1.22, this corresponds to Y = 0.55.

2.4.3 GLYCEROL FERMENTATION

For the sake of completeness, the fermentation of the small amount of glycerol generated by lipid hydrolysis needs to be accounted for. Since no data exist, the rate and yield are assumed to be the same as for glucose. The acidogenesis and cell synthesis reactions are (assuming for the sake of simplicity that acetic acid is the sole product):

$$CH_2OHCHOHCH_2OH + H_2O \rightarrow CH_3COOH + 3H_2 + CO_2 \quad [2.54]$$

$$2CH_2OHCHOHCH_2OH + NH_3 \rightarrow C_5H_7O_2N + CO_2 + 2H_2O + 4H_2 \quad [2.55]$$

2.5 BETA OXIDATION OF LONG CHAIN FATTY ACIDS

According to Knoop's Theory (Sawyer and McCarty, 1989) the breakdown of long chain fatty acids occurs by oxidation of the beta carbon atom, resulting in the formation of acetic acid and hydrogen. The process is repeated and the fatty acid is shortened by two carbon atoms in each step. If the molecule has an even number of carbon atoms only acetic acid results. An odd numbered molecule will result in the formation of both acetic and propionic acids (McInery and Bryant, 1981). The general stoichiometry for beta-oxidation as given by Gujer and Zehnder (1983) is:

$$(-CH_2-CH_2-) + 2H_2O \rightarrow CH_3COOH + 2H_2 \quad [2.56]$$

For the specific case of palmitic acid the overall reaction is:

$$CH_3(CH_2)_{14}COOH + 14H_2O \rightarrow 8CH_3COOH + 14H_2 \quad [2.57]$$

Monod kinetic parameters for the breakdown of a number of LCFAs, as calculated by Gujer and Zehnder (1983), based on the data of Novak and Carlson (1970), are given in Table 2.4.

Table 2.4 : Monod kinetic parameters for long chain fatty acid beta oxidation at 37°C. Values from Gujer and Zehnder based on data from Novak and Carlson (1970). Yields and decay rates averaged for all experiments. Yield values may contain methanogenic biomass.

Fatty acid	μ_{max} d^{-1}	Y mg biomass/ Mg fatty acid	K_s Mg acid/L	b d^{-1}
Stearic	0.10	~0.3	143	~0.01
Palmitic	0.12	~0.3	49.8	~0.01
Myristic	0.11	~0.3	37.5	~0.01
Oleic	0.45	~0.3	1116	~0.01
Linoleic	0.56	~0.3	637	~0.01

The large amount of hydrogen generated by beta-oxidation has been shown to be inhibitory (Novak and Carlson, 1970). A non-competitive model has been shown to describe the behaviour of hydrogen inhibition of acetogenesis (see below). Since beta-oxidation of LCFAs is closely related to acetogenesis of SCFAs, it is hypothesized that a non-competitive model is also valid here. It is further assumed that the internal cell mechanisms are similar enough to allow the calculation of the inhibition constant from Equation 2.34.

If palmitic acid is taken as representative of all the LCFA present, the relevant cell synthesis reaction is:

$$5CH_3(CH_2)_{14}COOH + 16NH_3 + 22H_2O \rightarrow 16C_5H_7O_2N + 75H_2 \quad [2.58]$$

2.6 ACETOGENESIS

2.6.1 BASIC KINETICS AND STOICHIOMETRY

The process by which intermediate short chain fatty acids are degraded to acetate and hydrogen is termed acetogenesis. A number of bacteria capable of degrading butyrate and higher fatty acids have been identified (e.g. *Syntrophomonas wolfei* and *Syntrophomonas sapovorans*), however, to date only one acetogenic species capable of degrading propionate (and only propionate) has been identified, *Syntrophobacter wolinii* (McCarty and Mosey, 1991). Hence, for the purpose of modelling acetogenesis these two groups should be kept separate.

Propionate as Substrate

The reactions describing the anaerobic oxidation of propionate (McCarty and Mosey, 1991) and the production of biomass are:

$$CH_3CH_2COOH + 2H_2O \rightarrow CH_3COOH + CO_2 + 3H_2 \quad [2.59]$$

$$5CH_3CH_2COOH + NH_3 \rightarrow 3C_5H_7O_2N + 4H_2O + 5H_2 \quad [2.60]$$

A summary of Monod kinetic constants for propionate oxidation, compiled from a literature survey, is given in Table 2.5.

Butyrate and Higher Fatty Acids as Substrate

Butyrate oxidation and biomass production are represented by:

$$CH_3CH_2CH_2COOH + 2H_2O \rightarrow 2CH_3COOH + 2H_2 \quad [2.61]$$

$$5CH_3CH_2CH_2COOH + 4NH_3 \rightarrow 4C_5H_7O_2N + 2H_2O + 10H_2 \quad [2.62]$$

Kinetic constants for the anaerobic oxidation of butyrate, as taken from the literature, are given in Table 2.6.

Table 2.5 : Monod kinetic parameters for propionate utilizing acetogens. Adapted from Pavlostathis and Giraldo-Gomez (1991) and Oude Elferink *et al.* (1994).

Reference	Culture	T °C	Y mg biomass/mg propionate	μ_{max} d^{-1}	K_S mg PrH/l	$K_{I,H2S}$ mg H_2S/l	b d^{-1}
Lawrence and McCarty (1969)	Propionic acid utilisation	25	0.077 [1]	0.36	40		0.04
Lawrence and McCarty (1969)	Propionic acid utilisation	35	0.064 [1]	0.31	758		0.01
Heyes annd Hall (1983)	Propionic acid utilisation	35		0.13-1.2	11-331		
Maillacheruvu and Parkin (1996)	Propionic acid utilisation		0.063	0.15 [2]	17.9	26.6 [3]	0.021
Mosey (1983)	Propionic acid utilisation		0.13 [4]				
Dörner (1992); Boone and Bryant (1980)	*Syntrophobacter wolinii*			0.02-0.21			
Stams *et al.* (1993)	Strain MPOB			0.15-0.17			
Dörner (1992)	Strain KoPropl			0.07			
Wu *et al.* (1992)	Culture PT			0.01			
Wu *et al.* (1992)	Culture PW			0.14			

[1]Includes biomass formed in methanogenesis, [2]Reported as k, [3]Uncompetitive Inhibition, [4]Based on ATP yield

Table 2.6 : Monod kinetic parameters butyrate utilisation acetogens. Adapted from Pavlostathis and Giraldo-Gomez (1991) and Oude Elferink *et al.* (1994)

References	Culture	T °C	Y mg biomass/ mg butyrate	μ_{max} d^{-1}	K_S mg BuH/l	b d^{-1}
Lawrence and McCarty (1969)	Butyrate acid utilisation	35	0.085 [1]	0.37	7.2	0.027
Massey and Pohland (1978)	Butyrate acid utilisation	37		0.86	164	
Mosey (1983)	Butyrate acid utilisation		0.13 [2]			
Wu *et al.* (1992); Stieb and Schink (1985); Zhao *et al.* (1990)	*Syntrophospora (Clostridium) bryantii BH*			0.252		
Roy *et al.* (1986)	*Syntrophomonas sapovorans*			0.6		
McInerney *et al.* (1981); McInerney *et al.* (1979); Dörner (1992)	*Syntrophomonas wolfei*			0.19-0.31		
Zhao *et al* (1993)	*Syntrophomonas strain FSM2*			0.32		
Zhao *et al* (1993)	*Syntrophomonas FSS7*			0.34		
Zhao *et al* (1993)	Syntrophomonas FM4			0.24		

[1] Includes biomass formed in methanogenesis. [2] Based on ATP yield

2.6.2 INHIBITION KINETICS

Hydrogen Inhibition

Both the oxidation and biomass synthesis reactions result in the production of hydrogen. The oxidation reactions are thermodynamically unfavourable and can only proceed if accompanied by efficient hydrogen removal (Mosey, 1983, Pavlostathis and Giraldo-Gomez, 1991). Using the same reasoning as applied to the metabolism of glucose, Mosey determined that hydrogen regulation of propionate and butyrate uptake could be accounted for by a non-competitive inhibition model. As before the inhibition constants are calculated from Equation 2.34.

Fatty Acid Inhibition

As with acidogenic bacteria, high unionized fatty acid levels have been shown to be inhibitory to acetogens (Denac, 1986). Costello *et al* (1991), based on the results of Denac, used a competitive inhibition model to account for this, reporting inhibition constants of 3.0 and 30.0 mmole/l for propionate and butyrate utilizing acetogens respectively.

pH Inhibition

To date, no specific studies have been conducted to determine the optimal pH range for acetogenic bacteria. Costello *et al* have argued that, in a two stage digester with the stages operated at pH 6 and pH 7 respectively, due to the high hydrogen partial pressure in the first stage, acetogenic bacteria are more likely to predominate in the second methanogenic stage. They therefore assume that selection pressure would favour acetogenic bacteria with the same optimal pH range as methanogenic bacteria. While their argument is not complete, in the absence of any better data, the same pH inhibition function as that for methanogenesis (see below) can be assumed.

Hydrogen Sulfide Inhibition

Maillacheruvu and Parkin (1996) found that an uncompetitive inhibition model best described the inhibition of propionate oxidation due to unionized hydrogen sulfide. The reported inhibition constant is 26.6 mg H_2S/l. No sulfide inhibition constants for butyrate and h higher fatty acid utilizing acetogens are to be found in the literature.

2.7 HOMOACETOGENESIS

Homoacetogenesis refers to the production of acetic acid from carbon dioxide and hydrogen. The reaction given by McCarty and Mosey (1991) is:

$$4H_2 + 2CO_2 \rightarrow CH_3COOH + 2H_2O \qquad [2.63]$$

A suitable biomass synthesis reaction is:

$$5CO_2 + NH_3 + 10\ H_2 \rightarrow C_5H_7O_2N + 5H_2O \qquad [2.64]$$

No rate data for homoacetogenesis are to be found in the literature. According to Nozhevnikova and Kotsuyrbenko (1995), homoacetogenesis is only significant in relation to hydrogen consuming methanogenesis at temperatures below 20°C.

2.8 METHANOGENESIS

2.8.1 BASIC KINETICS AND STOICHIOMETRY

In an anaerobic system, the ultimate sink for carbon is methane. Although a number of species are methanogenic, only acetic acid or carbon dioxide and hydrogen can be utilized as substrates.

Hydrogen/Carbon Dioxide as Substrate

Methanogenesis, utilizing H_2 and CO_2, can be represented by the reaction:

$$4H_2 + CO_2 \rightarrow CH_4 + 2H_2O \qquad [2.63]$$

Autotrophic cell synthesis can be represented by:

$$5CO_2 + 10H_2 + NH_3 \rightarrow C_5H_7O_2N + 8H_2O \qquad [2.64]$$

A large amount of kinetic data, describing methanogenesis using hydrogen and carbon dioxide as substrates, is present in the literature. A summary of Monod kinetic parameters as taken from a number of sources is given in Table 2.7. The values have been converted to a common unit basis. For some bases, some assumptions have had to be made for this to be possible. These are recorded in the footnotes.

Acetate as Substrate

The overall reaction, for the biological production of methane from acetate, is given by:

$$CH_3COOH \rightarrow CH_4 + CO_2 \qquad [2.65]$$

Biomass synthesis can be described by:

$$5CH_3COOH + 2NH_3 \rightarrow 2C_5H_7O_2N + 6H_2O \quad [2.66]$$

As with hydrogen utilizing methanogenesis, a large amount of kinetic data can be found in the literature. This is summarized in Table 2.8.

Table 2.7 : Monod kinetic parameters for methanogenesis using hydrogen as substrate. Adapted from Oude Elferink *et al.* (1994), Pavlostathis and Giraldo-Gomez (1991) and Harper and Pohland (1986).

Reference	Culture	Conditions	T °C	Y mg biomass/ mg Hydrogen	μ_{max} d^{-1}	K_S µg H_2/l	$K_{I,H2S}$ mg H_2S/l	b d^{-1}
Robinson and Tiedje (1984)	*Methanospirillum hungatei* JF-1	Batch	37	0.16 – 0.24 [1]	1.24 – 1.29	11.7 – 14.7		
Wu *et al.* (1984)	*Methanospirillum hungatei* BD				2.4 – 2.8			
Robinson and Tiedje (1984)	Mean of several species				1.3	13		
Hungate (1967)	Rumen bacteria		37		5.4	0.03		
Robinson and Tiedje (1982)	Digesting sludge					0.03		
Kaspar and Wuhrmann (1978)	Digesting sludge					166 [4]		
Kristjansson *et al.* (1982)	*Methanobrevibacter arboriphilus* AZ	Continuous	35			12.1		
Zehnder and Wuhrmann (1977)	*Methanobrevibacter arboriphilus* AZ			0.3 –0.35	1.4 – 3.4			
Zeikus and Henning (1975)	*Methanobrevibacter arboriphilus* DH1			0.5 – 0.6				
Pavlotathis *et al.* (1990)	*Methanobrevibacte smithii*		37	0.36	4.02	2.3		
Archer and Powell (1985)	*Methanobrevibacte smithii*		37		4.07			
Maillacheruvu and Parkin (1996)	Enriched MPB	Batch		0.39 [2]	0.18 [2,3]	30 [2,4]	664 [2]	0.013
Weiner and Zeikus (1978b)	*Methanosarcina barkeri* MS			0.8	1.4			
Smith and Mar (1978)	*Methanosarcina barkeri* 227			1.1				
Wu *et al.* (1992)	*Methanosarcina mazei* T18				1.4 – 1.7			
Jain *et al.* (1987)	*Methanobacterium ivanovii*			0.54	0.8 – 1.7			
Wu *et al.* (1992)	*Methanobacterium formicicum* T1N				2.1 – 2.8			
Schauer and Ferry (1980)	*Methanobacterium formicicum* JF1			0.4	1.2 – 2.8			
Jain *et al.* (1987)	*Methanobacterium bryantii* MOH			0.3	0.3 – 0.4			

[1] Based on cell protein of 0.5 g protein / g biomass [2] Uncompetitive Inhibition [3] Reported as k [4] Converted using Henry's law

Table 2.8 Monod kinetic parameters for methanogenesis using acetate as substrate. Adapted from Harper and Pohland (1986), Gujer and Zehnnder (1983) and Pavlostathis and Giraldo-Gomez (1991)

Reference	Culture	Conditions	T °C	Y mg biomass/ mg acetate	μ_{max} d^{-1}	K_S mg acetate/l	$K_{I,H2S}$ mg H_2S/l	b d^{-1}
Gupta *et al.* (1994a,b)	Mixed SRB and MPB	Continuous	35	0.0375 [1]		6.00		
Bhattacharya *et al.* (1996)	Mixed SRB and MPB	Batch	35	0.0346	0.112 [2]	115.5		0
Visser *et al.* (1993)	Mixed SRB and MPB	UASB			0.055	0.07		
Maillacheruvu and Parkin (1996)	Enriched MPB	Batch		0.041 [3]	0.14 [2, 3]	27 [3]	117 [3]	0.013
Lawrence and McCarty (1969)	Enriched MPB	Continuous	25	0.054	0.250	869		0.011
	Enriched MPB	Continuous	30	0.058	0.270	333		0.037
	Enriched MPB	Continuous	35	0.04	0.357	154		0.015
	Enriched MPB	Continuous	37	0.04	0.39	168		0.02
Kugelman and Chin (1971)	Enriched MPB	Continuous	35		0.34	170		0.036
Moletta t al. (1986)	Mixed MPB	Batch	35	0.82	0.138	3		
Van der Berg (1977)	Mixed MPB	Batch	20	0.05	0.13 [2]			
		Batch	30	0.02	0.052-0.10 [2]			
		Batch	35	0.02	0.052-0.10 [2]			
Visser (1995)	Granular sludge	UASB	30		0.09 – 0.12	54		
Visser (1995)	Suspended sludge	UASB	30		0.03 – 0.09	29		
Wandrey and Aivasidis (1983)	*Methanosarcina barkeri*	Continuous	37	0.024	0.206	230		0.004
Schönheit *et al.* (1982)	*Methanosarcina barkeri*	Batch				180		
Weimer and Ziekus (1978a)	*Methanosarcina barkeri*		37	0.03				
Smith and Mar (1980)	*Methanosarcina barkeri*		36	0.05	0.44			
Smith and Mar (1978)	*Methanosarcina barkeri* 277		36	0.04	0.60	299		
Zinder and Mar (1979)	*Methanosarcina*		55	0.03	1.4	271		
Zehnder *et al.* (1980)	*Methanothrix soehngenii*		33	0.03	0.11	28		
Huser *et al.* (1982)	*Methanothrix soehngenii*		37	0.02	0.16	42		
Cappenburg (1975)	*Methanothrix* species		30	0.01	0.26	10		

[1] Based on biomass COD of 1.41 mg COD / mg biomass [2] Reported as k [3] Uncompetitive Inhibition

2.8.2 INHIBITION KINETICS

Sulfide Inhibition

The inhibitory effect of sulfide on methanogenesis has been well documented. Hydrogen sulfide levels resulting in a 50% inhibition of methanogenesis range from 50mg/l to 250 mg/l (Visser, 1995). Hilton and Oleszkiewicz (1988) studied the effect of sulfide on methanogenesis utilizing acetate as a substrate over a pH range of 6.5 to 8.0. They concluded that it is the unionized H_2S and total sulfide that is inhibitory. They were also able to confirm the generally accepted level of 200mg/l H_2S, above which methanogenesis is severely or completely retarded. Maillacheruvu and Parkin (1996) have reported kinetic constants for sulfide inhibition for a number of anaerobic reactions including methanogenesis (both acetate and H_2/CO_2 substrates). They concluded that an uncompetitive inhibition model gives the best fit to the data. The constants reported by these researchers are given in Tables 2.8 and 2.9.

Acid Inhibition

Another factor, which has been shown to be inhibitory to methane production, is the presence of high concentrations of unionized acetic and other volatile fatty acids. In their general model of an anaerobic digester, Moletta *et al* (1986) used a non-competitive inhibition model to describe the kinetics of acetate substrate methanogenesis. The reported inhibition constant is 40 mg AcH/l.

pH Inhibition

In contrast to acidogenic bacteria, which have an optimal growth at pH 6.0, methanogenic bacteria are seriously inhibited below pH 6.5 (Sawyer and McCarty, 1989). Huser *et al* (1982) report the optimal pH to be 7.4-7.8, with complete cessation of methane production below pH 6.8 and above pH 8.2. Visser (1995) reports similar results but notes that granular sludge is more tolerant of pH extremes. This is presumably due to concentration gradients within the particles.

The narrow pH range indicates a rapid onset of inhibition, and consequently the inhibition parameters α_{LL} and α_{UL} should be large (around 20). pH_{LL} and pH_{UL} were chosen to be 7.1 and 8.0. The resulting empirical plot of the pH inhibition function (Figure 2.7) reflects the behaviour observed by Visser (1995) and Huser *et al.* (1982).

Absence of Hydrogen Inhibition

In contrast to the biological reactions discussed above, methanogenesis is not affected by elevated hydrogen concentrations (Mosey, 1983).

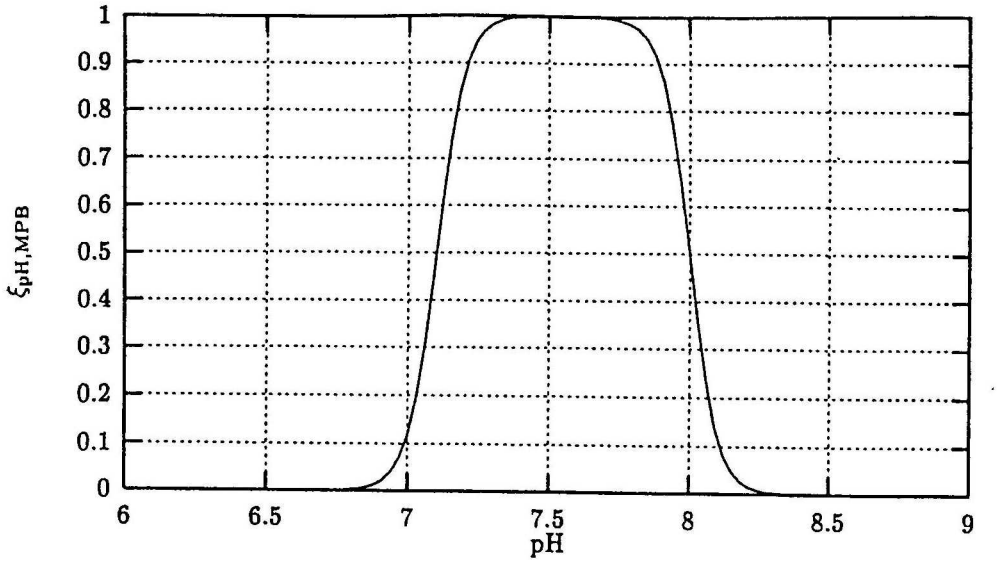

Figure 2.7: Plot of pH inhibition of methanogenesis based on data from Huser *et al.* (1982) α_{LL} = 20, α_{UL} = 20, pH_{LL} = 7.7, pH_{UL} = 8.0.

2.9 SULFATE REDUCTION

Sulfate reducing bacteria have been shown to be able to utilize a large number of substrates as electron donors. These include hydrogen, volatile fatty acids up to C_{20}, alcohols, several amino acids, monomeric sugars and a large number of aromatic compounds (Hansen, 1993). However in the sort of digester under consideration, many of the above components may not be present in significant quantities (e.g. aromatic compounds). In addition, the sulfate reducers may favour certain substrates, or may not be able to compete with other organisms utilizing the same substrates. Consequently, in the development of the model, only hydrogen and some of the short chain fatty acids were considered as substrates.

2.9.1 BASIC KINETICS AND STOICHIOMETRY

Hydrogen as Substrate

Along with acetate, hydrogen is probably the most important electron donor for sulfate reducing organisms. While both incompletely- and completely oxidizing sulfate reducers are able to utilize

hydrogen as a electron donor, only the complete oxidizers are capable of true autotrophic growth on H_2/CO_2 (Colleran *et al.* 1995). The energy producing reaction is:

$$4H_2 + H_2SO_4 \rightarrow H_2S + 4H_2O \quad [2.67]$$

and the reaction for autotrophic cell synthesis utilizing CO_2 as the carbon source is:

$$5CO_2 + NH_3 + 10H_2 \rightarrow C_5H_7O_2N + 8H_2O \quad [2.68]$$

Growth kinetic constants obtained from literature are given in Table 2.9.

Acetate as Substrate

The reactions describing sulfate reduction and biomass production, using acetic acid as the electron donor and carbon source are:

$$CH_3COOH + H_2SO_4 \rightarrow H_2S + CO_2 \quad [2.69]$$

$$5CH_3COOH + 2NH_3 \rightarrow 2C_5H_7O_2N + 6H_2O \quad [2.70]$$

Monod kinetic parameters as taken from the literature are given in Table 2.9.

Propionate as Substrate

Propionate can be utilized by both completely- and incompletely oxidizing sulfate reducers. The reactions for complete and incomplete oxidation are respectively (Visser, 1995):

$$4CH_3CH_2COOH + 7H_2SO_4 \rightarrow 12CO_2 + 7H_2S + 12H_2O \quad [2.71]$$

$$4CH_3CH_2COOH + 3H_2SO_4 \rightarrow 4CH_3COOH + 4CO_2 + 3H_2S + 4H_2O \quad [2.72]$$

However, the growth rates of complete oxidizers utilizing propionate are low (Colleran *et al*, 1995); and from thermodynamic analysis, incomplete propionate oxidation is expected to be the preferred pathway (Maillacheruvu and Parkin, 1996). Consequently only incomplete oxidation is expected to be of any importance.

The proposed biomass synthesis reaction is:

$$20CH_3CH_2COOH + 12NH_3 + 5H_2SO_4 \rightarrow 12C_5H_7O_2N + 36H_2O + 5H_2S \quad [2.73]$$

It should be noted that sulfate reduction has been incorporated in the cell synthesis reaction. If sulfate reduction is not included, it is impossible to write a synthesis reaction that does not result in the formation of hydrogen. This is unlikely to occur in reality. Monod kinetics are shown in Table 2.11.

Lactate as Substrate

The reactions for incomplete oxidation and cell synthesis utilizing lactate as a substrate are:

$$2CH_3CHOHCOOH + H_2SO_4 \rightarrow 2CH_3COOH + H_2S + 2CO_2 + 2H_2O \quad [2.74]$$

$$5CH_3CHOHCOOH + 3NH_3 \rightarrow 3C_5H_7O_2N + 9H_2O \quad [2.75]$$

Kinetic parameters taken from literature are given in Table 2.12.

Table 2.9 : Monod kinetic parameters for sulfate reduction using hydrogen as substrate. Table in part taken from Oude Elferink *et al.* (1994)

Reference	Culture	Conditions	T °C	Y mg biomass/ mg hydrogen	μ_{max} d^{-1}	K_S mg H_2/l	$K_{I,H2S}$ mg H_2S/l	b d^{-1}
Robinson and Tiedje (1984)	Desulfovibrio G11	Batch	37	0.70 - 0.98 [1]	1.17 – 1.57	4.88 – 8.41		
Robinson and Tiedje (1984)	Mean of several species			0.84 [1]	1.4	6.7		
Maillacheruvu and Parkin (1996)	Enriched SRB	Batch		0.33	0.18 [2]	25	149 [3]	0.013
Kristjansson *et al.* (1982); Badziong and Thauer (1978); Badziong *et al.* (1978); Branndis and Thauer (1981)	*Desulfovibrio vulgaris* (Marburg)			0.55 – 1.3	3.6 – 5.5			
Badziong *et al.* (1978); Lupton and Zeikus (1984)	*Desulfovibrio vulgaris* (Madison)			0.3 – 0.55	0.7 – 5.5			
Brandis annd Thauer (1981)	*Desulfovibrio desulfuricans*			0.94	2.6			
Nanninga and Gottschal (1987)	*Desulfovibrio desulfuricans*				2.8 – 4.3			
Widdel (1987)	*Desulfobacter hydrogenophilus*				0.98			
Brysch *et al.* (1987)	*Desulfbacterium autotrophicum*				0.83 – 1.04			
Widdel and Pfennig (1982)	*Desulfobulbus propionnicus* lpr3				1.66			
Nanninga and Gottschal (1987)	*Desulfobulbus propionnicus*				0.23 – 0.59			

[1] based on protein cell content of 0.5 g protein / g biomass [2] Reported as k [3] Uncompetitive Inhibition [4] Reported as k

Table 2.10 : Monod kinetic parameters for sulfate reduction using acetate as substrate. Experimental conditions as follows: C Chemostat, B Batch, CL Carbon Limited, SL Sulfate limited, SR Sulfate removal. Table in part adapted from Oude Elferink *et al.* (1994)

Reference	Culture	Conditions	T °C	Y mg biomass/ mg AcH	μ_{max} d^{-1}	$K_{S,\ AcH}$ mg AcH/l	$K_{S,SO_4^{2-}}$ mg SO_4^{2-}/l	$K_{I,H2S}$ mg H_2S/l	b d^{-1}
Middleton and Lawrence (1977)	Enriched SRB	B, C, CL	20	0.065	0.33 [1]	250			0.00
			25	0.065	0.46 [1]	92			0.00
			31	0.065	0.57 [1]	5.7			0.00
Maillacheruvu and Parkin (1996)	Enriched SRB	B		0.025 [2]	0.11 [1,2]	46.7 [2]		8.5 [2]	0.013
Bhattacharya *et al* (1996)	Mixed SRB and MPB	B	35	0.0602	0.14 [1]	102.1			0
Gupta *et al.* (1994a,b)	Mixed SRB and MPB	C, SR	35	0.0469 [3,2]		0.84			
Visser *et al.* (1993)	Mixed SRB and MPB	UASB			0.07	5			
Visser (1995)	Granular sludge	UASB	30		0.11-0.12	55	33		
Visser (1995)	Suspended sludge	UASB	30		0.001-0.05	10	18		
Ingvorsen *et al.* (1984)	*Desulfobacter postgatei*	C, SL	30	0.072	0.32 [4,1]	3.84 [4]	20.4 [4]		
Ingvorsen *et al.* (1984)		C, CL	30	0.072	0.33 [4,1]	4.62 [4]	21.1 [4]		
Ingvorsen *et al.* (1984)		B	30				16.3 [4]		
Schönheit *et al.* (1982)	*Desulfobacter postgatei*	B				12			
Brandis-Heep *et al.* (1983)	*Desulfobacter postgatei*		28	0.04	1.03	14			
Schauder *et al.* (1986)	*Desulfobacter postgatei*		30		0.6 [5]				
Widdel (1987)	*Desulfobacter lactus*				0.79				
Widdel (1987)	*Desulfobacter hydrogenophilus*		30		0.92 [5]				
Widdel (1987)	*Desulfobacter curvatus*				0.79				
Widdel and Pfenning (1977)	*Desulfomaculum acetoxidans*		30	5.6	0.65-1.39				

[1] Reported as k [2] Uncompetitive Inhibition [3] Based on biomass COD / mg biomass [4] Reported as Michaelis-Menton parameter [5] Estimated from doubling time

Table 2.11 : Monod kinetic parameters for sulfate reduction using propionate as substrate. Taken in part from Okabe and Characklis (1992) and Visser (1995)

Reference	Culture	Conditions	T °C	Y mg biomass/ mg propionate	μ_{max} d^{-1}	$K_{S, PrH}$ mg PrH/l	$K_{I,H2S}$ mg H_2S/l	b d^{-1}
Maillacheruvu and Parkin (1996)	Enriched SRB	Batch		0.048 [1]	0.11 [1,2]	27.2 [1]	206 [1]	0.021
Nanninga and Gottschal (1987)	*Desulfobulbus propionicus*	Batch	35		2.64			
Widdel and Pfennig (1982)	*Desulfobulbus propionicus*	Batch	39	0.071	1.66			
Widdel and Pfennig (1977)	*Desulfomaculum acetoxidans*	Batch	36		1.10			
Hunter (1989)	Mixed population	Continuous	35	0.022	1.68	90.0		
Samain *et al.* (1984)	*Desulfobulbus elongatus*				1.39			
Stieb and Schink	*Desulfcoccus multivorans*				0.17 – 0.23			

[1] Uncompetitive inhibition [2] Reported as k

Table 2.12 : Monod kinetic parameters for sulfate reduction using lactate as substrate. Adapted from Okabe and Characklis (1992)

Reference	Culture	Conditions	Y mg biomass/ mg LaH	μ_{max} d^{-1}	$K_{S, LaH}$ mg LaH/l	$K_{S,SO4^{2-}}$ mg SO_4^{2-}/l
Cappenburg (1975)	*Desulfovibrio desulfuricans*	Continuous	0.343	8.64	4.4	
Traore *et al.* (1982)	*Desulfovibrio desulfuricans*	Batch	0.046	2.5		
Traore *et al.* (1982)	*Desulfovibrio africans*	Batch	0.019	1.44		
Traore *et al.* (1982)	*Desulfovibrio gigus*	Batch	0.042	2.01		
Traore *et al.* (1982)	*Desulfovibrio vulgaris*	Batch	0.075			
Ingvorsen and Jørgensen (1984)	*Desulfovibrio vulgaris*	Batch		0.264		0.5
Ingvorsen and Jørgensen (1984)	*Desulfovibrio sapovarans*	Batch		0.168		0.7
Ingvorsen and Jørgensen (1984)	*Desulfovibrio salexigens*	Batch		0.504		7.4

Butyrate as Substrate

The reactions for partial oxidation and cell synthesis, using butyrate as a substrate are:

$$2CH_3CH_2CH_2COOH + H_2SO_4 \rightarrow 4CH_3COOH + H_2S \quad [2.76]$$

$$20CH_3CH_2CH_2COOH + 16NH_3 + 10H_2SO_4 \rightarrow 10C_5H_7O_2N + 48H_2O + 10H_2S \quad [2.77]$$

As explained above, sulfate reduction has been included in the biomass synthesis reaction to avoid the production of hydrogen.

Kinetic parameters for butyrate sulfate reduction are given in Table 2.13.

Table 2.13 : Monod kinetic parameters for sulfate reduction using butyrate as substrate. Taken in part from Visser (1995) and Okabe and Characklis (1992)

Reference	**Culture**	**Conditions**	μ_{max} d^{-1}
Schauder *et al.* (1986)	*Desulfovibrio baarsi*	Batch	0.14
Nanninga and Gottschal (1987)	*Desulfovibrio sapovorans*	Batch	1.58
Stieb and Schink (1989)	*Desulfococcus multivorans*		0.17–0.23
Widdel and Pfennig (1981)	*Desulfotomaculum acetoxidans*		1.11
Kuever *et al.* (1993)	*Desulfotomaculum strain Gro11*		1.19–1.3
Brysch *et al.* (1987)	*Desulphobacterium autotrophicum*		0.67–1.11

Sulfate Uptake

In order for the above sulfate reducing reactions to occur, sulfate must be present in sufficient quantities. Under sulfate limiting conditions, a reduced rate results. This is usually accounted for by using dual substrate kinetics, i.e.:

$$\mu = \mu_{max} \frac{S}{K_S + S} \frac{S_{SO_4^{2-}}}{K_{S,SO_4^{2-}} + S_{SO_4^{2-}}} \quad [2.78]$$

At present, $K_{S,SO4^{2-}}$ values have only been reported for acetate and lactate utilizing sulfate reducers. Ingvorsen *et al* (1984) give a range of 11.5-31.7 mg/l with an average of around 20mg/l for *Desulfobacter postgatei*. This is in accord with the results of Visser (1995), who reports values of 33 mg/l and 18 mg/l for mixed methanogenic and sulfate reducing, granular and suspended sludges in a UASB reactor.

2.9.2 INHIBITION KINETICS

Sulfide Inhibition

In contrast to the other microbial reactions where only the undissociated form of hydrogen sulfide has been shown to be inhibitory, there is some debate as to whether total sulfide or only undissociated hydrogen sulfide is inhibitory to sulfate reducers. Hilton and Oleskiewicz (1988) examined the effect of sulfide on sulfate reduction over a pH range of 6.5 to 8.0. They found that even under alkaline conditions, where the concentration of undissociated sulfide is small, the sulfate reducers were inhibited. It was concluded that total sulfide was inhibitory. In their study of VFA degradation in a sulfidogenic reactor, Omil *et al* (1996) found that a decrease in reactor pH from 8 to 7 resulted an increase in free sulfide levels. This was found to inhibit methanogenesis severely, while having little effect of sulfate reduction. This suggests that free sulfide and not total sulfide is inhibitory.

In contrast Reis *et al* (1991) found that only the undissociated form was inhibitory over a pH range of 6.2-6.6. The same conclusion can be drawn from Visser (1995), whose results show that loss of activity has a better correlation with undissociated sulfide concentration, than with total sulfide. This is also in accord with the theory that only undissociated H_2S is able to penetrate the cell membrane (Speece 1983).

Maillacheruvu and Parkin (1996) have shown that an uncompetitive model describes sulfide inhibition and have reported inhibition constants for partial propionate oxidizing, acetate oxidizing and hydrogen utilizing sulfate-reducing bacteria. Values were reported for both total sulfide concentration and hydrogen sulfide concentration. Okabe *et al* (1995) found that a non-competitive model described sulfide inhibition of *Desulfovibrio desulfuricans* using lactate as a carbon source. A summary of sulfide inhibition constants for sulfate reducers is given in table 2.14. An important point worth mentioning at this stage is the lower inhibition constants of the sulfate reducers as compared to methanogens. The implications of this are discussed below.

Table 2.14 : Summary of sulfide inhibition constants for sulfate reducers

		Noncompetitive		Uncompetitive	
Reference	**Substrate**	**$K_{I,TS}$ mg S/l**	**$K_{I,H2S}$ mg H_2S/**	**$K_{I,TS}$ mg S/l**	**$K_{I,H2S}$ mg H_2S/**
Maillacheruvu and Parkin (1996)	Hydrogen			422	149
Maillacheruvu and Parkin (1996)	Acetate			35	8.5
Maillacheruvu and Parkin (1996)	Propionate			681	206
Okabe *et al.* (1995)	Lactate	251	74 [1]		

[1]Calculated from equilibrium at pH = 7

Acid Inhibition

As with the other microbial reactions occurring in an anaerobic digester, undissociated volatile fatty acids are inhibitory to sulfate reducers. Reis *et al* (1990) examined the effect of undissociated acetic acid over a pH range of 5.8 to 7.0 on a sulfate reducing culture fed lactate. They concluded that a modified non-competitive model describes the effect of acetic acid inhibition on sulfate reducers. Their equation is:

$$\frac{\mu}{\mu_{max}} = \frac{1}{1+\left(\frac{S_{AcH}}{K_{I,AcH}}\right)^{1.08}} \qquad [2.79]$$

with an inhibition constant of $K_{I,AcH}$ = 54 mg/l.

pH Inhibition

The optimal pH range for acetate utilizing sulfate reducers is about 7.0-7.8 with minimum and maximum values of around 5.5 and 9.0 (Visser, 1995; Fauque, 1995). However, Visser (1995) found that sulfate reducers in a sludge from a UASB reactor had an optimal range of 6.9 to 8.5, and were active up to a pH of 10. Presumably this is due to concentration gradients within the sludge particles. Based on these data, the following values for a pH inhibition function are estimated: α_{LL} = 10, α_{UL} = 10, pH_{LL} = 6.3 and pH_{UL} = 8.4.

2.10 SULFATE REDUCTION IN COMPETITION WITH METHANOGENESIS

The outcome of competition between the sulfate reducing bacteria and the methanogenic bacteria present in a sulfate reducing anaerobic reactor is important for several reasons. The most obvious point of consideration is that "useless" methanogenic bacteria can be viewed as being in competition with "useful" sulfate reducing bacteria for hydrogen and acetate substrates. As such, it would be desirable to operate a reactor in which sulfate reducing bacteria predominate. However, methanogenic bacteria have at least two "useful" roles. In the first instance hydrogen utilizing methanogenic bacteria have a symbiotic relationship with fermenting bacteria. In order for effective fermentation to occur, a low hydrogen partial pressure is required (Harper and Pohland, 1986). The methanogenic bacteria are intimately associated with the fermenters and consequently the hydrogen produced by fermentation is rapidly consumed. The second useful function provided by methanogenic bacteria is their role in producing large

biomass flocs. Sulfate reducing bacteria are poor extracellular polymeric substance (EPS) producers as compared to methanogens, and consequently do not do well in pure culture retained biomass systems such as UASB rectors. Methanogenic bacteria on the other hand secrete a larger amount of EPS and hence form good flocs in which both MPB and SRB are retained. Some methanogens would therefore be required in a retained biomass system or a system in which the biomass is thickened and returned (i.e. high rate system).

Several studies have been conducted into the outcome of competition between SRB and MPB (Krisjansson *et al*, 1982, Schönheit *et al*, 1982; Robinson and Tiedje, 1984; Isa *et al*, 1986a,b; Oude Elferink *et al*, 1994; Gupta *et al*, 1994a; Harada *et al*, 1994; Bhattacharya *et al*, 1996; Shin *et al*, 1996; Omil *et al*, 1998). From a kinetic point of view, the Monod constants μ_{max} and K_S can give insight as to which group will predominate. At high substrate levels the Monod equation approximates first order kinetics and consequently the group with the higher maximum specific growth rate can be expected to enjoy an advantage. Under low substrate conditions, the group with the greater affinity for the substrate (i.e. lower K_S value) will have an advantage. From an inspection of Tables 2.7 to 2.10, it is apparent that under first order conditions the two groups will have similar growth rates (the specific growth rates are of the same order of magnitude). However, under low substrate conditions, sulfate-reducing bacteria will have an advantage as their half velocity constants are typically an order of magnitude less than those of the methanogens. Gupta *et al* (1994a,b) have suggested that the ratios of the respective half velocity constants may be used as an indicator of the length of time it will take for one group to become extinct in a CSTR. The closer the ratio is to unity, the longer it will take for one group to be come the sole user of substrate.

The above kinetic argument is valid for a continuous stirred type reactor. In a retained biomass type system (i.e. where SRT > HRT) such as UASB reactor, the better floc forming nature of methanogens can be expected to result in better retention. This is in accord with the results of Omil *et al* (1998), who have reported that a shorter solids retention time results in a decrease in the time taken for SRB to predominate, and with the results of Isa *et al* (1986b) who found that despite the lower growth rates of MPB they were able to dominate in a high-rate anaerobic reactor. Visser (1995) studied the biofilm and granulation forming abilities of pure methanogenic, mixed SRB/MP and pure sulfate reducing cultures in an UASB. He concluded that methanogens were necessary for the formation of sludge granules containing sulfate reducers. However, in a mixed culture over a period of months, sulfate reducers came to dominate - but not completely out compete - methanogens. In contrast to the results of Isa *et al*,

Visser observed that in a mixed culture the sludge immobilization capacity of the two groups are similar.

Another factor that will influence the outcome of competition is the relative sensitivities of the two groups to various inhibitory compounds. For example Maillacheruvu and Parkin (1996) have reported lower sulfide inhibition constants (i.e. greater inhibition) for both hydrogen and acetate utilizing SRB as compared to hydrogen and acetate utilizing methanogens. As has been observed by McCartney and Oleszkiewicz (1991) the greater sensitivity of the sulfate reducers to sulfide can be expected to negate some of the advantage gained from lower K_S values.

The optimal pH ranges for sulfate reducers and methanogens are roughly similar. However Visser (1995) has shown that in a mixed culture UASB, methanogenic species enjoy higher growth rates than sulfate reducers at pH values below 6.9. Between 6.9 and 8.5 the growth rates are roughly the same, and above pH 8.5 sulfate reducers have an advantage.

Other factors potentially affecting which group will predominate are sulfate concentration and the nature of the inoculum. Gupta *et al* (1994a) have hypothesized that there is only a very narrow range of operating parameters in which SRB and MPB are able to coexist, and that a very slight change in one variable will result in the domination of one group over the other. It is hence apparent that in designing an anaerobic sulfate-reducing reactor, careful attention needs to be paid to ensure that the reactor conditions are optimal for maximum sulfate removal.

3 MODELLING OF A RECYCLING SLUDGE BED REACTOR USING AQUASIM

3.1 INTRODUCTION

This chapter is a summary of the work carried out under the WRC Consultancy Agreement No. K8/312 during 1998/9. It is included here for completeness of this report. The objective was to develop a simulation model of the biological process treating acid mine drainage (AMD) using settled sewage sludge as electron donor and a falling bed sludge reactor configuration (Ramachandra and Giraldo-Gomez, 1976). AMD characteristically has a high acidity (pH = 2 - 3), high levels of metals (Al = 50 - 2000 $mg.l^{-1}$; Fe = 10 - 6700 $mg.l^{-1}$; Zn = 10 - 100 $mg.l^{-1}$), high sulfate concentration (3 - 30 $g.l^{-1}$), and high total dissolved solids (TDS = 1800 - 45000 $mg.l^{-1}$) (Christensen *et al*, 1996)

The development of a model using AQUASIM, a simulation program traditionally used in the area of activated sludge research, was as a means of gaining some insight into the biological reaction system and reactor configuration. The simulation model does not consider the aqueous chemistry. In addition, the degrees of freedom available in the model mean that it is formulated and calibrated specifically for the recycling sludge bed reactor configuration and is not applicable to other systems. The process of development of the AQUASIM model as well as the model itself has successfully fulfilled its objective. Insight into the particular system has been greatly enhanced during model development and a basic model exists from which more fundamental models may be developed.

The aim of the Recycling sludge bed reactor (RSBR) is to hydrolyse the particulate organic matter, so that sulfate reduction can take place in the baffled reactor that follows the RSBR in the treatment process. The RSBR allows the particulates to settle into the three valleys, and then recycles them back to the feed. This increases the solid retention time, allowing greater hydrolysis to take place.

In order to prevent the soluble organic matter being converted to methane by the methane-producing bacteria (MPB), the AMD is added to the RSBR. In so doing, the SRB will not be sulfate limited, and since they have a greater affinity for the organic substrate, and a greater maximum specific growth rate, they will dominate in the system, and minimal soluble organic matter will be wasted on methane production.

3.2 MODEL FORMULATION AND DEVELOPMENT

To model the system, the reaction scheme, rate equations and kinetic constants for the processes taking place in the RSBR were chosen from the literature. The organic feed to the RSBR consisted of primary settled sewage sludge, and the composition of primary settled sewage sludge, as given by Eastman and Ferguson (1981) was used in the model to define the organic feed (Table 3.1).

An extensive literature survey was performed in order to find an adequate reaction pathway to describe the reactions taking place in the system. The reaction scheme proposed by Gujer and Zehnder (1983), based on the work of Kasper and Wuhrmann (1977) was chosen for the anaerobic digestion of particulate organic matter, from hydrolysis to methane production (Figure 2.1).

Table 3.1: The Composition of Primary Municipal Sludge as given by Eastman and Ferguson (1981)

Feed component	% of total feed COD
VSS	73.5
lipids	21.0
cellulose	19.9
protein	28.7
Volatile fatty acids	5.0
ash	26.5

The stoichiometry of the various reactions was given in terms of COD, and this was used as the stoichiometry in the model. The reaction scheme grouped a number of organic substrates into groups, so that only one rate equation would be needed to describe the degradation of all of the substrates from that group. Therefore, for the sulfate reducing reactions, only three substrates were available in the model. These included propionate (volatile fatty acids, VFA's), acetate and hydrogen. These three stoichiometric reactions were converted to units of COD for consistency in the model.

A rate equation was then chosen from the literature for each of the reactions. For the hydrolysis reactions, a first order reaction was used. For the biological reactions, the model proposed by Kalyuzhnyi and Fedorovich (1988) was used as a basis, since it was developed for the degradation of a mixture of sucrose, propionate, acetate and sulfate. The rate equations included terms for sulfide inhibition in all of the reactions, as well as sulfate limitation in the three sulfate reducing reactions. The rate equation for the anaerobic oxidation of the long chain fatty acids was modified from the Monod equation, where a sulfide inhibition term has been included. A

competitive acetic acid inhibition term was included for the fermentation reaction, while a non-competitive acetic acid term was included for the acetogenic reaction (Costello *et al*, 1991).

Kinetic constants for the hydrolysis reactions were taken from O'Rourke (1968), for the hydrolysis of particulate proteins, carbohydrates and lipids. The kinetic constants for the rest of the bioreactions were taken from Kalyuzhnyi and Fedorovich (1988). The anaerobic oxidation of long chain fatty acids was not included in the model proposed by Kalyuzhnyi and Fedorovich (1988), and these constants were taken from the review paper by Pavlostathis and Giraldo-Gomez (1991).

The kinetic constants from all of these references were for processes taking place at 35°C, while the pilot plant ambient temperature was at 15°C. The kinetic parameters chosen from the literature therefore needed to be converted to these reduced temperatures. The temperature dependence of microbial rate equations is such that the half saturation constant is not strongly dependent on temperature, the yield coefficient is slightly dependent on temperature, but that this variation can be ignored, and that the maximum specific growth rate is largely dependent on temperature (Rose *et al*, 1999).

The temperature dependence for the maximum specific growth rate constant is roughly that the maximum specific growth rate will double for a 10 to 15°C increase in temperature. To apply this rule of thumb, the maximum specific growth rate constants and hydrolysis rate constants were all divided by 4, reducing the rate equations from 35°C to roughly 15°C. The summary of the reactions, their rate equations, kinetic constants and stoichiometry is shown in Table 3.2.

Sulfide inhibition and acetic acid inhibition terms have been included in the rate equations. However, the concentration of these undissociated compounds is dependent on the pH of the system. Acid-base equilibrium reactions were included to determine the equilibrium concentrations of each of these compounds, assuming that the pH in the system is constant at 7. The following reactions were used to calculate these equilibria, consistent with the method proposed by Musvoto *et al* (1997):

$$K_a = \frac{[HS^-][H^+]}{[H_2S]} = 0.75\,10^{-7} \qquad [3.1]$$

For: $$H_2S \xrightarrow{k_1} H^+ + HS^- \qquad [3.2]$$

the rate of reaction is: $$r_{HS^-} = k_1[H_2S] \qquad [3.3]$$

where: $k_1 = 10000$

Then, for: $$H^+ + HS^- \xrightarrow{k_2} H_2S \quad [3.4]$$

the rate of reaction is: $$r_{H_2S} = k_2 [HS^-] \quad [3.5]$$

where: $$k_2 = \frac{k_1}{K_a} 10^{-pH} \quad [3.6]$$

The rate of each of these reactions is far greater than the rate of any of the biological reactions, and therefore equilibrium concentrations would be calculated immediately. The same algorithm was used for the acetic acid dissociation, using the equilibrium constant at 15°C (van Loosdrecht, 1993):

$$K_a = \frac{[Ac^-][H^+]}{[HAc]} = 1.745\,10^{-5} \quad [3.7]$$

The value of k_1 was set at 10^6, since the value of K_a is bigger than for the sulfide equilibrium, and by elevating the reaction rate constant, the rate of the reverse reaction will still be sufficiently higher than the biological reactions to ensure equilibrium values are obtained. The activities of the ions in solution were not taken into account, since the model did not require this level of accuracy.

Once these reactions had been defined, they were incorporated into AQUASIM. AQUASIM is a wastewater treatment package that was originally designed for simulation of nitrification and denitrification systems.

Table 3.2: A summary of the reactions , rate equations, stoichiometry and kinetic constants used in the model.

Process	Reaction	RATE EQUATION	Constants	Stoichiometry	References
hydrolysis of proteins	proteins → amino acids	$r_{proteins} = k_{hprotein}.[protein]$	$k_{h_{protein}}$ = 0.0075 d^{-1}	proteins: -1 SAA: 1	O'Rourke (10)
hydrolysis of lipids	lipids → long chain fatty acids	$r_{lipids} = k_{h_{lipids}}.[lipids]$	$k_{h_{lipids}}$ = 0.0425 d^{-1}	lipids: -1 FA: 1	O'Rourke (10)
hydrolysis of cellulose	cellulose → sugars	$r_{cellulose} = k_{h_{cellulose}}.[cellulose]$	$k_{h_{celllose}}$ = 0.3025 d^{-1}	cellulose: -1 SAA: 1	O'Rourke (10)
fermentation	sugars + amino acids → propionate + acetate + hydrogen	$-r_{Sf} = \frac{\mu_{max,f} C_f}{Y_f\left(1+\frac{K_{S,f}}{[SAA]}\right)\left(1+\frac{[HAc]}{K_{If,HAc}}\right)}\left(1-\frac{[H_2S]}{K_{If,H_2S}}\right)$	$u_{max,f}$ = 2.0 day^{-1} $K_{S,f}$ = 28 $gCOD.m^{-3}$ Y_f = 0.043 $gVSS.gCOD^{-1}$ $K_{If,H2S}$ = 550 g $S.m^{-3}$ $K_{If,HAc}$ = 604 $gCOD.m^{-3}$	SAA: -66 HAc: 35 HPr: 20 H2: 11	Kinetic constants and sulfide inhibition from Kalyuzhnyi and Fedorovich (7) Acetate inhibition equation and constant from Costello (4)
growth of fermenting bacteria	sugars + amino acids → biomass	$r_{Xf} = \frac{\mu_{max,f} C_f}{\left(1+\frac{K_{S,f}}{[SAA]}\right)\left(1+\frac{[HAc]}{K_{If,HAc}}\right)}\left(1-\frac{[H_2S]}{K_{If,H_2S}}\right)$	$u_{max,f}$ = 2.0 day^{-1} $K_{S,f}$ = 28 $gCOD.m^{-3}$ Y_f = 0.043 $gVSS.gCOD^{-1}$ $K_{If,H2S}$ = 550 g $S.m^{-3}$ $K_{If,HAc}$ = 604 $gCOD.m^{-3}$	SAA: $-1/Y_f$ C_f: 1	Kinetic constants and sulfide inhibition from Kalyuzhnyi and Fedorovich (7) Acetate inhibition equation and constant from Costello (4)
anaerobic oxidation	long chain fatty acids → acetate + hydrogen	$-r_{So} = \frac{\mu_{max,o} C_o}{Y_o\left(1+\frac{K_{S,o}}{[FA]}\right)}\left(1-\frac{[H_2S]}{K_{Io}}\right)$	$u_{max,o}$ = 0.1375 day^{-1} $K_{S,o}$ = 1.816 $gCOD.m^{-3}$ Y_o = 0.11 $gVSS.gCOD^{-1}$ $K_{I,o}$ = 550 g $S.m^{-3}$	FA: -34 HAc: 23 H_2: 11	Kinetic constants and sulfide inhibition from Kalyuzhnyi and Fedorovich (7)
growth of oxidisers	long chain fatty acids → biomass	$r_{Xo} = \frac{\mu_{max,o} C_o}{1+\frac{K_{S,o}}{[FA]}}\left(1-\frac{[H_2S]}{K_{Io}}\right)$	$u_{max,o}$ = 0.1375 day^{-1} $K_{S,o}$ = 1.816 $gCOD.m^{-3}$ Y_o = 0.11 $gVSS.gCOD^{-1}$ $K_{I,o}$ = 550 g $S.m^{-3}$	FA: $-1/Y_o$ C_o: 1	Kinetic constants and sulfide inhibition from Kalyuzhnyi and Fedorovich (7)
aceticlastic sulfidogenesis	propionate + sulfate → acetate + sulfide	$-r_{Sps} = \frac{\mu_{max,ps} C_{ps}}{Y_{ps}\left(1+\frac{K_{S,ps}}{[HPr]}\right)\left(1+\frac{K_{S,SO_4}}{[SO_4^{2-}]}\right)}\left(1-\frac{[H_2S]}{K_{Ips}}\right)$	$u_{max,ps}$ = 0.2025 day^{-1} $K_{S,ps}$ = 295 $gCOD.m^{-3}$ Y_{ps} = 0.035 $gVSS.gCOD^{-1}$ $K_{I,ps}$ = 285 g $S.m^{-3}$ $K_{S,SO4}$ = 7.4 $gCOD.m^{-3}$	HPr: -224 SO_4^{2-}: -144 HAc: 128 HS^{-1}: 93	Kinetic constants and sulfide inhibition from Kalyuzhnyi and Fedorovich (7)
growth of aceticlastic sulfidogens	propionate + sulfate → biomass	$r_{Xps} = \frac{\mu_{max,ps} C_{ps}}{\left(1+\frac{K_{S,ps}}{[HPr]}\right)\left(1+\frac{K_{S,SO_4}}{[SO_4^{2-}]}\right)}\left(1-\frac{[H_2S]}{K_{Ips}}\right)$	$u_{max,ps}$ = 0.2025 day^{-1} $K_{S,ps}$ = 295 $gCOD.m^{-3}$ Y_{ps} = 0.035 $gVSS.gCOD^{-1}$ $K_{I,ps}$ = 285 g $S.m^{-3}$ $K_{S,SO4}$ = 7.4 $gCOD.m^{-3}$	HPr: $-1/Y_{ps}$ p-SRB: 1	Kinetic constants and sulfide inhibition from Kalyuzhnyi and Fedorovich (7)
acetogenesis	propionate → acetate + hydrogen	$-r_{Sa} = \frac{\mu_{max,a} C_a}{Y_a\left(1+\frac{K_{S,a}}{[HPr]\left(1+\frac{[HAc]}{K_{Ia,HAc}}\right)}\right)}\left(1-\frac{[H_2S]}{K_{Ia,H_2S}}\right)$	$u_{max,a}$ = 0.04 day^{-1} $K_{S,a}$ = 247 $gCOD.m^{-3}$ Y_a = 0.018 $gVSS.gCOD^{-1}$ $K_{I,aH2S}$ = 215 g $S.m^{-3}$ $K_{Ia,HAc}$ = 181 $gCOD.m^{-3}$	HPr: -7 HAc: 4 H_2: 3	Kinetic constants and sulfide inhibition from Kalyuzhnyi and Fedorovich (7) Acetate inhibition equation and constant from Costello (4)

growth of acetogens	propionate → biomass	$r_{Xa} = \frac{\mu_{max,a} C_a}{\left(1+\frac{K_{S,a}}{[HPr]}\left(1+\frac{[HAc]}{K_{Ia,HAc}}\right)\right)}\left(1-\frac{[H_2S]}{K_{Ia,H_2S}}\right)$	$u_{max,a}$ = 0.04 day^{-1} $K_{S,a}$ = 247 $gCOD.m^{-3}$ Y_a = 0.018 $gVSS.gCOD^{-1}$ $K_{I,aH2S}$ = 215 g $S.m^{-3}$ $K_{Ia,HAc}$ = 181 $gCOD.m^{-3}$	HPr: -1/Y_a C_a: 1	Kinetic constants and sulphide inhibition from Kalyuzhnyi and Fedorovich (7) Acetate inhibition equation and constant from Costello (4)
aceticlastic methanogenesis	acetate → methane	$-r_{Sam} = \frac{\mu_{max,am} C_{am}}{Y_{am}\left(1+\frac{K_{S,am}}{[HAc]}\right)}\left(1-\frac{[H_2S]}{K_{Iam}}\right)$	$u_{max,am}$ = 0.06 day^{-1} $K_{S,am}$ = 56 $gCOD.m^{-3}$ Y_{am} = 0.026 $gVSS.gCOD^{-1}$ $K_{I,am}$ = 285 g $S.m^{-3}$	HAc: -64 CH_4: 64	Kinetic constants and sulphide inhibition from Kalyuzhnyi and Fedorovich (7)
growth of aceticlastic methanogens	acetate → biomass	$r_{Xam} = \frac{\mu_{max,am} C_{am}}{1+\frac{K_{S,am}}{[HAc]}}\left(1-\frac{[H_2S]}{K_{Iam}}\right)$	$u_{max,am}$ = 0.06 day^{-1} $K_{S,am}$ = 56 $gCOD.m^{-3}$ Y_{am} = 0.026 $gVSS.gCOD^{-1}$ $K_{I,am}$ = 285 g $S.m^{-3}$	HAc: -1/Yam a-MPB: 1	Kinetic constants and sulphide inhibition from Kalyuzhnyi and Fedorovich (7)
hydrogenotrophic methanogenesis	hydrogen → methane	$-r_{Shm} = \frac{\mu_{max,hm} C_{hm}}{Y_{hm}\left(1+\frac{K_{S,hm}}{[H_2]}\right)}\left(1-\frac{[H_2S]}{K_{Ihm}}\right)$	$u_{max,hm}$ = 0.25 day^{-1} $K_{S,hm}$ = 0.13 $gCOD.m^{-3}$ Y_{hm} = 0.018 $gVSS.gCOD^{-1}$ $K_{I,hm}$ = 215 g $S.m^{-3}$	H_2: -48 CH_4: 48	Kinetic constants and sulphide inhibition from Kalyuzhnyi and Fedorovich (7)
growth of hydrogenotrophic methanogens	hydrogen → biomass	$r_{Xhm} = \frac{\mu_{max,hm} C_{hm}}{1+\frac{K_{S,hm}}{[H_2]}}\left(1-\frac{[H_2S]}{K_{Ihm}}\right)$	$u_{max,hm}$ = 0.25 day^{-1} $K_{S,hm}$ = 0.13 $gCOD.m^{-3}$ Y_{hm} = 0.018 $gVSS.gCOD^{-1}$ $K_{I,hm}$ = 215 g $S.m^{-3}$	H_2: -1/Y_{hm} h-MPB: 1	Kinetic constants and sulphide inhibition from Kalyuzhnyi and Fedorovich (7)
aceticlastic sulfidogenesis	acetate + sulphate → sulphide	$-r_{Sas} = \frac{\mu_{max,as} C_{as}}{Y_{as}\left(1+\frac{K_{S,as}}{[HAc]}\right)\left(1+\frac{K_{S,SO_4}}{[SO_4^{2-}]}\right)}\left(1-\frac{[H_2S]}{K_{Ias}}\right)$	$u_{max,as}$ = 0.1275 day^{-1} $K_{S,as}$ = 24 $gCOD.m^{-3}$ Y_{as} = 0.041 $gVSS.gCOD^{-1}$ $K_{I,as}$ = 285 g $S.m^{-3}$ $K_{S,SO4}$ = 19.2 $gCOD.m^{-3}$	HAc: -64 SO_4^{2-}: -96 HS^{-1}: 62	Kinetic constants and sulphide inhibition from Kalyuzhnyi and Fedorovich (7)
growth of aceticlastic sulfidogens	acetate + sulphate → biomass	$r_{Xas} = \frac{\mu_{max,as} C_{as}}{\left(1+\frac{K_{S,as}}{[HAc]}\right)\left(1+\frac{K_{S,SO_4}}{[SO_4^{2-}]}\right)}\left(1-\frac{[H_2S]}{K_{Ias}}\right)$	$u_{max,as}$ = 0.1275 day^{-1} $K_{S,as}$ = 24 $gCOD.m^{-3}$ Y_{as} = 0.041 $gVSS.gCOD^{-1}$ $K_{I,as}$ = 285 g $S.m^{-3}$ $K_{S,SO4}$ = 19.2 $gCOD.m^{-3}$	HAc: -1/Y_{as} a-SRB: 1	Kinetic constants and sulphide inhibition from Kalyuzhnyi and Fedorovich (7)
hydrogenotrophic sulfidogenesis	hydrogen + sulphate → sulphide	$-r_{Shs} = \frac{\mu_{max,hs} C_{hs}}{Y_{hs}\left(1+\frac{K_{S,hs}}{[H_2]}\right)\left(1+\frac{K_{S,SO_4}}{[SO_4^{2-}]}\right)}\left(1-\frac{[H_2S]}{K_{Ihs}}\right)$	$u_{max,hs}$ = 1.25 day^{-1} $K_{S,hs}$ = 0.05 $gCOD.m^{-3}$ Y_{hs} = 0.077 $gVSS.gCOD^{-1}$ $K_{I,hs}$ = 550 g $S.m^{-3}$ $K_{S,SO4}$ = 0.9 $gCOD.m^{-3}$	H_2: -48 SO_4^{2-}: -96 HS^{-1}: 62	Kinetic constants and sulphide inhibition from Kalyuzhnyi and Fedorovich (7)
growth of hydrogenotrophic sulfidogens	hydrogen + sulphate → biomass	$r_{Xhs} = \frac{\mu_{max,hs} C_{hs}}{\left(1+\frac{K_{S,hs}}{[H_2]}\right)\left(1+\frac{K_{S,SO_4}}{[SO_4^{2-}]}\right)}\left(1-\frac{[H_2S]}{K_{Ihs}}\right)$	$u_{max,hs}$ = 1.25 day^{-1} $K_{S,hs}$ = 0.05 $gCOD.m^{-3}$ Y_{hs} = 0.077 $gVSS.gCOD^{-1}$ $K_{I,hs}$ = 550 g $S.m^{-3}$ $K_{S,SO4}$ = 0.9 $gCOD.m^{-3}$	H_2: -1/Y_{hs} h-SRB: 1	Kinetic constants and sulphide inhibition from Kalyuzhnyi and Fedorovich (7)

3.3 REACTOR CONFIGURATION

The RSBR was constructed from a rectangular shipping container, and has the dimensions and configuration illustrated in Figure 3.1.

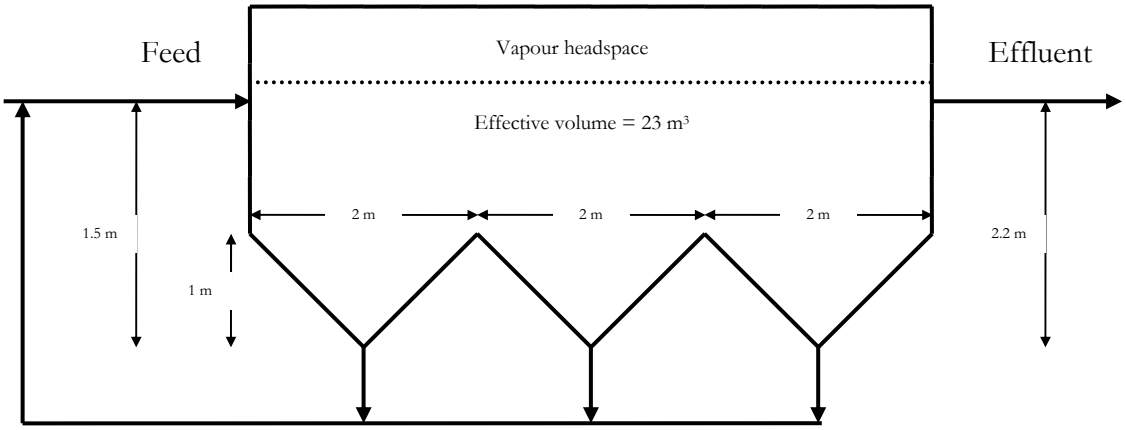

Figure 3.1: The dimensions and configuration on the RSBR pilot plant

The feed and recycled sludge enters at the top of one end of the bioreactor, and settles into each of the three troughs, forming a high solids density bed, while the liquid flows across the top of the bioreactor. This shape and operation allows for a high solids recycle rate, and therefore high solids residence time. There is therefore a concentration profile in both the horizontal and vertical directions. There is an increase in biomass and particulate organic matter concentration from the top to the bottom of the bioreactor, while substrate concentrations tend to decrease with an increase in reactor depth. There is also a distribution of biomass between the three troughs, due to the different recycle rates from each trough, as well as the differential settling of larger particulates into the first trough. The soluble substrate concentrations decrease along the length of the RSBR, as the reaction time and substrate conversion increases.

The model made use of a number of mixed reactor compartments in AQUASIM. The entire volume was divided into compartments, each represented by a mixed reactor, in order to represent the concentration variations. The RSBR was divided into nine separate reactors in the model, as shown by the dotted lines in Figure 3.2.

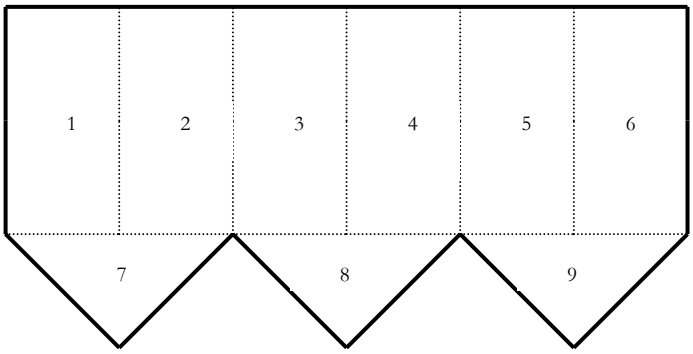

Figure 3.2 : The RSBR was divided into 9 compartments for the AQUASIM model

This configuration essentially allows for plug flow of the liquid and dissolved components across the top of the reactor, with settling of the solids into the three troughs.

The model makes use of three different streams to represent the different flow patterns in the reactor. The first stream type is the flow of water, with the dissolved compounds and the particulates, from the inlet compartment to the outlet, as well as to the three valleys due to the recycle (Figure 3.3).

A greater amount of liquid flow is expected in the first of the three troughs because of the longer time that the recycle pump draws from this trough. The flow of water into each trough was determined by the rate at which the recycle pump is drawing water from each.

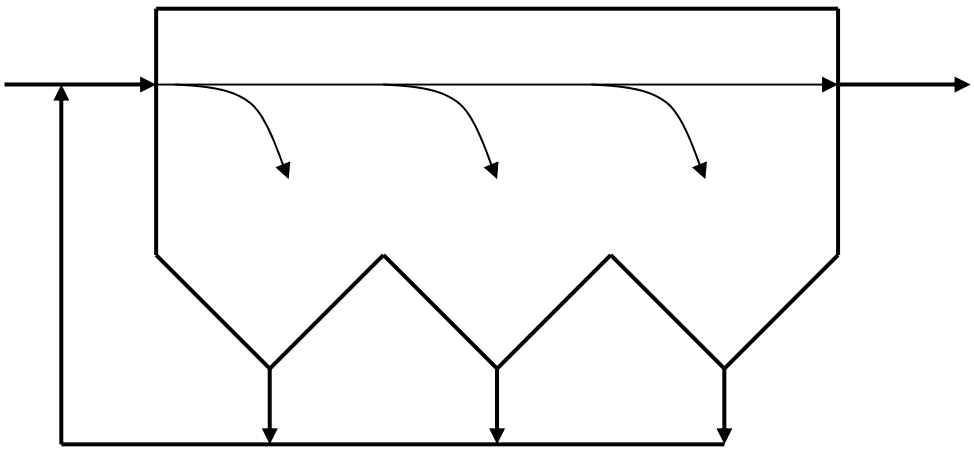

Figure 3.3 : The flow of water and soluble substrates through the RSBR

The second type of stream used in the model shows the settling of the particulates into the troughs. This velocity profile is superimposed on the liquid flow, due to the differential forces of gravity on the particulates (Figure 3.4). The larger particles will settle faster than the smaller ones, and therefore preferentially into the first of the three troughs. However, this overall effect

is probably more due to the higher recycle and liquid flow rate from the first trough, than the RSBR acting as a settling basin.

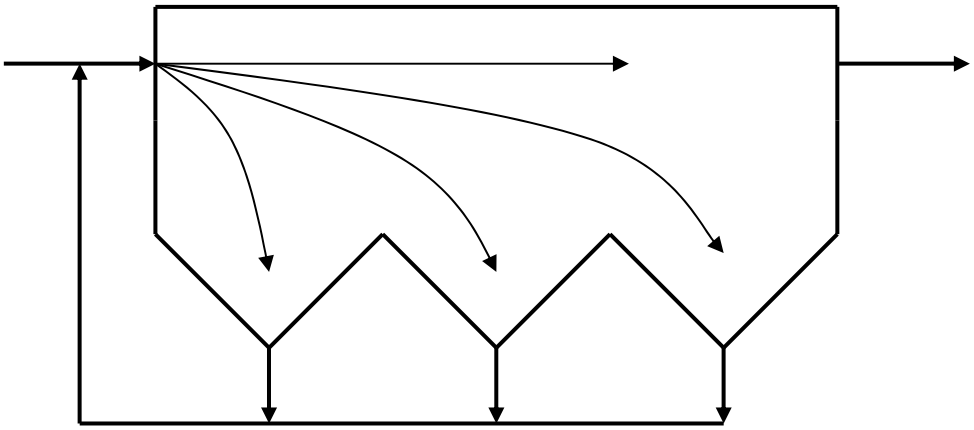

Figure 3.4 : The flow of solids in the RSBR

The final stream used in the model represents the overflow of particulate matter from one valley to the next. This is due to the filling of the first trough caused by the immediate settling of the majority of the particulates, thereby causing the sludge bed to overflow to the adjacent valley. It is also partially due to the liquid movement across the top of the valleys, possibly causing the particles to spill into the next valley. However, this is modelled as purely a solid flux from one valley to the next. Figure 3.5 illustrates the flow patterns taking place in one section of the reactor, and the subsequent representation of this section in AQUASIM.

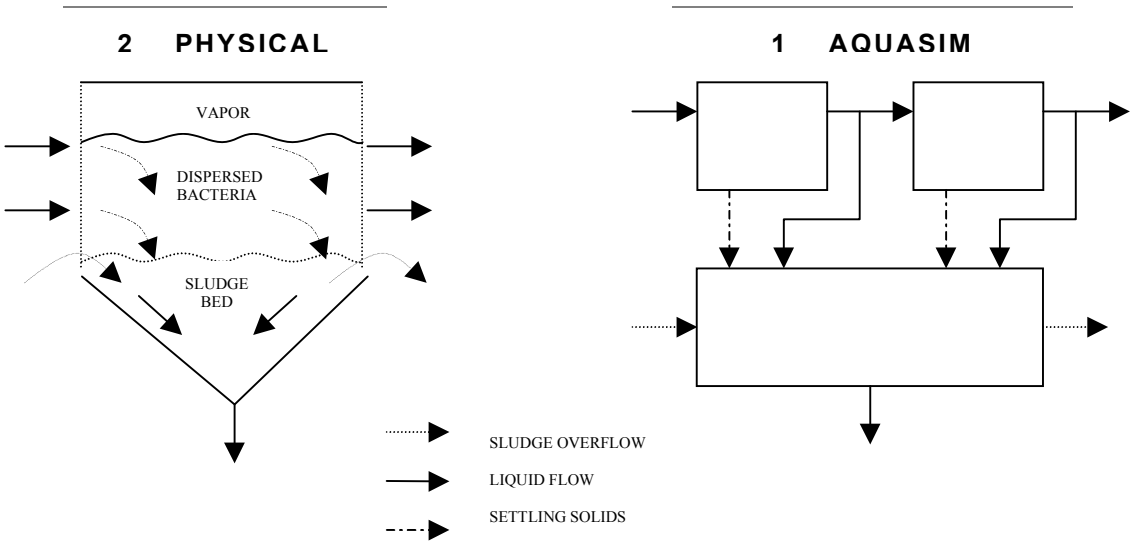

Figure 3.5 : The flow patterns taking place in one section of the reactor, and the subsequent representation of this section in AQUASIM

The complete reactor configuration used in the model is shown in Figure 3.6.

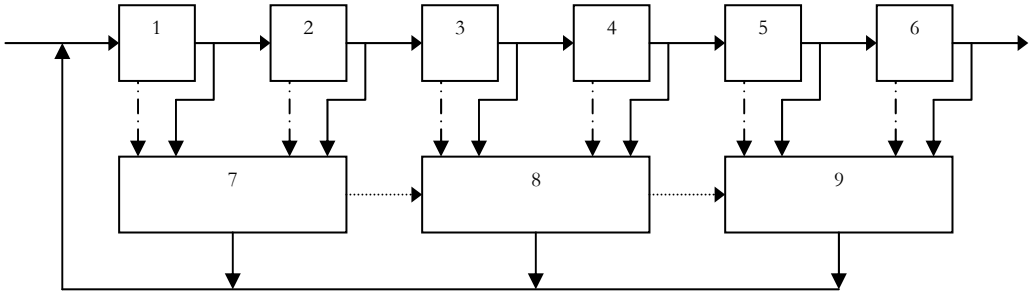

Figure 3.6 : The AQUASIM representation of the RSBR showing the compartments and the connecting streams

3.4 MODEL CALIBRATION

In developing the model, it was assumed that no anaerobic digestion or sulfate reduction takes place prior to entering the reactor, i.e. in the storage tanks or the blend tank. By assuming this, the feed to the reactor is accepted as been constant over a period of time. The model was calibrated using a feed COD: SO_4^{2-} ratio of 2:1 (mass), i.e. a sulfate concentration of 1700 $mg.l^{-1}$, and a COD value of 3400 mg $COD.l^{-1}$. The values of the sulfate concentration in the effluent, or the overall sulfate conversion, were measured, as well as the total COD values in each of the three troughs. These concentrations were used for the model calibration. Table 3.3 shows the

comparison of the measured and simulated values for the COD in each of the three valleys, and the sulfate in the effluent.

Table 3.2 : Comparison of measured and simulated concentrations

SAMPLE POINT	**Measured value**	**Simulated value**	**% deviation**
trough 1 (gCOD.m^{-3})	61816	61500	0.46
trough 2 (gCOD.m^{-3})	50050	50900	1.67
trough 3 (gCOD.m^{-3})	53655	52000	3.07
EFFLUENT SULFATE CONCENTRATION	1100 mg.l^{-1}	1300 mg.l^{-1}	15.4

3.5 MODEL VERIFICATION

The reactor was run at two other operating points, where the feed COD: SO_4^{2-} ratio was changed. Table 3.4 shows the comparison of these measured concentrations to the simulated concentrations. Table 4 shows that the model accurately predicts the performance of the pilot plant at various operating conditions, and was then used with confidence to further predict the performance of the pilot plant under different operating conditions.

Table 3.3 : Comparisons of measured values to simulated values for the model verification

COD:SO_4^{2-}	2 : 1	1.33 : 1	2.82 : 1
COD in (gCOD.m^{-3})	3400	2365	4375
sulfate in (mg.l^{-1})	1700	1772	1551
sulfate out (mg.l^{-1})	1100	1496	820
simulated sulfate out (mg.l^{-1})	1300	1481	1048
% deviation	15.4	1.00	21.7

3.5.1 EFFECTS OF HYDRAULIC RETENTION TIME

In order to obtain simulated trends from variations in the hydraulic retention time (HRT), the feed rate to the bioreactor was varied. Although the feed pump capacity at the pilot plant was 14.64 m^3.d^{-1}, the simulations were performed at feed rates of up to 46 m^3.d^{-1}, resulting in a 0.5 day HRT. A maximum HRT of 2.5 days was simulated, requiring a feed rate of 9.2 m^3.d^{-1}.

Figure 3.7 shows the fraction of the feed entering the bioreactor that is leaving as either particulate COD, biomass, soluble COD, methane, or that has been used for sulfate reduction and is leaving as a sulfide species.

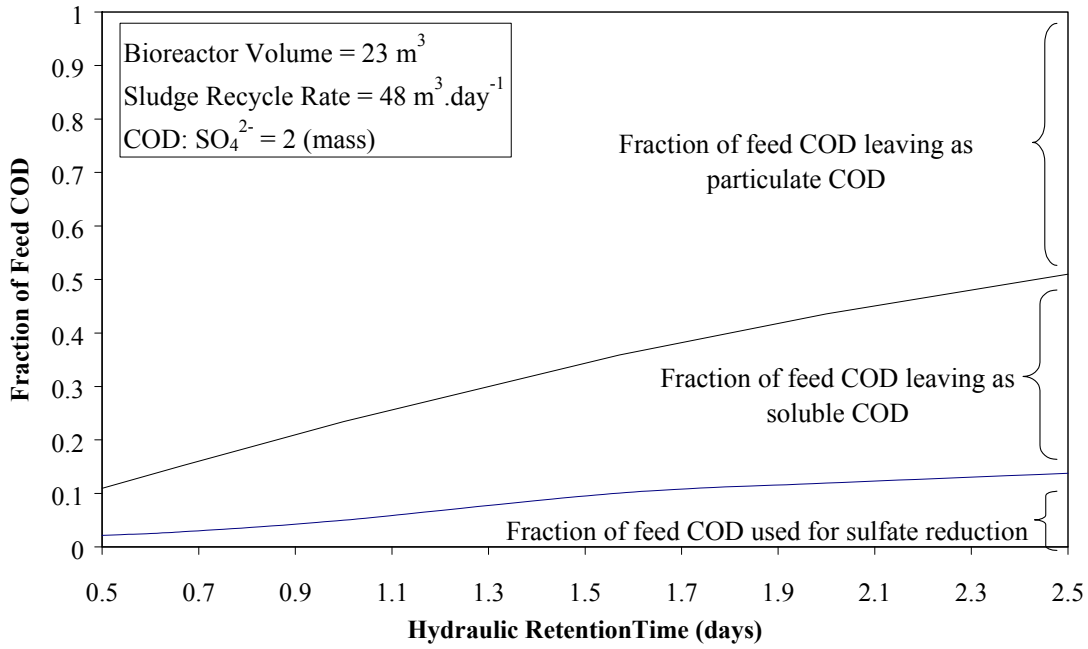

Figure 3.7 : Model predictions of the fraction of the feed COD that is leaving the bioreactor as particulate COD, soluble COD, biomass, methane and sulfide, as the feed to the bioreactor is varied, varying the hydraulic retention time (COD: SO_4^{2-} = 2)

In order to increase the performance of the bioreactor, the fraction that is leaving as particulate COD and as methane needs to be minimised, while the ratios between the fractions leaving as sulfide, soluble COD or biomass is of secondary importance. Figure 3.7 shows that the model predicts that an increase in the HRT will decrease the fraction of the product stream that is particulate. The fraction of the COD leaving as methane and as biomass is insignificant compared to the other groups, and do not appear in Figure 3.7. The fraction leaving as sulfide increases significantly from a HRT of 0.5 until around 1.7, when the amount seems to remain constant. The fraction leaving as soluble COD increases as the HRT is increased across the whole range.

The decrease in the fraction leaving as particulate COD would be expected since the rate of hydrolysis is first order with respect to the particulate COD concentration, and an increase in the HRT would allow for an increased reaction time, which would in turn lead to greater reaction conversion.

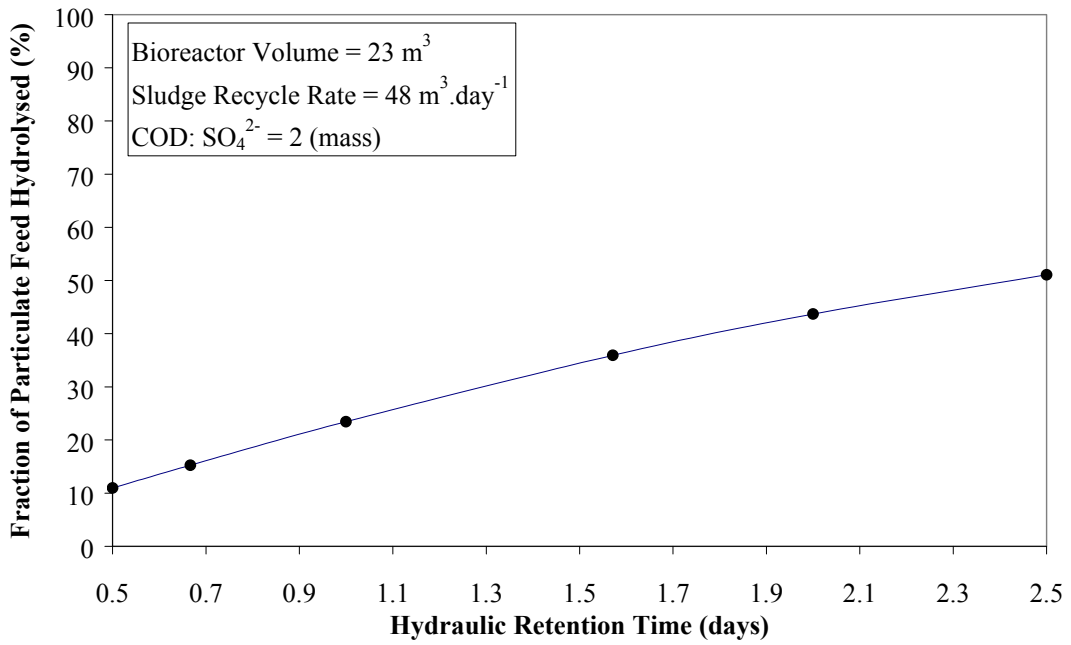

Figure 3.8 : Model predictions of the fraction of the feed particulate COD that is being hydrolysed, as the feed to the bioreactor is varied, varying the hydraulic retention time (COD: SO_4^{2-} = 2)

Figure 3.8 shows the model predictions of the fraction of the feed particulate COD that is being hydrolysed as a function of the HRT. It can be seen that the fraction hydrolysed increases from about 10% at a HRT of 0.5, to about 50% at a HRT of 2.5. The trend in Figure 3.8 is certainly not linear, and a maximum fraction of hydrolysis could be expected at a higher HRT. However, the higher the HRT, the greater the bioreactor volume is required. Low values of HRT are therefore favourable to avoid high capital costs in constructing the bioreactor. There is therefore a trade off between the amount of particulates that will be hydrolysed and the cost of the bioreactor.

Figure 3.7 indicated that the model predicted that the fraction of the feed COD leaving the bioreactor as methane is insignificant. The model predicts that the greatest concentration of methane produced in the system is 2.7 x 10^{-5} g COD.m^{-3} at a HRT of 1.57 days. This is favourable in the bioreactor operation, in that there is very little of the COD being wasted on methane production.

It can be seen from Figure 3.7 that the fraction of the feed COD that is leaving as sulfide is substantial compared to methane. The idea of adding sulfate to the bioreactor to prevent methane formation is therefore justified, since the sulfate reducing bacteria out-compete the methane-producing bacteria for the organic substrate. The fraction of the COD that the model

predicts is leaving the bioreactor as sulfide also increases with an increase in the HRT. However, the trend seems to level off at HRT greater than 1.6. It would be expected that the sulfate conversion would increase with an increase in HRT for many reasons. The first is that the amount of particulates being hydrolysed increases, increasing the amount of available organic substrate. Secondly, the increased HRT increases the reaction time available to the sulfate reducing bacteria, and more sulfate conversion would be expected.

Figure 3.9 shows the predicted trend in the sulfate conversion as the HRT is varied. It can be seen that the sulfate conversion increases with an increase in the HRT. The shape of the curve however does not resemble any of the other trends so far predicted. There is an inflection point in the sulfate conversion at a HRT of about 1.5 days.

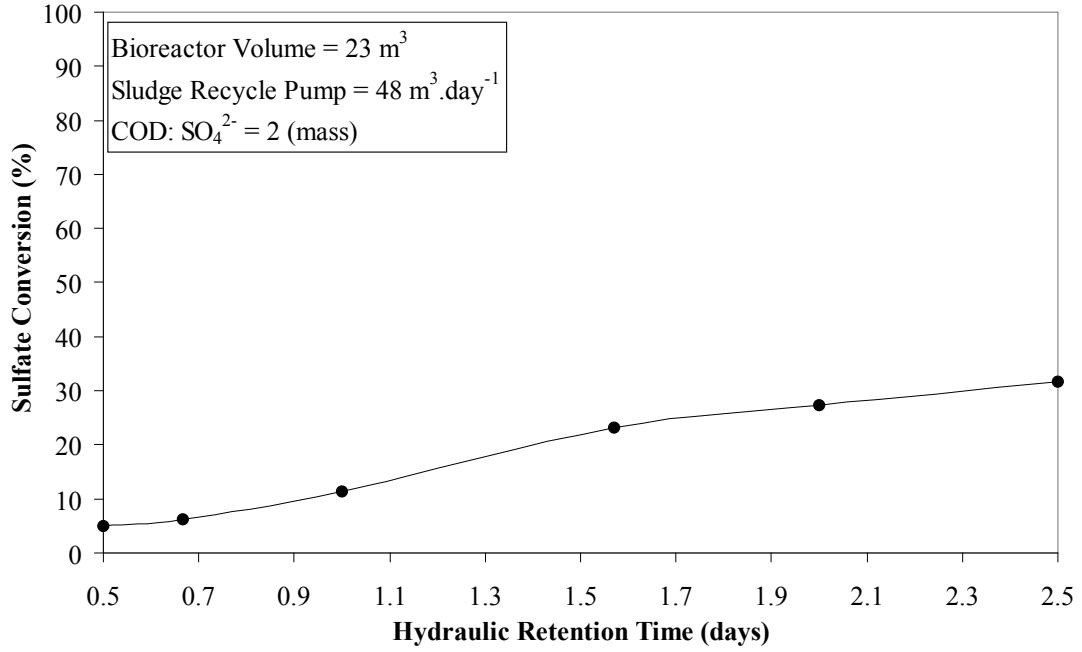

Figure 3.9 : Model predictions of the sulfate conversion, as the feed to the bioreactor is varied, varying the hydraulic retention time (COD: SO_4^{2-} = 2)

In an attempt to explain this inflection point, the rate equation for the specific growth rate of the p-SRB will be used as given in Table 3.2. The equation can be rewritten to separate the terms for organic substrate limitation, sulfate substrate limitation, and sulfide inhibition, as in Equation 3.8:

$$\frac{\mu}{\mu_{max}} = \left(\frac{[HPr]}{K_S + [HPr]}\right)\left(\frac{[SO_4^{2-}]}{K_{SO_4^{2-}} + [SO_4^{2-}]}\right)\left(1 - \frac{[H_2S]}{K_{H_2S}}\right) \qquad [3.8]$$

This equation suggests that when the concentration of propionate is much higher than the value of the half saturation constant, the term for organic substrate limitation will be close to 1, and will not effect the value of the specific growth rate in Equation 3.9. Similarly, when the sulfate concentration is much higher than the half saturation constant for sulfate, this term will be close to 1, and not effect the specific growth rate. When the concentration of undissociated hydrogen sulfide is much smaller than the sulfide inhibition constant, the term for sulfide inhibition will be close to 1 and not effect the specific growth rate. If all three of the above terms are close to 1, the specific growth rate will be equal to the maximum specific growth rate for the bacteria.

Therefore, by calculating the value for each of these terms individually, and then calculating the product of the three terms, the term most affecting the specific growth rate can be determined.

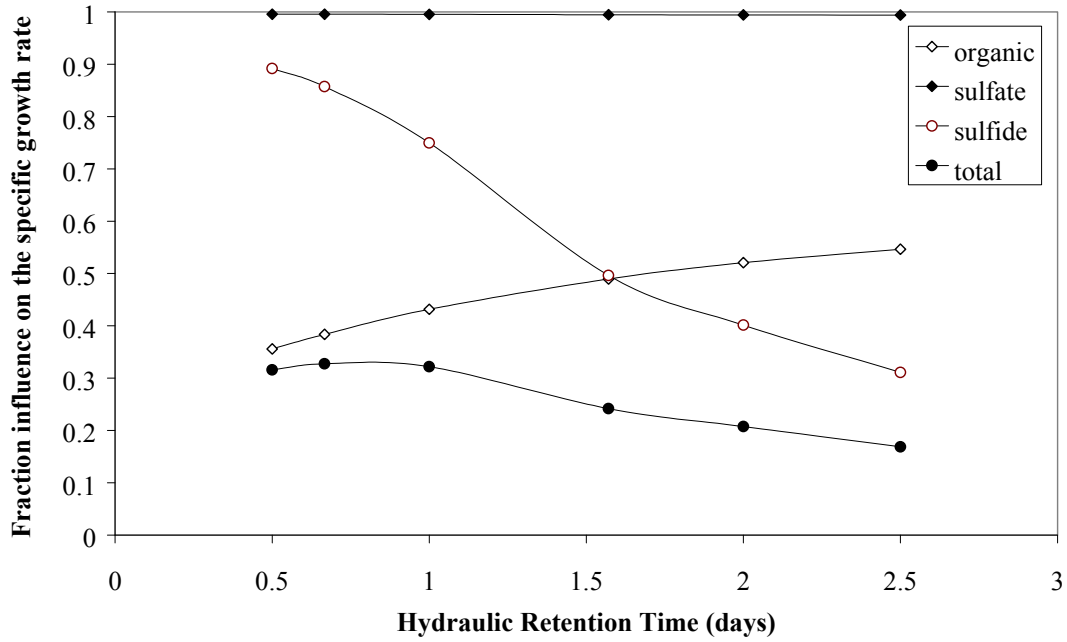

Figure 3.10 : Model predictions of the terms for substrate limitation, sulfate limitation, sulfide inhibition, and the product of the three terms, for the acetogenic sulfidogens, as the feed to the bioreactor is varied, varying the hydraulic retention time (COD: SO_4^{2-} = 2)

Figure 3.10 is a plot of the terms for substrate limitation, sulfate limitation, sulfide inhibition, and the product of the three terms, for the acetogenic sulfidogens, as predicted by the model, as the HRT is varied. Figure 3.10 shows that the values for the sulfate limitation are close to 1 throughout, suggesting that the bacteria are never sulfate limited. The value for the organic substrate limitation increases with an increase in the HRT. This would be expected, as more hydrolysis is taking place as the HRT is increased, resulting in more soluble COD being formed.

Figure 3.7 showed that the fraction of the feed COD leaving the bioreactor as soluble COD increased with an increase in HRT. This would then suggest that the propionate concentration would increase, resulting in less substrate limitation of the p-SRB.

Thirdly, the sulfide inhibition term decreases with an increase in the HRT. This would be expected since the sulfate conversion increases (Figure 3.10), resulting in more sulfide being produced. As this value increases, the bacteria become more inhibited.

Most importantly, the model predicts that the term most affecting the specific growth rate is the organic substrate limitation term, at a HRT of less than 1.5 days, while it is the sulfide inhibition term at a HRT of greater than 1.5 days.

Therefore, as the sulfate conversion increases with an increase in the HRT, forming more sulfide, the bacteria become sulfide inhibited. The rate of hydrolysis is not affected by the sulfide concentration in the model, and forms more soluble COD at higher hydraulic retention times. There is therefore more soluble substrate being formed, but the bacteria are becoming more inhibited, causing the soluble COD to accumulate. This explains the increase in the fraction of the feed COD leaving the bioreactor as soluble COD, as shown in Figure 3.7.

3.5.2 EFFECTS OF SLUDGE RECYCLE RATIO

One of the main features of the RSBR is the high solids density in each of the three troughs, with the subsequent recycle of this high-density sludge back to the feed stream. The classical definition of recycle ratio is a fraction of the effluent stream being fed back to the feed stream. For the RSBR, the sludge recycle ratio (SRR) is defined as the total volumetric flow rate of the combined recycle streams as a ratio of the total volumetric flow rate of the feed stream (Figure 3.11).

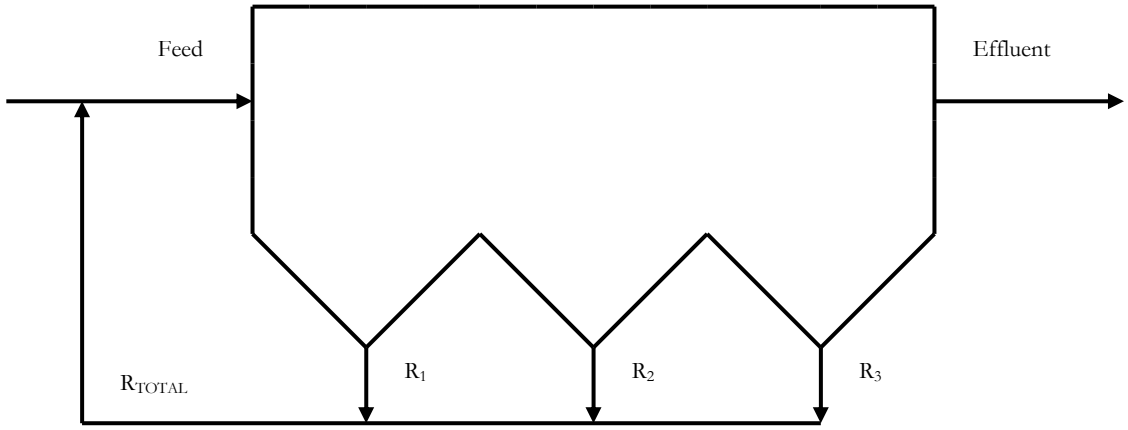

Figure 3.11 : A schematic representation of the RSBR to show the recycle streams, in order to define the Sludge Recycle Ratio (SRR)

The sludge recycle ratio is then defined as:

$$SRR = \frac{R_{TOTAL}}{Feed} \qquad [3.9]$$

In AQUASIM, the various flows of both solids and liquid streams are dependent on the recycle stream, since this determines the liquid flow in the RSBR. AQUASIM calculates the flow rate of the liquid streams across the top of the reactor using a mass balance. The total flow of water into each of the compartments is equal to the total flow out. The solid lines in Figure 3.6 represent these liquid flow lines. Between the top six compartments, the liquid stream is split, and this split stream flows to the compartment below. The flow rate of each of these streams is set by the flow rate of liquid from each of the bottom compartments. These flow rates are in turn set by the total flow of the recycle pump, since the pump draws from each of these compartments for a set time.

However, the dotted lines representing solids flow do not depend on the recycle pump rate directly. These are calculated from the total discharge from a compartment, which will be influenced by the recycle flow rate. For example, the protein fraction that will settle out of the first top compartment to the first bottom compartment is calculated as the product of the discharge from the compartment, the concentration of protein in the compartment, and a user defined fraction. It is this fraction that was varied in order to calibrate the model, to get the model to predict the correct distribution of solids in the RSBR.

Therefore, the model will predict the settling of solids into the bottom three compartments even in the absence of a recycle flow rate. However, there will be no flow from one bottom

compartment to the next, as there is not discharge from these compartments. There will also be no flow of solids back into the top six compartments. Therefore, the recycle flow rate cannot be set to 0 in the model, because the hydrodynamic flow patterns in the RSBR will not be simulated.

The total recycle pump capacity can be varied to determine the effects of the SRR on the performance of the RSBR. At the pilot plant, the recycle pump had a capacity of 2000 $l.h^{-1}$ (48 $m^3.d^{-1}$), while the feed flow rate was 610 $l.h^{-1}$ (14.64 $m^3.d^{-1}$), giving a SRR of 3.28. To obtain simulated trends from varying the SRR, the capacity of the recycle pump was varied. A minimum SRR of 0.25 was simulated, needing a recycle pump capacity of 3.66 $m^3.d^{-1}$, while simulated trends up to a maximum SRR of 4 are shown.

Figure 3.12 shows the model prediction of the fraction of the feed COD that is leaving the RSBR as particulate COD, soluble COD, biomass, methane, or used for sulfide reduction, as a function of the SRR.

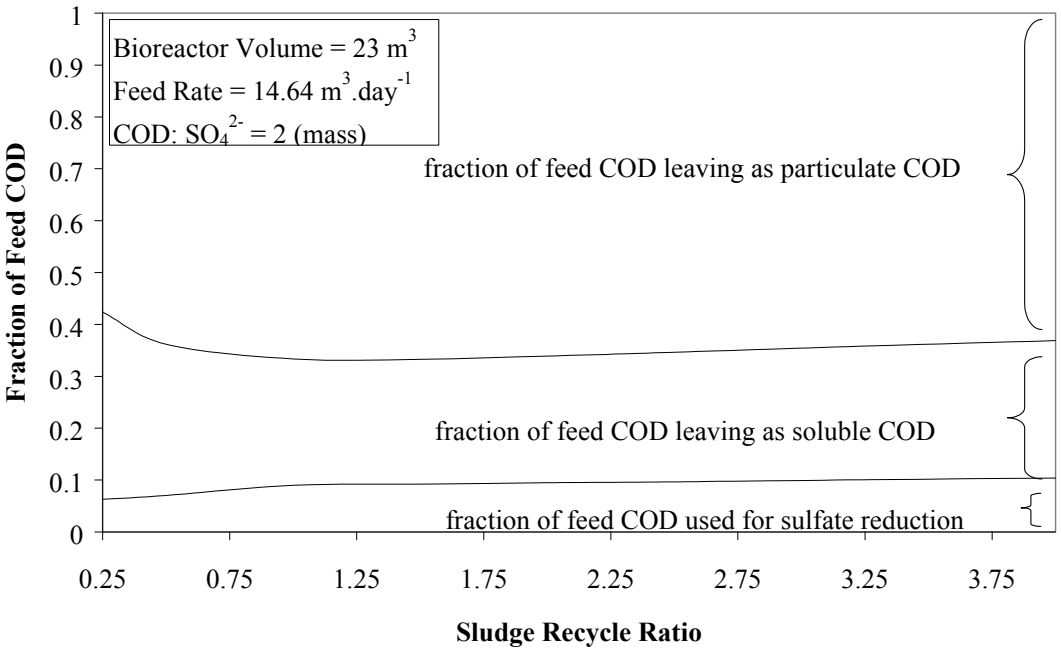

Figure 3.12 : Model prediction of the fraction of the feed COD leaving the RSBR as particulate COD, soluble COD, biomass, methane, or used for sulfide reduction, as a function of the SRR (HRT = 1.57; COD: SO_4^{2-} = 2)

Figure 3.12 shows that the model predicts that a SRR of greater than 1 has little effect on the fractions of the various groups. There is very little biomass and methane produced, but this can be expected at this HRT and COD: SO_4^{2-} ratio.

However, at a SRR below 1, there is a change in the simulated trends. The fraction of the feed COD leaving as particulate COD decreases, together with a change in the COD being used for sulfate reduction. Unfortunately, for values of SRR of less than 0.25, AQUASIM experienced calculation errors.

Figure 3.13 shows the fraction of the feed particulate COD that is being hydrolysed, as a function of the SRR. Figure 3.13 shows a slight increase in the fraction being hydrolysed for SRR values greater than 1, but at SRR values below 1, there is a sudden increase in the fraction being hydrolysed.

At lower recycle ratios, there is less of the high-density sludge being mixed with the feed, resulting in a lower concentration of particulates in the inlet compartment. There are then fewer solids that have to settle out of this liquid stream into the high solids density compartments below, with fewer not settling sufficiently, and being washed out of the bioreactor with the effluent stream. This would result in a higher solids retention time than at higher solids recycle ratios, where more solids would be washed out unhydrolysed. With a higher reaction time available, greater solids hydrolysis is possible.

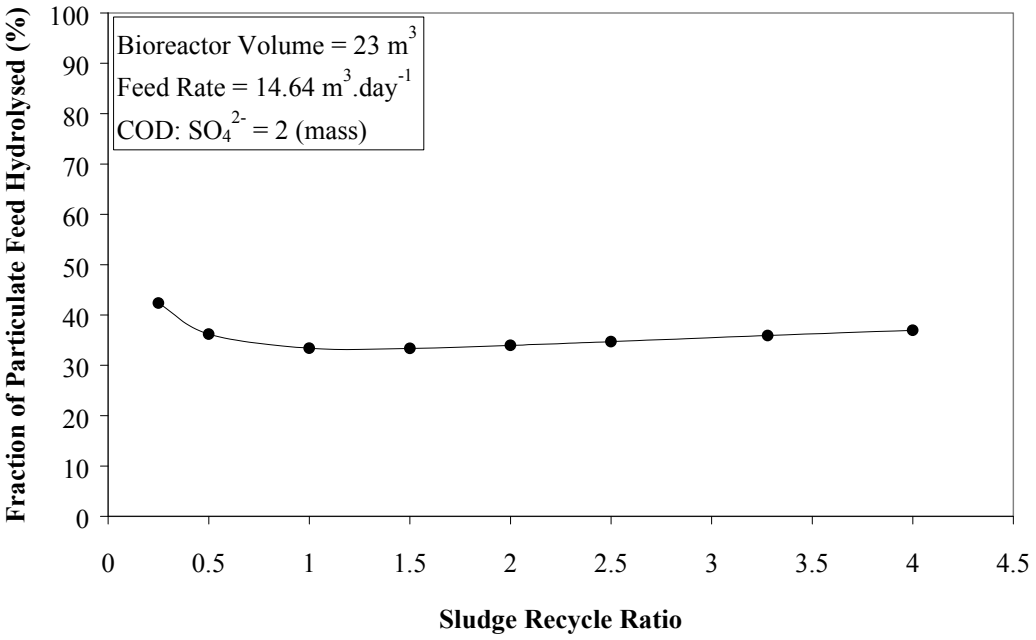

Figure 3.13 : Model prediction of the fraction of the feed particulate COD being hydrolysed as a function of the SRR (HRT = 1.57; COD: SO_4^{2-} = 2)

With greater solids hydrolysis taking place, more sulfate conversion would be expected, since there is more organic substrate available. However, Figure 3.12 shows that the fraction of the feed COD being used for sulfate reduction actually decreases at SRR values of less than 1.

Figure 3.14 shows the sulfate conversion as a function of the SRR. At SRR values of greater than 1, there is a slight increase in the amount of sulfate converted. However, there is a decline in the sulfate conversion for values of SRR of less than 1.

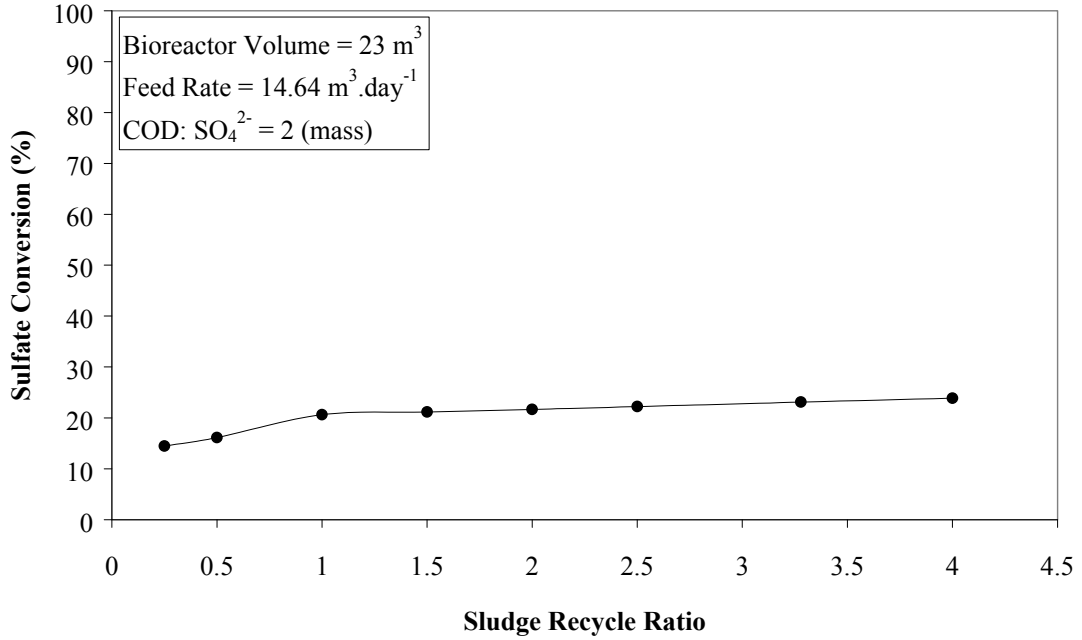

Figure 3.14 : Model prediction of the fraction of sulfate converted as a function of the SRR (HRT = 1.57; COD: SO_4^{2-} = 2)

Figure 3.15 shows the concentration of methane in the bioreactor outlet as a function of the SRR. There is a definite increase in the amount of methane being produced as the SRR increases, but this concentration is still very small compared to the amount of sulfide being produced.

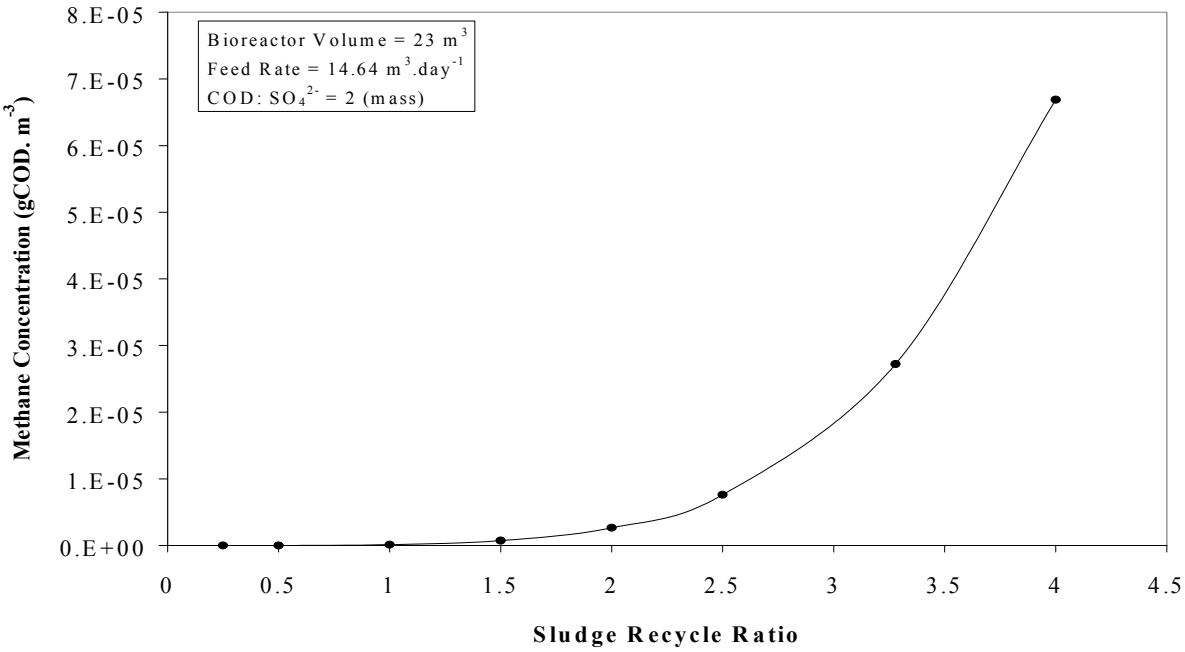

Figure 3.15: Model prediction of the effluent methane concentration, indicating methane production, as a function of the SRR (HRT = 1.57; COD: SO_4^{2-} = 2)

3.5.3 EFFECTS OF COD: SO_4^{2-} RATIO

Theoretically, in anaerobic systems, a COD: SO_4^{2-} ratio of 0.67 will result in all of the sulfate being reduced to sulfide, using all the available COD. For example, in the reaction where acetate is used as the organic electron donor, conversion of the units of the stoichiometric reaction gives the following:

In moles: $CH_3COOH + SO_4^{2-} + 2H^+ \rightarrow 2H_2O + 2CO_2 + H_2S$ [3.10]

In grams: $60g\ CH_3COOH + 96g\ SO_4^{2-} + 2g\ H^+ \rightarrow 36g\ H_2O + 88g\ CO_2 + 34g\ H_2S$ [3.11]

In grams COD: $64g\ COD + 96g\ SO_4^{2-} \rightarrow 64g\ COD\ H_2S$ [3.12]

Normalised: $0.67g\ COD + 1g\ SO_4^{2-} \rightarrow 0.67\ g\ COD\ H_2S$ [3.13]

However, the aim of the RSBR is not to reduce all the sulfate added to the bioreactor, but rather to hydrolyse as much of the particulate COD being added as possible. The soluble products from this bioreactor enter a baffled reactor, where the majority of the sulfate reduction takes place.

The aim of the simulations is to predict the maximum amount of particulate organic matter that can be added with the minimum amount of sulfate, so that the production of methane is avoided, while the hydrolysis of the particulate organic matter is maximised.

It has been mentioned earlier that the rate of hydrolysis is increased in the presence of sulfate and sulfate reducing bacteria. This was observed during operation of the pilot plant. The exact effect that the sulfate concentration has on the rate of hydrolysis is as yet unknown, and therefore the model cannot predict this effect. The model can only be used to predict the effect of the COD: SO_4^{2-} ratio on the competition between the methanogens and the sulfate reducing bacteria.

The effect of the hydrogen partial pressure on anaerobic digestion systems has been discussed earlier in the report, and mention was made of process failure at high organic loading rates. However, the effects of the hydrogen partial pressure were not included in the model, since the reaction scheme used in the model was more general than would be needed to compute the hydrogen partial pressure effects. For example, the exact reaction stoichiometry would be needed for all reactions involving hydrogen, in order to calculate the Gibbs Free Energy change for the reaction. This would require the concentration of each of the reactants and products at any time during the simulation, to determine the spontaneity of the reaction, and the ratio of products formed. This would drastically increase the complexity of the model. Hydrogen partial pressure effects have therefore been omitted. The model predictions will therefore become more uncertain at high organic loading rates, where the hydrogen partial pressure would be expected to increase. A maximum COD: SO_4^{2-} ratio of 4 was used, giving an organic feed rate of 100 g COD. d^{-1}.

Figure 3.16 shows the model prediction of the fraction of the feed COD that is leaving the RSBR as particulate COD, soluble COD, biomass, methane, or that has been consumed during sulfate reduction.

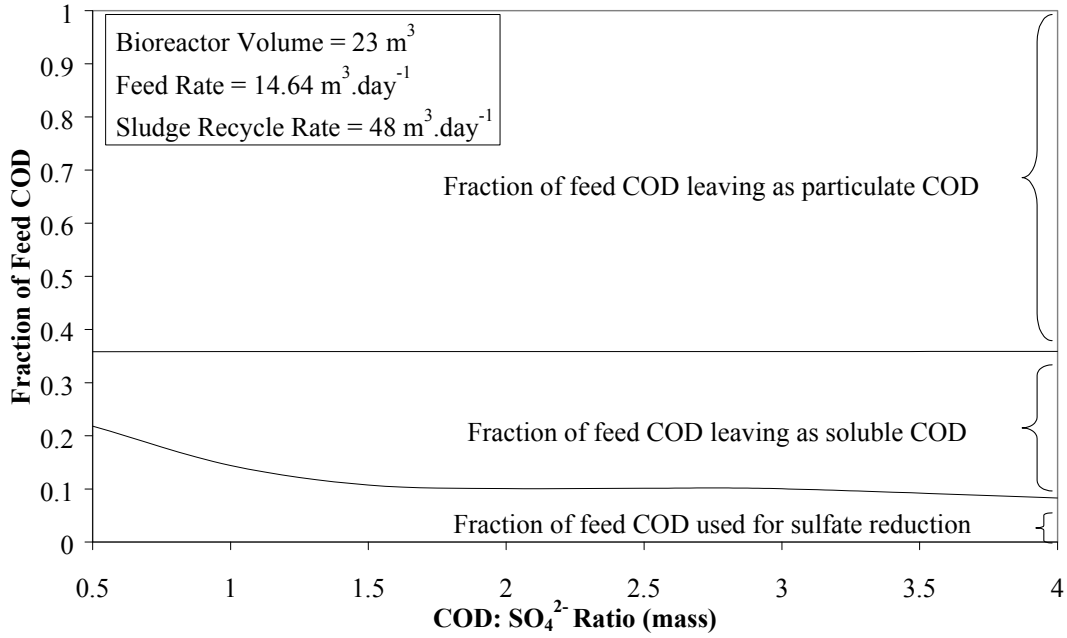

Figure 3.16 : Model prediction of the fraction of feed COD that is leaving the bioreactor as either particulate COD, soluble COD, biomass, methane or sulfide, at various COD: SO_4^{2-} ratios (HRT = 1.57; SRR = 3.28)

Figure 3.16 shows that the majority of the feed COD is leaving the bioreactor still as particulate COD. Figure 3.16 also shows that the fraction of the feed COD that is leaving as soluble COD is increasing with an increase in the COD: SO_4^{2-} ratio, while the fraction of the feed COD being used for sulfate reduction is decreasing with an increase in the COD: SO_4^{2-} ratio. The fraction of the feed COD being used to produce biomass and methane is of such minor quantities that these fractions do not appear in the figure. This suggests that very little methane is being produced, and that very little biomass is being produced.

Once again, the effects of sulfate on the rate of hydrolysis are not known, and not included in the model. Therefore, the only factor affecting the rate of hydrolysis is the concentration of the particulate COD and the available reaction time. Figure 3.17 shows the model prediction of the fraction of the feed particulate COD that is hydrolysed, as a function of the COD: SO_4^{2-} ratio. The model predicts that as more particulate COD is added to the bioreactor, more is leaving the bioreactor, with the same fraction being hydrolysed.

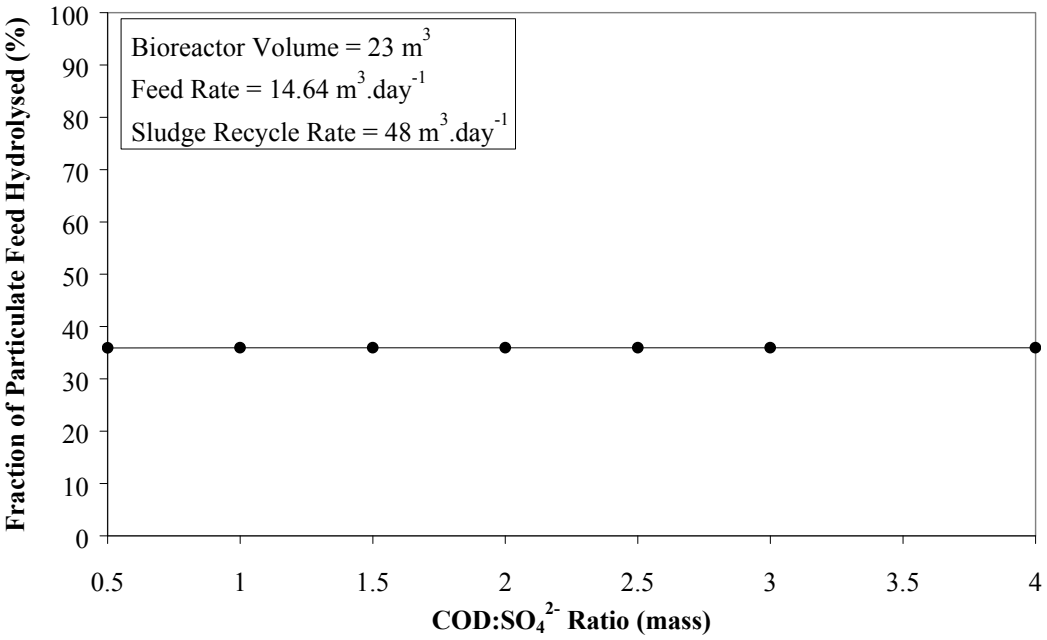

Figure 3.17 : Model prediction of the fraction of feed COD that is leaving the bioreactor as either particulate COD, soluble, biomass, methane or sulfide, at various COD: SO_4^{2-} ratios (HRT = 1.57; SRR = 3.28)

An increase in the COD: SO_4^{2-} ratio is a result of more COD being added, since the SO_4^{2-} concentration is constant. The rate of hydrolysis is first order with respect to the particulate COD concentration. Therefore, at higher feed concentrations, the rate of hydrolysis would increase. The higher reaction rate would cause greater conversion of the reactants for the same reaction time (HRT). The overall result is that more soluble COD is produced with an increase in the COD: SO_4^{2-} ratio.

In fact, Figure 3.17 shows that the fraction of the feed particulate COD that is hydrolysed is constant. Therefore, the variations in reactant concentration in the feed and the subsequent variations in the reaction rate result in the same fraction of hydrolysis. The model therefore predicts that the COD: SO_4^{2-} ratio does not affect the fraction of the feed particulate COD that is hydrolysed in the bioreactor. However, it does allow for greater amounts of soluble COD to be produced. This would be beneficial to the second bioreactor in the process, in that there would now be more substrate available for sulfate reduction in this bioreactor.

It would also mean that there is more soluble substrate available for sulfate reduction and methane production in the RSBR.

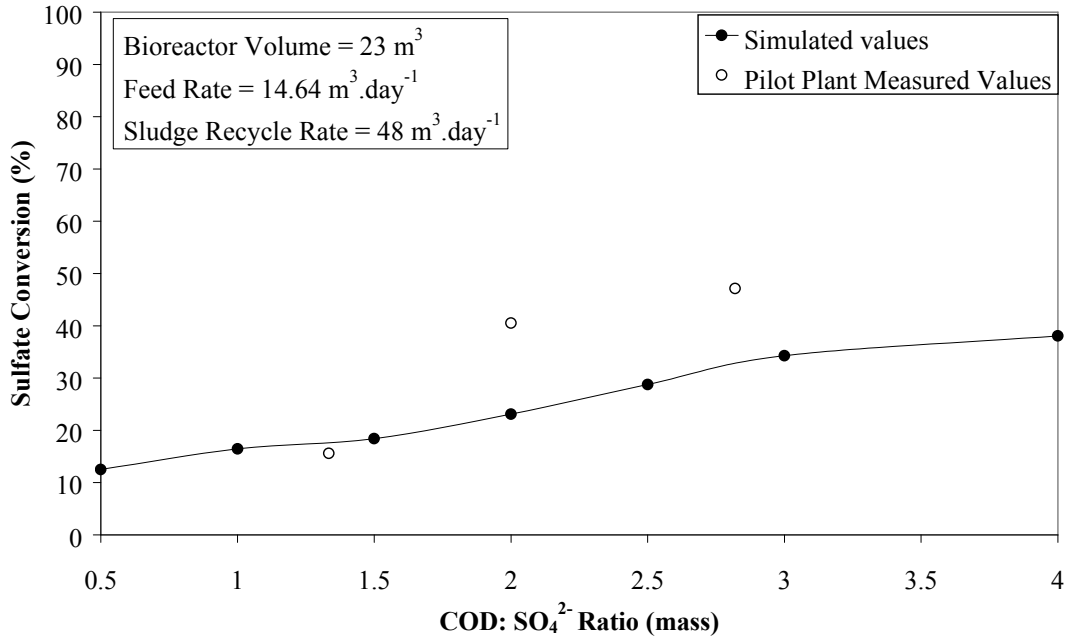

Figure 3.18 : Model prediction of the sulfate conversion at various COD: SO_4^{2-} ratios, together with the three measured concentrations used for the model calibration and verification (HRT = 1.57; SRR = 3.28)

Figure 3.18 shows the predicted sulfate conversion taking place in the bioreactor. Also plotted in Figure 3.18 are the measured sulfate conversion points from the pilot plant RSBR. The sulfate conversion does increase with an increase in the COD: SO_4^{2-} ratio. However, Figure 3.16 shows that the fraction of the total feed COD being used for sulfate reduction does not increase with an increase in the COD: SO_4^{2-} ratio. This means that although the amount of sulfate reduced does increase with an increase in the COD: SO_4^{2-} ratio, the SRB are effected by something other than the organic substrate concentration.

Figure 3.19 shows the predicted concentration of methane being produced in the system. Figure 3.19 shows that the maximum methane production occurs at a COD: SO_4^{2-} ratio of 1, but results in an effluent concentration of less than 2×10^{-4} g COD.m^{-3}. This means than very little methane is being produced in the system, and that less is being produced at higher COD: SO_4^{2-} ratios, even as the soluble COD concentration increases.

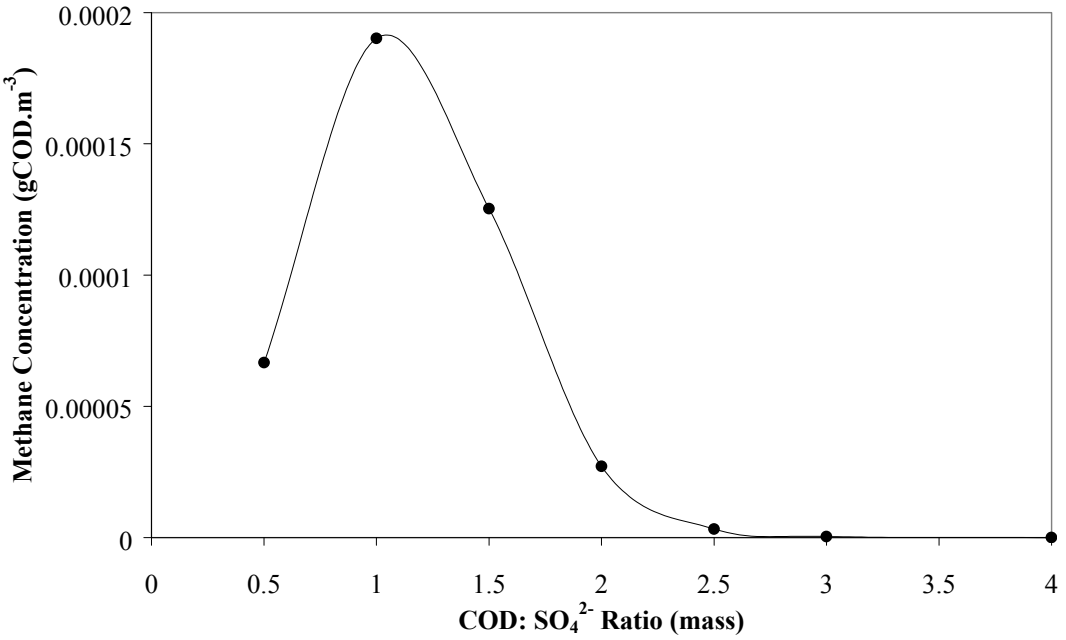

Figure 3.19 : Model prediction of the concentration of methane leaving the bioreactor, indicating methane production, at various COD: SO_4^{2-} ratios (HRT = 1.57; SRR = 3.28)

In order to explain the inactivity of the bacteria at these higher COD: SO_4^{2-} ratios, the specific growth rate is divided into terms for substrate limitation and other inhibition terms. For the acetogenic sulfidogens, Equation 3.9 was again calculated for each COD: SO_4^{2-} ratio, as well as each of the three terms, namely organic substrate limitation, sulfate substrate limitation and undissociated sulfide inhibition.

Figure 3.20 is a plot of each of these individual effects on the specific growth rate, as well as the overall effect of each of these combined. Figure 3.20 shows that the sulfate limitation is close to 1 at all COD: SO_4^{2-} ratios, suggesting that the sulfate concentration is never substrate limiting. Figure 21 also shows that the value for the organic substrate limitation increases significantly with an increase in the COD: SO_4^{2-} ratio. This means that the organic substrate is becoming less limiting at higher COD: SO_4^{2-} ratios. This would be expected, as we have seen previously that the soluble COD concentration in the system increases with an increase in the COD: SO_4^{2-} ratio.

Figure 3.20 shows that the sulfide inhibition value decreases with an increase in the COD: SO_4^{2-} ratio. This indicates that the bacteria are becoming more inhibited by the undissociated hydrogen sulfide. This would indicate an increase in the undissociated hydrogen sulfide concentration, which would be expected, as Figure 3.18 shows an increase in the sulfate conversion with an increase in the COD: SO_4^{2-} ratio, which produces undissociated hydrogen sulfide. Finally, Figure 3.20 shows that for a COD: SO_4^{2-} ratio of less than two, the bacteria are

mostly effected by organic substrate limitation, while at COD: SO_4^{2-} ratios greater than 2, they are mostly effected by the sulfide inhibition.

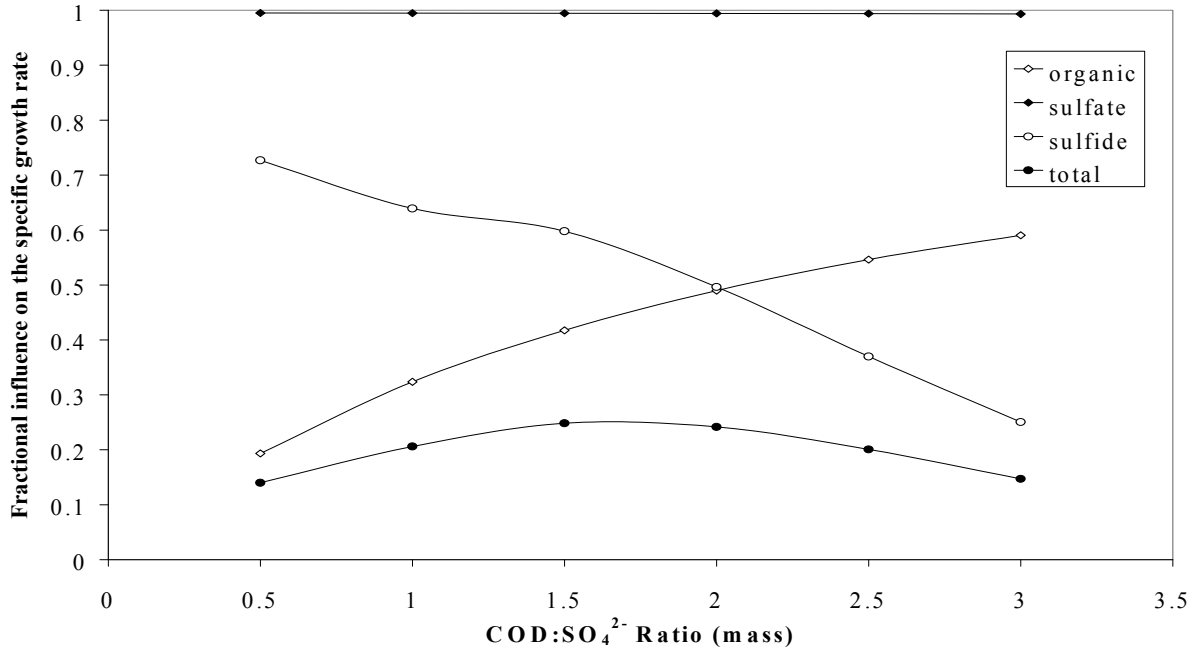

Figure 3.20 : Model predictions of the terms for substrate limitation, sulfate limitation, sulfide inhibition, and the product of the three terms, for the acetogenic sulfidogens, as the COD: SO_4^{2-} ratio of feed to the bioreactor is varied (HRT = 1.57; SRR = 3.28)

A similar trend is observed for the other sulfate reducing bacteria, as well as for the methane-producing bacteria. This suggests that at low COD: SO_4^{2-} ratios, the bacteria are competing for the organic substrate, while at higher COD: SO_4^{2-} ratios, the bacteria are more inhibited by the undissociated hydrogen sulfide concentration. The model predicts that the sulfate reducing bacteria are less affected by the undissociated hydrogen sulfide than the methane producing bacteria, as well as competing more effectively for the available organic substrate, resulting in an insignificant amount of methane being produced.

3.6 CONCLUSIONS

The model predicts that the performance of the recycling sludge bed reactor (RSBR) is mainly dependent on the hydraulic retention time (HRT). An increase in the HRT leads to the predicted increase in the amount of particulate COD that is hydrolysed, which is the primary aim of the RSBR. Secondly, at the sludge recycle ratio (SRR) and COD: SO_4^{2-} ratio used, the model predicts that the production of methane is insignificant, resulting in more soluble COD being available for sulfate reduction in the baffled reactor. Thirdly, the model predicts that the amount

of biomass produced is also insignificant. The overall effect is that an increase in the HRT would improve the performance of the RSBR.

The model predicts that the SRR has very little effect on the bioreactor performance when the ratio varies from 1 to 10. However, at SRR values below 1, there is an increase in the bioreactor performance with a decrease in the SRR. At these low SRR, the flow patterns in the RSBR differ compared to higher SRR, and the RSBR is acting more as a settler than a completely mixed reactor. Unfortunately, the pilot plant cannot verify these trends. However, the model-predicted trend does show that the recycle pump capacity can be reduced from 48 $m^3.d^{-1}$ to 15 $m^3.d^{-1}$, saving on operational costs, without jeopardising the bioreactor performance.

Finally, the model predicts that the COD: SO_4^{2-} ratio does not affect the fraction of the feed particulate COD that is solubilised. However, for the same HRT and SRR, when more particulate COD is added to the RSBR, the same fraction is hydrolysed, resulting in more soluble COD being produced.

The model does not predict the influence of the hydrogen partial pressure, which would influence the system at high organic loading rates. The influence of the high organic loading rate cannot be determined. Also, the influence of the sulfate and sulfide concentrations on the rate of hydrolysis cannot be predicted, so the effect of the COD: SO_4^{2-} ratio is not entirely rigorous.

The model predicts that the methane production in the RSBR is negligible, even at high COD: SO_4^{2-} ratios, suggesting that sufficient sulfate is being added to the RSBR to allow the sulfate reducing bacteria to out-compete the methane producing bacteria for the available organic substrate.

In conclusion, the objective of gaining insight into this particular reaction system and reactor configuration has been achieved through the AQUASIM model development. The model does not consider the effects of aqueous chemistry and speciation and is also specifically calibrated for RSBR. These shortcomings are addressed in the development of a process simulation using a high level mathematical modelling language in Chapter 4. This more fundamental model was developed using octave/matlab, and is a generic model applicable to any reactor configuration and incorporating aqueous chemistry.

4 PROCESS SIMULATION USING A HIGH LEVEL MATHEMATICAL MODELLING LANGUAGE

While general anaerobic mathematical models, beginning with that of Graef and Andrews (1974) have been developed for several decades, only in recent years have models incorporating sulfate reduction emerged (e.g. Kalyuzhnyi and Fedorovich (1997); Vasiliev *et al* (1993), Vavilin *et al* (1995)). In some respects, these models are not yet mature, in that they omit some of the more advanced features of the older non-sulfate models. For example, Costello *et al* (1991) include the effects of pH inhibition, hydrogen partial pressure and undissociated fatty acid inhibition in their dynamic digester model. In addition, in the sulfate reducing models, not all of the possible electron donor substrates have been considered. This is usually the result of a deliberate simplification, but does limit the usefulness of the models in some cases.

The aim of this chapter is to describe the development of a comprehensive mathematical model describing the anaerobic treatment of high sulfate wastewaters. The model is a fundamentally based one, taking into account the biological and chemical reactions as well as the vapour-liquid equilibria pertinent to the treatment systems. Particular requirements are that the model should be applicable for a number of carbon sources (both simple and complex); should account for pH, sulfide, hydrogen and fatty acid inhibition, and should be valid for a number of commonly used reactor types.

An additional objective of this work was that the process of model development should interact strongly with the laboratory-based studies, giving insight to both the experimenters and modellers for the system under consideration. The model should eventually be used to simulate areas of critical experimental interest, generating predictions that can be verified by experimental results.

At this stage of the work, no laboratory data was incorporated into the model. Data for the model's development and calibration was taken from literature. In addition, this work is confined to the anaerobic stage of the treatment process.

While the overall focus of the model has been, in general, to describe the anaerobic treatment of high sulfate waste waters, a particular focus of the work has been on the Recycling sludge bed reactor system developed under WRC contracts 869 and 972 by the Department of Microbiology at Biotechnology at Rhodes University. This treatment system uses primary settled sewage sludge as both electron donor and carbon source for the microbial treatment system.

4.1 MODEL DEVELOPMENT

The model development incorporated the following: biological reactions, aqueous chemistry, vapour liquid equilibrium and reactor geometry.

All of the following microbial processes have been included in the model framework. This gives the model a large range of applicability, covering many possible substrates, from complex primary sludge to the simple case of a H_2/CO_2 fed reactor.

- Colonisation of the sludge particles by acid fermenting bacteria. The particles are hydrolysed extracellularly by enzymes secreted by the bacteria. The carbohydrate fractions of the sludge is broken down to sugars, the protein fraction to amino acids and the lipid portion to long chain fatty acids (LCFAs) and polyols such as glycerol.
- Acid fermentation (acidogenesis) of the sugars and amino acids to hydrogen; carbon dioxide and short chain fatty acids (SCFAs) such as acetic, propionic, butyric and lactic acids.
- Beta-oxidation of the long chain fatty acids to yield acetate, propionate and hydrogen.
- Anaerobic oxidation (acetogenesis) of propionate and higher SCFAs to acetate, hydrogen and carbon dioxide.
- Methanogenesis using hydrogen and acetate as substrates.
- Biological sulfate reduction using hydrogen, acetate, propionate and potentially other intermediate SCFAs as substrates.

The following categories of components were assumed to be representative of those found in an anaerobic, high sulfate system:

- Insoluble components (e.g. carbohydrate)
- Non-dissociating soluble components (e.g. amino acids)
- Dissociating soluble components (e.g. short chain fatty acids)
- Vapour phase components (e.g. hydrogen)

Based on the substrates utilised, twelve different microbial groups (not species) were assumed to be present. Apart from the fermenters, which use amino acids, glucose and glycerol, all other species were assumed to use only one compound as a substrate.

4.2 MICROBIAL REACTION RATES

The rate of hydrolysis is based on a first order model (Eastman and Ferguson (1981), Lilley *et al* (1990), Eliosov and Argaman (1995) and Shimizu *et al* (1993)).

In contrast, more complex expressions are required to account for the rate of utilisation of other substrates. Both the rate of biomass production and of substrate uptake are functions of the μ, the specific biomass growth rate. μ itself can be expressed as a product of μ_{max} (the maximum specific growth rate) and several modifying factors i.e.

$$\mu = \mu_{max} \prod_i \xi_i \qquad [4.1]$$

where ξ_i are appropriate factors for substrate utilisation and various inhibitions. This approach has been used to describe the acetogenic, methanogenic and sulfate-reducing reactions, where the rates are expressed as functions of substrate concentration, undissociated acid concentration, sulfide concentration and pH. The rates of acidogenesis and acetogenesis are also functions of hydrogen partial pressure (Mosey, 1983).

Acidogenesis was modelled using the theory of Mosey (1983) modified by Costello *et al* (1991a,b), as presented in the literature review.

Since the beta-oxidation of LCFAs is closely related to acetogenesis of SCFAs, it is hypothesised that a similar non-competitive model to describe the hydrogen inhibition is also valid here.

4.3 MICROBIAL REACTION STOICHIOMETRY

The microbial reaction stoichiometry is presented in the literature review.

4.4 SOLUTION CHEMISTRY AND MASS TRANSFER

Mass transfer of the four gas phase components between the vapour and the liquid phases is calculated from:

$$N = k_l a\left(\frac{p}{H} - c\right) \qquad [4.2]$$

where:

N = Gas mass transfer rate per unit volume (mmole.l^{-1}.day^{-1})

$k_l a$ = product of gas mass transfer coefficient and specific interfacial area (day^{-1})

p = partial pressure of species (atm)

H = Henry's law constant (atm $(mg/l)^{-1}$

c = molar concentration in the liquid phase ($mmole.l^{-1}$)

For the k_la values, the rates given in Table 4.1were found in the literature.

Table 4.1 : k_la values for gaseous products of anaerobic digestion

Gas species	**K_{ea}**	**Reference**
Carbon dioxide	100 day^{-1}	Graef and Andrews (1974)
Hydrogen sulfide	4320 day^{-1}	Janssen (1996)
Hydrogen	2082 – 3205 day^{-1}	Van Houten *et al* (1994)

No values were given for methane. However, since methane is only very sparingly soluble in water and does not have an effect on microbial rates (as the hydrogen, carbon dioxide and hydrogen sulfide do), not knowing the exact rate of its mass transfer is a minor inaccuracy in the model. Consequently, in the model, a very large value was assumed, which has the effect of allowing the liquid and vapour concentrations to come to equilibrium very rapidly.

The acid/base ionisation reactions are assumed to be in equilibrium. The state of dissociation is calculated from an activity-based expression. The necessary activity coefficients are obtained from the Davies equation (van Haandel and Lettinga, (1994)).

In addition, the hydrogen ion concentration is either calculated from a charge balance or, if the pH of the reactor is specified, from the pH itself. The acid/base reactions included in the model are listed in Table 4.2.

Table 4.2 : Acid/base dissociation reactions included in the model

$$CH_3COOH \Leftrightarrow CH_3COO^- + H^+$$

$$CH_3CH_2COOH \Leftrightarrow CH_3CH_2COO^- + H^+$$

$$CH_3(CH_2)_2COOH \Leftrightarrow CH_3(CH_2)_2COO^- + H^+$$

$$CH_3CHOHCOOH \Leftrightarrow CH_3CHOHCOO^- + H^+$$

$$H_2S_{(l)} \Leftrightarrow HS^- + H^+$$

$$HS^- \Leftrightarrow S^{2-} + H^+$$

$$CO_{2(l)} + H_2O \Leftrightarrow HCO_3^- + H^+$$

$$HCO_3^- \Leftrightarrow CO_3^{2-} + H^+$$

$$H_2SO_4 \Leftrightarrow HSO_4^- + H^+$$

$$HSO_4^- \Leftrightarrow SO_4^{2-} + H^+$$

$$NH_4^+ \Leftrightarrow NH_3 + H^+$$

$$H_2O \Leftrightarrow OH^- + H^+$$

4.5 REACTOR GEOMETRY

A number of different designs are available for anaerobic reactors. These include UASB, packed beds, the contact process and baffle plate reactors. The primary aim of these designs is to achieve a higher rate by ensuring good biomass retention. In other words, the solids residence time is typically higher than the hydraulic residence time.

A simple approach to modelling high rate reactors is to separate the two residence times. The equations describing the dynamic behaviour of the soluble (S) and insoluble (X) components are:

$$\frac{dS_2}{dt} = \frac{{}_1S_1 - S_2}{\tau_{h1}} + r_s(X_2)\frac{\tau_s}{\tau_h} - N \qquad [4.3]$$

where:

S = the vector of the soluble concentrations of the input (1) and output (2) streams ($mg.l^{-1}$)

r_s = the vector of the rate of production of the soluble components ($mg.l^{-1}d^{-1}$)

τs = the solids residence time (d)

τ_h = the hydraulic residence time (d)

N = vector of mass transfer rates between the vapour and liquid phases ($mg.l^{-1}d^{-1}$)

A similar expression can be written for the insoluble components. A mass balance over the vapour phase will yield an expression that is a function of p, a vector of partial pressures, and QG, the gas flow rate leaving the reactor.

By setting the differentials to zero, the model is reduced to the steady state case. Reactor geometries for which the flow is closer to plug flow can be modelled by a number of mixed reactors in series. For example, an anaerobic baffled plate reactor (ABR) can be regarded as a number of UASB reactors in series (Bachmann *et al* (1985)). Similarly, Grobiki and Stuckey (1992) have used residence time distribution studies to demonstrate that the hydraulic flow of an ABR can be characterised by a number of theoretical perfectly mixed reactors in series – the number of ideal reactors required being equal to the number of reactor compartments.

4.6 MODEL IMPLEMENTATION

In choosing a modelling package, there are essentially two options. The first approach is to use a purpose written process simulation package such as Aspen Plus ™ or Hysis. The alternative is to write the model from scratch using a high level programming or modelling language. For a discussion of the relative merits of these two approaches, see Lewis and Knobel (2000). The model was implemented using the high level mathematical modelling language Octave (http://www.che.wisc.edu/octave/). A number of different modules describing the rate of biological reactions, the equilibrium solution chemistry, the vapour liquid mass transfer and the reactor geometry were constructed. Combined, these result in a system of differential algebraic equations for the dynamic case or a system of non-linear algebraic equations for the steady state case. These were then solved using Octave's built in numerical routines.

Apart from Henry's Law constants, K_a values, molecular weights and COD values, which are easily calculated or obtained from standard chemistry textbooks, the model has a large number of parameters required for the calculation of the rates of the biological reactions. In particular, the following are required:

- For the hydrolysis reactions the rate constants and the fraction of sludge which is degradable

- For the soluble substrate reactions, the four Monod constants Y, K_S, μ_{max} and b, as well as undissociated fatty acid and sulfide inhibition constants
- For the inclusion of pH inhibition, additional data is required to calculate the value of the switching function.

The required constants were obtained from a survey of published anaerobic kinetic constants, a summary of which is given by Knobel (1999). Values were not obtained for all constants. In particular, acid and sulfide inhibition constants and K_{SO42-} values are only known for some of the reactions. In these cases, values from other related biological reactions were used.

4.7 RESULTS

The model has been successfully used to simulate a number of different reactor configurations and feeds (including primary sludge) under both steady state and dynamic conditions. A case study of a dynamic simulation emulating an experiment described in the literature is presented here.

4.8 MODEL CALIBRATION

The calibration of the model takes place with reference to a particular system configuration. Numerous calibration/verification cases were used. For the first case, data from an upflow packed bed reactor was used. Maree *et al* (1987) operated an upflow packed bed reactor for 200 days on a feed of molasses and acid mine drainage. Two thirds of the 1 litre reactor was packed with dolomite pebbles with a void ratio of 50%. The relevant operating parameters for the duration of the experiment are given in Table 4.3.

Table 4.3 : Experimental conditions for molasses fed packed bed reactor (Maree *et al*, 1987)

Period	**1**	**2**	**3**
Days	**1-90**	**91-122**	**123-200**
Retention time (h)	20	15	10
Molasses (mg/l)	2000	2000	3000
Sulfate (mg/l)	2480	2480	2480

Since the physical reactor had a high recycle rate relative to the feed flow (20l/day against 1.8l/day), the reactor hydraulic phase was modelled as an ideal CSTR. The molasses feed was approximated as glucose, giving a simulated feed COD of 3210mg/l (as compared to 3360mg/l

in reality). Since there is no sewage sludge component, the hydrolysis reactor can be excluded. The initial concentrations of each microbial species were unknown and arbitrary values of 1mg/l were assumed. The long duration of the experiment allowed the simulated species to grow (or washout) to steady state concentrations. The first period (days 1-90) was used as the calibration case. As the solids residence time (SRT) was not reported, different sludge ages between 2 and 7 days were tested to see which gave the best estimate of COD and sulfate concentrations.

The error was quantified by summing the absolute difference between the experimental and model predicted values. A coarse plot taken at intervals of 0.5 days SRT, indicated that the SRT giving the best fit to the data is around 3.5 days. A more detailed plot around this point indicated that a SRT of 3.4 days gives the best prediction of COD, while a SRT of 3.6 days gives a better prediction for sulfate. Consequently, a SRT of 3.5 days was used in the simulations for the 2nd and 3rd periods, which were used as the verification periods. This value is well within the range that might be expected of a reactor of this type.

Plots of actual and simulated sulfate and COD concentrations in the effluent are shown in Figure 4.1 and 4.2.

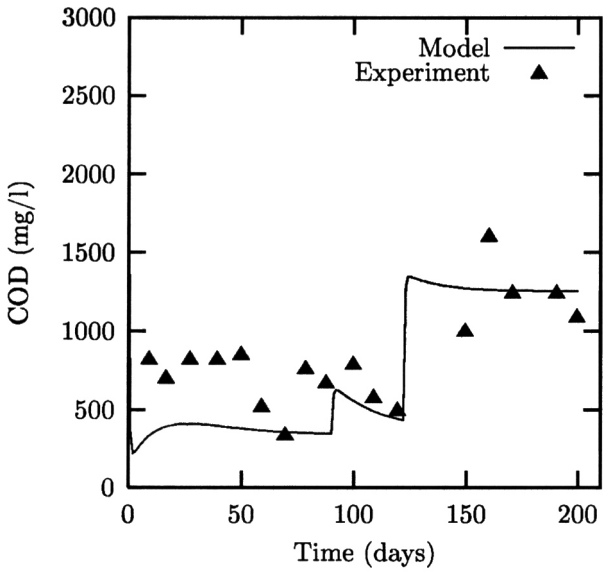

Figure 4.1 : Actual and simulated COD in a molasses fed packed bed reactor.

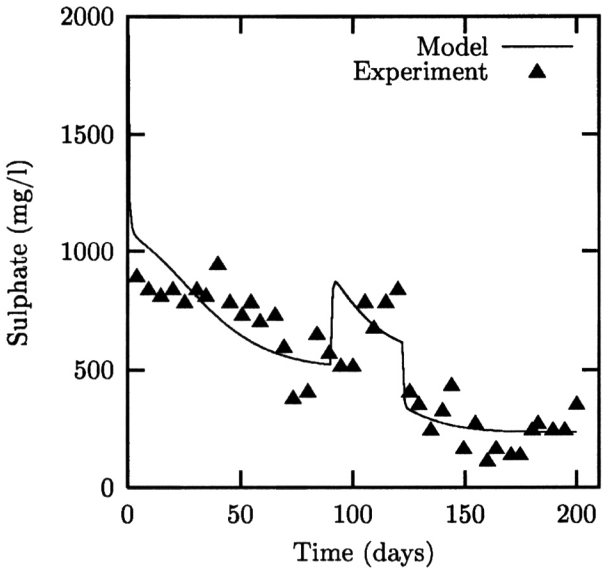

Figure 4.2 : Actual and simulated sulfate concentrations in a molasses fed packed bed reactor.

On a purely visual basis, the predicted sulfate level appears to be in good agreement with the experimental values. The COD is slightly underestimated, although it is still within the range of experimental values. The COD is in better agreement in the second and third time periods of the experiment, even though the first period was used as the calibration case for the SRT. Presumably this is due to the fact that the initial biomass concentration (as input into the model) has less of an effect later in time.

4.8.1 ERROR ESTIMATION AND MEASUREMENT OF UNCERTAINTY – THE SENSITIVITY ANALYSIS

However, a judgement of the goodness-of-fit of the model predictions cannot be made on a visual basis alone. Press *et al* (1992) refer to this practice as "chi-by-eye". To be genuinely useful, the match of the model predictions to the data needs to be quantified in some way. This can be achieved by summing the squares of the residuals and coming up with a number that is a measure of the error in the current model. The model is then changed in some way, and the procedure is repeated. The model that gives the smallest value for the error is the one that fits the measured data most accurately. In addition, in the model presented here, many of the model parameters are either unknown or are poorly known. One of the valuable functions of the model is the ability to quantify the effect of these uncertainties. This allows the critical parts of the model to be identified. These are the parts that have the largest impact and for which the most accurate data is required. A sensitivity analysis is a formal procedure that can be used both

for quantifying the error in the model and the sensitivity of the model parameters on the predicted results.

The simplest approach is to vary one model parameter while keeping the others constant. The results of each simulation are recorded and plotted as a function of the varied model. A more elegant (and powerful) approach to a sensitivity analysis is to define a sensitivity coefficient matrix as the partial derivative of each state variable (i.e. concentration etc) with respect to each model parameter (Lutz *et al*, 1988). This is described in more detail in Lewis and Knobel (2000).

4.9 CONCLUSIONS

A mathematical model using a high level mathematical modelling language (Octave) has been developed. The model describes the dynamic and steady state behaviour of an anaerobic digester treating high sulfate wastewaters. It is applicable for a number of different carbon sources (both simple and complex). It accounts for pH, sulfide, hydrogen and fatty acid inhibition. It has been shown to be capable of predicting a number of different scenarios, including the time dependent concentration of sulfate and COD in a molasses fed packed bed reactor.

In summary:

The development of the model encompassed:

- A formal evaluation of the various kinetics, by comparing their dynamic and steady state behaviour.
- The synthesis of the model equations on the basis of a thorough review of anaerobic and sulfate reduction kinetic data present in the literature.
- Implementation of the model using the high level mathematical language Octave.
- Calibration and verification of the model using a number of different case studies based in the literature.

5 KINETICS OF CONVERSION OF SULFATES TO SULFIDE BY SULFATE REDUCING BACTERIA IN CHEMOSTAT

5.1 A PRELIMINARY INVESTIGATION OF THE EFFECT OF SULFATE CONCENTRATION ON THE KINETICS OF ANAEROBIC SULFATE REDUCTION USING ETHANOL AS THE ELECTRON DONOR AND CARBON SOURCE

5.1.1 THE SELECTION OF ETHANOL AS AN APPROPRIATE ORGANIC SOURCE

Electron donors are widely available and can be divided into two main categories: organic waste materials and bulk chemicals. The use of organic waste materials may be accompanied by further pollution of the wastewater stream, which would require subsequent downstream processing to produce a clean effluent. Furthermore, intermediates from the degradation of complex organic matter may cause complications in the treatment process. The use of pure, fully degradable bulk chemicals is advantageous because no remaining pollution exists after the biological treatment process and no post-treatment is required. Pure chemicals also have a well-defined composition and thus it is easier to predict and describe the process of biological sulfate reduction.

Possible candidates for use as bulk chemicals are ethanol, methanol and synthesis gas. It was found by van Houten (1996) that ethanol was a cheaper bulk chemical than synthesis gas for small-scale applications (< 0.05 – 0.1 kg sulfate per hour). In South Africa, ethanol is a freely available, cheap bulk chemical. This fact, coupled with the advantage that ethanol has been identified as a possible growth substrate for acidogens, MPB and SRB existing in co-culture, makes it a justifiable choice for kinetic studies in mixed microbial systems for sulfate-reduction applications.

Ethanol is the electron donor of choice in the Thiopaq® Process developed and patented by Paques Biosystems (The Netherlands), specifically for the treatment of acidic, high sulfate wastewaters. This technology has been successfully employed industrially in the United States (Buisman, 1996), and operated at pilot scale in South Africa.

A Brief review of relevant literature

Traditionally, COD removal from wastewater streams using anaerobic biological methods was focused on the optimisation of the production of methane as a valuable by-product. Sulfate and sulfate-reducing bacteria were seen as unwanted contaminants resulting in COD wastage and thus a reduction in optimal COD oxidation to methane. With the recent investigations into microbiological methods specifically for the treatment of sulfate-rich wastewaters, it has become necessary to optimise the system in favour of the sulfate-reducing bacteria, treating methane-producers as unwanted competitors for COD.

Acetate has been extensively used in this regard (Maillacheruvu and Parkin, 1996; Visser, 1995; Gupta *et al*, 1994a,b; Isa *et al*, 1986a,b; Schonheit *et al*, 1982; Middelton and Lawrence, 1977), with many studies on microbial kinetics and inhibition published. Acetate is a "restrictive" substrate in that it allows the growth of methane producers and sulfate reducers only, eliminating acid-forming bacteria that are a vital part of the anaerobic consortia.

The use of ethanol allows for the growth of acidogenic and fermentative species. The advantage of sustaining a mixed culture with acidogens is that the culture is more resistant to process perturbations (particularly with respect to longer chain volatile fatty acids), allowing for a more stable treatment process. Figure 5.1 illustrates the possible reaction mechanisms using ethanol as the growth substrate. The reactions 1 – 8 as well as the Gibbs free energies of reaction are summarised in Table 5.1 (adapted from Thauer *et al.* (1977).

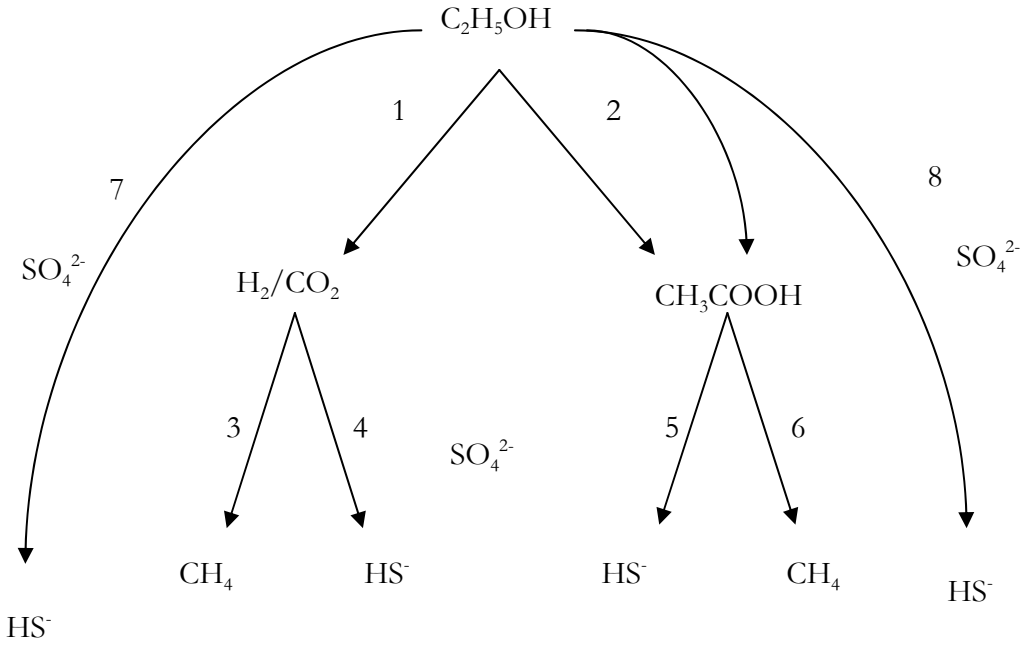

Figure 5.1 : Mechanism of ethanol utilisation in anaerobic mixed cultures

Observing the Gibbs free energy changes of these reactions reveals that sulfate-to-sulfide reduction with simultaneous ethanol oxidation (reactions 7 and 8) is thermodynamically more likely to occur than the corresponding sulfate reduction reactions using hydrogen and acetate (reaction 4 and 5 respectively). Ethanol is also thermodynamically more likely to be partially oxidised to acetate (reaction 8) than completely oxidised to carbon dioxide (reaction 7). Ethanol oxidation to hydrogen and acetate (reaction 1 or 2) are thermodynamically impossible unless they are coupled to acetate and hydrogen consumption reactions (3-6). The kinetics of sulfate reduction using the ethanol electron donor is predicted to be faster than the kinetics of acetate consumption as growth on ethanol is less likely to be thermodynamically inhibited. In a mixed culture of AB, MPB and SRB, it would be expected that, thermodynamically, SRB would dominate and cause an accumulation of acetate in the system.

Table 5.1: Possible reactions in anaerobic sulfate reduction by a mixed culture using ethanol as the carbon source and electron donor (Thauer *et al.*, 1977)

	REACTION	**ΔG° (KJ/MOL)**
1	$C_2H_5OH + 2H_2O \rightarrow CH_3COO^- + H^+ + 2H_2$	+9.6
2	$C_2H_5OH + 2H_2O \rightarrow CH_3COO^- + H^+ + 2H_2$	+9.6
3	$4H_2 + HCO_3^- + H^+ \rightarrow CH_4 + 3H_2O$	-33.9
4	$4H_2 + SO_4^{2-} + H^+ \rightarrow HS^- + H_2O$	-38.1
5	$CH_3COO^- + SO_4^{2-} \rightarrow 2HCO_3^- + HS^-$	-47.6
6	$CH_3COO^- + H_2O \rightarrow CH_4 + HCO_3^-$	-31.0
7	$2C_2H_5OH + 3SO_4^{2-} \rightarrow 4HCO_3^- + H^+ + 2H_20 + 3HS^-$	-118.0
8	$2C_2H_5OH + SO_4^{2-} \rightarrow 2CH_3COO^- + H^+ + 2H_20 + HS^-$	-151.9

5.1.2 KINETICS OF SULFATE REDUCTION ON ETHANOL

Owing to the traditional focus of anaerobic biotechnology, and the relatively recent investigations into ethanol usage, there is very little published kinetic data on the biological treatment of sulfate wastewater using ethanol as the growth substrate.

De Smul *et al.* (1997) successfully ran a high-rate UASB reactor fed with ethanol and sulfate wastewater. The temperature effects on high-rate sulfate reduction processes in UASB reactors were investigated (De Smul, 1998) as well as COD:SO_4^{2-} ratios, however no microbial kinetics were reported.

Szezwyk and Pfennig (1990) investigated the competition for ethanol between SRB and fermenting bacteria in a mix of pure cultures of *Desulfobulbus*, *Desulfovibrio*, *Desulfotomaculum* SRB and *Pelobacter* and *Acetobacterium* fermenting bacteria. They found that maximum specific growth rate, μ^{max}, was higher for the fermenting bacteria ($0.096h^{-1}$) than the SRB ($0.03h^{-1}$) but that the half velocity constants (K_s) were lower for SRB ($\approx 5\mu M$) than fermenting bacteria ($\geq 50\mu M$). This indicates that although the SRB are slower growing, they have a higher affinity for their carbon substrate (in this case ethanol) and will dominate competition in nutrient-limited conditions or low dilution rates.

The accumulation of acetate in high-rate processes has been documented (Lettinga *et al.*, 1981; Tatton *et al.*, 1989; O'Flaherty *et al.*, 1999). Acetate has the net effect of inhibiting microbial growth if excessive accumulation occurs. Acetate removal by some mechanism is essential in maintaining the activity of the culture. The most feasible means is to allow the growth of acid-consuming bacteria in the microbial community.

Hydrogen sulfide, originating from the microbial reduction of sulfate, is also toxic and inhibitory. Although there is some discrepancy in the literature of the exact levels of sulfide causing inhibition, it is generally accepted that methane producers are more susceptible to sulfide toxicity ($120\text{-}240mg.l^{-1}$) than SRB ($160\text{-}200mg.l^{-1}$)(Choi and Rim, 1991; Maillacheruvu and Parkin, 1996).

As pH values are seldom reported, it is not possible to determine the equilibrium between species of sulfide (H_2S/HS^-) when sulfide toxicity is reported. Assuming that most anaerobic digesters operate at around a pH of 7.5-8.0, it can be assumed that soluble unionised sulfide is in the range of $70mg.l^{-1}$. It has also been postulated that the SRB are inhibited by total sulfide concentration, whereas methane producers are most affected by unionised H_2S.

5.1.3 SUBTASK OBJECTIVES

Due to the acute lack of kinetic parameters for ethanol-consuming bacteria, it was necessary to conduct kinetic studies to obtain growth parameters in order to develop models that will help in the engineering design and optimisation of biological wastewater treatment processes. To do this, both batch and continuous bioreactors treating synthetic sulfate wastewater, using ethanol as carbon source and electron donor, were established, and measurements of the batch concentration-time trends, as well as the steady state substrate and product concentrations over a range of dilution rates were made.

In the task as a whole, the effect of sulfate concentration, sulfate loading rate and sulfide concentration on sulfate removal rates and sulfate removal efficiencies will be investigated. Thus far, sulfate concentration and sulfate loading rate have been investigated. These studies are described in detail in the MSc. Dissertation of Erasmus (2000).

5.1.4 EXPERIMENTAL APPARATUS AND MEASUREMENTS

Batch and continuous experiments were carried out in 1-litre vessels maintained at 35°C, and pH 7.3-7.8. pH control was carried out manually, by nitrogen sparging and acid/base addition. Table 5.2 summarises the parameters that were monitored in the experiments.

Table 5.2 : Parameters monitored in kinetic investigations

CONCENTRATION	PHASE	METHOD
Sulfate	Aqueous	Barium Sulfate Precipitation/Ion Chromatography
Acetate	Aqueous	HPLC
Ethanol	Aqueous	GC
Hydrogen Sulfide	Gas	GC
Methane	Gas	GC
pH	Aqueous	

5.1.5 RESULTS

Several batch tests were performed at a variety of sulfate concentrations varying from 1.0 $gSO_4^{2-}.l^{-1}$ to 7.5 $gSO_4^{2-}.l^{-1}$. The results of a typical batch run, lasting between 14 and 21 days

are illustrated in Figure 5.2. Based on these concentration times trends, it can be determined that the microbial lag phase is approximately 3.8 days, and the sulfate removal rate is approximately 0.46 $g.l^{-1}.day^{-1}$ with a corresponding removal efficiency of 90%.

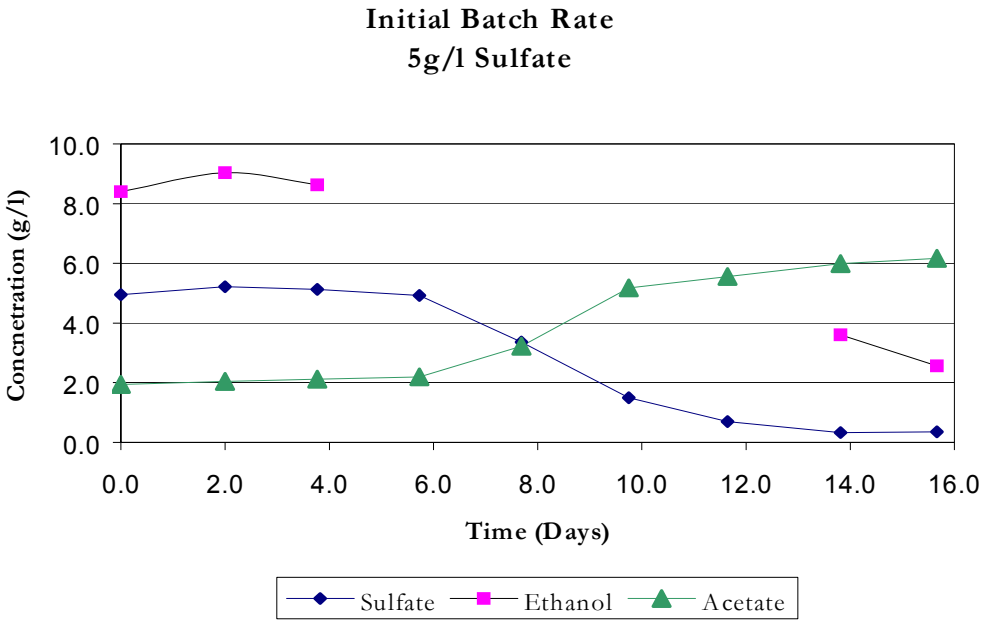

Figure 5.2 : Concentration-time trends for a typical batch experiment with an initial sulfate concentration of $5g.l^{-1}$.

Ethanol is in stoichiometric excess in all experiments in order that sulfate is the growth limiting substrate. Kinetic parameters can then be based on sulfate concentration instead of on the organic source, as typically reported in the literature.

Acetate accumulates in the batch system. This indicates that partially oxidising SRB are predominant (reaction 8) and suggests that the acetate consuming microbial species are either present and inactive or not present at all. Acetate is consumed in the absence of ethanol (data not shown), and thus it can be concluded that acetotrophic microorganisms are inactive in the presence of excess ethanol.

Continuous experiments were run at 10 and 6 days residence times. The steady state data obtained from these experiments as well as calculations of sulfate loading and removal rates are summarised in Table 5.3. The rates of sulfate removal approximate the following trends:

- *increased* with *increasing* dilution rate

- *increased* with *increasing* feed sulfate concentrations at *low* sulfate

- *decreased* with *increasing* feed sulfate concentrations at *high* sulfate

Sulfate removal efficiency decreased as feed sulfate concentration increased. This is an indication that sulfate is inhibitory. Product inhibition by hydrogen sulfide may also occur and the residual total sulfide concentrations fall within the bounds of the known toxicity range (0.1 - 0.8 $g.l^{-1}$).

Table 5.3 : Summary of steady state operating parameters for chemostats at hydraulic residence times of 10 and 6 days

Feed Sulfate (g/l)	1		2.5		5		7.5	
Residence Time (days)	10	6	10	6	10	6	10	6
Run Time (days)	-	57	82	78	107	25	125	28
Residual Sulfate (g/l)	-	0.3	0.75	1	3	3.5	7	6.5
Total Sulfide (g/l)	-	0.24	0.6	0.52	0.69	0.52	0.17	0.34
Loading Rate (g/l.day)	-	0.17	0.25	0.42	0.5	0.83	0.75	1.3
Removal Rate (g/l.day)	-	0.12	0.18	0.25	0.2	0.25	0.05	0.17
Reduction (%)	-	70	70	60	40	30	6.7	13

5.1.6 CONCLUSIONS

Sulfate reduction operates more efficiently at low sulfate concentrations (1 - 2.5 $g.l^{-1}$). This is postulated to be because of the absence of sulfate and sulfide toxicity. Sulfate removal rates are increased at high dilution rates, but this is countered by lower extents of reduction. Biomass concentrations are reduced at higher dilution rates, resulting in the lower extents of sulfate removal. There is a trade-off between high-rate efficiency applications and systems need to be operated at conditions that are optimal to a particular process.

The ideal wastewater treatment system would treat low sulfate wastewater at high dilution rates with biomass retention to increase removal rates. Reactor configurations can be manipulated (for example with recycle) to deal with wastewater streams that have particularly harsh chemical characteristics (very acidic pH and excessively high sulfate concentrations) that cannot be directly treated in anaerobic bioreactors.

5.2 A KINETIC STUDY OF A MIXED POPULATION OF SULFATE REDUCING BACTERIA USING ACETATE AS THE ELECTRON DONOR AND CARBON SOURCE

5.2.1 THE EFFECT OF FEED SULFATE CONCENTRATION

Introduction

As discussed in Chapter 2, sulfate is used as the terminal electron acceptor during the oxidation of a carbon source / electron donor. Possible electron donors include: hydrogen, organic acids such as formate, acetate, propionate and butyrate, various alcohols such as methanol, ethanol as well as fumarate, succinate and aromatic compounds (Postgate, 1984; Hansen, 1988; Widdel, 1988, Widdel & Hansen, 1992; Colleran *et al.*, 1995). Sulfate concentration in the feed has been shown to affect the activity of sulfate reducing bacteria (White and Gadd, 1996; Dries *et al.*, 1998). Using an expanded granular sludge bed with acetate as the organic and electron donor source they found that as the feed sulfate concentration was increased from 0.4 to 0.8 kgm^{-3} the sulfate conversion increased from 70 to 90 %. A subsequent increase in the feed sulfate concentration to 1.0 kgm^{-3} resulted in a decrease in the sulfate conversion to 60 %. The reactor was run at a retention time of 2 hours.

In this sub-task, we have aimed at extending the kinetic data available on the biological reduction of sulfate, using acetate as the electron donor. In particular, the influence of the initial sulfate concentration, sulfate loading rate and temperature were considered. The trends and kinetic data obtained have been used to develop the rate equation.

Materials and Methods

Microorganisms and medium

A mixed culture of anaerobic bacteria containing acidogenic bacteria, methanogenic bacteria and SRB was obtained from the Council for Scientific and Industrial Research (CSIR), Pretoria, South Africa. The culture had previously been used for treatment of a sulfate containing wastewater. The medium used for growth and maintenance of the culture consisted of essential organic substrates, inorganic salts and trace metals (Table 5.4). This medium has been recommended for the growth of anaerobic microorganisms (Grobicki , 1989). All reagents were analytical grade. Sodium sulfate was used as a source of sulfate. The stock cultures were grown in a medium containing 2.5 kg m^{-3} of sulfate ions (3.7 kg m^{-3} of Na_2SO_4). Initially glucose at a

concentration of 1.4 kg m^{-3} was used as the organic carbon source. This was replaced by sodium acetate. The substitution of glucose with acetate restricted the growth of the acidogenic bacteria. To suppress the activity of methanogenic bacteria, bromo-ethane-sulfonic-acid (BESA) at a concentration of 3.2 kg m^{-3} was added to the culture (Visser, 1995). The anaerobic culture was maintained in 1-litre bottles at 35°C on a rotary shaker at 160 rpm and was subcultured on a weekly basis (50% v/v inoculum). In order to remove the oxygen, the medium was purged with filter sterilized gaseous nitrogen prior to inoculation. No pH adjustment was made.

Table 5.4 : Composition of the medium used for growth and maintenance of the anaerobic mixed culture.

Components	Weight (g)
Acetate	20.000
Peptone	0.400
Lab-Lemco[1]	0.133
K_2HPO_4	0.040
$NaHCO_3$	1.250
Na_2SO_4	3.700
Deionised Water	500 mL
Trace Metals	
$CoCl_2.6H_2O$	0.0119
$FeCl_2.4H_2O$	0.0785
$MnCl_2.4H_2O$	0.0038
$NaMoO_4.2H_2O$	0.0038
$NiCl_2.6H_2O$	0.0045
Deionised Water	500 mL

Experimental procedure

The experiments were performed in four identical bioreactors with a capacity of one litre. Mixing was achieved using overhead stirrers with Rushton impellers (D/T = 0.303) at a speed of 400 rpm. To maintain the anaerobic conditions the glass lids of the vessels and other glass fittings were sealed with vacuum grease. Fresh medium was fed into the bioreactor by a variable speed peristaltic pump. To avoid channelling, feed was introduced near the bottom of the reactor. The effluent was discharged by gravity through an overflow tube. The reaction

[1] An extract used for general bacteriological purposes containing 12.4% N and 5.7% NaCl (Oxoid)

temperature was maintained at 35°C, using a circulating waterbath. The pH was controlled at 8.0 ± 0.2 with the addition of either concentrated HCl or a saturated NaOH solution. Figure 5.3 shows a schematic diagram of the experimental set-up used for the kinetic studies.

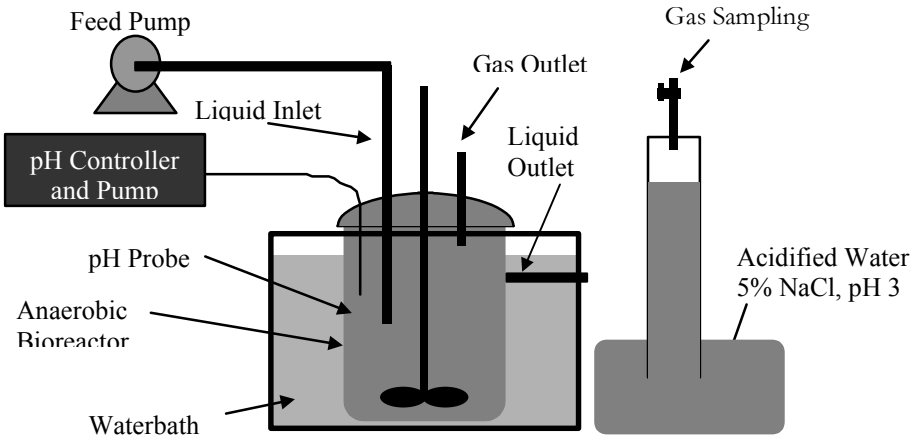

Figure 5.3: Schematic diagram of the experimental set-up

In order to study the effects of sulfate concentration and its volumetric loading on the kinetics of sulfate reduction and microbial growth, four independent experimental runs were conducted. Media (Table 5.4, except for acetate which was added at a various concentrations) containing 1.0, 2.5, 5.0 and 10.0 kg m^{-3} of sulfate were used. In each experiment the bioreactor was charged with 800 mL medium and 200 mL of inoculum (20% v/v). In the experiments with media containing 1.0 and 2.5 kg m^{-3} of sulfate, the stock culture was used as an inoculum. The inoculum for the experiments with media containing 5.0 and 10.0 kg m^{-3} of sulfate were taken from the bioreactors operating with 2.5 and 5.0 kg m^{-3} of sulfate, respectively.

The bioreactors were operated batchwise initially. During the batch operation, the concentration of acetate was increased stepwise from 2.5 to 17.5 kg m^{-3}. This ensured that organic carbon was not the limiting substrate. Once a sufficient reduction of sulfate (90 to 95%) was achieved, the bioreactors were switched to continuous mode. For each medium, increasing feed flow rates in the range 0.004 to 0.042 L h^{-1} (residence times between 10 days and 1 day) were applied. Steady state conditions were used at each flow rate to calculate the kinetics of bacterial growth and sulfate reduction. Steady state conditions were assumed to be established when both the residual sulfate concentration and bacterial concentration varied by less than 10% during a period of operation equal to three retention times. Liquid samples were taken on a daily basis and analysed for sulfate, acetate and bacterial concentrations.

Analytical procedures

A turbidimetric method was used to measure the concentration of sulfate (APHA, 1975). Prior to sulfate determination, suspended solids were removed from the sample by centrifugation. After addition of 0.25 mL conditioning reagent (50 mL glycerol, 30 mL concentrated HCl, 75 g NaCl, 100 mL ethanol and 300 mL deionised water) to 5 mL of sample, an excess amount of finely ground $BaCl_2$ was added and the sample was stirred for 1 minute on a vortex mixer. The absorbance of the sample was measured at a wavelength of 420 nm. The absorbance of the sample was used to calculate the concentration of sulfate. A calibration curve for dependency of adsorption on sulfate concentration was obtained using a similar procedure. Acetate concentration was determined with a High Performance Liquid Chromatograph (HPLC, Beckmann, System Gold), with a UV detector (Detector no 168) and a glass lined Wakosil column. Phosphoric acid solution (20 mM) with a pH of 2.5 was used as the mobile phase. The pH of the mobile phase was adjusted with sodium dihydrogen orthophosphate. The bacterial concentration was determined by measurement of dry weight at 80°C.

Results

The kinetic data for bacterial growth and bioreduction of sulfate at initial concentrations of 1.0, 2.5, 5.0 and 10.0 kg m^{-3} are shown in Figures 5.4, 5.5, 5.6 and 5.7 respectively. The volumetric reduction rate, calculated on the basis of initial concentration of sulfate, flow rate of the feed, working volume of the reactor and conversion, was used to ascertain the kinetics of the reaction.

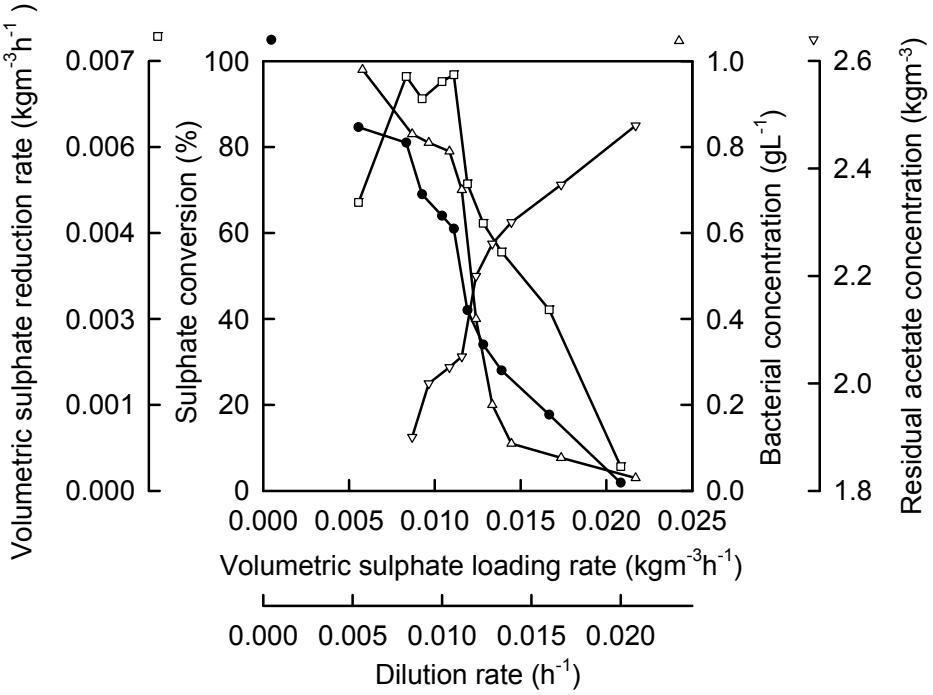

Figure 5.4 : Steady state kinetics of continuous reduction of sulfate in a feed medium containing 1.0 kg m^{-3} sulfate and 2.5 kg m^{-3} acetate at 35°C and pH 7.8. Steady state data presented includes volumetric sulfate reduction rate (□), sulfate conversion (●), bacterial concentration (Δ) and residual acetate concentration (∇).

In the reactor with a feed sulfate concentration of 1.0 kg m^{-3} (Figure 5.4), the maximum bacterial concentration of 0.98 gL^{-1} was observed at a dilution rate of 0.005 h^{-1}. Increasing dilution rates in the range 0.006 to 0.011 h^{-1} resulted in a decrease in bacterial concentration. This decreasing trend became sharper as the dilution rate was increased above 0.011 h^{-1}. As can be seen in Figure 5.4, a high conversion of sulfate to sulfide of 80 to 85%, was observed at volumetric loading rates in the range 0.006 to 0.008 kg m^{-3} h^{-1}. The corresponding reduction rate was 0.007 kg m^{-3} h^{-1}. Increasing the volumetric loading rate in the range 0.008 to 0.011 kg m^{-3} h^{-1}, a relatively constant reduction rate of 0.006 kg m^{-3} h^{-1} was observed. This however, was accompanied by a descending conversion of sulfate. Further increase in loading rate led to a sharp decrease in both conversion and reduction rate of sulfate. The maximum reduction rate in this set of experiments was 0.007 kg m^{-3} h^{-1}, achieved at a retention time of 3.75 days. The corresponding conversion of sulfate was 61%. The trend of acetate utilization was similar to that for sulfate reduction. At low volumetric loadings, corresponding to a high reduction of sulfate, high level of acetate was utilized. The decrease in reduction of sulfate at higher volumetric loadings led to a decrease in utilization of acetate. The ratio of sulfate reduced to acetate utilized

was relatively constant for the range of applied loading rates and was around 0.84 mol sulfate/mol acetate.

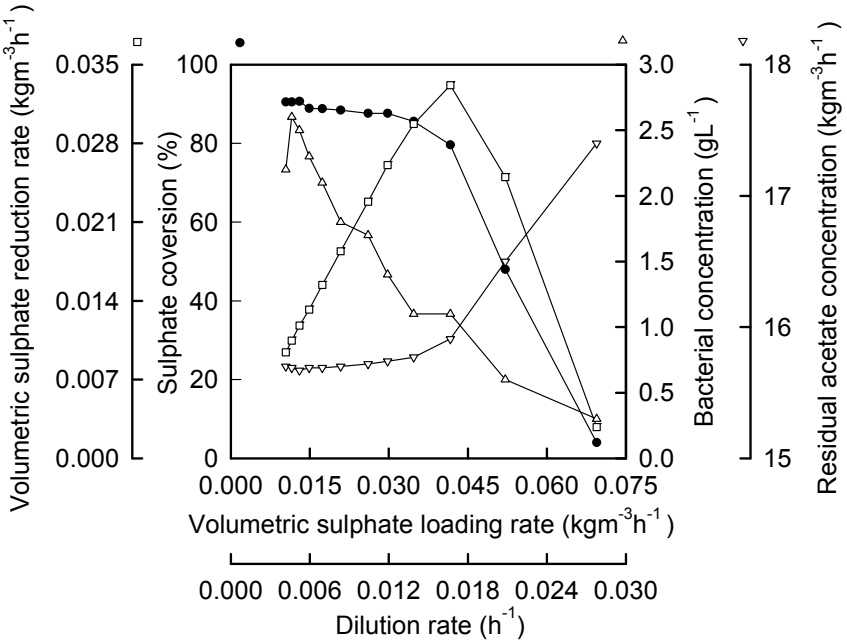

Figure 5.5 : Steady state kinetics of continuous reduction of sulfate in a feed medium containing 2.5 kg m^{-3} sulfate and 17.5 kg m^{-3} acetate at 35°C and pH 7.8. Steady state data presented includes volumetric sulfate reduction rate (□), sulfate conversion (●), bacterial concentration (Δ) and residual acetate concentration (∇).

With a feed medium containing 2.5 kg m^{-3} of sulfate (Figure 5.5) bacterial concentration showed a consistent decrease, due to an increase in dilution rate. The maximum bacterial concentration was 2.6 g L^{-1}, observed at a dilution rate of 0.005 h^{-1}. High conversion of sulfate (80% to 90%) was observed for loading rates in the range 0.010 to 0.040 kgm^{-3} h^{-1}. The increasing of volumetric loadings in this range was accompanied by an enhancement in reduction rate from 0.009 to 0.032 kg m^{-3} h^{-1}. The maximum reduction rate of 0.032 kg m^{-3} h^{-1}, was obtained at a retention time of 2.5 days. The conversion of sulfate at this retention time was 80 %. Applying higher volumetric loading rates led to a substantial decrease in the reduction rate of sulfate. The dependency of acetate utilization and sulfate reduction was similar to the previous run with a constant ratio of 0.77 mole of sulfate reduced /mole of acetate utilized.

In the presence of the feed medium containing 5.0 kg m^{-3} of sulfate (Figure 5.6) the bacterial concentration decreased gradually from 3.1 g L^{-1} to 2.6 g L^{-1} as the dilution rate was increased from 0.005 to 0.014 h^{-1}. This decreasing trend became more pronounced as the dilution rate was increased to values above 0.014 h^{-1}. Applying loading rates ranging from 0.021 to 0.07 kg m^{-3} h^{-1}

the conversion of sulfate varied from 93 to 86 %. Over this range of volumetric loadings a linear increase in reduction rate of sulfate was observed. Further increase of volumetric loading up to 0.14 kg m^{-3} h^{-1} led to a semi-plateau region in the reduction rate curve, accompanied by a sharper decrease in conversion of sulfate. The maximum reduction rate of sulfate in this set of experiments was 0.075 kg m^{-3} h^{-1}, achieved at a retention time 1.5 days. The corresponding conversion of sulfate was 54 %. The ratio of sulfate reduced to acetate utilized in this set of experiments was 0.83 mole of sulfate reduced /mole of acetate utilized.

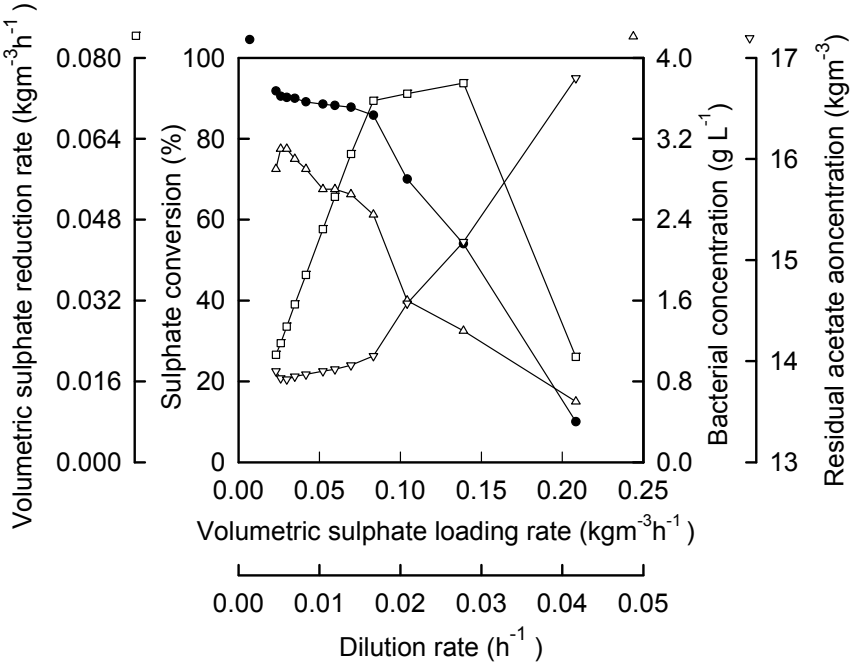

Figure 5.6 : Steady state kinetics of continuous reduction of sulfate in a feed medium containing 5.0 kg m^{-3} sulfate and 17.5 kg m^{-3} acetate at 35°C and pH 7.8. Steady state data presented includes volumetric sulfate reduction rate (□), sulfate conversion (●), bacterial concentration (Δ) and residual acetate concentration (∇).

With feed medium containing 10 kg m^{-3} of sulfate (Figure 5.7) a slight increase in bacterial concentration was observed when the dilution rates varied from 0.005 to 0.008 h^{-1}. The maximum bacterial concentration was 5.1 g L^{-1}. Further increase of dilution rate led to a decrease in bacterial concentration from 5.1 g L^{-1} to 0.6 g L^{-1}. For volumetric loadings in the range 0.04 to 0.21 kg m^{-3} h^{-1} a relatively constant and high conversion of sulfate to sulfide (87 % to 90 %) was observed. The increasing of volumetric loading in this range, however, led to a notable enhancement of sulfate reduction rate. The maximum reduction rate in this set of experiment was 0.17 kg $m^{-3}h^{-1}$ achieved at a retention time of 2 days. The corresponding sulfate

conversion was 82 %. Increasing the volumetric loading rate beyond 0.21 kg m^{-1} h^{-1} resulted in a dramatic decrease in both sulfate conversion and volumetric reduction rate. The coupling of acetate utilization and sulfate reduction was again observed. For the whole range of applied volumetric loading rates, the ratio of sulfate reduced to acetate utilized was around 0.76 mole sulfate /mole acetate.

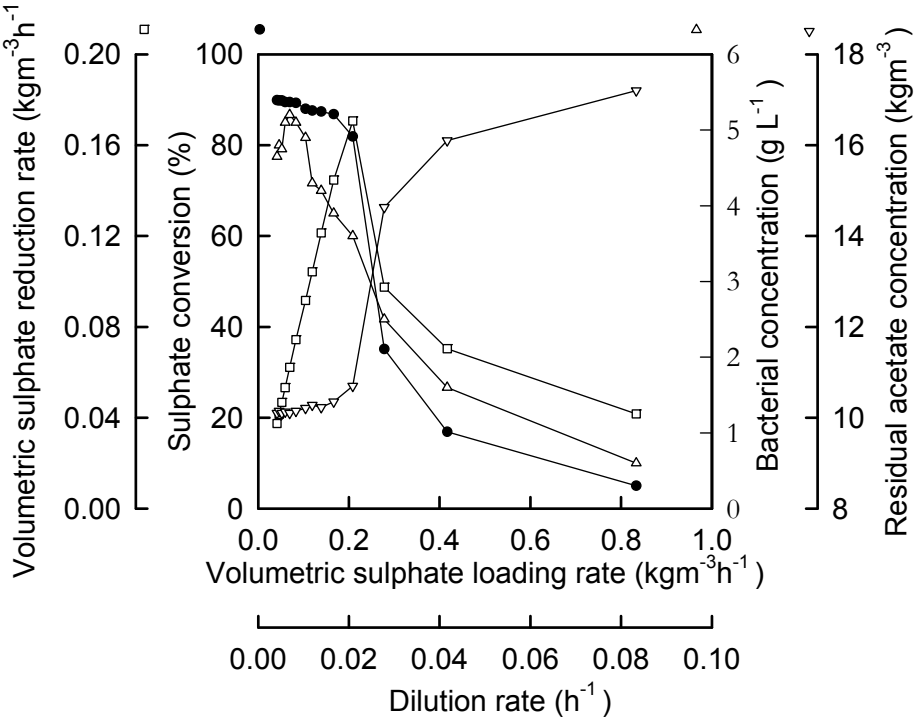

Figure 5.7 : Steady state kinetics of continuous reduction of sulfate in a feed medium containing 10.0 kg m^{-3} sulfate and 17.5 kg m^{-3} acetate at 35°C and pH 7.8. Steady state data presented includes volumetric sulfate reduction rate (□), sulfate conversion (●), bacterial concentration (Δ) and residual acetate concentration (∇).

Modelling of the experimental data

Our approach in development of a kinetic model for bioreduction of sulfate was based on the fundamental relationships between the kinetics of bacterial growth and anaerobic reduction of sulfate. For a growth associated biological reaction, the rate of substrate utilization (sulfate reduction in this case) can be related to the rate of biomass formation by Pirt equation (Pirt, 1975)

$$r_s = \frac{dS}{dt} = \frac{1}{Y_{x/S}} \frac{dX}{dt} + m_S[X] \qquad [5.1]$$

where:

r_s: rate of substrate utilization (reduction rate of sulfate or utilization rate of acetate) (kg m^{-3} h^{-1})

$Y_{x/s}$: yield coefficient (g of biomass produced /g of substrate utilized) (g biomass/g substrate)

dx/dt: $(\mu-k_d)[X]$, rate of biomass formation (h^{-1})

m_s: maintenance coefficient (h^{-1})

μ: specific growth rate (h^{-1})

[X]: biomass concentration (kg m^{-3})

Writing a mass balance for biomass, it can be shown that in a continuous system operating at steady state conditions the specific growth rate (μ) is related to dilution rate by the following expression:

$$D = \frac{F}{V} = \mu - k_d \qquad [5.2]$$

where:

D: dilution rate (h^{-1})

F: flow rate of the feed (m^3 h^{-1})

V: reactor working volume (m^3)

k_d: decay coefficient (h^{-1})

Using the residual concentration of sulfate, determined at various dilution rates it was possible to describe the dependency of the specific bacterial growth rate on concentration of sulfate. The experimental data were treated with a variety of unstructured, non-segregated models, including Monod (Eqn 5.3), Chen and Hashimoto (Eqn 5.4) and Contois models (Eqn 5.5) (Chen & Hashimoto, 1980). The Contois and Chen and Hashimoto models have been used for the prediction of growth rate as a function of residual substrate concentration at high feed substrate concentrations (Chen & Hashimoto, 1980). At high feed substrate concentrations, high biomass concentrations are supported, which in turn affects the mass transfer. This mass transfer effect may be taken into account by modification of K_s, the bulk substrate concentration at which growth occurs at 50 % of μ_m. These modifications are incorporated in Eqn 5.4 and 5.5, as suggested by Contois and Chen and Hashimoto (Chen & Hashimoto, 1980).

Monod Model: $$\mu = \frac{\mu_m [S]}{K_s + [S]} \quad [5.3]$$

where:

μ: growth rate (h^{-1})

μ_m: maximum specific growth rate (h^{-1})

S: limiting substrate concentration (kg m^{-3})

K_s: half saturation constant (kg m^{-3})

Chen and Hashimoto Model: $$\mu = \frac{\mu_m [S]}{K_S [S_o] + (1 - K_S)[S]} \quad [5.4]$$

Contois Model: $$\mu = \frac{\mu_m [S]}{K_s [X] + [S]} \quad [5.5]$$

where:

$[S_o]$: initial substrate concentration (kg m^{-3})

Using a non-linear regression programming, the value of various kinetic coefficients were determined for various initial concentration of sulfate. Among the tested models, Contois expression fitted the data with the highest accuracy, as it was evident from the lowest value for coefficient of variance (an average value of 10.7%) and parity chart (Figure 5.8).

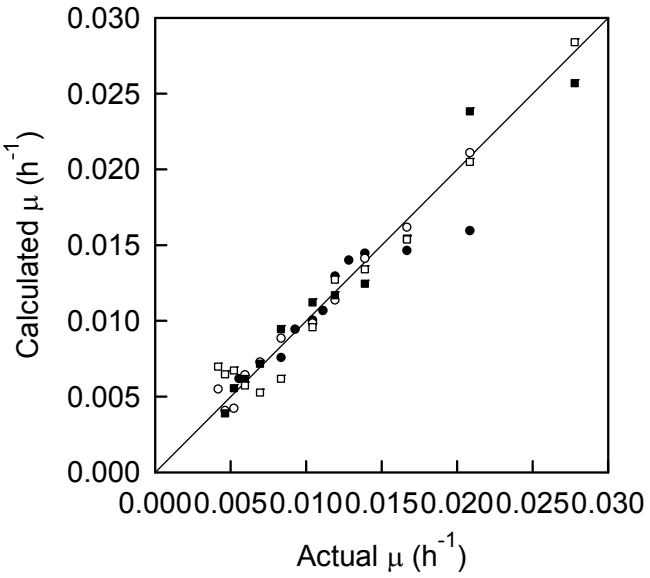

Figure 5.8 : Parity chart for the Contois bacterial kinetic model for continuous bioreactors reducing 1.0 (●), 2.5 (o), 5.0 (■) and 10.0 (□) kg m^{-3}. Data obtained from continuous bioreactors operated at a temperature of 35°C and pH 7.8.

The value of coefficients in the Contois model, as determined for various concentrations of sulfate, are summarized in Table 5.2. The value of μ_m is seen to increase slightly as the concentration of sulfate was increased in the range 1.0 to 10.0 kg m^{-3}. However, performing a t-test on the calculated value of μ_m showed that this dependency was statistically insignificant. The calculated average value of μ_m was 0.061 h^{-1}. The value of the decay coefficient (k_d) was independent of initial concentration of sulfate, with a relatively constant value of 0.035 h^{-1} determined in all cases. Saturation constant (K_s) increased significantly with increasing initial concentration of sulfate. A plot of saturation constant vs. initial concentration of sulfate (Figure 5.7) revealed a linear dependency between the value of K_s and sulfate initial concentration:

Table 5.5 : Kinetic constants obtained using the Contois kinetic model. The constants were obtained using a non-linear regression in Sigmaplot. The data was obtained from continuous bioreactors operating at 35°C and pH 7.8.

Initial sulfate concentration (kgm^{-3})	**μ_m (h^{-1})**	**K_s (kgm^{-3})**	**k_d (h^{-1})**
1.0	0.058	0.027	0.035
2.5	0.061	0.038	0.035
5.0	0.063	0.071	0.035
10.0	0.065	0.125	0.035

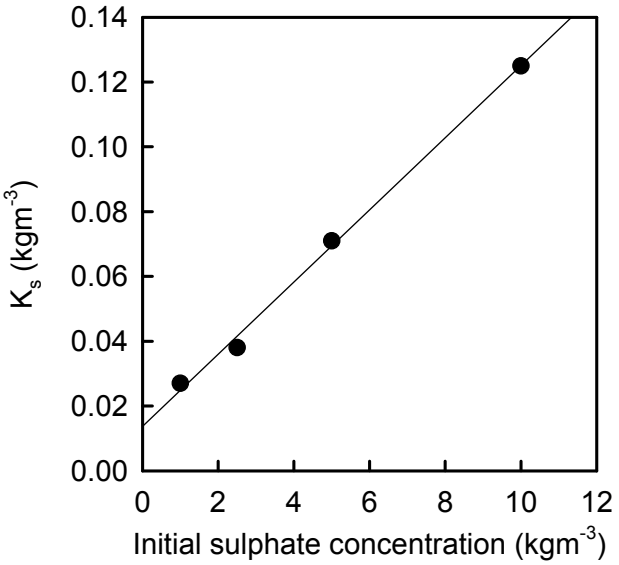

Figure 5.9 : Linear dependency of K_s on initial sulfate concentration.

$$K_s = K'_s [S_0] \quad [5.6]$$

where:

K'_s: apparent saturation constant

$[S_0]$: initial concentration of sulfate ($kg\ m^{-3}$)

The value of K'_s, calculated using the slope of the line, was 0.015. Substituting the rate of biomass production with $(\mu\text{-}k_d)[X]$ in Eqn 5.1, the rate of substrate utilization can be expressed in the following form:

$$\frac{dS}{dt} = \frac{1}{Y_{X/S}}(\mu - k_d)[X] + m_S[X] \quad [5.7]$$

This equation be rearranged to:

$$\frac{dS/dt}{[X]} = \frac{1}{Y_{X/S}}(\mu - k_d) + m_S \quad [5.8]$$

The value of bacterial yield and maintenance coefficient can be determined from a linear plot of specific utilization rate of substrate (sulfate or acetate) as a function of $(\mu\text{-}k_d)$, in which the reciprocal of the slope and intercept of the line represent the value of yield and maintenance coefficient respectively. Using the experimental data, the specific rate of sulfate reduction or specific rate of acetate utilization at different dilution rates, $(\mu\text{-}k_d)$ were calculated and used to

determine the value of bacterial yield and maintenance coefficient (Table 5.6). The value of the maintenance coefficient for the whole range of tested data was insignificant/negligible. The bacterial yield, based on sulfate or acetate, did not vary significantly by increase in initial concentration of sulfate, with the average values being 0.567 g biomass/ g sulfate and 0.574 g biomass/ g acetate.

Table 5.6 : Yield and maintenance coefficients calculated using the specific rate of sulfate and acetate utilization at different dilution rates.

Initial sulfate concentration (kgm^{-3})	**$Y_{x/sulfate}$ g bacteria/ g sulfate**	**$Y_{x/acetate}$ g bacteria/g acetate**	**m_s (h^{-1})**
1.0	0.584	0.575	-0.002
2.5	0.573	0.561	0.001
5.0	0.567	0.580	0.000
10.0	0.569	0.572	-0.001

Substituting the values of various coefficients, $Y_{X/S}$, μ_m, K'_s, k_d, into Eqn 5.8, an expression for the kinetics of sulfate reduction can be derived:

$$r_s = \left(\frac{0.061[S]}{0.015[S_0][X] + [S]} - 0.035 \right) \frac{[X]}{0.567} \qquad [5.9]$$

Using Eqn 5.9 and writing a material balance for sulfate concentration in the continuous bioreactor, volumetric reduction rate of sulfate at different volumetric loadings was calculated. The values of actual and calculated volumetric reduction rates are compared in Figure 5.10. As can be seen, the derived rate expression is able to predict the performance of the bioreactor with an acceptable level of accuracy, the error being less than 24 %.

The overall error of the model prediction can be determined for individual values of the sulfate reduction rate by applying the propagation of error concept. This involves taking the differential of r_S (Eqn 5.8) with respect to each variable or constant that contributes to the error. It is applicable where the variables are independent (Meyer, 1975). The contribution to the overall

error arises from the error in regressing the experimental data to ascertain $Y_{x/s}$ and μ and the experimental error arising from the determination of [X] and [S].

Considering all the contributory factors, the overall error can be estimated by the following expression:

$$\sigma_{r_s}^2 = \left(\frac{[x]}{Y_{x/s}}\right)^2 \sigma_\mu^2 + \left(\frac{\mu}{Y_{x/s}}\right)^2 \sigma_x^2 + \left(\frac{-\mu[X]}{Y_{x/s}{}^2}\right)\sigma_{Y_{x/s}}^2 \qquad [5.10]$$

where: σ = error

Using the equation for r_s shown above the percentage overall error is given by:

$$\frac{\sigma_{r_s}}{\bar{r}_s} = \sqrt{\frac{\sigma^2{}_\mu}{\bar{\mu}} + \frac{\sigma_X^2}{[\bar{X}]} + \frac{\sigma_{Y_{x/s}}^2}{\bar{Y}_{x/s}}} \qquad [5.11]$$

The percentage error in μ and $Y_{X/sulfate}$ results from error fitting the experimental data to the Contois model and Pirt equation respectively. The error associated with the model prediction (calculated to be around 24 %) is included as a line in the parity chart. The parity chart for experiments conducted at initial sulfate concentrations of 1.0, 2.5, 5.0 and 10.0 kg m^{-3} is shown as Figure 5.10. It can be seen that the calculated reduction rate points (y axis) lie within the error defined on the parity line. Hence the model predicts the data well, to within the limits allowed by the error propagation (24 %). Additionally, from χ^2 tests which are used to compare two sets of data for significant differences or similarities depending on the hypothesis (χ^2 is the sum of the ratio of the squares of the difference between the actual and the predicted value, $\sum \frac{(\text{Actual} - \text{Predicted})^2}{\text{Predicted}}$). For the four sulfate concentrations, it was found that the model was significant within the 95% confidence level (χ^2 less than 1.43).

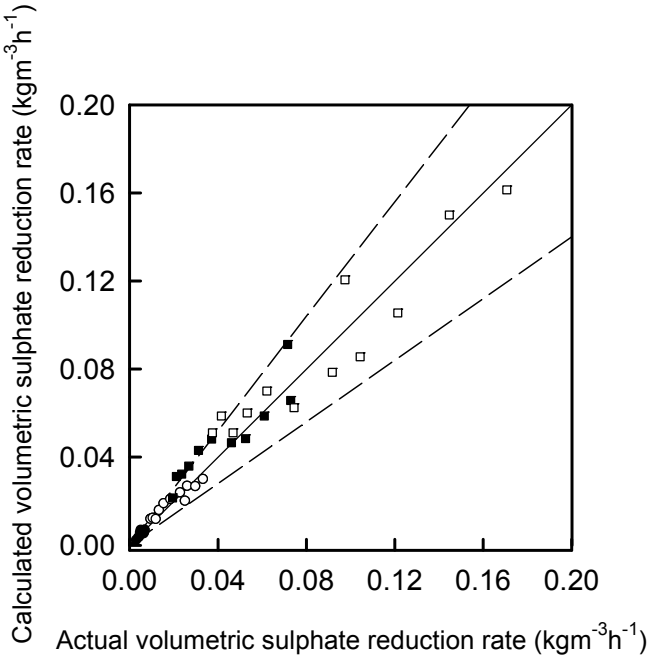

Figure 5.10 : Parity chart for volumetric sulfate reduction rates for the chemostat reducing 1.0 (●), 2.5 (○), 5.0 (▪) and 10.0 (□) kgm^{-3} sulfate. (—) represents parity line and (----) represents 24 % error line. Data obtained from chemostat operating at 35°C and pH 7.8

Discussion

The kinetics of anaerobic reduction of sulfate at various initial concentrations of 1.0, 2.5, 5.0 and 10.0 kg m^{-3} are compared in Figure 5.11. In all cases, the volumetric reduction rate of sulfate is enhanced linearly with an increase in volumetric loadings, where the dilution rate lies below washout value. The onset and progress of washout is gradual, due to the presence of various species of SRB in the mixed culture. Despite a similar trend in dependency of volumetric reaction rate on volumetric loading of sulfate, the increase in initial concentration of sulfate leads to improved reaction rates. For instance the maximum reaction rate with a medium containing 1.0 kg m^{-3} of sulfate is 0.007 kg m^{-3} h^{-1}, while in the presence of a medium containing 10.0 kg m^{-3} sulfate an enhanced rate of 0.17 kg m^{-3} h^{-1} is observed. The corresponding loading rate is also increased from 0.011 to 0.2 kg m^{-3} h^{-1}. This is consistent with observations of Stucki *et al.* (1993) in a biofilm system. Using a mixed SRB population in a fixed bed bioreactor, with acetate as an organic carbon source, Stucki *et al.* (1993) found that an increase in initial concentration of sulfate could lead to higher reaction rates.

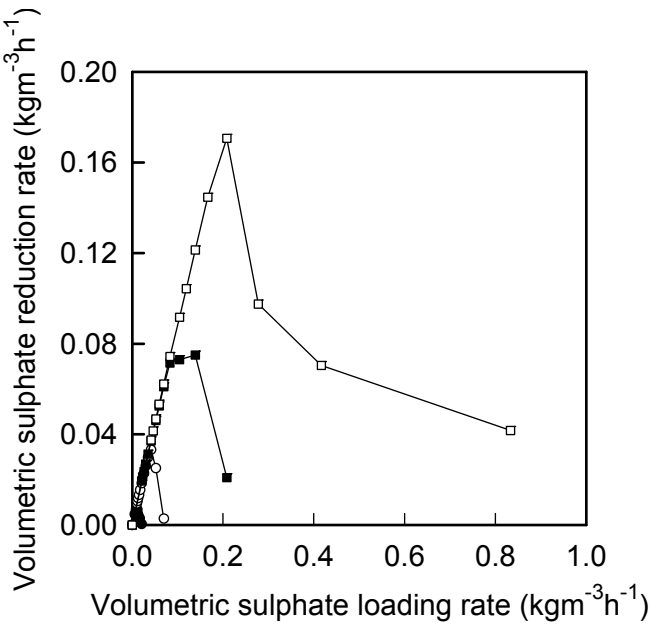

Figure 5.11: Dependency of steady state volumetric sulfate reduction rate on volumetric sulfate loading rate and initial sulfate concentration. Data obtained from continuous bioreactors operating with 1.0 (●), 2.5 (○), 5.0 (■) and 10.0 (□) kg.m^{-3} sulfate at 35°C and pH 7.8.

For a given dilution rate the bacterial concentration increased as higher concentrations of sulfate were used in the feed. The maximum specific growth rate (μ_m) and decay coefficient (k_d) were not dependent on initial concentration of sulfate, while saturation constant (K_s) displayed a linear increase with increase in concentration of sulfate. The average value of μ_m calculated in this work (0.061 h^{-1}) is in agreement with those reported in the literature. Widdel & Pfenning (1982) and O'Flaherty, *et al* (1998) reported values of 0.063 and 0.068 h^{-1} respectively for specific growth rate of *Desulfotomaculum acetooxidans*. Smaller values for SRB μ_m have also been reported in the literature. Investigating the competition between SRB and methanogens, Visser (1995) found that μ_m varied between 0.002 and 0.005 h^{-1}. A value of 0.013 h^{-1} was reported for the specific growth rate of *Desulfobacter postgatei* by Ingvorsen *et al.* (1984). These variations could be attributed to different bacterial species and various conditions applied in independent works.

The saturation constant (K_s) was found to be an increasing function of initial sulfate concentration. Studying the production of methane, with livestock waste as the carbon source, Chen & Hashimoto (1980) found that K_S remained constant as the COD was increased from 0.50 to 1.50 kg m^{-3}, while above a COD of 1.50 kg m^{-3} K_S increased as COD was increased in the feed. This increase in K_S was attributed to saturation of the system with substrate. K_s values

reported in literature for bioreduction of sulfate vary between 0.018 and 0.033 kg m^{-3} (Chen & Hashimoto, 1980). Studying the reduction of sulfate by a mixed SRB culture in a continuous UASB, Visser (1995) found K_s to be 0.033 kgm^{-3} for a granular biomass system and 0.018 kg m^{-3} for a freely suspended cell system. Growing a pure culture of *Desulfobacter postgatei* in a continuous stirred tank reactor under sulfate limitation, Ingvorsen *et al* (1984) found K_s to be 0.024 kg m^{-3}. The K_s values obtained for this work (0.027 to 0.125 kg m^{-3}) compare well with those reported in the literature for the anaerobic reduction of sulfate with acetate as the organic source.

The values of $Y_{x/sulfate}$ and $Y_{x/acetate}$ did not depend on initial concentration of sulfate. $Y_{x/sulfate}$ and $Y_{x/acetate}$ were 0.567 g biomass/g sulfate and 0.574 g biomass/g acetate respectively. Data for cell yield based on sulfate are not readily available in the literature. Ingvorsen *et al.* (1984) determined $Y_{x/sulfate}$ of *Desulfobacter postgatei* grown in batch to be 0.158 g bacteria/g sulfate. There is a large variation in yield coefficients based on acetate, $Y_{x/acetate}$, reported in the literature. Middelton and Lawrence (1977) observed that the overall yield for a mixed SRB culture grown on acetate-sulfate medium in a batch system was 0.065 g bacteria/g acetate. Widdel and Pfennig (1981) reported yield coefficients for *Desulfobacter postgatei* and *Desulfotomaculum acetoxidans* to be 0.074 and 0.095 g bacteria/kg acetate respectively. Employing a mixed anaerobic culture in a continuous system Visser (1995) calculated a yield coefficient of 0.043 g bacteria/g acetate. O' Flaherty *et al.* (1998) reported the yield coefficient for *Desulfotomaculum acetoxidans* and *Desulfonema magnum* to be 0.114 and 0.139 g bacteria/g acetate respectively.

In conclusion the results of the present study indicate that the growth of sulfate-reducing bacteria and the kinetics of anaerobic reduction of sulfate are influenced by initial concentration of sulfate and application of high concentrations of sulfate could enhance the rate of the reaction and lead to higher bacterial activity. The kinetic expression derived in this work describes the effects of initial and residual concentrations of sulfate, as well as bacterial concentration on the kinetics of sulfate bioreduction and is able to predict the experimental data with a reasonable accuracy.

5.2.2 EFFECT OF TEMPERATURE

Introduction

Anaerobic sulfate reduction is a complex reaction and as such is influenced by a variety of parameters. These include the availability of electron donor and its structure, pH, temperature, sulfate concentration, as well as the inhibitory effects of heavy metals and sulfide (Fauque *et al.*,

1980; Postgate, 1984; Legall and Fauque, 1988; Rintala and Lettinga, 1992, Oude Elferink *et al.*, 1994; Omil *et al.*, 1998)

Previous work has investigated the effects of initial sulfate concentration and its volumetric loading on the kinetics of reaction and activity of sulfate reducing bacteria (Moosa *et al*, 2001). The increase in initial concentration of sulfate in the range 1.0 to 10.0 kgm^{-3} enhanced the reaction rate from 0.007 to 0.17 $kgm^{-3}h^{-1}$. For a given initial concentration of sulfate and for dilution rates below washout value, an increase in volumetric loading of sulfate led to a linear increase in volumetric reduction rate of sulfate. The initial concentration did not have a significant on maximum specific growth rate (μ_m), decay coefficient (k_d) and bacterial yields ($Y_{X/sulfate}$ and $Y_{X/acetate}$), with the values of these coefficients being 0.061 h^{-1}, 0.035 h^{-1}, 0.567 g bacteria/g sulfate and 0.572 g bacteria/g acetate respectively. The saturation constant (K_s) was an increasing function of sulfate concentration, with the lowest and highest values of K_s being 0.027 and 0.125 kgm^{-3} respectively. Using the experimental data a kinetic model, incorporating terms for the effects of initial and residual concentrations of sulfate and biomass concentration, was developed.

Temperature is an important parameter, which affects the kinetics of sulfate reduction and the activity of SRB. Mesophilic strains of SRB, with growth temperatures in the range 28 to 45°C, as well as thermophilic strains with optimum growth temperatures ranging from 54 to 70°C, have been isolated (Johnson, 2000). Using a mixed SRB culture in a batch experiments, Middleton and Lawrence (1977) showed that the maximum specific rate of organic carbon utilization enhanced as the temperature increased from 20 to 31°C. For the same range of temperature the saturation constant (K_s) decreased, due to an increase in temperature. Using a continuous system Okabe and Characklis (1992) found that the maximum specific growth rate (μ_{max}) of *Desulfovibrio desulfuricans* was relatively constant for temperatures in the range 25 to 43°C, whereas, the saturation constant (K_s) increased with an increase in temperature. These authors reported that an increase in temperature led to a decrease in the yield coefficient. This contrasts with the results of Senez (1962), who reported a constant yield for Desulfovibrio desulfuricans over a range of temperatures.

The objective of this subtask was to assess the effect of temperature and volumetric loading of sulfate on the activity of a mixed population of SRB and to extend the kinetic model describing the effect of various physicochemical conditions, such as sulfate concentration and bacterial concentration developed in Section 5.2.1 to describe the effects of temperature on the kinetics of anaerobic reduction of sulfate.

Materials and Methods

The microorgansims used, medium and culture conditions, reactor set-up and analytical techniques employed are as described in section 5.2.1.

Experimental procedure.

In order to study the effects of temperature on the kinetics of sulfate reduction four independent experimental runs at 20, 25, 30 and 35°C were conducted. In each experiment the bioreactor was charged with 800 mL medium (Table 5.4, 5 kg m^{-3} of sulfate, 17.5 kg m^{-3} of acetate) and 200 mL of inoculum (20% v/v). The stock culture was used as an inoculum.

The bioreactors were initially operated batchwise. Once a sufficient reduction of sulfate (90 to 95%) was achieved the bioreactors were switched to continuous mode. In each experimental run, the flow rate of the feed was varied in the range 0.004 to 0.042 L h^{-1} (residence times between 10 days and 1 day). Steady state conditions were used at each flow rate to estimate the kinetics of sulfate reduction and bacterial growth. Steady state conditions were assumed to be established when both the residual sulfate concentration and bacterial concentration varied by less than 15 % during a period of operation equal to three retention times. Liquid samples were taken on a daily basis and analysed for sulfate, acetate and bacterial concentrations. Regular gas samples were taken from the headspace and analyzed for methane and hydrogen sulfide. In all cases methane was not detected due to the absence of methanogens and hydrogen sulfide was not detected due to the pH of the reactor being at 7.8.

Results

Kinetics of continuous bacterial reduction of sulfate at 20, 25, 30 and 35°C are shown in Figures 5.12, 5.13, 5.14 and 5.15 respectively. The volumetric reduction rate, calculated on the basis of initial concentration of sulfate, flow rate of the feed, working volume and conversion, was used to ascertain the kinetics of reaction.

Kinetics of continuous bacterial reduction of sulfate at 20°C, at an inlet sulfate concentration of 5.0 kg m^{-3} and a pH of 7.8 are shown as Figure 5.12. On operating the bioreactor at 20°C, a maximum bacterial concentration of 2.5 g L^{-1} was observed at a dilution rate of 0.007 h^{-1} (volumetric sulfate loading rate of 0.035 kg m^{-3}). Increasing the dilution rate in the range 0.007 to 0.042 h^{-1} (volumetric sulfate loading rate of 0.035 to 0.210 kg m^{-3}) resulted in a decrease in bacterial concentration. As can be seen in Figure 5.12, the conversion of sulfate at 20°C was relatively low, with a maximum value of 39 % at a loading rate 0.042 kg m^{-3} h^{-1} (dilution rate of

0.008 h^{-1}). The increasing of volumetric sulfate loading rate up to 0.139 kg m^{-3} h^{-1} (dilution rate of 0.028 h^{-1}) enhanced the sulfate reduction rate. The maximum volumetric sulfate reduction rate in this set of experiments was 0.030 kg m^{-3} h^{-1}, achieved at a volumetric sulfate loading rate of 0.139 kg m^{-3} h^{-1} (dilution rate of 0.028 h^{-1}). The corresponding conversion of sulfate was 22 %. Further increase in volumetric sulfate loading resulted in a dramatic decrease in the volumetric reduction rate of sulfate. The residual acetate concentration profile was similar to that for residual sulfate concentration (residual sulfate concentration profiles not shown). The ratio of sulfate reduced to acetate utilized was relatively constant at 0.80 ± 0.058 moles sulfate/moles acetate for the range of loading rates applied.

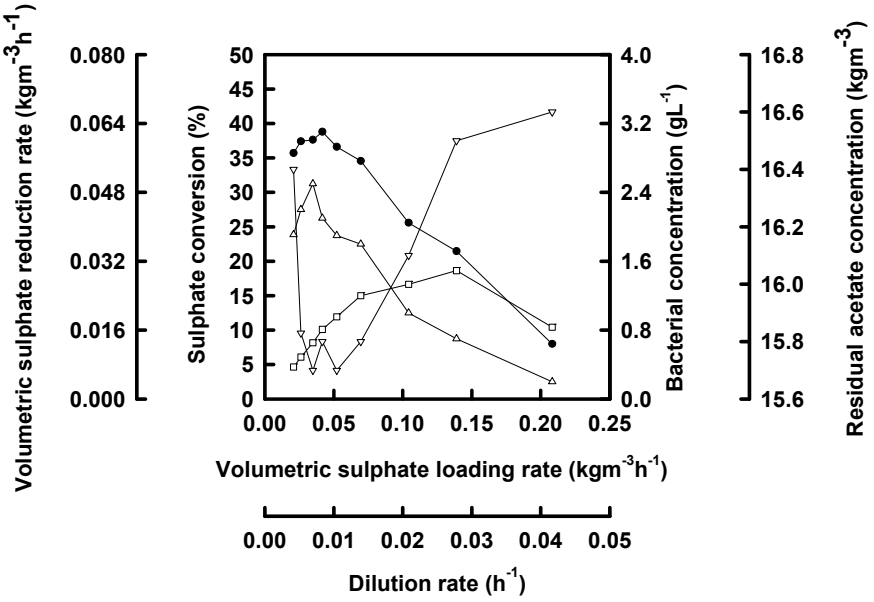

Figure 5.12 : Kinetic results of continuous reduction of sulfate at a temperature of 20°C

Figure 5.13 presents the kinetic results of the bioreactor operating at 25°C. A maximum bacterial concentration of 2.6 g L^{-1} was achieved at a dilution rate of 0.007 h^{-1} (volumetric sulfate loading rate of 0.035 kg $m^{-3}h^{-1}$). On further increase of dilution rate up to 0.042 h^{-1} (volumetric sulfate loading rate of 0.208 kg $m^{-3}h^{-1}$) the bacterial concentration decreased. Applying volumetric sulfate loading rates from 0.021 to 0.070 kg $m^{-3}h^{-1}$ (dilution rate range of 0.004 to 0.014 h^{-1}) the conversion of sulfate remained constant (44 to 48 %). Over this range of volumetric sulfate loadings, a linear increase in reduction rate of sulfate was observed. Further increase of volumetric sulfate loading up to 0.14 kg $m^{-3}h^{-1}$, while accompanied by a decrease in conversion of sulfate, led to a continued increase in sulfate reduction rates. The maximum reduction rate of sulfate in this set of experiments was 0.036 kg $m^{-3}h^{-1}$, achieved at a volumetric sulfate-loading rate of 0.139 kg m^{-3} h^{-1} (dilution rate of 0.028 h^{-1}). The corresponding conversion

was 26 %. The ratio of sulfate reduced to acetate utilized in this set of experiments was 0.76 ± 0.047 moles sulfate/moles acetate.

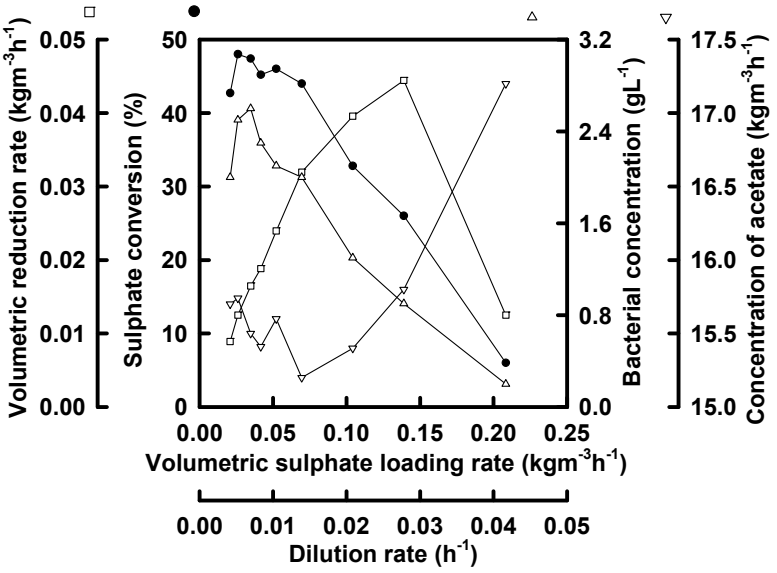

Figure 5.13 : Kinetic results of continuous reduction of sulfate at a temperature of 25°C

Operating the bioreactor at 30°C, the bacterial concentration exhibited a linear decrease over the range of dilution rates employed (Figure 5.14). The maximum bacterial concentration of 2.6 g L^{-1} was found at a dilution rate of 0.005 h^{-1} (volumetric sulfate loading rate of 0.026 kg $m^{-3}h^{-1}$). The maximum conversion of sulfate 75 %, was observed at a volumetric sulfate loading of 0.021 kg $m^{-3}h^{-1}$ (dilution rate of 0.005 h^{-1}). Increasing the volumetric sulfate-loading rate in the range 0.021 to 0.10 kg $m^{-3}h^{-1}$ (dilution rate range of 0.004 to 0.021 h^{-1}), while decreasing the conversion of sulfate to 62 %, led to a notable enhancement of the sulfate reduction rate. The maximum reduction rate achieved was 0.056 kg $m^{-3}h^{-1}$ at a volumetric sulfate-loading rate of 0.104 kg $m^{-3}h^{-1}$ (dilution rate of 0.208 h^{-1}). The corresponding sulfate conversion was 55 %. Increasing the volumetric loading rate beyond 0.140 kg $m^{-3}h^{-1}$ (dilution rate of 0.021 h^{-1}) resulted in a dramatic decrease in both sulfate conversion and volumetric reduction rate. For the range of applied volumetric loading rates, the ratio of reduced sulfate to acetate utilized was 0.81 ± 0.104.

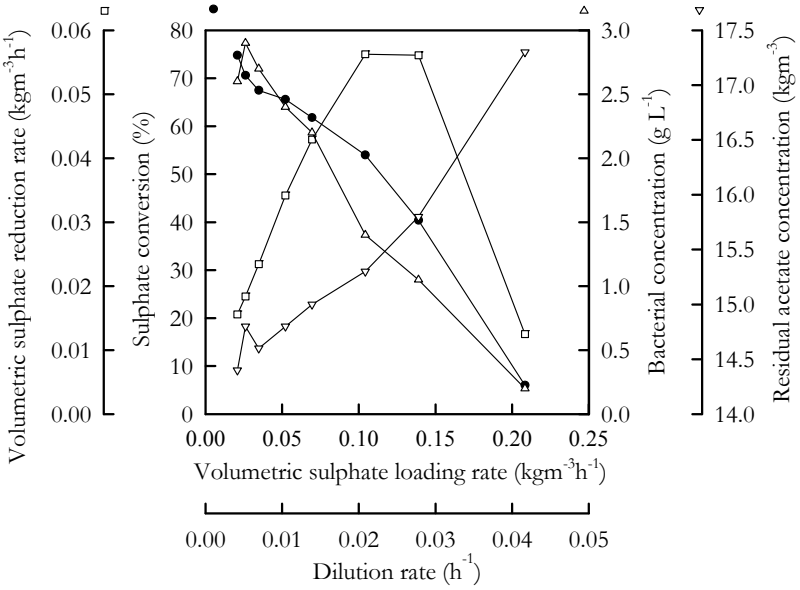

Figure 5.14 : Kinetic results of continuous reduction of sulfate at a temperature of 30°C

During the experiment at 35°C (Figure 5.15), the maximum bacterial concentration of 3.2 g L^{-1} was observed at a dilution rate of 0.004 h^{-1} (volumetric sulfate loading rate of 0.023 kg $m^{-3}h^{-1}$). Bacterial concentration decreased with increasing dilution rate over the range 0.005 to 0.042 h^{-1} (volumetric sulfate loading rate range of 0.026 to 0.0208 kg m^{3} h^{-1}).

For volumetric sulfate loading rates in the range 0.021 to 0.083 kg m^{-3} h^{-1} (dilution rate range of 0.004 to 0.017 h^{-1}), a relatively constant and high conversion of sulfate, of 87 to 90 %, was achieved. Over this range of volumetric sulfate loading rates a linear increase in the volumetric sulfate reduction rate from 0.019 to 0.072 kg $m^{-3}h^{-1}$ was found.

A further increase of volumetric sulfate loading rate to 0.139 kg $m^{-3}h^{-1}$ (dilution rate of 0.028 h^{-1}), while accompanied by a sharper decrease in conversion, led to a semi-plateau region in the reduction rate curve. The maximum reduction rate of sulfate in this set of experiments was 0.075 kg $m^{-3}h^{-1}$ achieved at a volumetric sulfate-loading rate of 0.139 kg m^{-3} h^{-1} (dilution rate of 0.028 h^{-1}). The corresponding sulfate conversion was 54 %. The molar ratio of sulfate reduced to acetate utilized was 0.83 ± 0.014 for the range of applied loading rates.

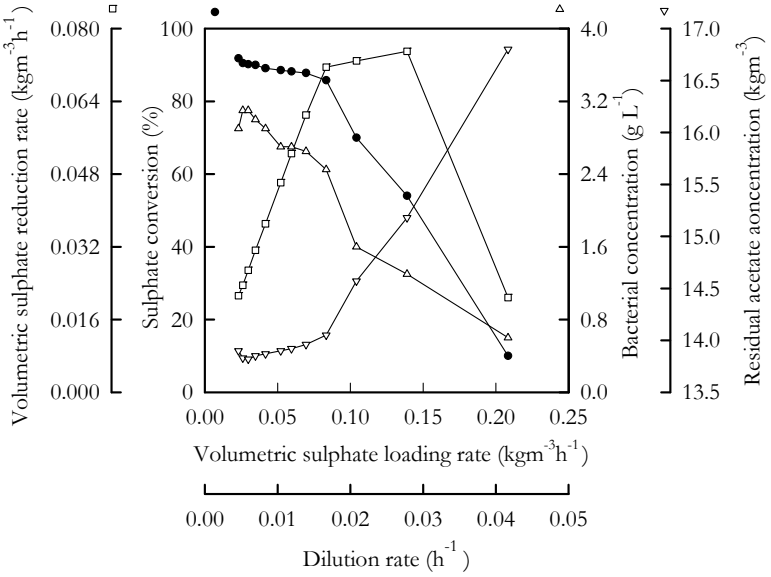

Figure 5.15 : Kinetic results of continuous reduction of sulfate at a temperature of 35°C

Model Development

In order to incorporate the effect of temperature into the derived model (Eqn 5.19), the experimental data was fitted to Eqn 5.5, the Contois equation, and the values of maximum specific growth rate (μ_m), the saturation constant (K_s) and the decay coefficient (k_d) were calculated for the four temperatures investigated in this work. These are given in Table 5.7. The coefficient obtained is given in Table 5.8 and the parity charts are presented in Figure 5.16.

Table 5.7 : Kinetic constants obtained using the Contois kinetic model. The constants were obtained using a non-linear regression package Sigmaplot.

Temperature	μ_m	K_s	k_d
°C	**h^{-1}**	**kg m^{-3}**	**h^{-1}**
20	0.06	4.746	0.008
25	0.06	1.467	0.022
30	0.06	0.613	0.025
35	0.06	0.078	0.038

Table 5.8 : Dependency of coefficient of variance (CV) on temperature in the range 20 to 35°C for the prediction of μ using the Contois equation

Temperature (°C)	**20**	**25**	**30**	**35**
CV (%)	14.578	13.269	9.153	10.840

The maximum specific growth rate, μ_m, of 0.061 ± 0.001 h^{-1}, was found to be constant at the 99 % significance level from a t-test. The value of the decay coefficient (k_d) increased from 0.008 to 0.035 h^{-1}as the temperature was increased from 20 to 35°C. The dependency of k_d on temperature can be described by an Arrhenius function (Eqn. 5.12). The Arrhenius behaviour is illustrated in Figure 5.17 (R^2 of 0.99). An Arrhenius constant of 8.8×10^{11} kg m^{-3}, and an activation energy of 78.7 kJ K^{-1} mol^{-1}, was determined. The saturation constant (K_s) decreased with increasing temperature. The dependency of K_s on temperature can also be described by an Arrhenius type equation (Eqn. 5.12). The 'Arrhenius type' dependence of the saturation constant on temperature is shown in Figure 5.18 (R^2 of 0.96). The values of K_0 and E_a determined were 3.26×10^{-35} kgm^{-3} and –198 $kJK^{-1}mol^{-1}$ respectively.

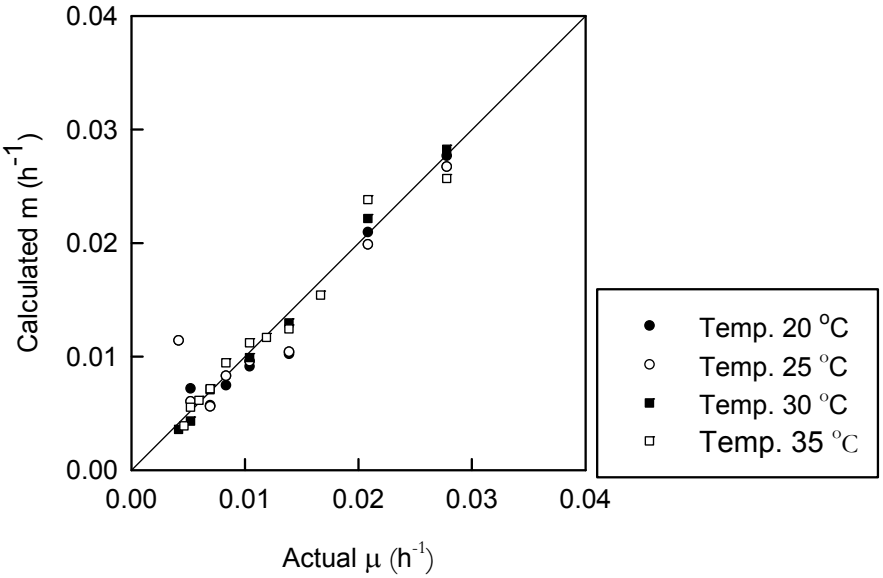

Figure 5.16 : Parity chart for the Contois model for the continuous reduction of sulfate at temperatures of 20, 25, 30 and 35°C

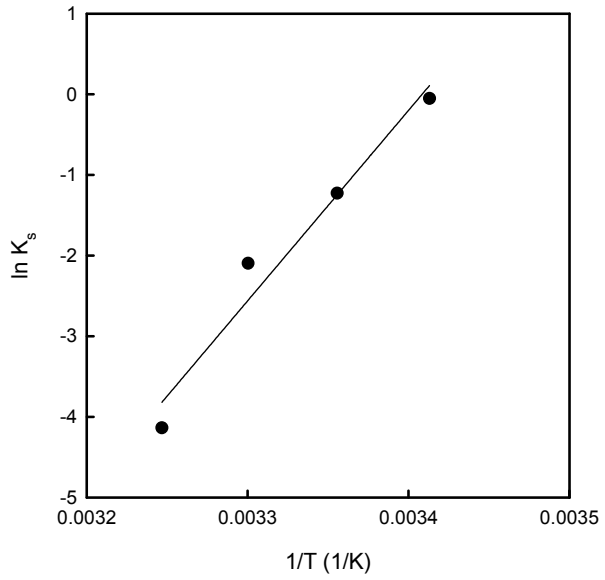

Figure 5.17 : Arrhenius plot for the dependency k_d on temperature $k_d = K_0 e^{-E_a/RT}$ [5.12] where $E_a$is the pseudo-activation energy (kJ mol^{-1}),R is the universal gas constant (kJ.K^{-1}.mol^{-1}), a K_0 a constant, (kg substrate m^{-3}) and T is the absolute temperature (K)

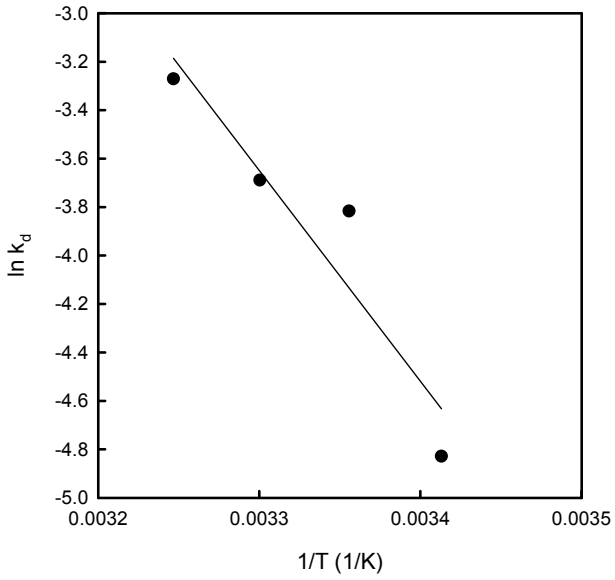

Figure 5.18 : Arrhenius plot for the dependency of K_s on temperature $K_S = K_0 e^{-E_a/RT}$ [5.13]

The value of bacterial yield and maintenance coefficient can be determined from a linear plot of specific utilization rate of substrate (sulfate or acetate) as a function of (μ-k_d), in which the reciprocal of the slope and intercept of the line represent the value of yield and maintenance

coefficient respectively. From the experimental data, the specific rate of sulfate reduction or specific rate of acetate utilization at different dilution rates, (μ-k_d) was calculated and used to determine the value of the bacterial yield and maintenance coefficients (Table 5.7). The value of the maintenance coefficient for the whole range of tested data was insignificant/negligible. The bacterial yield, based on sulfate or acetate, remained constant at the 99 % significance level (t-test, $Y_{X/Sulfate}$ had a variance of 1.2 % and $Y_{X/acetate}$ had a variance of 1.4 %) over the range of applied temperatures. The average value for $Y_{X/Sulfate}$ was 0.568±0.007 g biomass/g sulfate and $Y_{X/acetate}$ was 0.600±0.016 g biomass/g acetate.

The dependency of volumetric reduction rate of sulfate on bacterial concentration and residual sulfate concentration can be represented by Eqn 5.9. Dependence of the parameters K_s and k_d on temperature have been illustrated, while μ_m and $Y_{x/S}$ appear independent of temperature.

K_s can be substituted according to Eqn 5.14 to describe dependency on both temperature (T) and initial sulfate concentration (S_0).

$$K_S = 6.52 \times 10^{-36} e^{198/RT} [S_0] \qquad [5.14]$$

Similarly k_d can be substituted according to Eqn 5.15 to include the Arrhenius dependence on T.

$$k_d = 8.8 \times 10^{11} e^{-78.7/RT} \qquad [5.15]$$

The resultant model for volumetric sulfate reduction rate, including temperature dependency is:

$$r_S = \left(\frac{0.061[S]}{6.52 \times 10^{-35} e^{198/RT}[S_0][X]+[S]} - 8.8 \times 10^{11} e^{-78.7/RT} \right) \frac{[X]}{0.568} \qquad [5.16]$$

Using Eqn 5.16 as the governing expression for the kinetics of anaerobic reduction of sulfate and writing a mass balance, the performance of the continuous bioreactor, operating at different temperatures was assessed. The experimental error in the model prediction was calculated as outlined previously. An average error of 24 % was obtained. The parity chart for the range of reaction temperatures and a feed sulfate concentration of 5.0 kgm^{-3} is given as Figure 5.19. The model is significant at the 95 % confidence limit (χ^2 test).

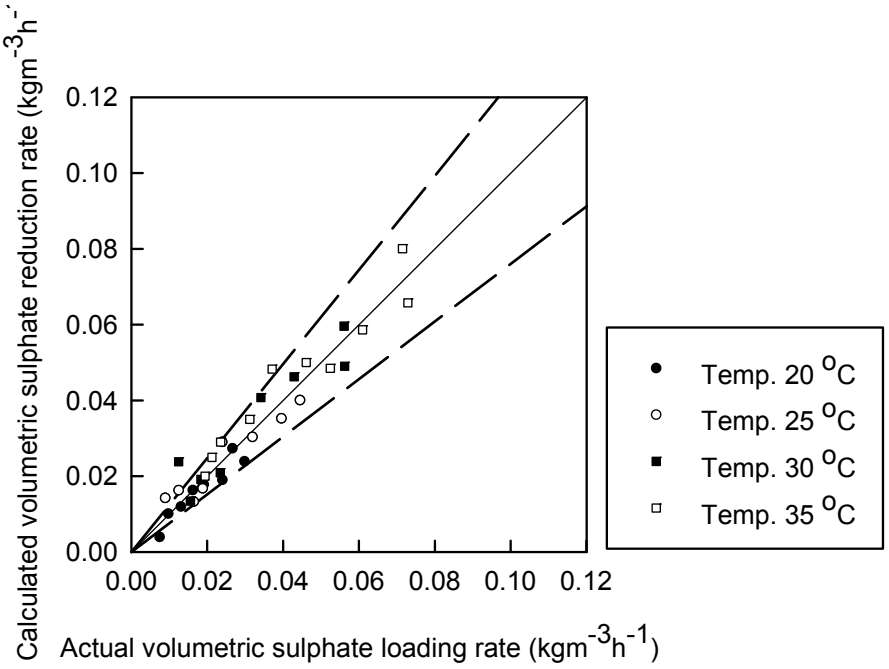

Figure 5.19 : Parity chart for volumetric sulfate reduction rate for the continuous reduction of sulfate at temperatures of 20, 25, 30 and 35°C

Discussion

The kinetics of anaerobic reduction of sulfate at temperatures of 20, 25, 30 and 35°C are compared in Figure 5.20. For the temperature range, 20 to 35°C, the increasing of volumetric sulfate loading rate from 0.021 to 0.080 $kgm^{-3}h^{-1}$ resulted in a linear increase in volumetric sulfate reduction rate. In the range 0.080 to 0.140 $kgm^{-3}h^{-1}$ the reduction rate showed a reduced dependence on volumetric sulfate loading rate. Further increase in volumetric sulfate loading rate resulted in a decrease in volumetric sulfate reduction rate linked to washout of biomass. The magnitude of the volumetric sulfate reduction rate increased with increasing temperature. As the temperature was increased in the range 20 to 35°C, the maximum reduction rate increased from 0.030 to 0.075 $kgm^{-3}h^{-1}$. The volumetric loading rate at which the maximum volumetric sulfate reduction rate occurred was similar for all temperatures applied. A similar trend of increasing sulfate volumetric loading rate with temperature was observed by Middleton and Lawrence (1977). They investigated the effect on batch microbial growth kinetics of a mixed SRB population at temperatures of 20, 25 and 31°C with acetate was the limiting organic nutrient. An increase in volumetric sulfate reduction rate from 0.0009 $kgm^{-3}h^{-1}$ to 0.0019 $kgm^{-3}h^{-1}$ was reported as the temperature increased from 20 to 31°C. Investigating the effect of two temperatures (22 and 31°C) on the continuous conversion of sulfate in a 1.6 l stirred tank using lactic acid as the limiting organic nutrient, Barnes *et al* (1992a) observed a similar response to

increased temperature in terms of volumetric sulfate reduction rate with increasing volumetric sulfate loading to that observed for this work.

The biomass concentration did not display a significant change with increasing temperature. The maximum specific growth rate (μ_m) was not dependent on temperature, while the decay coefficient (k_d) displayed an increase with temperature and the saturation constant (K_S) decreased with increasing temperature. The average value of μ_m calculated for this work (0.061 h^{-1}) is in agreement those reported in literature.

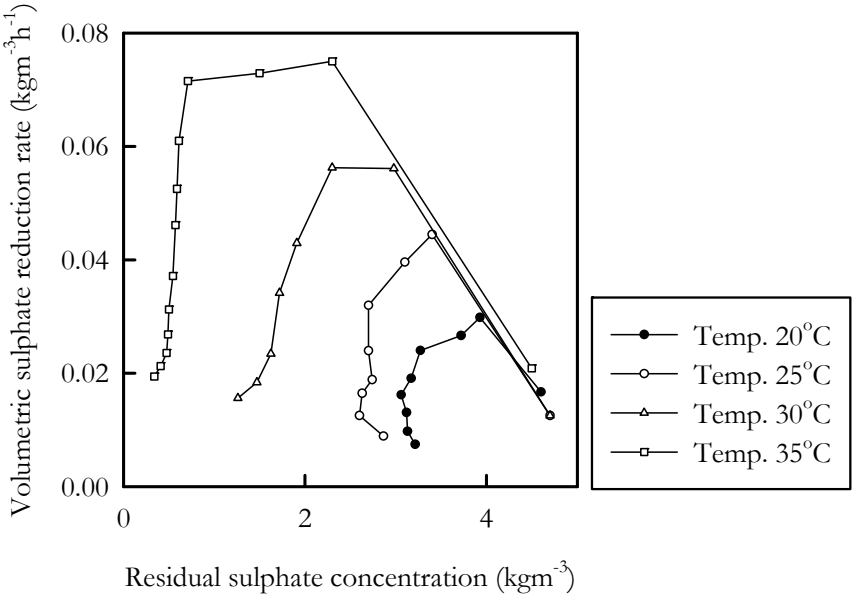

Figure 5.20 : Performance of the continuous bioreactor at 20, 25, 30 and 35°C

The denaturation of proteins and enzymes in a microbial system is highly temperature dependent (Roëls, 1983). The values of the decay coefficient, k_d, increased due to an increase in temperature. A similar trend was observed by Lawrence and McCarty (1969) for the anaerobic degradation of acetate by methanogens.

K_s was found to be a decreasing function of temperature explained by an "Arrhenius" type function. While a decrease in K_s represents enhanced affinity of the bacterial enzymatic system for the substrate (sulfate), the decrease in K_s may also be explained by enhanced mass transfer with increasing temperature. Information in the literature regarding the effect of temperature on K_s for SRB is inconsistent. A decrease in K_s (acetate) from 0.250 to 0.006 kg m^{-3} with increasing temperature in the range 20 to 31°C was observed by Middleton and Lawrence (1977) while studying the continuous reduction of sulfate in a chemostat with acetate as the limiting organic nutrient. Using data from a batch system, Characklis *et al.* (1989) reported an increase in K_s with

an increase in temperature. However, analysing data from a continuous system, they report a decrease K_s with increasing temperature. Okabe and Characklis (1992), conducting chemostat studies with lactate as the limiting carbon source, noted that K_s for *Desulfovibrio desulfuricans* remained relatively constant as the temperature was increased from 25 to 35°C. Morris (1976), studying the batch anaerobic degradation of dairy manure, showed that K_S decreased from 1.02 to 2.03 kg m^{-3} as the temperature was increased from 20 to 32.5°C. For the methanogenic process using acetate, K_s has been shown to be sensitive to temperature. Lawrence and McCarty (1969) developed the following Arrhenius equation to describe the relation between temperature and K_s for general anaerobic digestion (Speece, 1996):

$$\log \frac{(K_s)_2}{(K_s)_1} = 6980\left(\frac{1}{T_2} - \frac{1}{T_1}\right) \qquad [5.17]$$

where:

$(K_S)_1$ = Saturation constant at temperature 1 (kg m^{-3})

$(K_S)_2$ = Saturation constant at temperature 2 (kg m^{-3})

T_1 = Temperature 1 (K)

T_2 = Temperature 2 (K)

Lin (1987, in Speece, 1996) proposed the following equation for the temperature dependence of K_s for the methanogenesis of volatile fatty acids across the range 15 to 35°C:

$$K_s = 230(0.939)^{(T-25)} \qquad [5.18]$$

The bacterial yield, based on sulfate or acetate, remained constant at the 99 % significance level (t-test, $Y_{X/Sulfate}$ had a variance of 1.2 % and $Y_{X/acetate}$ had a variance of 1.4 %) over the range of applied temperatures. The average value for $Y_{X/Sukphate}$ was 0.568 g biomass/g sulfate and $Y_{X/acetate}$ was 0.600 g biomass/g acetate. The trend of yield coefficient with temperature observed for this work is similar to that observed by other researchers. Using a pure culture of *Desulfobacter desulfuricans*, Sanez (1962 in Okabe and Characklis, 1992) and Okabe and Characklis (1992) concluded that temperature had no effect on yield coefficient calculated in terms of organic substrate. The values reported in literature for $Y_{x/acetate}$ range between 0.065 and 0.141 kg bacteria (kg acetate)$^{-1}$. For $Y_{x/Sulfate}$ a value of 0.158 kg bacteria (kg sulfate)$^{-1}$ is reported (Middelton and Lawrence, 1977; Widdel and Pfennig, 1981; Visser, 1995; O' Flaherty *et al.*, 1998; Ingvorsen *et al.*, 1984).

5.3 CONCLUSIONS

Improved kinetic data on biological sulfate reduction across a broad range of sulfate feed concentrations (1 to 10 $g.l^{-1}$) has been presented using both ethanol and acetate as carbon source and electron donor.

The preliminary ethanol studies confirmed that incomplete oxidation results in an acetate accumulation in the presence of excess ethanol. Further, sulfate reduction was more efficient with feed concentrations of 1-2.5 $g.l^{-1}$ compared with 5-7.5 $g.l^{-1}$. The sulfate reduction rate increased with increasing dilution rate, while the extent of reduction decreased. Initial evidence of process inhibition by both undissociated H_2S and total sulfide was illustrated.

Similar studies using chemostat culture were performed using acetate as carbon source and electron donor. The results show that the volumetric loading of sulfate, as well as temperature, influences the kinetics of anaerobic reduction of sulfate. For the whole range of applied temperatures, 20 to 35 °C, the increasing of volumetric loading rate up to 0.08 to 0.01 kg m^{-3} h^{-1}, results in a linear increase in reduction rate. Beyond this level the reduction rate becomes independent of volumetric loading. Despite the similar patterns, the extent of reaction rate is influenced by temperature. An increase in temperature leads to enhanced reduction rates.

A comphrehensive kinetic model was derived and calibrated to describe the sulfate reduction rate. The rate expression derived, Equation 5.16, incorporates terms for sulfate and bacterial concentrations, as well as temperature and is able to predict the experimental data extremely well.

A future goal will be to evaluate the kinetics of sulfate reduction at higher concentrations of sulfate and to investigate the effect of sulfide on the kinetics of this reaction. The possibility of improving the kinetic model further to comprise terms describing the sulfide effect will be investigated as a part of WRC 1251.

6 METAL RECOVERY STUDIES

6.1 INTRODUCTION

An overview of the diversity of mine waters and their aqueous chemistry indicates that mine waters can be broadly classified into:

- high iron (≥ 1200mg Fe/l) and sulfate (≥ 5000mg SO_4/l), low carbonate waters originating from gold mining operations and typical of the West Rand and
- low iron (≤ 400mg Fe/l) and sulfate (≤ 1500mg SO_4/l), high carbonate waters, typical of the East Rand, such as at Grootvlei.

These two different types of mine waters have been considered separately with high iron, low carbonate waters forming part of the work of WRC contract 1079 and low iron, high carbonate waters forming part of the work of WRC contract 1080 and reported on in this document.

Two crucial issues arise when considering the process of developing a model to simulate metal removal via precipitation from an acid mine drainage stream.

The first one is related to kinetics. In the viable pH range of the biological system, a simulation model based only on solubility products will predict that most metals will precipitate out. The kinetic considerations, which are of great concern in the biological model, are a very minor issue in the precipitation system. In many precipitation systems, the characteristic reaction and nucleation times are very short, of the order of milliseconds or less (Sohnel and Garside, 1992). In contrast, the time scales for the various mixing and hydrodynamic processes are much larger and thus more significant that those for the reactions. Hence, any investigation into precipitation processes will not be overly concerned with kinetics, but will focus on issues of hydrodynamics, nucleation and consequent issues of particle size distribution, fines formation and solid-liquid separation.

The second issue is related directly to the system chemistry. Although the particle characteristics are the determining factor in a precipitation process, the solution chemistry does play a significant role. An understanding of the solution chemistry will provide insight into the effect of process variables on species precipitation and provide information as to which chemical species will precipitate under which conditions. This is significant information, although it does not indicate whether it will be possible to separate out the precipitated phase. Commercially

available software, such as ASPEN PLUS™ and OLI Systems Inc ESP, incorporate extensive databases containing most of the information necessary for carrying out the solution chemistry modelling.

In summary, the chemical and biological systems do not logically form part of the same model (at this stage), and incorporating a chemical precipitation model directly into the existing biological model will trivialise the precipitation issues. Hence, chemical modelling of metal removal has been carried out separately to the modelling of the biological sulfate reduction and associated processes. ASPEN PLUS™ and OLI Systems Inc ESP are the software of choice since they incorporate databases that already contain all the necessary information. Both simulation packages have been used to carry out the modelling study in order to compare their results with a view to switching to OLI Systems Inc ESP as the preferred modelling software in the future. This is in contrast to the biological system, where no such database exists.

Consequently, metal recovery from low iron waters has been examined using two approaches:

Theoretical modelling, using commercially available databases and simulation programmes. The theoretical modelling focussed on a mixed metal sulfide system incorporating five representative divalent metal ions: Ca^{2+}, Cu^{2+}, Zn^{2+}, Ni^{2+} and Mg^{2+}.

Experimental studies at the laboratory scale. The experimental studies focussed specifically on nickel precipitation within the carbonate system. The precipitation method used was on foreign seeds in a fluidised bed reactor with the seeds facilitating nucleation and providing surface area for growth and agglomeration.

6.2 THEORY AND LITERATURE REVIEW

Precipitation is one of the most widely used methods of removing metallic species from waste effluents (Mishra, 1999). The most common route is the precipitation of hydroxides through addition of lime or caustic soda directly to the waste effluent stream. Sulfide is also one of the commonly used precipitants. Carbonate precipitation for heavy metals has also been investigated (Patterson *et al*, 1977).

The drawbacks of hydroxide precipitation include large sludge volumes, gelatinous sludges, poor filterability and high operational costs (McNally and Benefield, 1984).

Advantages of metal sulfide over hydroxide precipitation are (McNally and Benefield, 1984):

- Good removal efficiency can be expected with metal sulfides because of their low solubility;
- Sulfide will precipitate metals complexed with most complexing agents;

Sulfide precipitates exhibit less of an amphoteric nature than hydroxide precipitates and have less of a tendency to resolubilise;

- Lower sludge volumes are experienced with sulfide compared to hydroxide treatment.

However, metal sulfide precipitates are often colloidal, making solid liquid separation difficult. In addition, they are frequently amorphous in nature, so that improvement of the particulate properties is an important factor for metal removal (Peters *et al*, 1984). The literature is sparse with respect to studies carried out into particle size or filterability improvements.

Using carbonate instead of hydroxide as the precipitation ion lowers the precipitation pH and thus the operating costs and the cost of neutralisation effluents. It has been suggested that the precipitate formed separates readily from the solution and produces a dense sludge (McNally and Benefield, 1984). However, Patterson *et al* (1977) maintain that the sludge properties are fundamentally the same as for hydroxide precipitation i.e. low filterability, gelatinous sludge and large sludge volumes.

6.2.1 PH

Solubility diagrams are commonly used in order to predict the nature of the precipitating species. As the determination of all the species present in solution is generally impossible, the concept of a "solubility domain" has to be defined, instead of having a precise solubility model for each species (Tunay *et al*, 1995). This solubility domain is constructed through interpretation of thermodynamic and kinetic constants found in the literature. To be strictly correct, the solubility domain of a particular metal must be defined for a solution containing both sulfide and hydroxide or carbonate and hydroxide ions, as sulfide or carbonate precipitation will never occur alone, but in competition with hydroxide precipitation. The final solubility domain will be determined from a superposition of the hydroxide and sulfide or hydroxide and carbonate solubility diagrams.

Figure 6.1 shows the relationship between pH and solubility for a mixed metal hydroxide and sulfide system.

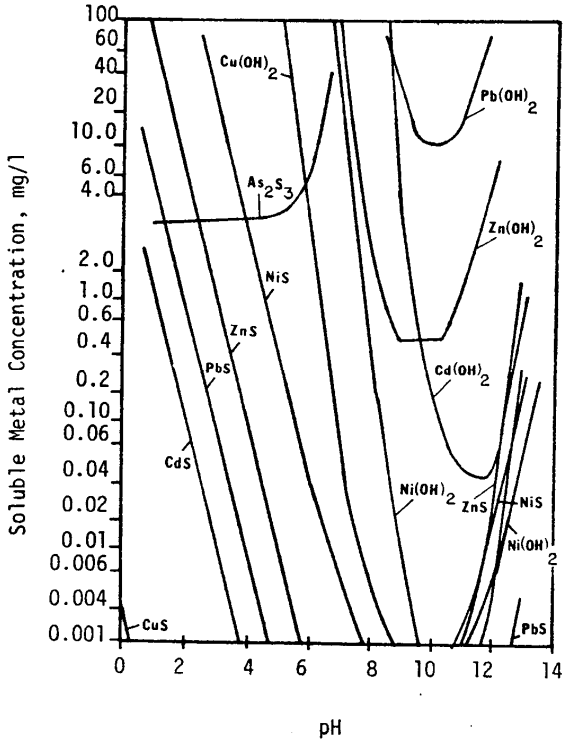

Figure 6.1 : Solubilities of metal sulfides and metal hydroxides as a function of pH (Peters *et al*, 1984)

From Figure 6.1, it is apparent that a suitable pH for precipitation of most metal sulfides in a mixed sulfide/hydroxide system is approximately $8 < pH < 11$. Operation in this pH range

would not remove aluminium (shown in Figure 6.1), magnesium or manganese (not shown in Figure 6.1).

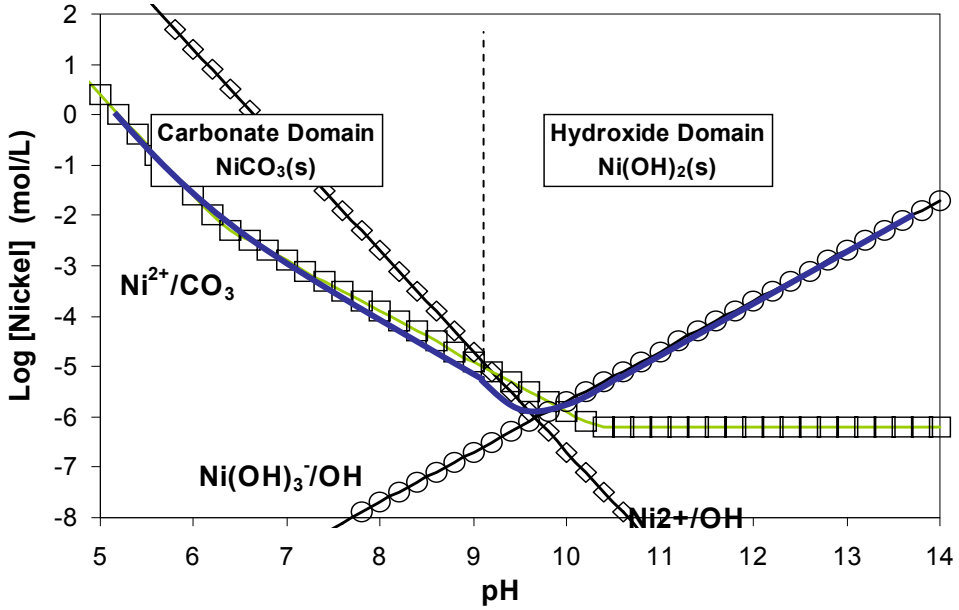

Figure 6.2 : Nickel hydroxide carbonate diagram $C_T = 10^{-2}$ mol/l (Guillard *et al*, 2000)

Figure 6.2 shows the relationship between pH and solubility for the combined Ni-OH-CO_3 system. From Figure 6.2, it can be seen that the optimum pH for precipitation of nickel carbonate is $9 < pH < 10$. Operation in this domain would remove nickel as a mixed nickel carbonate/ hydroxide.

6.2.2 REAGENT ADDITION AND SUPERSATURATION

The method of reagent addition directly influences the supersaturation within the system. For precipitation to occur, supersaturation must exist i.e. the concentration of a solute must exceed its solubility. However, the supersaturation alone does not ensure phase change by nucleation or crystal growth. It is the level of supersaturation, as well as the hydrodynamic conditions and the presence of other materials in suspension or in solution that affect the form and degree of growth. The supersaturation drives all the crystallisation process, as illustrated in Figure 6.3.

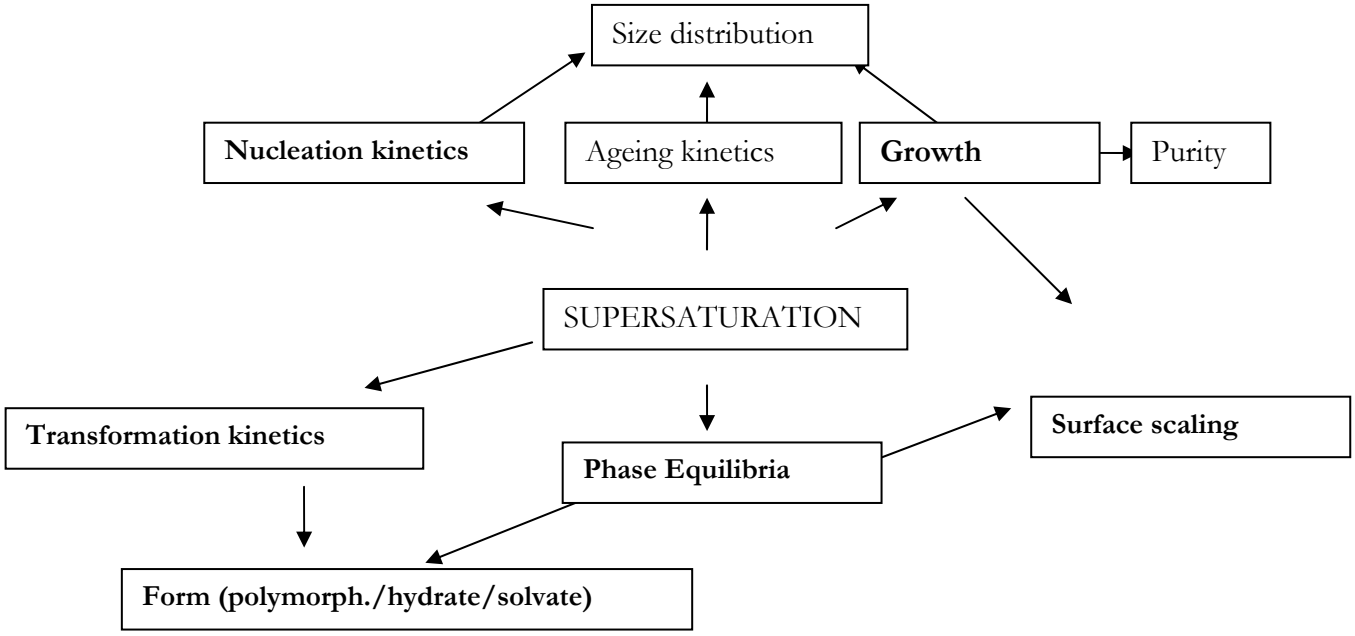

Figure 6.3 : Influence of supersaturation on the precipitation process (Sohnel and Garside, 1992)

A direct consequence of the low solubility of precipitates is the development of high supersaturation, which ensures a high primary nucleation rate. This produces a large number of particles and reduces the average size of the population.

In the sulfide system, direct addition of sulfide ion causes a relatively high concentration of dissolved sulfide to be present in the solution (Peters *et al*, 1984). The high sulfide concentration causes the rapid precipitation of metal sulfides (i.e. high nucleation rates), resulting in small particulate fines and hydrated colloidal particles. Consequently, poor settling or filtering flocs often develop. Classical homogeneous nucleation theory confirms this. At the high supersaturations that occur with addition of soluble sulfide, homogeneous nucleation occurs, and formation of nuclei is rapid (Sohnel and Garside, 1992).

In a seeded system such as a fluidised bed, however, the seeds provide a surface for nucleation and the formation of colloids can be avoided. Nonetheless, all precipitation processes involving direct reagent addition will suffer from high local supersaturation at the reactant inlets.

All the precipitation processes within a fluidised bed depend on the supersaturation profile, which, because of reagent addition at the bottom of the bed, is not constant over the bed. A gradient is observed, with high supersaturation occurring at the bottom of the bed and decreasing with bed height. Some high local supersaturation can also develop at the reactant inlets although the inlet flow should maintain the bottom of the bed under a slight

supersaturation, as the supersaturation acts as a driving force for the very fast precipitation on the seeds. It is the local supersaturation level that determines the nature of the crystalline phase as well as the kinetics of nucleation, growth and agglomeration. As a result of the variation in supersaturation over the bed, the precipitated product will consist of a mixture of various crystalline and amorphous materials with slightly different solubilities and formulas. For purposes of description of the precipitation process, it will be assumed that the product is composed of only one single compound, with characteristics independent of the bed position.

In a fluidised bed, excessive local supersaturation may cause one of the two unwanted processes to occur: spontaneous primary nucleation or abrasion of the mineral coating of the pellets. Both processes lead to the formation of fines, which are not retained by the bed, and therefore not recovered in the reactor.

6.2.3 PARTICLE SIZE DISTRIBUTION OF PRECIPITATES

Few of the published studies report on the particle size distributions of precipitated metal salts. For zinc sulfide precipitation, the maximum particle size obtained for any experimental conditions was 14μm (Peters *et al*, 1984). In addition, since the experimental system involved very low concentrations and suspension densities (approx. 100mg/l zinc), the chances for particle-particle contact were slight, particularly with the very small sizes of the particles.

In a seeded pellet reactor, the particle size distribution of the product will essentially be that of the initial dose of seeds. The precipitation of the metal salt causes the pellet size to increase. As the efficiency of the metal removal depends on the active surface of the seeds, the pellet size has to remain very small, usually less than 1 millimetre. To ensure this, the biggest seeds are removed periodically from the bottom part of the fluidised bed, where they automatically concentrate, while new seeding material is added from the top of the reactor. Keeping a small average seed size also prevents an increase of fines formation by pellet abrasion.

Fluidised bed reactor

Fluidised bed reactors (also called pellet reactors) where the process reaction occurs directly on seeds to form pellets, have many advantages over other heavy metal industrial precipitation methods. The advantages are that:

- The metal precipitates form a dense solid on the pellet surface;
- The process requires minimal supervision and maintenance
- Cost of chemicals and sludge disposal are very low and

- The investment costs are low because of the simplicity of the operating devices. (Van Dijk *et al*, 1986).

The pellet reactor provides an ideal environment for controlled crystallisation of metal salts in a very stable process. The large crystal surface area provided by the pellets favours heterogeneous nucleation on the seeds, and allows operation with a slightly supersaturated solution that avoids homogeneous nucleation of fines that are not easily separated from the stream. The relatively high fluid velocity in the reactor, typically in the range of 10 to 35cm/s, prevents the cementing of the pellets by ensuring their fluidisation. Very good mixing of the reactants also occurs. In many precipitating systems, the sedimentation velocity of the sludge is a limiting factor to heavy metal load on the reactor. In the case of pellet reactors, the precipitate density on the pellets can be much higher than in other precipitation processes as the sedimentation velocity of the grains is much greater than flocs. The permitted waste metal load can thus be 20 - 100 times that of a sludge process.

6.2.4 NICKEL CARBONATE SYSTEM IN THE FLUIDISED BED REACTOR

Process Efficiency

In practice, nickel effluent streams at a range of concentrations from 0.01 - 100g/l can be treated (Van Dijk, *et al*, 1987). Low concentration effluents do not need any re-circulation for efficient nickel removal, whereas more concentrated effluents require a re-circulation to improve the nickel removal efficiency.

The main problem encountered is the carryover of nickel-containing fines or amorphous nickel out of the top of the bed. Although most of the nickel precipitates onto the seeds, the presence of local high supersaturation zones, due to poor mixing at the reactant inlets, or to partial channelling of the bed, causes the formation of nickel carbonate and hydroxide primary nucleates. Secondly, the abrasion of the pellets can also cause the presence of fines in the upward flow. As the precipitation of nickel carbonate within the fluidised bed is time limited, most of the amorphous nickel formed does not have the opportunity to agglomerate onto the seeding material, and is recovered in the outlet flow of the column. The pellet attrition generally occurs at the bottom of the column, as observed by Seckler (1994), as well as just above the input nozzle of the fluidisation flow. Therefore, the re-circulation flow rate must be optimised to ensure process efficiency. Increasing the recirculation rate improves the nickel removal but also increases the Reynolds number, and thus the turbulence and the attrition within the reactor.

On the other hand, a low recirculation rate reduces nickel removal although it increases the residence time of the metal in the reactor.

In general, if nickel removal greater than 80% is required, a filtration step must be added after the reactor (Sekler, 1994 and Wilms, 1988). Using sand filters in conjunction with industrial scale columns is common. The backwash water of the filters can be diluted with the inlet effluent and the nickel re-dissolved and recovered within the column (Van Dijk, 1987). Nickel removal efficiencies up to 99.95% can be expected when using the post-filtration stage. This process can be extended with similar efficiencies to other heavy metals like Zn, Cu, Co, Cd, Mn, Ba, Sr, Ag, Pb and Hg.

Product purity

Van Dijk *et al* (1987) found that, for the nickel carbonate system, the pellets were quite pure: 99.8% nickel and only 0.2% other metals for a solution prepared with tap water. Van Dijk *et al* (1987) also showed that 50-60% of the ions were carbonates, and the rest mainly hydroxides under their operating conditions.

Metal recovery

The nickel on the pellets can be reused, after dissolving the pellets in strong acids such as HCl or H_2SO_4. The carbonate would be released as carbon dioxide, and the seeding material could be reused in the reactor.

6.3 THEORETICAL MODELLING OF METAL REMOVAL

6.3.1 MODEL CONFIGURATION

Equilibrium simulations of a typical iron-free acid mine drainage precipitation system have been developed using both ASPEN PLUS™ and OLI Systems Inc ESP software. The composition of the simulated acid mine drainage is defined in Table 6.1.

Table 6.1 : Composition of simulated acid mine drainage

Mineral	Metal	Species	Concentration (mg mineral /l)
$Ca(NO_3)_2$	Ca	Nitrate	240
$MgSO_4$	Mg	Sulfate	38
$ZnSO_4$	Zn	Sulfate	50
$CuSO_4$	Cu	Sulfate	50
$NiSO_4$	Ni	Sulfate	50

The simulation flowsheet is illustrated in Figure 6.4.

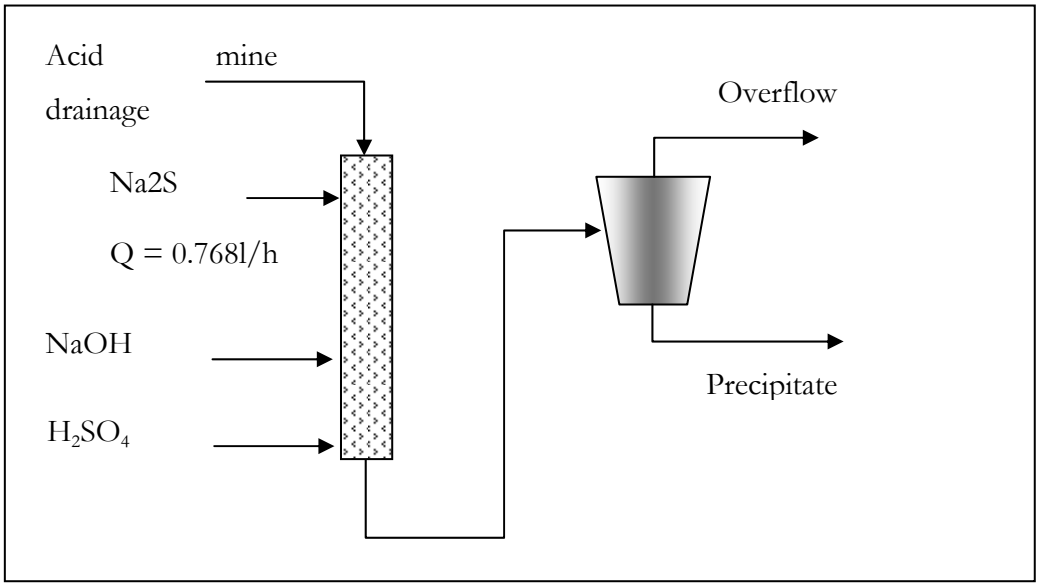

Figure 6.4 : Simulation flowsheet for metal removal modelling

The simulated flowrates were those that were selected for an equivalent experimental configuration. The sulfide stream was in excess.

ASPEN PLUS™ simulation

For the ASPEN PLUS™ simulation, an electrolyte model was developed. In ASPEN PLUS™, an electrolyte system is defined as one in which some of the molecular species dissociate partially or completely into ions in a liquid solvent and/or some of the molecular species precipitate as salts. These dissociation and precipitation reactions are assumed to occur fast enough that the reactions can be considered to be at chemical equilibrium (Aspen, 1994).

The liquid phase equilibrium reactions (the solution chemistry) have a major impact on the simulation of electrolyte systems. They also affect physical property calculations and phase equilibrium calculations as the presence of ions in the liquid phase causes highly non-ideal thermodynamic behaviour. The liquid phase properties were calculated using the Electrolyte Non Random Two Liquid activity coefficient model and the vapour phase properties were calculated from the Redlich-Kwong equation of state. Henry's Law was used to calculate phase equilibria for volatile species.

The reactions considered are defined in Table 6.2. Twelve equilibrium reactions, six dissociation reactions and 46 precipitation reactions were taken into account.

Table 6.2 : Reactions considered in ASPEN PLUS™ simulation of mixed metal sulfide precipitation

	Type	**Reaction**
1	Equilibrium	$2\,H_2O \Leftrightarrow H_3O^+ + OH^-$
2	Equilibrium	$H_2S + H_2O \Leftrightarrow H_3O^+ + HS^-$
3	Equilibrium	$HS^- + H_2O \Leftrightarrow H_3O^+ + S^{--}$
4	Equilibrium	$H_2SO_4 + H_2O \Leftrightarrow H_3O^+ + HSO_4^-$
5	Equilibrium	$HSO_4^- + H_2O \Leftrightarrow H_3O^+ + SO_4^{--}$
6	Equilibrium	$HNO_3 + H_2O \Leftrightarrow H3O^+ + NO_3^-$
7	Equilibrium	$MgOH^+ \Leftrightarrow Mg^{++} + OH^-$
8	Equilibrium	$Ni^{++} + 2\,H_2O \Leftrightarrow H_3O^+ + NiOH^+$
9	Equilibrium	$Zn^{++} + 4\,OH^- \Leftrightarrow Zn(OH)^{4-}$
10	Equilibrium	$Zn^{++} + 3\,OH^- \Leftrightarrow Zn(OH)^{3-}$
11	Equilibrium	$CaOH^+ \Leftrightarrow Ca^{++} + OH^-$
12	Equilibrium	$ZnOH^+ \Leftrightarrow Zn^{++} + OH^-$
$Ca(NO_3)_2$	Dissociation	$Ca(NO_3)_2 \Rightarrow Ca^{++} + 2\,NO_3^-$
$CuSO_4$	Dissociation	$CuSO_4 \Rightarrow Cu^{++} + SO_4^{--}$
$MgSO_4$	Dissociation	$MgSO_4 \Rightarrow Mg^{++} + SO_4^{2---}$
$CuSO_4$	Dissociation	$CuSO_4 \Rightarrow 2\,Na + S^{--}$
$ZnSO_4$	Dissociation	$ZnSO_4 \Rightarrow Zn^{++} + SO_4^{--}$
$NiSO_4$	Dissociation	$NiSO_4 \Rightarrow Ni^{++} + {}_{SO4}{}^{2---}$
Na_2SO_4	Salt	$Na_2SO_4 \Leftrightarrow 2\,Na^+ + SO_4^{--}$
$Na_2SO_4.10H_2O$	Salt	$Na_2SO_4.10H_2O \Leftrightarrow 2\,Na^+ + SO_4^{2-} + 10\,H_2O$
Na_3SO_4OH	Salt	$Na_3SO_4OH \Leftrightarrow 3\,Na^+ + SO_4^{2-} + OH^-$
NaOH(S)	Salt	$NaOH(S) \Leftrightarrow Na^+ + OH^-$
$NaOH.H_2O$	Salt	$NaOH.H_2O\,(S) \Leftrightarrow Na^+ + OH^- + H_2O$
$Ca(NO_3)_2$	Salt	$Ca(NO_3)_2 \Leftrightarrow Ca^{++} + 2\,NO^{3-}$
$Ca(NO_3)_2.4H_2O$	Salt	$Ca(NO_3)_2.4H_2O \Leftrightarrow Ca^{++} + 2\,NO^{3-} + 4\,H_2O$
$Ca(NO_3)_2.3H_2O$	Salt	$Ca(NO_3)_2.3H_2O \Leftrightarrow Ca^{++} + 2\,NO^{3-} + 3\,H_2O$
$Ca(NO_3)_2.2H_2O$	Salt	$Ca(NO_3)_2.2H_2O \Leftrightarrow Ca^{++} + 2\,NO3- + 2\,H_2O$
$CaSO_4(S)$	Salt	$CaSO_4(S) \Leftrightarrow Ca^{++} + SO_4^{--}$

$CaSO_4 0.5H_2O$	Salt	$CaSO_4 0.5H_2O \Leftrightarrow Ca^{++} + SO_4^{2-} + 0.5\ H_2O$
$CaSO_4.2H_2O$	Salt	$CaSO_4.2H_2O \Leftrightarrow Ca^{++} + SO_4^{2---} + 2\ H_2O$
$Ca(OH)_2$	Salt	$Ca(OH)_2 \Leftrightarrow CaOH^+ + OH^-$
CuS(S)	Salt	$CuS(S) \Leftrightarrow Cu^{++} + S^{--}$
$CuSO_4(S)$	Salt	$CuSO_4(S) \Leftrightarrow Cu^{++} + SO_4^{2-}$
$CuSO_4.H_2O$	Salt	$CuSO_4.H_2O \Leftrightarrow Cu^{++} + SO_4^{2-} + H_2O$
$CuSO_4.3H_2O$	Salt	$CuSO_4.3H_2O \Leftrightarrow Cu^{++} + SO_4^{2-} + 3\ H_2O$
$CuSO_4.4H_2O$	Salt	$CuSO_4.4H_2O \Leftrightarrow Cu^{++} + SO_4^{2-} + 5\ H_2O$
$Mg(NO_3)_2$	Salt	$Mg(NO_3)_2 \Leftrightarrow Mg^{++} + 2\ NO3-$
$Mg(NO_3)_2.\ 6H_2O$	Salt	$Mg(NO_3)_2.\ 6H_2O \Leftrightarrow Mg^{++} + 2\ NO3- + 6\ H_2O$
$Mg(NO_3)_2.2H_2O$	Salt	$Mg(NO_3)_2.2H_2O\ (S) \Leftrightarrow Mg^{++} + 2\ NO3- + 2\ H_2O$
$MgSO_4.7H_2O$	Salt	$MgSO_4.7H_2O \Leftrightarrow Mg^{++} + SO_4^{2-} + 7\ H_2O$
$MgSO_4.6H_2O$	Salt	$MgSO_4.6H_2O \Leftrightarrow Mg^{++} + SO_4^{2-} + 6\ H_2O$
$MgSO_4.H_2O$	Salt	$MgSO_4.H_2O \Leftrightarrow Mg^{++} + SO_4^{2-} + H_2O$
$MgSO_4.2H_2O$	Salt	$MgSO_4.2H_2O \Leftrightarrow Mg^{++} + SO_4^{2-} + 2\ H_2O$
$MgSO_4.4H_2O$	Salt	$MgSO_4.4H_2O \Leftrightarrow Mg^{++} + SO_4^{2-} + 4\ H_2O$
$MgSO_4$	Salt	$MgSO_4 \Leftrightarrow Mg^{++} + SO_4^{2-}$
$Ni(NO_3)_2.6H_2O$	Salt	$Ni(NO_3)_2.6H_2O \Leftrightarrow Ni^{++} + 2\ NO^{3-} + 6\ H_2O$
$NaNO_3$	Salt	$NaNO_3(S) \Leftrightarrow Na^+ + NO^{3-}$
$Na_2S(S)$	Salt	$Na_2S \Leftrightarrow 2\ Na^+ + S^{--}$
$Zn(NO_3)_2$	Salt	$Zn(NO_3)_2 \Leftrightarrow Zn^{++} + 2\ NO^{3-}$
$Zn(NO_3)_2.6H_2O$	Salt	$Zn(NO_3)_2.6H_2O \Leftrightarrow Zn^{++} + 2\ NO^{3-} + 6\ H_2O$
$Zn(NO_3)_2.4H_2O$	Salt	$Zn(NO_3)_2.4H_2O \Leftrightarrow Zn^{++} + 2\ NO^{3-} + 4\ H_2O$
$Zn(NO_3)_2.2H_2O$	Salt	$Zn(NO_3)_2.2H_2O \Leftrightarrow Zn^{++} + 2\ NO^{3-} + 2\ H_2O$
$Zn(NO_3)_2.H_2O$	Salt	$Zn(NO_3)_2.H_2O \Leftrightarrow Zn^{++} + 2\ NO^{3-} + H_2O$
$ZnSO_4$	Salt	$ZnSO_4(S) \Leftrightarrow Zn^{++} + SO_4^{2-}$
$ZnSO_4.7H_2O$	Salt	$ZnSO_4.7H_2O \Leftrightarrow Zn^{++} + SO_4^{2-} + 7\ H_2O$
$ZnSO_4.6H_2O$	Salt	$ZnSO_4.6H_2O \Leftrightarrow Zn^{++} + SO_4^{2-} + 6\ H_2O$
$ZnSO_4.H_2O$	Salt	$ZnSO_4.H_2O \Leftrightarrow Zn^{++} + SO_4^{2-} + H_2O$
$ZnSO_4.2H_2O$	Salt	$ZnSO_4.2H_2O \Leftrightarrow Zn^{++} + SO_4^{2-} + 2\ H_2O$
$Mg(OH)_2$	Salt	$Mg(OH)_2 \Leftrightarrow MgOH^+ + OH^-$
$Zn(OH)_2$	Salt	$Zn(OH)_2 \Leftrightarrow ZnOH^+ + OH^-$
CaS	Salt	$CaS \Leftrightarrow Ca^{++} + S^{--}$
MgS	Salt	$MgS \Leftrightarrow Mg^{++} + S^{--}$
ZnS	Salt	$ZnS \Leftrightarrow Zn^{++} + S--$
NiS	Salt	$NiS \Leftrightarrow Ni^{++} + S--$

These reactions are developed in terms of H_3O^+ instead of the usual H^+ because H_3O^+ is better able to represent most electrolyte vapour liquid equilibrium behaviour. (Aspen Plus, 1994).

The pH of the system was varied (by addition of appropriate quantities of acid or base) from pH = 1 to pH = 12 and the effect of the change in pH on metal salt precipitation was examined.

OLI Systems Inc ESP simulation

For the OLI Systems Inc ESP simulation, a similar electrolyte model was developed. The activity coefficient model for representing solution non-ideality used an extended form of the expression developed by Bromley (1973) (cited in Zemaitis, 1986). The Bromley equation is a combination of the Debye-Huckel term for long-range electrostatic interactions and a semi-empirical expression for short-range interactions between cations and anions. For ion-molecule and molecule-molecule interactions, the model of Pitzer (1973) (cited in Zemaitis, 1986) was used. The Helgeson-Kirkham-Flowers (1981) equation of state was used for standard state properties and vapour phase fugacity coefficients were determined using the SRK equation of state.

The reactions considered are defined in Table 6.3. Sixty-four equilibrium reactions and twenty-five precipitation reactions were taken into account.

Table 6.3 : Reactions considered in OLI Systems Inc ESP simulation of mixed metal sulfide precipitation

EQUILIBRIUM	**PRECIPITATION**
$Ca(NO_3)_2 .3H_2O \Leftrightarrow Ca^{++} + 2NO_3^{--} + 3.H_2O$	CaNO32PPT=CAION+2NO3ION
$Ca(NO_3)_2 .4H_2O \Leftrightarrow Ca^{++} + 2NO_3^{--} + 4.H_2O$	CAOH2PPT=CAION+2OHION
$Ca(NO_3)- \Leftrightarrow Ca^{++} + NO_3^-$	CASO4PPT=CAION+SO4ION
$CaOH \Leftrightarrow Ca^{++} + OH^-$	CASPPT=CAION+SION
$CaSO_4.2H_2O \Leftrightarrow Ca^{++} + SO_4^{2-} + 2H_2O$	CUOH2PPT=CUION+2OHION
$CaSO_4. \Leftrightarrow Ca^{++} + SO_4^{2-}$	CUSO4PPT=CUION+SO4ION
$Cu(NO_3)_2 .2.5H_2O \Leftrightarrow Cu^{++} + 2NO_3^{--} + 2.5H_2O$	CUSPPT=CUION+SION
$Cu(NO_3)_2 .6H_2O \Leftrightarrow Cu^{++} + 2NO_3^{--} + 6H_2O$	MGNO32PPT=MGION+2NO3ION
$Cu(NO_3)_2 \Leftrightarrow Cu^{++} + 2NO_3^{--}$	MGOH2PPT=MGION+2OHION
$Cu(NO_3)^+ \Leftrightarrow Cu^{++} + NO_3^{--}$	MGSO4OHPPT=1.5MGION+SO4ION+OHION
$Cu(OH)_2 \Leftrightarrow CuOH^+ + OH^{--}$	MGSO4PPT=MGION+SO4ION
$Cu(OH)_3^- \Leftrightarrow Cu(OH)_2 + OH^{--}$	MGSPPT=MGION+SION
$Cu(OH)_4^{--} \Leftrightarrow Cu(OH)_3 + OH^{--}$	NA2SO4PPT=2NAION+SO4ION
CUOHION=CUION+OHION	NA2SPPT=2NAION+SION
CUSO4.3H2O=CUION+SO4ION+3H2O	NA3HSO42PPT=3NAION+HSO4ION+SO4ION
CUSO4.5H2O=CUION+SO4ION+5H2O	NAHSO4PPT=NAION+HSO4ION
H2O=HION+OHION	NANO3PPT=NAION+NO3ION
H2OVAP=H2O	NAOHPPT=NAION+OHION
H2SAQ=HION+HSION	NINO32PPT=NIION+2NO3ION
H2SO4AQ=HION+HSO4ION	NIOH2PPT=NIION+2OHION
H2SO4VAP=H2SO4AQ	NISO4PPT=NIION+SO4ION
H2SVAP=H2SAQ	NISPPT=NIION+SION

HNO3AQ=HION+NO3ION

HNO3VAP=HNO3AQ

HSION=HION+SION

HSO4ION=HION+SO4ION

MGNO32.2H2O=MGION+2NO3ION+2H2O

MGNO32.6H2O=MGION+2NO3ION+6H2O

MGOHION=MGION+OHION

MGSO4.1H2O=MGION+SO4ION+1H2O

MGSO4.6H2O=MGION+SO4ION+6H2O

MGSO4.7H2O=MGION+SO4ION+7H2O

MGSO4AQ=MGION+SO4ION

MGSO4OH.0.5H2O=1.25MGION+SO4ION+0.5OHION+0.5 H2O

NA2S.9H2O=2NAION+SION+9H2O

NA2SO4.10H2O=2NAION+SO4ION+10H2O

NANO3AQ=NAION+NO3ION

NAOH.1H2O=NAION+OHION+H2O

NASO4ION=NAION+SO4ION

NINO32.2H2O=NIION+2NO3ION+2H2O

NINO32.4H2O=NIION+2NO3ION+4H2O

NINO32.6H2O=NIION+2NO3ION+6H2O

NINO3ION=NIION+NO3ION

NIOH2AQ=NIOHION+OHION

GEN NIOH3ION=NIOH2AQ+OHION

NIOHION=NIION+OHION

NISO4.6H2O=NIION+SO4ION+6H2O

NISO4.7H2O=NIION+SO4ION+7H2O

NISO4AQ=NIION+SO4ION

SO3AQ+H2O=H2SO4AQ

SO3VAP=SO3AQ

ZNNO32.1H2O=ZNION+2NO3ION+H2O

ZNNO32.2H2O=ZNION+2NO3ION+2H2O

ZNNO32.4H2O=ZNION+2NO3ION+4H2O

ZNNO32.6H2O=ZNION+2NO3ION+6H2O

ZNNO32AQ=ZNION+2NO3ION

ZNNO3ION=ZNION+NO3ION

ZNOH2AQ=ZNOHION+OHION

ZNOH3ION=ZNOH2AQ+OHION

ZNOH4ION=ZNOH3ION+OHION

ZNOHION=ZNION+OHION

ZNSO4.1H2O=ZNION+SO4ION+1H2O

ZNSO4.6H2O=ZNION+SO4ION+6H2O

ZNSO4.7H2O=ZNION+SO4ION+7H2O

ZNNO32PPT=ZNION+2NO3ION

ZNOH2PPT=ZNION+2OHION

ZNSO4PPT=ZNION+SO4ION

6.3.2 RESULTS

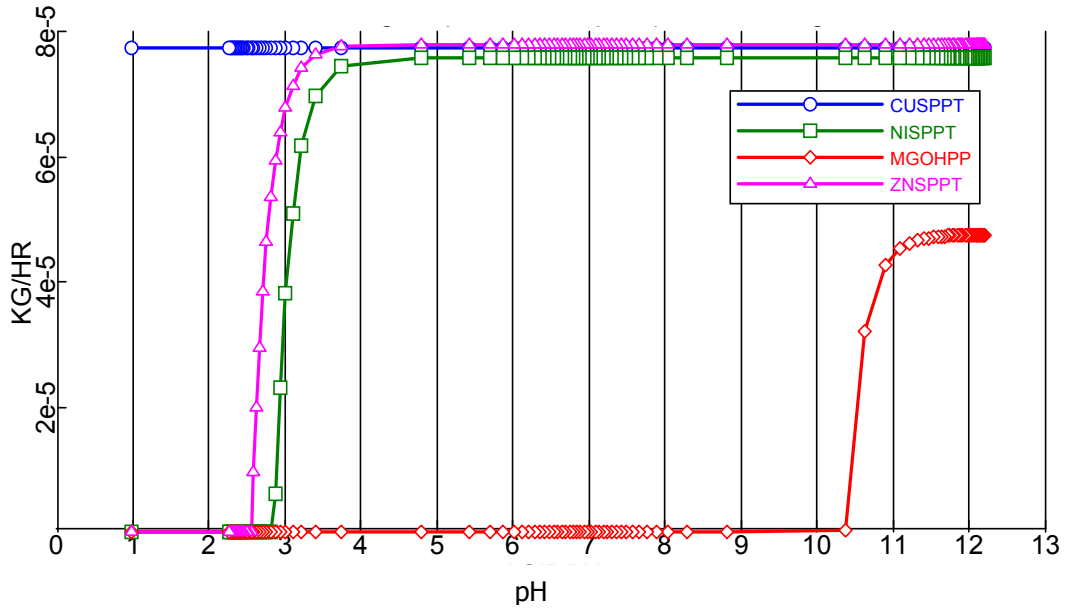

Figure 6.5 : Effect of change in pH on metal precipitation – ASPEN PLUS™

Figure 6.5 shows the effect of changing pH on all precipitated salts using the ASPEN PLUS™ simulation. The figure reflects all salts that precipitated i.e. of the 46 possible salts that could precipitate, only four were found to occur under these conditions. ASPEN PLUS™ predicts that copper sulfide will precipitate completely at all pH's between 1 and 12, that zinc sulfide will precipitate completely above a pH of 2, nickel sulfide above a pH of 3, and that magnesium will precipitate completely as magnesium hydroxide above a pH of 11. Magnesium sulfide does not occur. The incoming calcium does not precipitate as a salt.

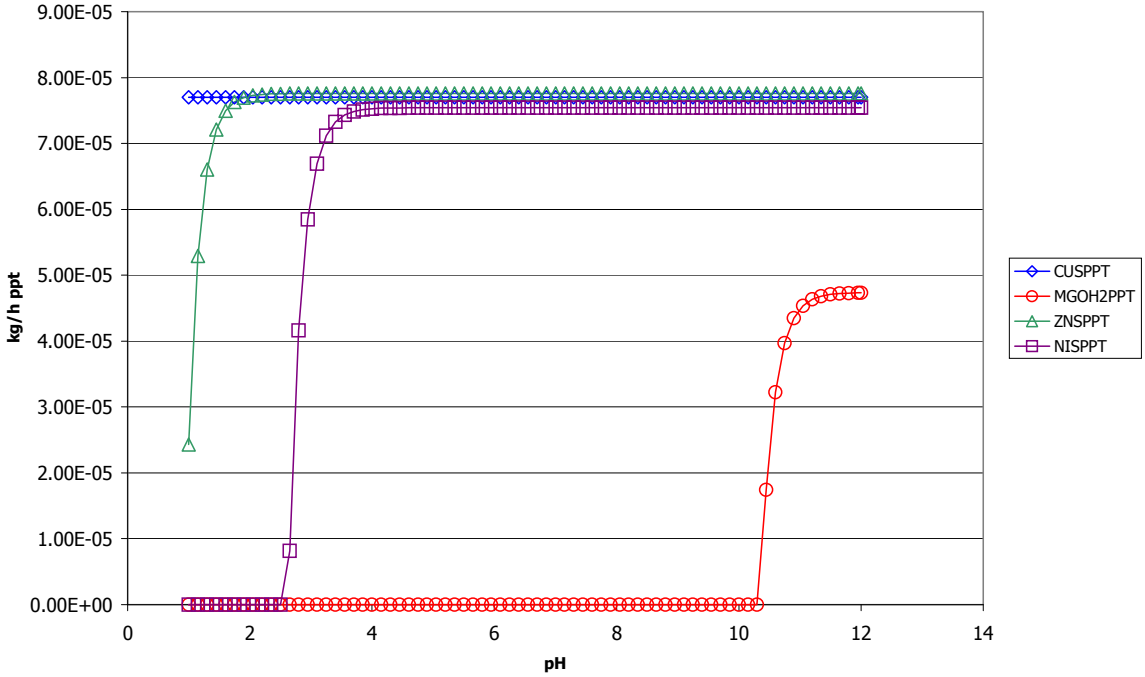

Figure 6.6 : Effect of change in pH on metal precipitation – OLI Systems Inc ESP

Very similar results are obtained when carrying out the simulation using OLI Systems Inc ESP. Of the 25 possible precipitated salts, only four were found to occur. The predicted precipitating salts (CuS, ZnS, NiS and MgOH) were the same as those predicted by ASPEN PLUS™ and occurred in the same pH ranges.

6.3.3 MASS BALANCE

The mass balance for the simulation flowsheet was carried out independently and the values in the last column of Table 6.4 compared with the equilibrium predictions of both simulations in Figure 6.5 and Figure 6.5. From this information, it is apparent that both of the simulations correctly preserve the mass balance over the simulation system.

Table 6.4 : Independent material balance on simulation flowsheet for the effect of change in pH on metal precipitation

	Metals input				metals output	
	mg/l species	g/h Species	gmol/h species	gmol/h metal		g/h species
$Ca(NO_3)_2$	240	0.6192	3.7738E-03	3.7738E-03		
$MgSO_4$	38	0.0980	8.1496E-04	8.1496E-04	$Mg(OH)_2$	4.75E-02
$ZnSO_4$	50	0.1290	7.9936E-04	7.9936E-04	ZnS	7.78E-02
$CuSO_4$	50	0.1290	8.0852E-04	8.0852E-04	CuS	7.73E-02
$NiSO_4$	50	0.1290	8.3387E-04	8.3387E-04	NiS	7.56E-02

6.3.4 DISCUSSION

One of the major uses of the simulation studies presented above is in the prediction of which species will precipitate under the various pH conditions. From a possible 46 (ASPEN PLUS™) and 25 (OLI Systems Inc ESP) precipitation reactions, both models predict the precipitation of the same four metal salts.

Once it has been established which salts to expect, it is the task of the experimental programme to investigate the feasibility of separating out these metal salts from solution. This experimental work is the subject of a future WRC research contract.

6.4 EXPERIMENTAL STUDIES

The experimental studies focussed specifically on nickel precipitation within the carbonate system using nickel sulfate and nickel carbonate solutions as reactants. The precipitation method used was on foreign seeds in a fluidised bed reactor.

6.4.1 EXPERIMENTAL PROCEDURE

The nickel carbonate precipitation reaction occurs within the height of the fluidised bed (Figure 6.7), the precipitation being achieved by mixing of a solution of nickel sulfate and sodium carbonate.

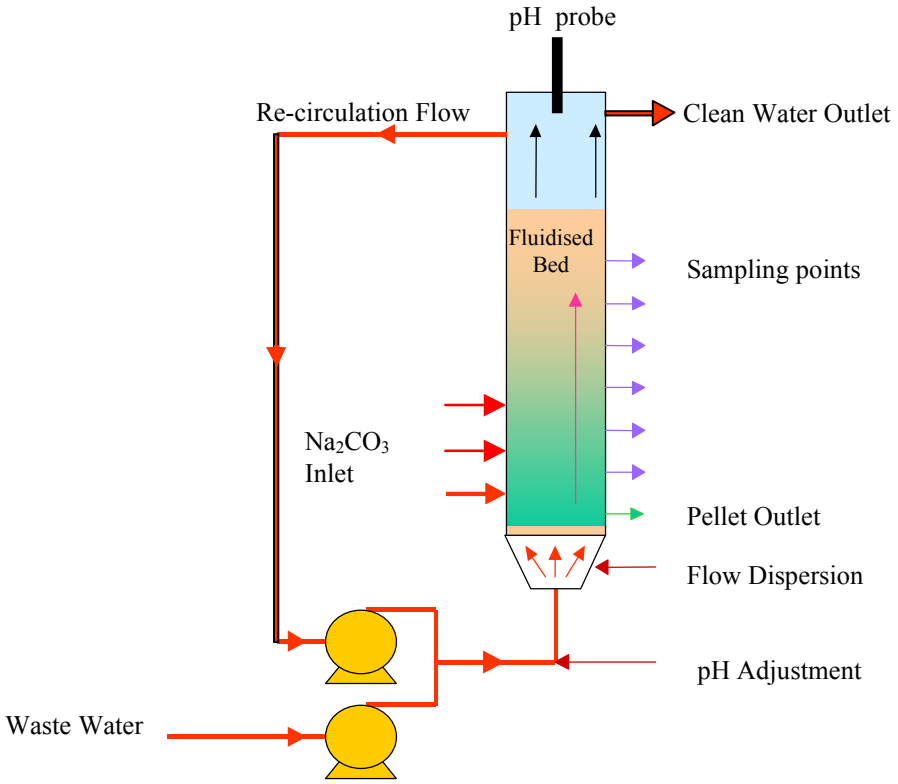

Figure 6.7 : Schematic representation of the pellet reactor

The pellet reactor consisted of a cylindrical vessel 1m high and 0.025m ID sealed from the atmosphere. The inlet flow distribution mechanism at the bottom of the column consisted of a conical glass fitting incorporating a plastic nozzle with large holes. This fitting was filled with glass beads of decreasing diameters that allowed uniform distribution of the upward flow as well as provided a support for the seeds (Figure 6.8). The reactor was filled with white quartz sand with particle size from 50 -70 mesh. The height of the bed at rest was 60±5cm and the fluidisation was achieved mainly through the recirculation flow.

There were up to three possible inlets for the carbonate solution on the side of the column. Each inlet was controlled with a separate valve, and consisted of a steel tube, 1mm ID. The inlets were spaced every 10cm starting 15cm from the bottom of the bed (Figure 6.7). One, two or three inlet points could be used simultaneously. By dividing the flow of carbonate, the supersaturation of the solution at the bottom of the column was significantly lowered, hence enhancing the efficiency of nickel removal.

There were seven sampling points, spaced every ten centimetres from the bottom of the column (Figure 6.7) the sampling tubes being 10mm OD. The outlet points allowed the withdrawal of solution as well as pellets from the reactor at different heights. At the top of the column, there

were 2 similar outlets (glass tube of 10mm OD), which were used for the re-circulation flow and the reactor outlet.

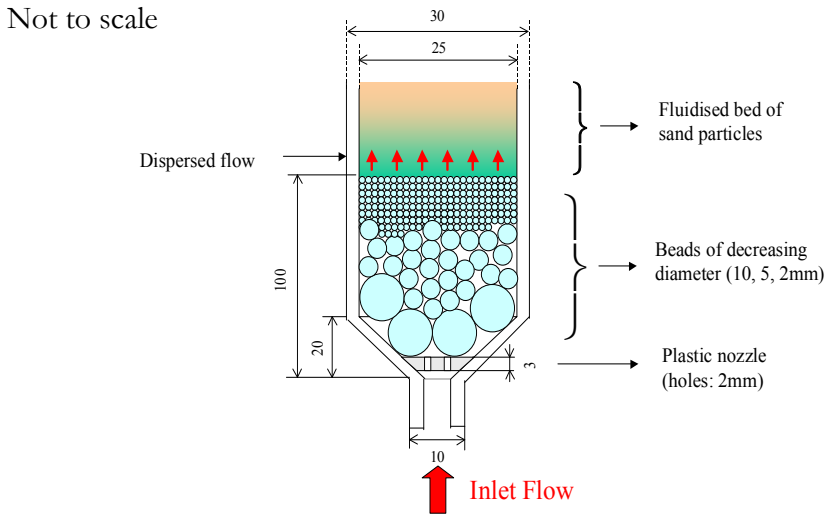

Figure 6.8 : Pellet reactor inlet nozzle

A pH probe was situated at the top of the column, allowing continuous monitoring of the system pH. The operating pH varied between 8 and 11 and was maintained by addition of acid or base in the re-circulation loop. The pH pump was a custom-made pump that allowed very small flow rates and the pH adjustment solutions were 0.01 -0.1 molar of hydrochloric acid and sodium hydroxide. Under normal operating conditions, the operating pH was very stable because of the buffering effect of the carbonates and the flow re-circulation.

The re-circulation pump was a Watson-Marlow peristaltic pump used with Masterflex 16 tubing. The maximum re-circulation corresponded to a re-circulation to inlet flow ratio of 1.66. The reagent inlet pump was a double pump-head Masterflex used with 14 and 16 tubing for the carbonate and nickel solutions respectively.

The synthetic nickel solution fed to the reactor had a concentration of 50-150ppm of nickel ($8.5*10^{-4}$ - $2.6*10^{-3}$mol/l) depending on the experiment. This corresponds to a nickel load of 367 -1098g/h/m^2 reactor XSA. The solution was prepared with nickel sulfate hexahydrate (MM=262.8g/mol) dissolved with tap water containing less than 0.1ppm of nickel. The carbonate solution had a concentration of $2.8*10^{-3}$ - $3.4*10^{-2}$ mol/l of carbonate. This corresponds to a relative carbonate to nickel ratio of 1:4 when fed to the reactor. The carbonate used was anhydrous sodium carbonate (MM=105.99g/mol). The flow rates of nickel and

carbonate solutions were constant: Q_{Ni}=3.6L/h and Q_{CO3}=1.08L/h and the temperature of the bed and solution was 22 ± 4 °C.

The samples were taken from the side of the bed and from the stream outlet. These were used to determine the nickel removal efficiency of the reactor as well as to establish concentration and pH profiles of the fluidised bed. For every sample drawn from the column, half was filtered using a 0.45micron filter, the other half being left as drawn. A comparison of the total and dissolved nickel was then possible. The two half samples were then acidified with 5 drops of hydrochloric acid 0.1 M to prevent further precipitation and to allow the re-dissolution of the fines. Analysis was carried out using Atomic Adsorption Spectrophotometry.

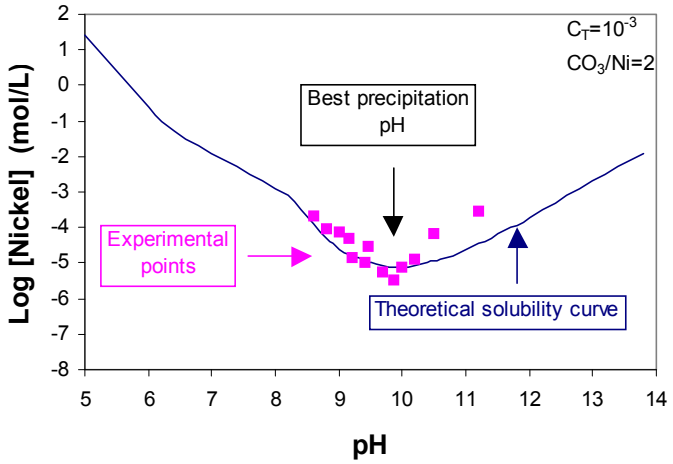

Figure 6.9 : Preliminary results – C_t = 10^{-3} and CO_3: Ni ratio = 2

6.4.2 PRELIMINARY RESULTS

Figure 6.9 shows a comparison of theoretical and actual nickel carbonate solubility under one set of operating conditions. This data was collected for various CO_3: Ni ratios. From the figure, it can be seen that there is relatively good agreement between the experimental points and the theoretical solubility curve from pH ≈ 8 until pH ≈ 10.5. Above pH = 10.5, the experimental points lie significantly above the theoretical solubility curve.

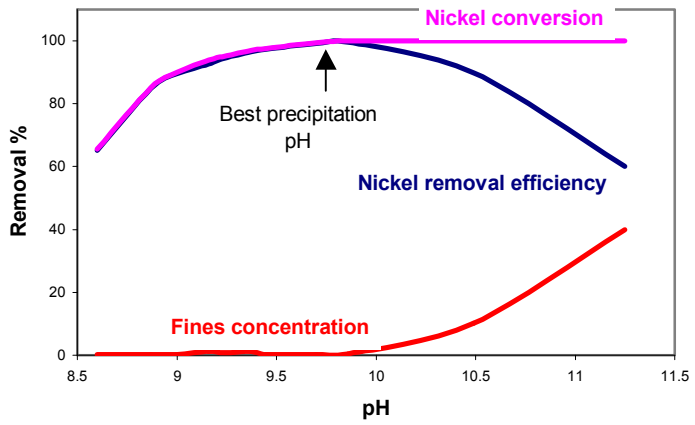

Figure 6.10 : Effect of pH on nickel removal efficiency, nickel conversion and fines formation

Figure 6.10 shows the effect of pH on nickel removal efficiency, nickel conversion and fines formation.

Nickel removal efficiency is defined as:

$$\eta(\%) = \frac{(\text{nickel introduced} - \text{total nickel in outlet}) \times 100}{\text{nickel introduced}} \qquad [6.1]$$

Nickel conversion is defined as:

$$\chi(\%) = \frac{(\text{nickel introduced} - \text{total nickel in outlet}) \times 100}{\text{nickel introduced}} \qquad [6.2]$$

Fines concentration is reported as percentage of introduced nickel.

From Figure 6.10, it is apparent that nickel conversion increases steadily with increasing pH until pH ≈ 9.8 and then levels out at a value of 100%. The nickel removal increases with increasing pH, reaches a peak at pH ≈ 9.8 and thereafter decreases with increasing pH. The fines concentration is minimal until pH ≈ 9.8, whereafter it begins to increase, reaching its maximum value of 40% coinciding with the maximum measured pH value.

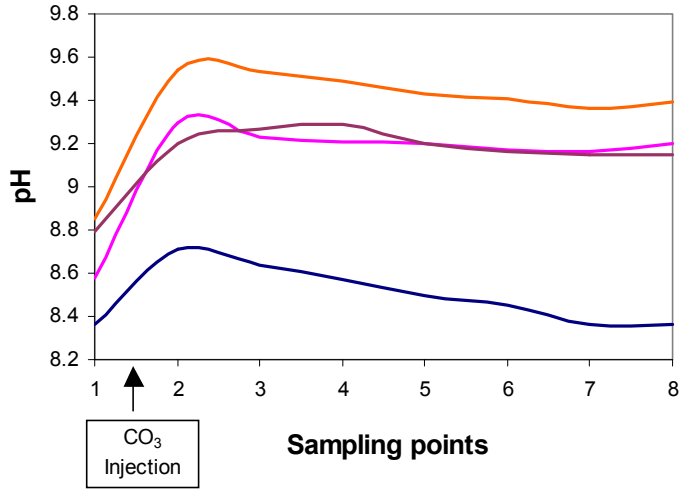

Figure 6.11 : pH profile within the fluidised bed

Figure 6.11 shows the pH profile in the fluidised bed. Each of the lines represents a different pH setpoint, which is monitored and controlled through the pH probe at the top of the column. The setpoints were pH = 9.4, 9.2, 9.15 and 8.4. For all but one of the measurements, the pH values are at the lowest at the bottom of the bed. For the setpoints of 9.4, 9.2 and 8.4, the pH profiles experience a peak at the carbonate injection point, as the incoming carbonate solution causes the pH to increase. Thereafter, the pH steadily decreases, due to carbonate consumption by the nickel carbonate precipitation reaction. For the setpoint of 9.15, the increase in pH over the height of the bed is much more gradual, with the highest pH value occurring at sample point 4.

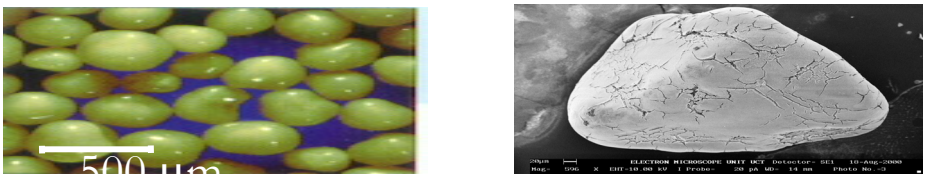

Figure 6.12: Nickel carbonate pellets as seen under top lit microscope (left) and scanning electron microscope (right)

6.4.3 DISCUSSION

The nickel in the outlet stream can occur both as dissolved nickel and as fines. The fines are washed out with the outlet stream and thus are not considered to be part of the nickel removal.

Fines can be formed either by attrition of the precipitate already on the pellets or by a primary nucleation mechanism occurring in the bulk of the solution, as illustrated in Figure 6.13. It is possible, given sufficient residence time in the reactor, for the fines to agglomerate onto the pellet.

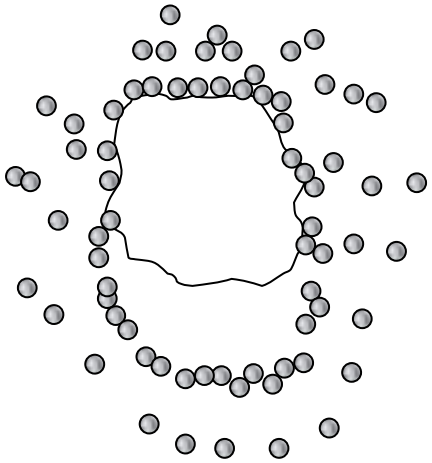

Figure 6.13 : Schematic representation of nucleated precipitation and fines formation (Zhou *et al*, 1999)

As the pH is increased, the supersaturation at the inlet point also increases due to the increased concentration of OH^- ions and thus spontaneous formation of solid phase within the liquid medium (fines formation) is favoured. This phenomenon explains the presence of the two outliers in Figure 6.9. The reason that the two outliers are above the theoretical solubility curve is that they include the significant fines formation found above pH = 10.5.

It is this same phenomenon that prevents the nickel removal efficiency from remaining at 100% at all pH values ≥ 9.8 (see Figure 6.10). Although at pH ≥ 9.8 the nickel conversion = 100%, the nickel removal efficiency decreases due to the increase of total nickel in the outlet. At high pH values, the total nickel is made up mostly of fines. This is confirmed by the fact that the fines concentration curve is almost zero until pH ≥ 9.8. At pH ≥ 9.8, significant fines formation begins to occur. It was found that, above pH = 9.8, fines formation causes filter blockages. Below pH = 9.8, the fines formation was found to be negligible and no filtration problems were experienced.

The change in pH over the height of the reactor is due to the fact that the pH probe is at the top of the reactor and that the measurement and control take place there. This means that the

setpoint is only really achieved at the top of the reactor (see Figure 6.11). Since the pH affects the supersaturation, which is the most critical variable governing all the precipitation processes in the bed, this variation can have significant effects on the control of measured phenomena in the reactor.

6.5 FUTURE WORK

From results so far obtained as well as from a theoretical standpoint, it is clear that the local supersaturation within the bed has a major influence on the precipitation processes. It affects:

- The ratio between primary and secondary nucleation,
- The kinetics of nucleation, growth and agglomeration as well as
- The characteristics of the precipitate.

In addition, the hydrodynamics also play a critical role, as they affect:

- The kinetics of agglomeration and
- The formation of fines by attrition.

7 CONCLUSIONS

1. The literature on the kinetics of anaerobic digestion and bacterial sulfate reduction has been reviewed. There is kinetic data available on the various microbial steps in each of the processes. The rate equations and kinetic constants for all the processes from the hydrolysis of sewage sludge to methanogenesis and sulfidogenesis have been assessed and those appropriate for inclusion in a simulation model tabulated. However, the literature review shows that while the effect of sulfide on anaerobic digestion is well described, there is a lack of kinetic data on bacterial sulfate reduction, and in particular on the inhibitory effect of high sulfate and sulfide concentrations most likely to be found in systems treating acid mine drainage.

2. A model has been developed in AQUASIM using kinetic data from the literature and this model was able to describe the limited steady state data available from the Rhodes University, Biosure process. In a parallel modelling exercise a mathematical model using a high level mathematical language (Octave) has been developed. The model describes the dynamic and steady state behaviour of an anaerobic digester treating high sulfate wastewaters. It is applicable for a number of different carbon sources (both simple and complex). It accounts for pH, sulfide, hydrogen and fatty acid inhibition. It has been shown to be capable of predicting a number of different scenarios, including the time dependent concentration of sulfate and COD in a molasses fed packed bed reactor. It was also able to predict bacterial sulfate reduction performance.

3. Experimental investigations on the kinetics of bacterial sulfate reduction using acetate and using ethanol were carried out. The former was extensive, based on chemostat culture in a well-mixed stirred tank. It investigated kinetics of sulfate reduction and bacterial growth as a function of sulfate loading (affected by both residence time and feed concentration) and temperature. The investigation using ethanol was preliminary. Both showed that the kinetics are inhibited by sulfide and possibly by sulfate. For the case of the acetate-based sulfate reduction, the effect of sulfate concentration and temperature are reported and a rate equation describing the kinetics proposed.

4. Equilibrium simulations of a typical iron-free acid mine drainage precipitation systems were developed using both ASPEN PLUS™ and OLI Systems Inc ESP software. The simulation studies produced useful results and provided a basis from which both

experimental studies and further modelling could be carried out. Both simulation programs predicted the precipitation of the same four metal salts for the test case examined.

5. The experimental studies showed that the pellet reactor is an appropriate technology for the precipitation of a metal hydroxy-carbonate salt from a synthetic nickel sulfate stream. The seeded precipitation means that no sludge is formed. Instead, a dense precipitate permitting easy solid-liquid separation and reuse of the metal occurs.

6. The results suggest that the fines are formed mostly by the spontaneous nucleation of solid phase in the liquid medium generated by a high supersaturation zone, often at the reactant inlet.

7. The Patterson *et al.* (1977) solubility diagram can predict accurately the nickel conversion when two solid phases are taken into account: nickel hydroxide and nickel carbonate. The model is employed to determine the pH zone of the lowest soluble nickel concentration, i.e. the maximal conversion to solid nickel.

8. The equilibrium model may not be used to predict removal efficiency, since it does not take into account fines formation. Hence, the experimental data of nickel removal fits the Patterson *et al* (1977) model well when a low supersaturation, and thus minimal fines generation, is employed within the bed. At high supersaturation, (pH above 9.8, or carbonate to nickel ratio above 4), a significant concentration of fines is found in the outlet stream and thus the removal of the nickel is reduced. Maximal removal efficiencies of 99.6% (ratio 2) and 97.2% (ratio 4) are found at pH = 9.8 for the synthetic stream used during the experiments. At increasing pH, the nickel conversion reaches a steady level of 100%, while the removal efficiency decreases below 80% at pH 11 for both ratios. The Patterson *et al* solubility model cannot thus be employed alone for nickel removal prediction.

9. The kinetics of precipitation are fast, and the soluble species reach near equilibrium with the solid phase after 20 centimetres of bed.

8 RECOMMENDATIONS

In the investigations of sulfate reduction, the volumetric sulfate reduction rates obtained were low. For full-scale implementation of the SRB process, enhancement of the volumetric sulfate reduction rate is required. This may be achieved by using reactor systems in which high cell density is favoured. Typically, these are immobilised cell systems or reactor designs that allow cell recirculation. Immobilised cell systems have been used successfully in other applications for the improvement of reduction rates (Nemati *et al.*, 1996) and show potential for application in the sulfate reduction systems. Consequently, it is recommended that sulfate reduction be studied in immobilised cell systems. This study should include the optimisation of sulfate reduction by a sulfate reducing consortia with respect to support media and reactor configuration.

The anaerobic sulfate reduction process was inhibited at a feed sulfate concentration of 15.0 kgm^{-3}. This inhibitory effect may result from the toxicity of sulfate, sulfide or sodium on SRB. Data presented allowed the hypothesis of sulfate toxicity, however this was not incorporated into the kinetic model. To include the inhibitory effect of sulfate in the kinetic model, further experiments are required across a range of sulfate concentrations that are inhibitory to the biological sulfate reduction process. This will allow for rigorous data collection so that a value for K_I (where I is the substrate) may be determined and used to extend the model. Typically, the study should be carried out in continuous bioreactor experiments receiving sulfate at concentrations between 10.0 and 15.0 kgm^{-3} and above 15.0 kgm^{-3}. Using sulfate concentrations between 10.0 and 15.0 kgm^{-3} will allow determination of the exact concentration at which the onset of sulfate inhibition occurs.

To eliminate the inhibitory effect of sulfide, experiments were carried out at a pH of 7.8 at which sulfide speciation is biased towards the non-toxic HS^- species. Most sulfate containing effluent streams (including AMD) are below this pH. It is therefore recommended that experimental studies be carried out across a range of pH values. The proposed study should be extended to ascertain the effect of sulfide on the kinetics of anaerobic sulfate reduction, since the toxicity of sulfide is pH dependent owing to the variation in sulfide speciation with pH. Using the results from the proposed study the kinetic model presented in this study can be extended to include the effect of pH and sulfide concentration. Furthermore, the combination of the pH and sulfide concentration studies will provide conclusive information regarding the relative toxicity of the sulfide species (H_2S, HS^- or S^{2-}) on sulfate reducing microorganisms.

On an industrial scale, the choice of organic source is motivated by availability and cost. Consequently, readily available and cost effective carbon and electron sources for anaerobic sulfate reduction need to be studied. Where long chain organic compounds are used, the involvement of acid producers and methanogens will occur. The kinetic results obtained can be used to extend the kinetic model developed for this study to include the methanogens and acid producer populations. Furthermore, kinetic data on complete and incomplete oxidising SRB require comparison.

It is envisaged this will provide data to inform the extension of the kinetic model developed, to include the inhibitory effect of sulfate and sulfide, the pH effect and to account for all the microbial groups involved in the conversion of sulfate to sulfide using long chain organic compounds. This model can be used to advise the design of full-scale processes for the biological treatment of sulfate containing effluents.

The modelling studies will continue as improved kinetic data become available from the experimental studies.

It is apparent that precipitation is strongly affected by the local supersaturation within the bed, and by the system hydrodynamics. It is recommended that these phenomena be further investigated.

It is also recommended that further evidence for the mechanism suggested in Figure 6.13 be collected. This would involve measuring the dissolved nickel, nickel removal and fines concentrations as they change with bed height.

Since it appears that agglomeration, not crystal growth, is the main mechanism of nickel removal, it is also recommended that the agglomeration potential of the system be investigated. Examining the zeta potential of the solution in the fluidised bed can provide evidence for the agglomeration potential in the system. Changing the zeta potential could influence the agglomeration mechanism, and promote further agglomeration under various conditions in the bed. This will be carried out as part of a future WRC research contract.

The improved kinetic data for microbial sulfate reduction ow available, as well as the improved understanding of metal precipitation will be integrated, and where appropriate, included in the overall model to allow the key sub-process steps to be identified for further experimental study and process improvement.

9 REFERENCES

1. Alibhai, K.R.K., I.Mehrotra and.C.F.Forster (1984) "Heavy metal binding to digested sludge" Water Res. **19** (12) 1483-1488.
2. Andrews, J.F. and S.P. Graef (1970) "Dynamic Modelling and Simulation of the Anaerobic Digestion Process." In: J.F. Andrews and S.P. Graef Eds, Anaerobic Biological Treatment Processes, Advances in Chemistry, Series 5, American Chemistry Society, Washington DC, pp. 126-162.
3. Andrews, J.F. (19??) "Kinetics of Biological Processes used for Wastewater Treatment" Clemson University, Clemson, pp. 1-35.
4. Andrews, J.F. (1973) "Dynamic Model and Control Strategies for Waste water Treatment Processes". Water Res. **8** 261-289.
5. Andrews, J.F. (1975) "The Development of a Dynamic Model and Control Strategies for the Anaerobic Digestion Process." Water and Sewage Works 62-65 and 74-77.
6. Antonio Giuseppe (1983) "Aerobic digestion of thickened activated sludge." Water Res.**17** (11) 1525-1531.
7. ASPEN PLUS™ (1994). "Modelling processes with electrolytes" ASPEN PLUS™ Release 9.
8. Bachmann, A., V.L. Beard and P.L. McCarty (1985) "Performance Characteristics of the Anaerobic Baffled Reactor." Water Res. **19** (1) 99-106.
9. Badziong, W. and R.K. Thauer (1978a) "Isolation and Characteristics of *Desulfovibrio* Growing on Hydrogen plus Sulfate as the Sole Energy Source." Arch. Microbiol. **116** 41-49.
10. Badziong, W. and R.K. Thauer (1978b) "Growth Yields and Growth Rates of *Desulfovibrio vulgaris* (Marburg) Growing on Hydrogen plus Sulfate and Hydrogen plus Thiosulfate as the Sole Energy Sources." Arch Microbiol. **117** 209-214.
11. Bailey, J. E. and Ollis, D. F. (1986), *Biochemical Engineering Fundamentals* McGraw-Hill Book Company, International Editions, Singapore.
12. Banister, S.S. and W.A. Pretorius (1998) "Optimisation of primary sludge acidogenic fermentation for biological nutrient removal." Water SA **24** (1) 35-41.
13. Barnes, L.J. (1990) "Removal of Heavy Metals and Sulfate from Contaminated Groundwater using Sulfate – Reducing Bacteria: Development of a Commercial Process." Report.
14. Barnes, L.J., F.J. Jansenn, P.J.H Scheeren, J.H. Versteegh and R.O. Koch (1992a) "Simultaneous microbial removal of sulfate and heavy metals from waste water." In: Proceedings of EMC '91: Non-ferrous Metallurgy – Present and Future, Elsevier Applied Science, London, UK, pp 391-402
15. Barnes, L.J., P.J.M Scheeren and C.J.N. Buisman (1992b) "Microbial Removal of Heavy Metals and Sulfate from contaminated Groundwaters." Bioremediation J., 38-49.
16. Barnes, L.J., Budelco. (1999) "THE SRB PROCESS. Process research study on the microbial removal of metals and sulfate from aqueous streams." Shell Research.
17. Barthakur, A., M. Bora and H.D. Singh (1991) "Kinetic Model for Substrate Utilization and Methane Production in the Anaerobic Digestion of Organic Feeds." Biotechnol. Prog. **7** 369-376
18. Barton, L.L. (1995) "Biotechnology Handbooks: Sulfate reducing bacteria, volume 8", Plenum Press, New York.
19. Bharathi, P. A. L., V. Sathe, D. Chandramohan (1990) "Effect of Lead, Mercury and Cadmium on a Sulfate-Reducing Bacterium." Environ. Pollut. **67** 361-3774.
20. Bhattacharya, S.K., V. Uberoi, M.M. Dronamraju (1996) "Interaction between Acetate Fed Sulfate Reducers and Methanogens." Water Res. **3** (10) 2239-2246.
21. Bhattacharyya, D., A.B. Jumawan, G. Sun, D. Sund-Hagelberg and K.Schwitzgebel (1980) "Precipitation of Heavy Metals with Sodium Sulfide: Bench Scale and Full Scale Experimental Results." Water 1980, AICHE Symposium Series 209 77 and 31-38.
22. Blanch, W.H. and D.S. Clark (1996) "Biochemical Engineering." Marcel Dekker, INC. pp 90-115

23. Bos, P. (1994) "Microbiology of Sulfur removal." Department of Microbiology and Enzymology, Delft University of Technology pp. 2-38.

24. Braun, M., H. Stolp (1985) "Degradation of Methanol by a Sulfate reducing bacterium" Arch Microbiol **142** 77-80.

25. Breed, A.W., C.J.N. Dempers, G.E. Searby, M.N. Gardner, D.E. Rawlings and G.S. Hansford (1999) "The Effect of Temperature on the Continuous Ferrous-iron Oxidation Kinetics of a Predominantly Leptospirillum ferrooxidans Culture." Biotechnol. Bioeng. **65** 44-53

26. Brierley, C.L. "Metals Bioremediation Bacteria." Appl. Environ. Microbiol. **33**: (5) 1162-1169.

27. Brown, D.E. G.R. Groves and J.D.A. Miller (1973) "pH and Eh Control of Cultures of Sulfate-reducing Bacteria." J. Appl. Chem. Biotechnol. **23** 141-149.

28. Brüne, G., S.M. Schoberth and H. Sahm (1982) "Anaerobic Treatment of an Industrial Wastewater containing Acetic Acid, Furfural and Sulfite." Process Biochem., pp. 20-35.

29. Bryant, M.P., L. Leon Campbell, C.A. Reddy and M.R. Crabil (1977) (Growth of *Desulfovibrio* in lactate or ethanol media low in sulfate in association with hydrogen utilising methanogenic bacteria." Appl. Environ. Microbiol. **33** (5) 1162-1169

30. Bryers, J.D. (1985) "Structural modelling of the anaerobic digestion of biomass particulates." Biotechnol. Bioeng. **27** 638–649.

31. Buisman, C.J.N. (1996) "Industrial applications of a new sulfur biotechnology." TMR Summer School Programme, Wageningen, pp. 3-30.

32. Buisman, C.J.N., B.G. Geraats, P. Ijspeert and G. Lettinga (1990) "Optimization of Sulfur Producing in a Biotechnological Sulfide-Removing Reactor." Biotechnol. Bioeng. **35** 50-56.

33. Bux, F., F.M. Swalaha and H.C. Kasan (1994) "Microbiological transformation of metal contaminated effluents." Report to the Water Research Commission.

34. Callander, I.J. and J.P. Barford (1983) "Precipitation, Chelation, and the Availability of Metals as Nutrients in Anaerobic Digestion. I. Methodology." Biotechnol Bioeng. **25** 1947-1957

35. Capone, D.G., D.D. Reese and R.P. Kiene (1983) "Effects of Metals on Methanogenesis, Sulfate Reduction, Carbon Dioxide Evolution, and Microbial Biomass in Anoxic Salt Marsh Sediments." Appl. Environ. Microbiol. 1586-1591.

36. Cappenberg, T.H.E. (1979) "Relationships between Sulfate-reducing and Methane-producing Bacteria" Plant and Soil **43** 125-139.

37. Carrol, J.J. (1990) "Reliably predict the solubility of H_2S in water." Chem. Eng. 227-229.

38. Characklis, W.G. (1989) "Kinetics of Microbial Transformations" Biofilms 233-264.

39. Characklis, W.G., G.A. Mcfeters and K.C. Marshall (1989) "Physiological Ecology in Biofilm Systems." Biofilms 341-394.

40. Characklis, W.G., M.H. Turakhia and N. Zelver (1989) "Transport and Interfacial transfer phenomena." Biofilms 265-340.

41. Chen, C.I., R.F. Mueller and T. Griebe (1994) "Kinetic Analysis of Microbial Sulfate Reduction by Desulfovibrio desulfuricans in an Anaerobic Upflow Porous Media Biofilm Reactor." Biotechnol. Bioeng. **43** 267-274.

42. Chen, Y.R. and A.G. Hashimoto (1980) "Substrate Utilization Kinetic Model for Biological Treatment Processes." Biotechnol. Bioeng. **22** 2081-2095.

43. Choi, E. and J.M. Rim (1991) "Competition and Inhibition of Sulfate reducers and Methane producers in anaerobic treatment." Water Sci. Technol. **23** 1259-1264.

44. Christensen, B., M. Laake and T. Lien (1996) "Treatment of Acid Mine Water by reducing Sulfate-reducing Bacteria; results from a bench scale experiment." Water Res. **30** (7) 1617-1624.

45. Cidu, R., R. Caboi, L. Fanfani and F. Frau (1997) "Acid drainage from sulfides hosting gold mineralization (Furtei, Sardinia)." Environ. Geol. **30** 231-237.

46. Cole, S. (1998) "The Emergence of Treatment Wetlands." Environ. Sci. Technol. 218-223.

47. Colleran, E. "Direct anaerobic treatment of citric acid production wastewater." TMR Summer School Programme pp. 2-27.

48. Colleran, E., S. Finnegan and P. Lens (1995) "Anaerobic treatment of sulfate-containing waste streams." Antonie van Leeuwenhoek **67** 29-46.

49. Colleran, E., S. Finnegan, Brendan, R. O' Keeffe (1994) "Anaerobic Digestion of high Sulfate – containing wastewater from the Industrial production of Citric Acid." Water Sci. and Technol. **30** (12) pp 265-273

50. Corbett (1999). Personal communication

51. Cord-Ruwisch, R., H. Seitz and R. Conrad (1988) "The capacity of hydrogenotrophic anaerobic bacteria to compete for traces of hydrogen depends on the redox potential of the terminal electron acceptor." Arch. Microbiol. **149** 350-357.

52. Costello, D.J., P.F Greenfield and P.L. Lee (1991) "Dynamic modelling of a single-stage high-rate anaerobic reactor-I. Model derivation." Water. Res. **25** (7) 847-858.

53. Counotte, G.H,M. and R.A. Prins (1979) "Calculation of K_m and V_{max} from Substrate Concentration Versus Time Plot." Appl. Environ. Microbiol. **38** (4) 758-760.

54. De Lima, A.C.F., M.M. Silva, S.G.F Leite, M.M.M. Goncalves and M. Granato (1996) "Anaerobic Sulfate-reducing microbial process using UASB reactor for heavy metal decontamination". University of Concepcion 141-152.

55. De Smul, A. (1998) "A combined biotechnological and physico-chemical process for the desulferisation of waste-waters" PhD Thesis, University of Gent, Gent, Belgium.

56. de Vegt, A.L., J.P. Krol and C.J. Buisman (1995) "Biological Sulfate removal and metal recovery from mine waters.

57. Delkor Technik (Pty) Ltd. (1998) "Acid Mine Drainage." Presentation by Dr Cees Buisman.

58. DeWalle, F.B., E.S.K Chian, J. Brush (1979) "Heavy Metal Removal with completely mixed anaerobic filter." Journal WPCF **51** (1) 22-36.

59. Dinopoulou, G., R.M. Sterritt and J.N. Lester (1988) "Anaerobic Acidogenesis of a Complex Wastewater : II. Kinetics of Growth, Inhibition, and Product Formation." Biotechnol. Bioeng. **31** 969-978.

60. Dolfing, J. (1988) "Acetogenesis" In: Biology of Anaerobic Microorganisms, ed. Zehnder, A.J.B., John Wiley and sons, New York, Chap. 9 417-468

61. Dries, J., De Smul, A., Goethals, L., Grootaerd, H. and Verstraete, W. (1998), "High rate biological treatment of sulfate-rich wastewater in an acetate-fed EGSB reactor". *Biodegradation*, **9**, 103-111.

62. Du Preez, L.A. and J.P. Maree (1994) "Pilot-scale Biological Sulfate and Nitrate removal utilizing producer gas as energy source." Seventh International Symposium on A/D, Cape Town, S.A. 190-204.

63. Dvorak, D.H., R.S. Hedin and H.M. Edenborn (1992) "Treatment of Metal-Contaminated Water Using Bacterial Sulfate Reduction: Results from Pilot- Scale Reactors". Biotechnol. Bioeng. **40** 609-616.

64. Eastman, J.A. and J.F. Ferguson (1981) "Solubilization of particulate organic carbon during the acid phase of anaerobic digestion." Journal WPCF **53** (3) 352-366.

65. Eliosov, B. and Y. Argaman (1995) "Hydrolysis of particulate organics in Activated Sludge systems." Water Res. **29** (1) 155-163.

66. Elliot, P., S. Ragusa and D. Catcheside (1998) "Growth of Sulfate-reducing Bacteria under acid conditions in an upflow anaerobic bioreactor as a treatment system for mine drainage." Water Res. **32** (12) 3724-3730.

67. Erasmus, C.L. (2000) "A preliminary investigation of the kinetics of biological sulfate reduction using ethanol as a carbon source and electron donor", MSc. Thesis, University of Cape Town, Cape Town, South Africa.

68. Fauque, G. D. (1995), "Ecology of sulphate reducing bacterium". In: Barton L. L. (Editor), *Sulphate Reducing Bacteria*, Plenum Press, New York.

69. Ferguson, J.F., B.J. Eis, and M.M. Benjamin (1984) "Neutralization in anaerobic treatment of an acid waste." Water Res. **18**: (5) 573-580.

70. Fourie, J. W. (1995) "A study on a mine reclamation test plant." Report to the Water Research Commission.

71. Fristoe, B.R., P.O. Nelson (1983) "Equilibrium chemical modelling of heavy metals in activated sludge." Water Res. **17** (7) 771-778.

72. Fukui, M. and S. Takii (1994) "Kinetics of sulfate respiration by free-living and particle-associated sulfate-reducing bacteria." FEMS Microbiol. Ecol., **13** 241-248.

73. Gabb, P.J., *et al* (1995). "The Kennecott smelter hydrometallurgical impurities process." Copper '95 – Cobre '95, Santiago, Chile.

74. Gazea, B., K. Adam and A. Kontopoulos (1996) "A Review of Passive systems for the treatment of Acid mine drainage." Min. Eng., **9** (1) 23-42.

75. Genschow, E., W. Hegemann and C. Maschke (1996) "Biological Sulfate removal from Tannery Wastewater in a two-stage anaerobic treatment." Water Res. **30** (9) 2072-2078.

76. Gerber, A. (1982) "The use of Mathematical models in the formulation of pollution control policies- an Overview." Water Sci. Technol., **14** 1045-1053.

77. Gibson, G.R. (1990) "Physiology and ecology of the sulfate-reducing bacteria." J Appl. Bacteriol., **69** 769-797.

78. Gould, M.S., E.J. Genetelli (1978) "The effect of Methylation and Hydrogen ion concentration on heavy metal binding by Anaerobically digested sludges." Water Res., **12** 889-892.

79. Grady, C.P.L. (1996) "Variability in Kinetic Parameter estimates : a review of possible causes and a proposed terminology." Water Res., **30** (3) 724-748.

80. Graef S.P. and J.F. Andrews (1974) "Mathematical modelling and control of anaerobic digestion." CEP Symposium Series **70** 101-128.

81. Gray, N.F. (1996) "Field assessment of acid mine drainage contamination in surface and ground water." Environ. Geol., **27** 358-361.

82. Gray, N.F. (1997) "Environmental impact and remediation of acid mine drainage: a management problem." Environ. Geol., **30** 62-71.

83. Grobicki, A. and D.C. Stuckey (1992) "Hydrodynamic characteristics of the anaerobic baffled reactor." Water Res. **26** (3) 371-378.

84. Grobicki, A. and S. Moosa. (1994) "High-Sulfate wastewater treatment using the Anaerobic baffled reactor." Department of Chemical Engineering, University of the Witwatersrand 375-382.

85. Grobicki, A.M.W., (1989), "Hydrodynamic characteristics and performance of an anaerobic baffled reactor", PhD thesis, Department of CHEMICAL Engineering, Imperial College, London, United Kingdom

86. Guillard, D., A.E. Lewis and B.K. Butler (2000). "Nickel carbonate precipitation in a pellet reactor." Minerals Engineering 2000, Cape Town, 13-15 November 2000.

87. Gujer, W., and A.J.B. Zehnder (1983) "Conversion processes in anaerobic digestion." Water Sci. Technol. **15** 127-167.

88. Gupta, A., J.R.F. Flora, G.D. Sayles and M.T. Suidan (1994b) "Methanogenesis and Sulfate reduction in Chemostats-II. Model development and verification." Water Res., **28** (4) 792-803.

89. Gupta, A., J.R.F. Flora, M. Gupta, G.D. Sayles and M.T. Suidan (1994a) "Methanogenesis and Sulfate reduction in Chemostats-I. Kinetic studies and experiments." Water Res., **28** (4) 781-793.

90. Hamelers, B., F. Scharff, A. Veeken and S. Kalyuzhnyi (1999) "Inhibition of Anaerobic Hydrolysis of Biowaste by pH and VFA: Experimental Observations and Simulations." J. Environ. Eng. 1- 27.

91. Hamilton, W. "Microbiology and Microbial ecology of Sulfate reducing bacteria." TMR Summer School Programme 2-41.

92. Hammack, R.W. and H.M. Edenborn (1993) "Use of Bacterial Sulfate reduction for removing Nickel from mine waters" 141-147.

93. Hammack, R.W., D.H. Dvorak, S.L. Borek, H.M. Edenborn and W.M. Haffner (1993) "Potential applications of biogenic H_2S in the treatment of metal-containing process waters and mine effluents." 211-216.

94. Hansen, T.A. (1988) "Physiology of Sulfate-reducing bacteria." Microbiol. Sci. **5** (3) 81-84.

95. Harada, H., S. Uemura and K. Momonoi (1994) "Interaction between Sulfate-reducing bacteria and Methane-producing bacteria in UASB reactors fed with low strength wastes containing different levels of Sulfate." Water Res., **28** (2) 355-365.

96. Harper, S.R and F.G. Pohland (1986) "Recent Developments in Hydrogen Management During Anaerobic Biological Wastewater Treatment." Biotechnol. Bioeng.**18** 585-602

97. Hayes. T.D. and T.L. Theis (1978) "The distribution of heavy metals in anaerobic digestion." Journal WPCF 61-72.

98. Heitz, E., H.C. Flemming and W. Sand (1996) "Microbially Influenced Corrosion of materials." Springer-Verlag, Berlin, Heidelberg, Germany.

99. Herlihy, A.T. and A.L. Mills (1985) "Sulfate reduction in freshwater sediments receiving Acid Mine Drainage." Appl. Environ. Microbiol. **49** (1) 179-186.

100. Herrera, L. (1996) "Biological process for Sulfate and metals abatement from mine effluents." Environ. Toxicol. Water Qual.,. **12** 125-134

101. Hickey, R.F., J. Vanderwielen and M.S. Switzenbaum (1989) "The effect of heavy metals on Methane production and Hydrogen and Carbon Monoxide levels during batch Anaerobic Sludge digestion." Water Res. **23** (2) 207-218.

102. Hilton, B.L. and J.A. Oleszkiewiez (1988) "Sulfide-induced inhibition of anaerobic digestion." J. Environ. Eng. **114** (6) 1377-1391.

103. Hilton, M.G. and D.B. Archer (1988) "Anaerobic Digestion of a Sulfate-rich Molasses Wastewater: Inhibition of Hydrogen Sulfide Production." Biotechnol. Bioeng. **31** 885-888.

104. Hoeks, F.W.J.M.M., H.J.G. Hoopen Ten, J.A. Roels and J.G. Kuenen (1984) "Anaerobic treatment of 'Acid Water' (Methane production in a Sulfate-rich environment)." Innovations in Biotechnology **20** 113-119.

105. Hoh, C.Y. and W.R. Cord-Ruwisch (1996) "A Practical Kinetic Model that Considers Endproduct Inhibition in Anaerobic Digestion Processes by including the Equilibrium Constant." Biotechnol. Bioeng., **51** 597-604.

106. Houten van, R.T., L.W. Pol and G. Lettinga (1994) "Biological Sulfate Reduction Using Gas-Lift Reactors Fed with Hydrogen and Carbon Dioxide as Energy and Carbon Source", Biotechnol. Bioeng., **44** 586-594.

107. Houten van, R.T., S. Yun, and G. Lettinga (1997) "Thermophilic Sulfate and Sulfite Reduction in Lab-Scale Gas-Lift Reactors Using H_2 and CO_2 as Energy and Carbon Source." Biotechnol. Bioeng., **55** (5) 807-814.

108. Hulshoff, Pol L.W. (2000) "Treatment of sulfate-rich wastewaters: microbial and process technological aspects." TMR Summer School Programme

109. Huser, B.A., K. Wuhrmann and A.J.B. Zehnder (1982) "Methanothrix soehngenii gen. nov. sp. nov., a New Acetotrophic Non-hydrogen-oxidizing Methane Bacterium." Arch. Microbiol. **132** 1-9.

110. Ingvorsen, K., A.J.B. Zehnder and B.B. Jorgensen (1984) "Kinetics of Sulfate and Acetate Uptake by Desulfobacter postgatei." Appl. Environ. Microbiol. **47** (2) 403-408.

111. Isa, Z., Y. Grusenmeyer and W. Verstraete (1986a) "Sulfate Reduction Relative to Methane Production in High- Rate Anaerobic Digestion: Technical Aspects." Appl. Environ. Microbiol., **51** (3) 572-579.

112. Isa, Z., Y. Grusenmeyer and W. Verstraete (1986b) "Sulfate Reduction Relative to Methane Production in High-Rate Anaerobic Digestion: Microbiological Aspects." Appl. Environ. Microbiol., **51** (3) 580-587.

113. Jackson Moss, C.A. and J.R. Duncan (1990) "The Effect of Iron on Anaerobic digestion." Biotech. Lett., **12** (2) 149-154.

114. Jackson, E., (1986). "Hydrometallurgical Extraction and Reclamation." Horwood Ellis Publishers, Chichester. 50-97

115. Jain, S., A.K. Lala, S.K. Bhatia and A.P. Kudchadker (1992) "Modelling of Hydrolysis Controlled Anaerobic Digestion." J. Chem. Technol. Biotechnol., **53** 337-344.

116. Jeffers, T.H., C.R. Ferguson and P.G. Bennert (1991) "Biosorption of Metal contaminators from Acidic mine waters." Salt Lake City Research Centre, pp. 290-298.

117. Jenke, D.R. and D.E. Diebold (1983) "Recovery of valuable metals from acid mine drainage by selective titration." Water Res. **17** (11) 1585-1590.

118. Jenke, D.R. and F.E. Diebold (1985) "Computer simulation of an Industrial wastewater treatment process." Water Res. **19** (6) 719-724.

119. Jensen, A.B. and C. Webb (1995) "Treatment of H_2S-containing gases: A review of microbiological alternatives." Enzyme and Microbial Technology **17** 2-10.

120. Jeyaseelan, S. (1997) "A simple mathematical model for Anaerobic Digestion process." Water. Sci. Technol., **35** (8) 185-191.

121. Kalin, M., A. Fyson and M.P. Smith (1991) "Passive treatment processes for the mineral sector" 363-374.

122. Kalin, M., J. Cairns and R. McCready (1991) "Ecological engineering methods for acid mine drainage treatment of coal wastes." Resour. Conserv. Recycling, **5** 265-275.

123. Kalyuzhnyi, S.V. and V.V. Fedorovich (1997) "Integrated mathematical model of UASB reactor for competition between Sulfate reduction and Methanogenesis." Water. Sci. Technol., **36**: (6/7) 201-208.

124. Kalyuzhnyi, S.V. and V.V. Fedorovich (1998a) "Mathematical modelling of competition between Sulfate reduction and Methanogenesis in Anaerobic reactors." Bioresour. Technol., **65** pp227-242

125. Kalyuzhnyi, S.V. and V.V. Fedorovich (1998b) "Mathematical modelling of competition between Sulfate reduction and Methanogenesis in Anaerobic reactors." Biodegradation **9** 187-199.

126. Kamaraj, P., S. Jacob, N. Sathyamurthy and D. Srinivasan (1991). "Sulfide Precipitation Technique in the Removal of Heavy Metals." Indian Journal of Environmental Health, **33** (2) 208-212.

127. Kasper, H.F. and K. Wuhrmann. (1977). "Kinetic parameters and relative turnover of some important catabolic reactions in digesting sludge." Appl. Environ. Microbiol., **36** (1) 1-7.

128. Knobel A.N., (1999) "A mathematical model of a high sulfate wastewater, anaerobic treatment system" MSc Thesis, UCT, Cape Town

129. Kolmert, A., T. Henrysson, R. Hallberg and B. Mattiasson (1997) "Optimization of sulfide production in an anaerobic continuous biofilm process with sulfate reducing bacteria." Biotech. Lett., **19** (10) 971-975.

130. Konishi, Y., N. Yoshida and S. Asai (1996) "Desorption of Hydrogen Sulfide during Batch Growth of the Sulfate-Reducing Bacterium *Desulfovibrio desulfuricans*." Biotechnol. Prog., **12** 322-330.

131. Kremer, D.R., H.E. Nienhuis-Kuiper and T.A. Hansen (1988) "Ethanol dissimilation in *Desulfovibrio*." Arch. Microbiol. **150** 552-557

132. Kristjansson, J.K., P. Schonheit and R.K. Thauer (1982) "Different K_s Values for Hydrogen of Methanogenic Bacteria and Sulfate Reducing Bacteria: An Explanation for the Apparent Inhibition of Methanogenesis by Sulfate." Arch. Microbiol. **131** 278: 282.

133. Krouse, H.R. and R.G.I. McCready (1992) "Biochemical cycling of Sulfur", pp. 401-430.

134. Kugelman, I.J. and P.L. McCarty (1965) "Cation Toxicity and stimulation in Anaerobic waste treatment." Journal WPCF **37** (1) 97-116.

135. Kuyucak, N. and P. St- Gemain (1994) "Evaluation of Sulfate reducing Bacteria and related process parameters for developing a passive treatment method." Mineral Bioprocessing II conference Proceedings, pp287-303

136. Kuyucak, N. and P. St-Germain (1994) "Passive treatment methods for acid mine drainage." 319-331.

137. Kuyucak, N. and P. St-Germain (1994) "Possible options for In Situ treatment of acid mine drainage seepages." International Land Reclamation and Mine Drainage Conference.

138. Kuyucak, N. and S. Payant (1995) "Enhanced Lime-neutralization methods for improving sludge density and final effluent quality." International Symposium on Waste Processing and Recycling in Mineral and Metallurgical Industries.

139. Laanbroek H.J., T. Abee and I.L. Voogd (1982) "Alcohol conversions by Sulfobulbus propionicus Lindhorst in the presence and absence of sulfate and hydrogen" Arch. Microbiol. **133** 178-184

140. Laanbroek, H.J., H.J. Geerligs, L. Sijtsma and H. Veldkamp (1984) "Competition for sulfate and ethanol among Desulfobacter, Desulfobulbus and Desulfovibrio species isolated from intertidal sediments." Appl. Environ. Microbiol. **47** 329-334

141. Lawrence, A.W. and P.L. McCarty (1965) "The role of Sulfide in Preventing heavy metal Toxicity in Anaerobic treatment." Journal WPCF **37** (3) 392-406.

142. Lawrence, A.W. and P.L. McCarty (1966) "The Effects of Sulfides on Anaerobic treatment." Air and Water Pollution International Journal. **10** 207-221.

143. Ledin, M., and K. Pederson (1996) "The Environmental impact of mine wastes – Roles of microorganisms and their significance in treatment of mine wastes." Earth-Sci. Rev., **41** 67-108.

144. Legall, J. and F. Fauque (1988) "Dissimilatory reduction of Sulfur compounds." Biology of Anaerobic Microorganisms 587-639.

145. Lens, P.N.L. and L.W. Hulshoff Pol (1998) "Biodegradation : Special issue. Biological sulfur cycle." Environmental Science and Technology. **9** (3/4), Kluwer Academic Publishers.

146. Lettinga, G. (1995) "Anaerobic digestion and wastewater treatment systems." Antonie van Leeuwenhoek **67** 3-28.

147. Lettinga, G., W. De Zeeuw and E. Ouborg (1981) "Anaerobic treatment of wastes containing methanol and higher alcohols." Water. Res., **15** 171-182.

148. Lewis, A. E. and A. N. Knobel (2000) "A primer for modelling and simulation: a case study of a mathematical model for a high sulfate wastewater, anaerobic treatment system." BIOY2K Millennium Meeting, Minewater Symposium, Grahamstown, SA.

149. Lewis, A. E. and J.G. Petrie (1998) "Process developments for biological treatment of metal Sulfate waste waters." 2nd International Conference on Advanced Wastewater Treatment, recycling and Re-use, Milan, Italy.

150. Li, Y., S. Lam and H.H.P. Fang (1996) "Interactions between Methanogenic, Sulfate-reducing and Syntrophic Acetogenic bacteria in the Anaerobic degradation of Benzoate." Water Res., **30** (7), 1552-1562

151. Lilley, I.D., M.C. Wentzel, R.E. Loewenthal and G.R. Marais (1990) "Acid fermentation of primary sludge at 20 C." UCT Department of Civil Engineering Water Research Commission Report.

152. Lin, C.Y. (1993) "Effect of heavy metals on Acidgenesis in Anaerobic digestion." Water. Res., **27** (1) 147-152

153. Loewenthal, R.E., G.A. Ekama and G.R. Marais (1989) "Mixed weak acid/base systems Part1 – Mixture characterisation." Water S.A., **15** (1) 3-23.

154. Loewenthal, R.E., G.A. Ekama and G.R. Marais (1989) "Mixed weak acid/base systems Part II : Dosing estimation, aqueous phase." Water S.A., **17** (2) 107-123.

155. Lovley, D.R. and M.J. Klug (1983) "Sulfate Reducers can Out-compete Methanogens at Freshwater Sulfate Concentrations." Appl. Environ. Microbiol. **40** (1) 187-192.

156. Lowe, S.E., M.K. Jain and J.G. Zeikusa (1993) "Biology, Ecology and Biotechnological Applications of Anaerobic Bacteria Adapted to Environmental Stresses in Temperature, pH, Salinity, or Substrates." Microbiol. Rev., **57** (2) 451-509.

157. Lyew, D. and J.D. Sheppard (1997) "Effects of physical Parameters of a Gravel Bed on the Activity of Sulfate-reducing Bacteria in the Presence of Acid Mine Drainage." J. Chem. Technol. Biotechnol., **70** 223-230.

158. Maillacheruvu, K.Y. and G.F. Parkin (1996) "Kinetics of growth, substrate utilization and sulfide toxicity for propionate, acetate, and hydrogen utilizers in anaerobic systems." Water Environ. Res., **68** (7) 1099-1106.

159. Maree, J.P. (1988) "Sulfate Removal from industrial effluents.", PhD Thesis in department of Chemistry, University of O.F.S., Bloemfontein.

160. Maree, J.P. and E. Hill (1989) "Biological removal of Sulfate from industrial effluents and concomitant production of Sulfur." Water. Sci. Technol., **21** 265-276.

161. Maree, J.P. and W.F. Strydom (1985) "Biological Sulfate removal in an upflow packed bed reactor." Water Res. **19** (9) 1101-1106.

162. Maree, J.P. and W.F. Strydom (1987) "Biological Sulfate removal from industrial effluent in an upflow packed bed reactor." Wat. Res., **21** (2) 141-146

163. Maree, J.P., A. Gerber and E. Hill (1987) "An integrated process for biological treatment of sulfate-containing industrial effluents." Journal of Water Pollution control federation. **12** 1069-1074.

164. McCartney, D.M. and J.A. Oleszkiewicz (1991) "Sulfide inhibition of anaerobic degradation of Lactate and Acetate." Water. Res., **25** (2) 203-209.

165. McCartney, D.M. and J.A. Oleszkiewicz (1993) "Competition between Methanogens and Sulfate reducers: effect of COD : Sulfate ratio and acclimation." Water Environ. Res., **65** 655-664.

166. McCarty, P.L. and F.E. Mosey (1991) "Modelling of Anaerobic digestion processes (A discussion of concepts)." Water. Sci. Technol. **24** (8) 17-33.

167. McNally, S., and Benefield, L. (1984) "Nickel Removal from a Synthetic Nickel-Plating Wastewater Using Sulfide and Carbonate for Precipitation and Co-precipitation." Sep. Sci. and Technol., **19** (2/3) 191-217.

168. Middleton, A.C. and A.W. Lawrence (1977) "Kinetics of microbial sulfate reduction." Journal of Water Pollution Control Federation. **49**, pp 1659-1670.

169. Mishra, S. K. (1999). "Resource recovery in waste treatment increasingly used." Min. Eng., April 1999.

170. Mizuno, O., Y.Y. Li and T. Noike (1994) "Effects of Sulfate concentration and sludge retention time on the interaction between Methane production and Sulfate reduction for Butyrate." Water. Sci. Technol., **30** (8) 45-54.

171. Moletta, R., G. Verrier and G. Albagnac (1986) "Dynamic Modelling of Anaerobic Digestion." Water Res., **20** (4) 427-434.

172. Moon, J (1995) "Quantification of Biomass in a Biooxidation system." MSc. Thesis, University of Cape Town, Cape Town, South Africa

173. Moosa, S. (2000) "A kinetic study on anaerobic sulfate reduction – effect of sulfate and temperature." PhD thesis, University of Cape Town, Cape Town, South Africa

174. Moosbrugger, R.E, M.C. Wentzel, G.A. Ekama and G.R. Marais (1992) "Simple titration procedures to determine H_2CO_3 Alkalinity and short-chain fatty acids in aqueous solutions containing known concentrations of Ammonium, Phosphate and Sulfide weak Acid/Bases." WRC Report No. TT 57/92.

175. Mosey, F.E. (1983) "Mathematical modelling of the anaerobic digestion process: Regulatory mechanisms for the formation of short-chain volatile acids from Glucose." Water Sci. Technol., **15** 209-232.

176. Mosey, F.E. and D.A. Hughes (1975) "The Toxicity of Heavy Metal Ions to Anaerobic Digestion." Water pollution control. 18-39.

177. Mosey, F.E., J.D. Swanwick and D.A. Hughes (1971) "Factors affecting the availability of Heavy Metals to inhibit Anaerobic Digestion." Water Pollut. Control. 668-680.

178. Mukai S., *et al* (1979). "Study on the Removal of Heavy Metal Ions in Wastewater by the Precipitation-Flotation method." Recent Developments in Separation Science. 27-39

179. Mulder, A. (1984) "The effects of high Sulfate concentrations on the Methane fermentation of wastewater." Innovations in Biotechnology 133-143.

180. Musvoto, E.V., M.C. Wentzel, R.E. Loewenthal and G.A. Ekama (1997) "Kinetic based model for mixed weak acid/base systems." Water S.A., **23** (4) 311-322.

181. Nakamura, K. (1987) "Biological Metal removal From mine drainage" 274-278.

182. Nemati, M. and C. Webb (1996) "Effect of ferrous iron concentration on the catalytic activity of immobilized cells of *Thiobacillus ferrooxidans*." Appl. Microbiol. Biotechnol. **46** 250-255.

183. Nemati, M. and C. Webb (1997) "A Kinetic Model For Biological Oxidation of Ferrous Iron by *Thiobacillus ferrooxidans*." Biotechnol. Bioeng. **53** (5) 478-485.

184. Nemati, M., (1998) Bioprocess Technology II:Enzyme Kinetics, Lecture notes.

185. Nemati, M., S.T.L. Harrison, G.S. Hansford and C. Webb (1998) "Biological oxidation of ferrous Sulfate by *Thiobacillus ferrooxidans*: a review on the kinetic aspects." Biochem. Eng. J., **1** 171-190

186. Nethe-Jaenchen, R., R.K. Thauer (1984) "Growth yields and saturation constant of *Desulfovibrio vulgaris* in chemostat culture." Arch. Microbiol. **137** 236-240.

187. O' Flaherty and E. Colleran (1998) "Effect of sulfate addition on volatile fatty acid and ethanol degradation in an anaerobic hybrid reactor: I. Process disturbance and remediation." Bioresour. Technol., **68** 101-107

188. O' Flaherty, V., T. Mahony, R. O'Kennedy and E. Colleran (1998) "Effect of pH on growth kinetics and Sulfide toxicity thresholds of a range of Methanogenic, Syntrophic and Sulfate-reducing bacteria." Process Biochem., 33 (5) 1-15.

189. Okabe, S. and W.G. Characklis (1992a) "Effects of Temperature and Phosphorous Concentration on Microbial Sulfate Reduction by *Desulfovibrio desulfuricans*." Biotechnol. Bioeng. **39** 1031-1042.

190. Okabe, S., P.H. Nielson and W.G. Characklis (1992b) "Factors Affecting Microbial Sulfate Reduction by *Desulfovibrio Desulfuricans* in Continuous Culture: Limiting Nutrients and Sulfide Concentration." Biotechnol. Bioeng., **40** 725-734.

191. Okabe, S., P.H. Nielson, W.L. Jones and W.G. Characklis (1995) "Sulfide product inhibition of *Desulfovibrio desulfuricans* in batch and continuous cultures." Water. Res. **29** (2) 571-578.

192. Oleszkiewicz, J.A. and B.L. Hilton (1986) "Anaerobic treatment of high-sulfate wastes." Can. J. Civ. Eng., **13** 423-428.

193. Omil, F., P. Lens, L.W. Hulshoff Pol and G. Lettinga (1996) "Effect of Upward Velocity and Sulfide Concentration on Volatile Fatty Acid Degradation in a Sulfidogenic Granular Sludge reactor." Process Biochem., **31** (7) 699-710.

194. Omil, F., P. Lens, L.W. Hulshoff Pol and G. Lettinga (1997) "Characterization of Biomass from a sulfidogenic, volatile fatty acid-degrading granular sludge reactor." Enzyme and Microbial Technology **20** 229-236.

195. Omil, F., P. Lens, L.W. Hulshoff Pol and G. Lettinga (1998) "Long-Term Competition between Sulfate reducing Methanogenic Bacteria in UASB Reactors treating Volatile Fatty Acids." Biotechnol. Bioeng. **57** (6) 676-685.

196. Ong, S. L. (1983) "Least Squares Estimation of Batch Culture Kinetic Parameters." Biotechnol. Bioeng., **15** 2345-2358.

197. Oremland, R.S. and S. Polcin (1982) "Methanogenesis and Sulfate reduction competitive and non-competitive substrates in Esturine Sediments." Appl. Environ. Microbiol., **44** (6) 1270-1276.

198. O'Rourke, J.T. (1968). "Kinetics of anaerobic treatment at reduced temperatures." PhD. Dissertation, Department of Civil Engineering, Stanford University.

199. Oude Elferink, S.J.W.H., A. Visser, L.W. Hulshoff Pol and A.J.M. Stams (1994) "Sulfate reduction reduction in methanogenic bioreactors." FEMS Microbiol. Reviews, **15** 119-136

200. Owen, W.F., D.C. Stuckey, J.B. Healy, L.Y. Young and P.L. McCarty (1979) "Bioassay for Monitoring Biochemical Methane Potential and Anaerobic Toxicity." Water. Res., **13** 485-492.

201. Paques Environmental Technology. "Biological treatment of photoprocessing wastewater."

202. Parkes. R.J., B.A. Cragg S.J. Bale, K. Goodman and J.C. Fry (1995) "A combined ecological and physiological approach to studying sulfate reduction within deep marine sediment layers." J. Microbiol. Methods, **23** 235-249.

203. Parkin, G. F., M.A. Sneve and H. Loos (1991) "Anaerobic filter treatment of Sulfate-containing wastewaters." Water Sci., **23** 1283-1291.

204. Patterson, J.W., J.J. Scala and H.E. Allen (1977) "Heavy Metal Treatment By Carbonate Precipitation." Journal Water Pollution Control Federation, December 2397-2410.

205. Pavlostathis, S.G. and E. Giraldo-Gomez (1991) "Kinetics of Anaerobic treatment." Water Sci. Technol., **24** (8) 35-59.

206. Peck, H.D. and T. Lissolo (19??) "Assimilatory and Dissimilatory Sulfate reduction: Enzymology and Bioenergetics." Biochemistry of Sulfate Reduction 109-131.

207. Perry, K.A. (1995) "Sulfate-reducing Bacteria and Immobilization of Metals." Mar. Geosour. Geotechnol., **13** 33-39.

208. Peters, R.W., K. Young and T. Chang (1984) "Heavy metal crystallisation kinetics in an MSMPR crystalliser employing sulfide precipitation." Advances in Crystallisation from Solutions, AICHE Symposium Series **240** (80) 55-75

209. Petrasek, A.C., I.J. Kugelman, B.K. Austern and T.A. Pressley (1983) "Fate of toxic organic compounds in wastewater treatment plants." Journal WPCF **55** (10) 1286-1296

210. Pfennig, N., F. Widdel and H.G. Truper (1981) "The Dissimilatory Sulfate-reducing Bacteria."

211. Polprasert, C. and C.N. Haas (1995) "Effects off Sulfate on Anaerobic processes fed with dual substrates." Water Sci. Technol., **31** (9) 101-107.

212. Postgate, J.R. (1984) "The sulfate reducing bacteria" (2nd ed.), Cambridge University press.

213. Press, W.H., B.P. Flannery, S.A. Teukolsky and W. T. Vetterling (1992), "Numerical Recipes: The Art of Scientific Computing." Cambridge University Press.

214. Ramachandra, R.S. and L.G. Hepler (1977). "Equilibrium constants and thermodynamics of ionisation of aqueous hydrogen sulfide." Hydrometallurgy **2**: 293-299.

215. Raskin, L., B.E. Rittmann, and D.A. Stahl (1996) "Competition and Coexistence of Sulfate-Reducing and Methanogenic Populations in Anaerobic Biofilms." Appl. Environ. Microbiol., **62** (10) 3847-3857.

216. Reis, M.A.M., J.S. Almeida, P.C. Lemos and M.J.T. Carrondo (1992) "Effect of Hydrogen Sulfide on Growth of Sulfate reducing Bacteria." Biotechnol. Bioeng., **40** 593-600.

217. Reis, M.A.M., L.M.D Goncalves and M.J.T. Carrondo (1998) "Sulfate removal in Acidogenic phase anaerobic digestion." Environ Technol. Lett., **9** 775-784.

218. Reis, M.A.M., P.C. Lemos, J.S. Almeida and M.J.T. Carrondo (1990) "Influence of produced Acetic Acid on growth of Sulfate reducing bacteria." Biotech. Lett., **12** (2) 145-148.

219. Reis, M.A.M., P.C. Lemos, J.S. Almeida and M.J.T. Carrondo (1991) "Evidence for the intrinsic toxicity of H_2S to Sulfate-reducing bacteria." Applied Microbiol. Biotechnol. **36** 145-147.

220. Reis, M.A.M., P.C. Lemos, J.S. Almeida, M.J. Martins, P.C. Costa, L.M.D. Goncalves and M.J.T. Carrondo (1991) "Influence of Sulfates and operational parameters on volatile fatty acids concentration profile in acidogenic phase." Bioprocess Eng., 145-151.

221. Rintala, J. and G. Lettinga (1992) "Effects of Temperature elevation from 37 to 55 ºC on anaerobic treatment of Sulfate rich acidified wastewaters." Environ. Technol., **37** 801-812.

222. Robinson, J.A. and J.M. Tiedje (1984) "Competition between sulfate-reducing and Methanogenic bacteria for H_2 under resting and growing conditions." Arch. Microbiol., **137** 26-32.

223. Roels, J.A. (1983) "Energetics and Kinetics in Biotechnology." Elsevier Biomedical Press.

224. Roig, M.G., T. Manzano and M. Diaz (1997) "Biochemical process for the removal of Uranium from acid mine drainage." Water. Res., **31** (8) 2973- 2083.

225. Rose, P (1999). Personal communication.

226. Rose, P.(19??) "Biological treatment of acid mine drainage." TMR Summer School Programme.

227. Rouse, J.V. (1976) "Removal of Heavy Metals from Industrial Effluents." Journal of the Environmental Engineering division. 929-936.

228. Rudd, T., R.M. Sterrit and J.N. Lester (1984) "Formation and conditional stability constants of complexes formed between heavy metals and bacterial extracellular polymers." Water Res. **18** (3) 379-384.

229. Salomons, W. (1995) "Environmental impact of metals derived from mining activities: Processes, predictions, prevention." J. Geochem. Explor. **52** 5-23.

230. Samain, E.,G. Albagnac, H.C. Dubourguier and J.P. Touzel (1982) " Characterisation of a new propionic acid bacterium that ferments ethanol and displays a growth factor-dependant association with a gram-negative homoacetogen" FEMS Microbiol. Lett., **15** 69-74

231. Sam-Soon, P., R.E. Loewenthal, P.L. Dold and G.R. Marais (1987) "Hypothesis for pelletisation in the Upflow Anaerobic Sludge Bed reactor." Water S.A., **13** (2).69-80.

232. Scheeren, P.J.H., R.O. Koch, C.J.N. Buisman, L.J. Barnes and J.H. Versteegh (1994) "New biological treatment plant for heavy metal-contaminated groundwater", Transactions of the Institute of Metallurgists, **101**, C190-C199.

233. Schink, B., T.J. Phelps, B. Eichler and J.G. Zeikus (1985) "Comparison of ethanol degradation pathways in anoxic freshwater sediments." J. Gen. Microbiol., **131** 651-660

234. Schonheit, P., J. Moll and R.K. Thauer (1980) "Growth Parameters of Methanobacterium thermoautotrophicum." Arch. Microbiol., **127** 59-65.

235. Schonheit, P., J.K. Krisrjansson and R.K. Thauer (1982) "Kinetic Mechanisms for the Ability of Sulfate Reducers to Out-Compete Methanogens for Acetate." Arch Microbiol., **132** 285-288.

236. Schsuder, R., B. Eikmanns, R.K. Thauer, F. Widdel and G. Fuchs (1986) "Acetate oxidation to CO_2 in anaerobic bacteria via a novel pathway not involving reactions of the citric acid cycle." Arch. Microbiol. **145** 162-172.

237. Seckler, M. (1994). "Calcium Phosphate Precipitation in a Fluidised bed." PhD. Thesis, Delft University of Technology, The Netherlands. 70-131

238. Senior, E. (1990) "Microbiology of landfill sites." CRC Press, Inc.

239. Senior, E., T.J. Britz and M. Senior Ter Laag (1992) Proceedings of Third Southern Africa anaerobic digestion symposium. Pietermaritzburg, SA.

240. Shimizu, T., K. Kudo and Y. Nasu (1993) "Anaerobic Waste-Activated Sludge Digestion – A bioconversion Mechanism and Kinetic Model." Biotechnol. Bioeng., **41** 1082-1091.

241. Shin, H.S., S.E. Oh and B.U. Bae (1996) "Competition between SRB and MPB according to temperature change in the anaerobic treatment of Tannery wastes containing high Sulfate." Environ. Technol., **17** 361-370.

242. Sohnel, O., and J. Garside (1992) "Precipitation: Basic principles and industrial applications." Butterworth-Henemann Ltd, Oxford.

243. Soto, M., R. Mendez and J.M. Lema (1993) "Sodium Inhibition and Sulfate Reduction in the Anaerobic Treatment of Mussel Processing Wastewaters." J. Chem. Technol. Biotechnol., **58** 1-7

244. Speece, R. E. (1983), "Anaerobic biotechnology for industrial wastewaters". Environ. Sci. Technol., **17**, 416A-427A.

245. Speece, R.E. (1996) "Anaerobic Biotechnology for industrial wastewaters." Archae Press, USA

246. Stams, A.J.M. and J.W.H. Elferink Oude (1997) "Understanding and advancing wastewater treatment." Environ. Biotechnol., **8** 328- 334.

247. Stieb, M. and B. Schink (1989) "Anaerobic degradation of isobutyrate by methanogenic enrichment cultures and by a *Desulfococcus multivorans* strain." Arch. Microbiol., 126-132.

248. Szewzyk, R. and N. Pfennig (1990) "Competition for Ethanol between Sulfate-reducing and fermenting bacteria." Arch. Microbiol., **153** 470-477.

249. Thiopaq Sulfur Systems. (2000)" Combined Biological removal of Sulfate and heavy metals from water.", leaflet

250. Tijero, J., E. Guardiola, F. Miranda and Cortijo. (1991) "Effect of Cu^{2+}, Ni^{2+} and Zn^{2+} on an anaerobic digestion system." J. Environ. Sci. Health **A26** (6) 779-811.

251. Traore, A.S., M.L. Fardeau, C.E. Hatchikian, J. Gall and J.P. Belaich (1983) "Energetics of growth of a Defined Mixed Culture of *Desulfovibrio vulgaris* and *Methanosarcina bakeri*: Interspecies Hydrogen Transfer in Batch and Continuous Cultures." Appl. Environ. Microbiol., **46** (5) 1152-1156.

252. Tunay, O., O. Tasli and D. Orhon (1992) "Factors affecting the performance of hydroxide precipitation of metals." 46th Purdue Indus Wastes Conf. Proc.

253. Tuttle, J.H., P.R. Dugan and C.I. Randles (1969) "Microbial Sulfate Reduction and Its Potential Utility as an Acid Mine water Pollution Abatement Procedure." Appl. Microbiol. **17** (2) 279-302.

254. Uberoi, V. and S.K. Bhattacharya (1995) "Interactions among Sulfate reducers, Acetogens, and Methanogens in Anaerobic Propionate systems." Water Environ.Res., **67** (3) 330-339.

255. Ueki, A., K. Ueki and K. Matsuda (1988) "Effect of Sulfate reduction on Methanogenensis in the anaerobic digestion of animal waste." J. Gen. Appl. Microbiol., **34** 297-301.

256. Ueki, A., K. Ueki, A. Oguma and C. Ohtsuki (1989) "Partition of Electrons between Methanogenesis and Sulfate reduction in the Anaerobic digestion of animal waste." J. Gen. Appl. Microbiol. **35** 151-162.

257. Ulrich, G.A., L.R. Krumholz and J.M. Suflita (1997) "A rapid and simple method for estimating Sulfate reduction activity and quantifying Inorganic Sulfides." Appl. Environ. Microbiol., **63** (4) 1627-1630.

258. Van Dijk, J.C., M. van Ammers, A. Graveland and P.A.N.M. Nuhn (1986) "State of the Art of Pellet Softening in the Netherlands." Water Supply **4** 223-235.

259. Van Haandel A.C. and G. Lettinga (1994) "Anaerobic Sewage Treatment – A Practical Guide for Regions with a Hot Climate." John Wiley and Sons, Chichester, England. 15-73

260. Van Houten, R.T. (1996) "Biological sulfate reduction with synthetic gas." PhD Thesis, Wageningen Agricultural University, Wageningen, The Netherlands.

261. Van Houten, R.T., L.W. Pol Hulshoff and G. Lettinga (1994) "Biological Sulfate Reduction using Gas-Lift reactors fed with Hydrogen and Carbon Dioxide as Energy and Carbon Source." Biotechnol. Bioeng., **44** 586-594.

262. Van Houten, R.T., S.Y. Yun and G. Lettinga (1997) "Thermophilic Sulfate and Sulfite Reduction in Lab-Scale Gas-Lift Reactors using H_2 and CO_2 as Energy and Carbon Source." Biotechnol. Bioeng., **55** (5) 807-814.

263. Van Loosdrecht, M.C.M. (1993). Personal communication.

264. Vasiliev, V.B., V.A. Vavilin, S.V. Rytow and A.V. Ponomarev (1993) "Simulation Model of Anaerobic Digestion of Organic Matter by a Microorganism Consortium: Basic Equations." Water Resour., **20** (6) 714-725.

265. Vavilin, V.A., S.V. Rytov and L.Y. Lokshina (1996) "A description of Hydrolysis kinetics in anaerobic degradation of Particulate Organic Matter." Bioresour. Technol., **56** 229-237.

266. Vavilin, V.A., V.B. Vasiliev, S.V. Rytov, and A.V. Ponomarev (1995) "Modelling Ammonia and Hydrogen Sulfide inhibition in anaerobic digestion." Water Reserve **29** (3) 827-835.

267. Visser, A. (1995), "The anaerobic treatment of sulphate containing wastewaters". PhD Thesis, Wageningen Agricultural University, Wageningen, The Netherlands.

268. Visser, A.., F. Van de Zee, I. Beekman, A.J.M. Stams and G. Lettinga (1993) "Anaerobic degradation of volatile fatty acids at different Sulfate concentrations." Appl. Microbiol. Biotechnol., **40** 549-556.

269. Wanner, O. and P. Reichert (1996) "Mathematical Modelling of Mixed-Culture Biofilms." Biotechnol.. Bioeng., **49** 172-184.

270. Weist, R.C. (1977) "Handbook of chemistry and physics", 58th edition.

271. Wentzel, M.C., Ekama, G.A. and G.R. Marais (1990) "Biological excess phosphorus removal – Steady state process design." Water S.A., **16** (1) 29-48.

272. Whang, J.S., *et al* (1982) "Soluble Sulfide Precipitation from Heavy Metals Removal from Wastewaters." Environmental Progress **1** (2)

273. White, C. and G.M. Gadd (1996) "Mixed sulfate reducing bacterial cultures for bioprecipitation of toxic metals : factorial and response surface analysis of the effects of dilution rate, Sulfate and substrate concentration." Microbiol., **142** 2197-2205.

274. Widdel, F. (1987) "New types of Acetate-oxidizing, Sulfate-reducing *Desulfobacter* species, *D. hydrogenophilus* sp. nov., *D. latus* sp. nov., and *D. curvatus* sp. nov." Arch. Microbiol., **148** 286-291.

275. Widdel, F. (1988) "Microbiology and Ecology of Sulfate and Sulfur-reducing bacteria." 469-585.

276. Widdel, F. and N. Pfennig (1977) "A New Anaerobic, Sporing, Acetate-Oxidizing, Sulfate-Reducing Bacterium, *Desulfotomaculum* (emend.) *acetoxidans*." Arch. Microbiol., **112** 119-122.

277. Widdel, F. and N. Pfennig (1981) "Dissimilatory Sulfate or Sulfate-reducing Bacteria" 663-679.

278. Widdel, F. and N. Pfennig (1981) "Sporulation and Further Nutritional Characteristics of *Desulfotomaculum acetoxidans*." Arch. Microbiol., **129** 401-402.

279. Widdel, F. and N. Pfennig (1981) "Studies on Dissimilatory Sulfate-Reducing Bacteria that Decompose Fatty Acids. I. Isolation of New Sulfate-Reducing Bacteria Enriched with Acetate from Saline environments. Description of *Desulfobacter postgatei* gen. nov., sp. nov." Arch. Microbiol., **129**, 395-400.

280. Widdel, F. and N. Pfennig (1982) "Studies on Dissimilatory Sulfate-reducing Bacteria that decompose Fatty Acids. II. Incomplete Oxidation of Propionate by *Desulfobulbus Propionicus* gen. nov., sp. nov." Arch. Microbiol., **131** 360-365.

281. Widdel, F., G.W. Kohring and F. Mayer (1983) "Studies on Dissimilatory Sulfate-Reducing Bacteria that Decomposes Fatty Acids III. Characterization of the Filamentous Gliding *Desulfonema limicola* gen. nov. sp. nov., and *Desulfonema magnum* sp. nov." Arch Microbiol., **134** 286-294.

282. Wiegant, W.M., M. Hennink and G. Lettinga (1986) "Separation of the Propionate degradation to improve the efficiency of Thermophilic Anaerobic treatment of Acidified wastewaters." Water Res., **20** (4) 517-524

283. Wijaya, S., W.D. Henderson, J.K. Bewtra and N. Biswas (1997) "Optimization of Dissolved heavy metals removal using Sulfate reducing Bacteria." 48th Purdue University Industrial Waste Conference Proceedings 469-481.

284. Wilms, D.A., (1988). "Recovery of nickel by crystallisation of nickel carbonates in a fluidised bed reactor." VTT Symposium on Non-Waste Technology, Espoo, Finland.

285. Wittington-Jones (1999). Personal communication.

286. Wood, P. M. (1978) "A Chemiosmotic Model for Sulfate respiration." FEBS Lett., **95** (1) 12-98.

287. Wu, M.M. and R.F. Hickey (1997) "Dynamic Model for UASB reactor including reactor Hydraulics, Reaction and Diffusion." J. Environ. Eng., 244-252.

288. Yadav, V.K. and D.B. Archer (1988) "Specific inhibition of Sulfate-reducing bacteria in Methanogenic co-culture." Lett. Appl. Microbiol., **7** 165-168.

289. Zehdner, J.B. (1988) "Ecology of Methane Formation." 349-376

290. Zehdner, J.B. (1988) "Environmental and Technological Aspects." Biology of Anaerobic Microorganisms, John Wiley and Sons, New York, 794-831

291. Zellner, G., F. Neudorfer and H. Diekmann (1994) "Degradation of Lactate by an Anaerobic mixed culture in a Fluidized-bed reactor." Water Res., **28** (6) 1337-1340.

292. Zemaitis, Jr., J.R., D.M. Clark, M. Rafal and N.C. Scrivner (1986). "Handbook of aqueous electrolyte thermodynamics." AIChE, New York, NY.

293. Zhou, P., J. Huang, A.W.F. Li and S. Wei (1999) "Heavy Metal Removal from Wastewater in Fluidised Bed Reactor." Wat.er Res., **33** (8) 1918-1924.

294. Zinder, S.H. (1984) "Microbiology of Anaerobic Conversion of Organic Wastes to Methane: Recent Developments." ASM News, **50** (7) 294-298.

295. Zoetmeyer, R.J., A.J.C.M. Matthijsen, A. Cohen and C. Boelhouwer (1982b) "Product Inhibition in the acid forming stage of the Anaerobic digestion process." Water Res., **16**, 633-638.

296. Zoetmeyer, R.J., J.C. Van Den Heuval and A. Cohen (1982a) "pH influence on Acidogenic dissimilation of Glucose in an Anaerobic Digester." Water Res., **16** 303-311.